

Kinetic Mechanism Reduction for Chemical Process Hazard Application

Richard Thomas James Porter

Submitted in accordance with the requirements for the degree of PhD.

The University of Leeds
The School of Process Environment and Materials
Engineering

June 2007

The candidate confirms that the work submitted is his own and that appropriate credit has been given where reference has been made to the work of others.

This copy has been supplied on the understanding that it is copyright material and that no quotation from this thesis may be published without proper acknowledgement.

Acknowledgements

It has sincerely been a pleasure to work under the supervision of Professor Mike Fairweather, Professor John Griffiths and Dr. Alison Tomlin. I am extremely grateful for their guidance, encouragement, patience and enthusiasm.

Many of the practical aspects of the work presented in this Thesis were performed in conjunction with Dr. Kevin Hughes as part of the SAFEKINEX project. I would like to thank him for his generous contributions in terms of training, technical guidance and use of code.

I am also grateful to Dr. Boyd Brad for the many helpful discussions during the first two years of my studies at Leeds.

My family have always supported and encouraged me throughout my studies and for that I am eternally grateful. I further thank my friends around the Houldsworth building for their moral support and for the good times we spent together.

Lastly, I would like to thank the European Union for financial assistance through the SAFEKINEX project and the other partners in the consortium of this project. The international and collaborative nature of the project, made the work very exciting and rewarding.

Abstract

Despite considerable knowledge of the potential hazards associated with chemical process industries, explosion hazards continue to occur during hydrocarbon processing under partial oxidation conditions. Among the reasons is the change of operations that arise from process intensification, combined with an incomplete knowledge of the combustion characteristics of the processed materials. The ability to couple chemical kinetics with fluid dynamics and simulate these processes in reactive multi-dimensional flows would be a powerful process engineering tool that would constitute a significant advance in methodologies available to predict such hazards.

Detailed combustion kinetic mechanisms for hydrocarbon oxidation may contain hundreds of chemical species and thousands of reactions, making them too computationally expensive to be solved in computational fluid dynamic (CFD) codes. By adopting formal mathematical procedures, more compact and computationally efficient models can be achieved by reducing the numbers of species and reactions from the detailed mechanisms, thus making the incorporation of chemical kinetic effects into CFD possible. In addition, reduced reaction mechanisms can be used to gain kinetic understanding and elucidate the effect of poorly known reaction rate parameters and thermochemistry. Currently, mechanism reduction can be achieved by running full models with multiple initial conditions in a non CFD-based environment, interpreting the results using local sensitivity methods, identifying and removing redundant species and reactions, and then testing the reduced mechanisms. Many hours can also be saved by automating these tasks using programming techniques.

In this work we present automatic methods for removing species and reactions from comprehensive reaction mechanisms without significant detriment to model performance. The software has been applied to a range of chemical mechanisms covering different fuels, including propane, n-butane and cyclohexane which were generated using the EXGAS program. Reduced chemical models which can be used in higher dimensional simulations are obtained as output. A method for the

automatic construction of closed vessel ignition diagrams is presented, with such diagrams used to evaluate the comprehensive and reduced models. The benchmark is set by the performance of the full scheme and the criteria for performance of the reduced models are matched to this.

Kinetic investigations have been carried out using the reduced mechanism. Global uncertainty analysis methods were applied within the SAFEKINEX project to the reduced propane mechanism to establish the main contributors to uncertainties in output predictions. Results from the application of a Monte Carlo uncertainty analysis are reported in comparison with analysis of the main element fluxes within the scheme during oxidation. The kinetic foundation of the reduced n-butane mechanism was then analysed by formal numerical methods to trace the origins of the dramatic shifts in autoignition temperature as conditions are changed. One of the key factors in the chemistry that promotes autoignition at low temperatures ($T < 700$ K) is the transition from a cool flame to a second stage, within a two-stage ignition, driven by the formation and decomposition of hydrogen peroxide. A quantitative investigation into the kinetic origins of hydrogen peroxide in the transition stage has been performed.

The quasi steady state approximation (QSSA) combined with reaction lumping was applied to the reduced cyclohexane mechanism to further eliminate a number of intermediate species whilst incurring little error to output ignition delay predictions. The QSS species are fast reacting species which locally equilibrate with respect to the slower species in the system. Thresholds were applied to the calculated instantaneous QSSA error for each species over all considered time points, thus providing an automatic way of identifying QSS species. Species were eliminated by the formulation of lumped reactions with corresponding lumped reaction rates. With the aid of element flux visualization software, analysis of the fluxes of carbon atoms during isothermal oxidation has been undertaken using the reduced cyclohexane mechanisms. This shows the major reaction pathways of fuel to oxygenated cyclic compounds, the breakage of the ring to form aldehydroperoxides and ketohdroperoxides and their subsequent decomposition.

Contents

1	Introduction	1
2	Background to Method	10
2.1	Combustion kinetics and computational methods	12
2.1.1	The generation of comprehensive combustion mechanisms and experimental background	14
2.2	Reduction Methodologies	20
2.2.1	Skeletal Reduction	21
2.2.2	Time-scale based reductions	28
3	General Methods	36
3.1	Physicochemical principles	37
3.1.1	Thermochemistry	37
3.1.2	Elementary chemical reaction rate equations	38
3.1.3	Third body and fall-off reactions	40
3.1.4	Rate of production and rate of temperature change	43
3.2	CHEMKIN	45
3.3	MECHMOD	47
3.4	The SPRINT Integrator	48
3.4.1	Measurement of computational run time	51
3.5	Converting mechanism data files	52
3.6	Summary	52

4	Comprehensive kinetic mechanisms and their validation	54
4.1	Ignition diagrams and the negative temperature coefficient of reaction rate	56
4.1.1	Automatic simulation of the numerically predicted ignition diagram	62
4.2	Comprehensive propane model evaluation	66
4.3	Comprehensive n-butane model evaluation	72
4.4	Comprehensive n-hexane model evaluation	75
4.5	Comprehensive n-heptane model evaluation	78
4.6	Comprehensive cyclohexane model evaluation	82
4.7	Trends between fuels and the prediction of minimum autoignition temperature (MIT)	84
4.7.1	Kinetic background to the reactivity of different alkane structure	84
4.7.2	Evaluation of numerically predicted p-T _a ignition diagrams of n-butane and n-hexane for stoichiometric mixtures in air	88
4.7.3	Predicted minimum autoignition temperature from comprehensive mechanisms for a range of alkanes and their isomers	90
4.8	Discussion and conclusions	94
5	Automated Sensitivity Analysis Based Reduction Methods and Rate of Production Analysis	96
5.1	Automatic selection of time points for sensitivity analysis	97
5.2	Removal of redundant species	100
5.3	Removal of redundant reactions: Sensitivity analysis	107
5.4	Principal component analysis	109
5.5	Rate of production analysis	110

5.6	Application of sensitivity and principal component analyses for the equimolar propane + oxygen scheme	111
5.6.1	Removal of species: Iterative Jacobian analysis	113
5.6.2	Removal of reactions: Principal component analysis	116
5.6.3	Final reduced propane scheme and computational speed-ups	118
5.7	Application of sensitivity and principal component analyses for the lean n-butane + air scheme	120
5.8	Application of sensitivity and principal component analyses for the stoichiometric cyclohexane + air scheme	124
5.8.1	Development of reduced cyclohexane mechanism applicable over a wide low temperature range	125
5.8.2	Generation of reduced cyclohexane mechanisms for the calculation of simulated autoignition temperature (AIT)	130
5.8.3	Summary of reduced cyclohexane mechanisms and their computational speed-ups	135
5.9	Comparison of reduction achievements	137
5.10	Conclusions	140
6	Kinetic analysis of reduced hydrocarbon oxidation mechanisms	142
6.1	Species and reaction elimination patterns between fuels	145
6.1.1	Redundant species patterns	145
6.1.2	Redundant reactions patterns	149
6.2	Quantitative assessment of the impact of uncertainties in parameter values of the propane mechanism	150
6.2.1	Summary of uncertainty analysis	156
6.3	Analysis of major oxidation pathways during 2-stage ignition of equimolar propane and oxygen using element flux analysis	157
6.4	Numerical study of the kinetic origins of two-stage autoignition in lean n-butane-air mixtures	164

6.5	Analysis of cyclohexane oxidation under fuel rich isothermal conditions	170
6.6	Conclusions	180
7	Application of the Quasi Steady State Approximation	182
7.1	The identification of quasi steady state species	186
7.2	Application of reaction lumping	188
7.3	Amalgamation of products	192
7.4	Application of the quasi steady state approximation and reaction lumping to the cyclohexane + air scheme	193
	7.4.1 Further skeletal reduction	202
	7.4.2 Computational speed ups	206
7.5	Comparison of quasi steady state approximation reduction achievements	208
7.6	Conclusions	211
8	Conclusions	213
	Bibliography	224
	Appendices	
A.1	Classes of reactions removed from the cyclohexane mechanism	253
A.2	Classes of reactions removed from the n-butane mechanism	254
B	Publications and Conference Presentations	255

List of Figures

1.1	Experimental p-T _a ignition diagram for n-butane	7
3.1	Numerical modelling software schematic	53
4.1	EXGAS primary mechanism schematic	56
4.2	Early experimental ignition boundary showing the effect of a trace additives on the AIT of H ₂ / O ₂ mixtures	57
4.3	Generic p-T _a ignition diagram for C ₃₊ alkanes and other hydrocarbons	59
4.4	The effect of various vessel coatings on the experimental p-T _a ignition diagram of n-butane / oxygen	61
4.5	Simulated p-T _a ignition diagram from the full, EXGAS propane mechanism	65
4.6	Experimental p-T _a ignition diagram for equimolar C ₃ H ₈ / O ₂ . . .	67
4.7	Simulated p-T _a ignition diagram from the full, Westbrook propane mechanism	68
4.8	Comparison of simulated and experimental p-T _a ignition digrams for equimolar C ₃ H ₈ / O ₂	68
4.9	Temperature – time profiles generated using the full EXGAS propane mechanism	70
4.10	The variation of ignition delay time with operating conditions . .	71
4.11	Simulated φ-T _a ignition diagram from the full, EXGAS n-butane mechanism	73
4.12	Simulated φ-T _a ignition diagram from the full, Westbrook n- butane mechanism	73

4.13	Comparison of experimental n-butane ϕ - T_a ignition diagram at different ambient pressures	74
4.14	Comparison of experimental and simulated n-butane ϕ - T_a ignition diagram	74
4.15	Simulated p- T_a ignition diagram from the full, EXGAS n-hexane mechanism	76
4.16	Experimental p- T_a ignition diagram for n-hexane	76
4.17	Comparison of experimental and simulated n-hexane p- T_a ignition diagram	77
4.18	Simulated p- T_a ignition diagram from the full, EXGAS n-heptane mechanism	79
4.19	Experimental p- T_a ignition diagram for n-heptane	79
4.20	Temperature – time profile generated using the full EXGAS n-heptane mechanism	80
4.21	Comparison of simulated p- T_a ignition diagrams for n-heptane	81
4.22	Comparison of experimental and simulated cyclohexane p- T_a ignition diagram	83
4.23	Variation of the MIT of n-alkanes	85
4.24	Comparison of experimental n-butane and n-hexane p- T_a ignition diagrams	89
4.25	Comparison of simulated n-butane and n-hexane p- T_a ignition diagrams	89
4.26	Variation of predicted AIT for a range of alkanes	92
5.1	Simulated n-butane ϕ - T_a ignition showing selected operating conditions for sensitivity analysis	99
5.2	Automatically selected time points for sensitivity analysis during two-stage ignition	100
5.3	Example results for the iterative analysis of the Jacobian matrix	102
5.4	Necessary species identified during two-stage ignition	104
5.5	The influence of reduction criteria on reduced mechanisms	105

5.6	The effect of algorithmic modifications to the overall sensitivity measure for reaction removal	109
5.7	Simulated p - T_a ignition diagram from the full, EXGAS propane mechanism showing operating conditions for sensitivity analysis	112
5.8	Two-stage species reduction temperature profiles	114
5.9	The effect of species reduction on the simulated propane p - T_a ignition diagram	115
5.10	The effect of species reduction on simulated propane temperature profiles	115
5.11	The effect of reaction reduction on the simulated propane p - T_a ignition diagram	117
5.12	The effect of reaction reduction on simulated propane temperature profiles	117
5.13	Simulated p - T_a ignition diagram from the reduced propane mechanism	119
5.14	Comparison of full and reduced simulated propane temperature profiles	119
5.15	Comparison of full and species reduced n-butane ϕ - T_a ignition diagrams	121
5.16	Comparison of full and reaction reduced n-butane ϕ - T_a ignition diagrams	121
5.17	Comparison of full and reduced n-butane temperature profiles . .	122
5.18	Comparison of reduced n-butane ϕ - T_a ignition boundaries	123
5.19	Simulated p - T_a ignition diagram from the full, EXGAS cyclohexane mechanism showing operating conditions for sensitivity analysis	125
5.20	The effect of species reduction on the simulated cyclohexane p - T_a ignition diagram	127
5.21	The effect of species reduction on simulated cyclohexane temperature profiles	127

5.22	The effect of reaction reduction on the simulated cyclohexane p- T _a ignition diagram	129
5.23	The effect of reaction reduction on simulated cyclohexane temperature profiles	129
5.24	Simulated low temperature ignition boundary from the full cyclohexane mechanism	131
5.25	Comparison of full and reduced cyclohexane temperature profiles	133
5.26	Comparison of full and reduced cyclohexane low temperature p- T _a ignition boundaries	134
5.27	Comparison of full and further reduced cyclohexane low temperature p-T _a ignition boundaries	135
6.1	Monte Carlo analysis of simulated output variables	155
6.2	Simulated propane p-T _a ignition diagram with adjusted thermochemistry	157
6.3	Reduced propane reaction schematic	160
6.4	Simulated heat release during two-stage ignition of n-butane . . .	166
6.5	Isothermal quadratic autocatalysis in a closed vessel	172
6.6	Experimental isothermal oxygen consumption of cyclohexane . .	173
6.7	Simulated isothermal oxygen consumption of cyclohexane	173
6.8	Gradient analysis of simulated isothermal oxygen consumption of cyclohexane	174
6.9	Reduced cyclohexane reaction schematic	175
6.10	Key to cyclohexane species	176
6.11	Simulated isothermal oxygen consumption of n-butane and gradient analysis	179
7.1	The difference between species lumping and reaction lumping . .	185
7.2	N-butane reaction sequence including QSS species	189
7.3	Schematic of simple QSS species coupling	195
7.4	Schematic of complex QSS species coupling	197

7.5	Effect of QSSA application on simulated p-T _a ignition diagram of cyclohexane	199
7.6	Effect of QSSA application on simulated temperature profiles of cyclohexane	199
7.7	Effect of product amalgamation on simulated p-T _a ignition diagram of cyclohexane	200
7.8	Effect of product amalgamation on simulated temperature profiles of cyclohexane	200
7.9	Post QSSA cyclohexane reaction schematic	202
7.10	Effect of further skeletal reduction on simulated p-T _a ignition diagram of cyclohexane	203
7.11	Effect of further skeletal reduction on simulated temperature profiles of cyclohexane	203
7.12	Effect of further product amalgamation on simulated p-T _a ignition diagram of cyclohexane	204
7.13	Effect of further product amalgamation on simulated temperature profiles of cyclohexane	204

List of Tables

4.1	Activation energies of H atom abstractions	87
4.2	Predicted and measured MIT for a range of alkanes	92
5.1	Species reduction criteria for cyclohexane	126
5.2	Further species reduction criteria for cyclohexane	132
5.3	Calculated and estimated computational runtimes from reduced cyclohexane mechanisms	136
5.4	Comparison of reduction achievements to DRG	139
6.1	Consistently redundant species	146
6.2	Consistently redundant classes of species	147
6.3	The 18 most important heats of the propane mechanism	151
6.4	The 50 most important reactions of the propane mechanism	152
6.5	Carbon flux thresholds used to produce the propane reaction schematic	159
6.6	Rates of production of crucial intermediates during the transition of cool flame to ignition of n-butane	167
6.7	Post cool flame heat releasing reactions during two-stage ignition of n-butane.	168
6.8	Pre-ignition heat releasing reactions during two-stage ignition of n-butane	168
6.9	Consumption reactions involving OH radicals during two-stage ignition of n-butane	169
6.10	Consumption reactions involving O ₂ molecules during isothermal oxidation of cyclohexane	177

7.1	Magnitudes of instantaneous QSSA errors for cyclohexane species	193
7.2	QSS specie identified in the cyclohexane mechanism	194
8.1	Summary of reduced mechanisms	219

Nomenclature

A	Pre-exponential factor in rate constant
A	Reactor surface area
A_0	Low pressure limit pre-exponential factor in rate constant
A_∞	High pressure limit pre-exponential factor in rate constant
a	(Subscript) Ambient
a_n	NASA polynomial coefficient
B_i	Overall sensitivity of species i
B_j	Overall sensitivity of reaction j
C_p	Molar heat capacity
c_i	Concentration of species i
Δc_i^s	Instantaneous, normalised, single species, quasi steady state approximation error
Δc_i^g	Instantaneous, normalised, group, quasi steady state approximation error
E	Activation energy
E_0	Low pressure limit activation energy
E_∞	High pressure limit activation energy
F	Fall-off reaction parameter
\tilde{F}	Rate parameter sensitivity matrix
f_i	Rate of production of species i
f_i^q	Rate of production of QSS species
H	Enthalpy
ΔH_j^o	Change of enthalpy that occurs in passing completely from reactants to products in j th reaction
J	Jacobian matrix
K_c	Equilibrium constant in concentration units
K_p	Equilibrium constant in pressure units
k_f	Forward rate parameter

k_j	Rate parameter of reaction j
k_r	Reverse rate parameter
M	Third body weight
N	Number of species
$N_{A,j}$	Total number of atoms A in reaction j
n	Number of reactions
n	(Superscript) Dimensionless exponent of Temperature in rate constant
$n_{A,i}$	Number of atoms A in species i
P_r	Reduced pressure of fall-off reactions
p	Pressure
R	Gas constant ($= 8.314 \text{ J mol}^{-1} \text{ K}^{-1}$)
R_j	Rate of elementary reaction j
S	Molar entropy
ΔS_j^o	Change of entropy that occurs in passing completely from reactants to products in j th reaction
\tilde{S}	Concentration rate sensitivity matrix
SS_j	The set of species in the left hand side of species j
T	Temperature
ΔT	Change in temperature
T_1	Temperature attained in the first stage of two-stage ignition
T^*	Troe parameter
T^{**}	Troe parameter
T^{***}	Troe parameter
t	Time
t_{ign}	Time to ignition
U	Heat transfer coefficient
V	Reactor volume
v	Overall reaction rate
Δv	Sum of stoichiometric coefficients
v_{ij}	Stoichiometric coefficient of species i in reaction j

v_{max} Maximum overall reaction rate

Greek Characters

α Troe parameter
 β_0 Low pressure limit exponent of temperature in rate constant
 β_∞ High pressure limit exponent of temperature in rate constant
 ζ Fractional extent of reaction of the primary reactant at time t
 ζ_0 Initial fraction of autocatalytic intermediate
 τ_1 Time to cool flame
 τ_2 Time to ignition
 φ Equivalence ratio

Abbreviations

AIT Autoignition temperature
CARM Computer aided reduction method
CFD Computational fluid dynamics
CMC Conditional moment closure
CSP Computational singular perturbation
CSTR Continuous-flow stirred tank reactor
DNS Direct numerical simulation
DR Detailed reduction
DRG Direct relation graph
GA Genetic algorithm
HCCI Homogenous charge compression ignition
ILDm Intrinsic low-dimensional manifold
ODE Ordinary differential equation
PCA Principal component analysis
PDE Partial differential equation
PDF Probability density function
PSR Perfectly stirred reactor
QSS Quasi steady state

QSSA Quasi steady state approximation
RCM Rapid compression machine

Chapter 1

Introduction

The provision of kinetic reduction software which can be used to reduce computational demand during the simulation of hydrocarbon oxidation processes using detailed kinetics, was a major objective of the SAFEKINEX project. The SAFEKINEX project (SAFE and Efficient hydrocarbon processes by KINETics and EXpertise and development of computational process engineering tools) was funded by the European Union and the participating partners were: Technical University of Delft, Centre National de la Recherche Scientifique - del. nord-est (Nancy), Vrije Universiteit Brussels, Bundesanstalt für Materialforschung und -prüfung (Berlin), Warsaw University of Technology, Technical University of Wroclaw, University of Leeds, University of Karlsruhe - Engler Bunte Institut, Institut Nat'l de l'Environnement et des Risques Industrielles (Creil, France), Shell International Chemicals, Gaz de France and Laborelec Belgium. The overall objectives were to acquire data and develop computer tools which will help to forecast and eliminate explosion hazards on plants which process hydrocarbons under partial oxidation conditions.

The partial oxidation of raw hydrocarbons in the chemical industries results in the production of many useful materials such as nylon from cyclohexane and maleic anhydride from n-butane. Despite our considerable knowledge of these chemical processes, many are poorly optimised and must maintain large safety margins due to an incomplete understanding of the gas phase oxidation characteristics of the processed materials in the operating conditions of

temperatures between 350 to 800 K and pressure up to 100 atm. Further, unexpected autoignitions take place on such processes when a mixture of fuel and oxidizer exist in an environment which exceeds the autoignition temperature (AIT) of that substance. The activation is provided by the ambient conditions rather than an external source of ignition, such as a spark or flame, and a chain branching exothermic reaction will follow. Autoignition hazards can also occur when fuel and oxidizer mixtures come into contact with hot surfaces or after residing in a hot chamber for a certain induction period known as an ignition delay time. However, the autoignition temperature for a given reactant will not be the same under different conditions, such as varying vessel size, reactant pressure or composition, and experiments have shown that a given fuel air mixture can ignite well below the value of its AIT defined by the statutory autoignition test procedure for that particular fuel [1]. Fluctuations in feed composition and other scalars can hence lead to operating conditions deemed to be safe becoming, dangerous [2,3].

Another important spontaneous phenomenon in hydrocarbon oxidation is the occurrence of cool flames at low ambient temperatures and pressures. A cool flame is a weakly chemiluminescent flame with a low temperature rise, typically with a $\Delta T < 200$ K, in which the reactants are only partially oxidised to products similar to those of a slow oxidation reaction rather than the products of complete oxidation, carbon dioxide and water. Although the occurrence of a single cool flame alone would not constitute a great danger, cool flames can initiate ignitions in their own right, as occurs during two-stage ignition, due to the accumulation and decomposition of reactive intermediates like formaldehyde and hydrogen peroxide in the resulting post cool flame mixture [4,5].

It follows that over the wide ranges of conditions encountered in the industrial processing of hydrocarbons, there are numerous potential hazards which can lead to ignition and explosions. These lead to wasted material, increased pollutant emissions, energy losses and lower profit margins. Unsafe situations generated by the rapid temperature and pressure rises related to autoignition hazards can and have previously caused industrial explosions that have resulted in injury, loss of life and damage to process infrastructure. In the UK, in 1986 alone there were 31

incidents reported in which thermal runaway occurred in batch reactor systems leading to the injury of 18 individuals [6]. Specific examples of fires and explosions on hydrocarbon oxidation plants, where the reactive mixtures inside units have entered the explosive range are covered by Kletz [7,8], including two incidents involving spontaneous ignition in gas recycles during the production of cyclohexanol and cyclohexanone from cyclohexane [7]. Several accidents in which explosions were initiated by cool flames (two-stage ignition) have been described by D'onofrio [9]. Other types of spontaneous ignition hazards include "lagging fires" [10] where process or heat exchange fluid leaks from a pipe and becomes entrapped in the piping insulation. The liquid may evaporate, mix with air and ignite on contact with the hot pipework.

A potential solution to this problem is through the use of detailed models of the relevant processes incorporating detailed chemical kinetics. Scientists and engineers use chemical kinetics to understand how reactions take place at the molecular level and thus predict their global behaviour. The interpretation of chemical experiments and mathematical models has led to the creation of chemical mechanisms consisting of large lists of elementary reactions and associated parameters. The reaction mechanisms usually involve some form of feedback whereby the intermediate products of the reaction influence the rates at which the other reaction steps proceed. As data of the elementary reactions has accumulated over time, the size and predictive accuracy of reaction mechanisms has increased and produced complex descriptions of the reacting systems.

The most common way to model the kinetics of a reaction in the gas phase is to establish a system of ordinary differential equations (ODEs) for the rates of change of concentration of each species over time in zero-dimensions, with spatial uniformity of concentration and temperature assumed. The rate of each reaction then depends on the concentrations of reactants and the rate parameter governed by the temperature and pressure of the system which is calculated using exponential Arrhenius expressions. Temperature changes can be calculated from the reaction rates and thermodynamic data associated with each species and hence variables can change as reaction time progresses.

Comprehensive reaction mechanisms for the description of the gas phase oxidation of hydrocarbons have been developed at research institutes for many decades by the assembly of large lists of reactions known to take place during an oxidation process [11-13]. The reactions contained in these lists are usually homogenous, although heterogeneous reactions between the gas mixture and vessel wall or catalyst may be introduced. The reactions, involving many intermediate species such as carbon monoxide or long chain hydroperoxy radicals, can be subdivided into three major categories, namely; initiation, propagation and termination [5]. Each set of associated rate parameters are found from either experiments or more recently theoretical rate determinations [14], and may have come under the scrutiny of rate data assessment panels. They can often be located in chemical reaction databases. The resulting mechanisms have a range of operating conditions to which they are applicable and are often characterised into low temperature (500 – 1000 K) or high temperature regimes (1000 – 2600 K). The comprehensive mechanisms used for this thesis will be focused on those of the low temperature regime as these are the operating conditions which are relevant to partial oxidation processes in industry. The end result must be validated by simulation and comparison to experiment although uncertainty in the rate parameters can often lead to discrepancies.

In order to be complete, comprehensive mechanisms can consist of thousands of reactions which makes their manual construction very labourious and prone to human error. The only way forward is the use of computers and development of automated procedures for the construction of the many required comprehensive oxidation mechanisms. Such procedures rely on insight gained from the manual construction and use rules for defining the structure of the output comprehensive mechanisms [15]. There have been a number of attempts at producing automatic software for this task, such as those of Matheu *et al* [16-18], although the most notably software is EXGAS, which has been developed at CNRS Nancy for two decades. This software is used for the automatic construction of detailed reaction mechanisms for gas phase oxidation with a hydrocarbon primary reactant and has been employed in this work [19-21].

Predictive tools for accurately forecasting and identifying combustion hazards are only scarcely available or missing. The ability to couple chemical kinetics with fluid dynamics and simulate industrial processes in reactive multi-dimensional flows would be a powerful process engineering tool that would constitute a significant advance in the available methodologies [22]. Such a tool would enable process engineers to optimise, increase efficiency and reduce running costs of existing processes and also aid in the design of future chemical processes. This could be achieved with the use of computational fluid dynamic (CFD) codes. Most currently available CFD codes use highly simplified kinetics in order to obtain a quick solution. As a result, their accuracy and usefulness is severely restricted. The incorporation of a detailed thermokinetic model, so that appropriate interactions between the physics and chemistry are considered, is necessary in order to predict phenomena such as autoignition, cool flames and the transitions between these regimes inside industrial units [3,23].

Detailed combustion mechanisms can contain vast numbers of species and reactions and require enormous computational power to be solved in CFD. The scale of the simultaneous equations makes the solution virtually impossible at present and for the foreseeable future. The computational time and cost can be reduced if the size of the mechanism is reduced, but this is useful only if the relevant qualitative features are not lost. In addition, due to the range of time-scales present in kinetic systems, the resulting chemical rate equations are classed as being “stiff”. The stiffness of the system is classified by the ratio of the slowest and fastest time-scales within the model and the presence of reactive radicals often leads to a high level of stiffness. The stiffness of the system has an impact on the computational methods that are used to solve the chemical rate equations, and therefore it is desirable to reduce not only the number of variables within the reduced model, but also the stiffness of the system [15]. Therefore, as a prerequisite to the simulation and prediction of hazards in large scale systems, formal procedures of mechanism reduction must be used to reduce the complexity of the comprehensive kinetic mechanism resulting in a reduced mechanism. A further, yet sometimes overlooked, justification for performing mechanism

reduction is that kinetic understanding can be gained from the analysis of reduced mechanisms. Global uncertainty analysis techniques can be used to elucidate poorly known Arrhenius or thermokinetic parameters which can cause discrepancies when model output is compared to experiment. These techniques involve running many simulations with both individual runtime and number of simulations scaling with mechanism size and so mechanism reduction is an established prerequisite [24]. Other kinetic techniques are greatly facilitated by the use of short mechanisms such as rate of production and element flux analyses.

To be valid, hydrocarbon oxidation mechanisms must be capable of reproducing the various autoignition phenomena seen in experiments over a wide range of operating conditions in both full and reduced form [25]. The usual ways to validate a kinetic mechanism include comparisons of the non-isothermal time-dependent behaviour or concentration profiles of chemically important species with experimental results, generally at high pressure. An alternative, rarely used method is the experimental comparison of the constructed ignition diagram, in which the various autoignition phenomena of cool flame, autoignition and slow reaction are classified as the initial conditions are varied and quantitative boundaries between the different regimes are defined. Further subclassifications of autoignition phenomena can be made, namely; multiple cool flames, i.e. two or more cool flames occurring one after another, and multiple stage ignition e.g. a three stage ignition is an ignition preceded by two cool flames. There are two types of ignition diagram, the $p-T_a$ diagram shows how the combustion characteristics change over a range of total pressure versus ambient temperature with mixture composition held constant, and the $\phi-T_a$ diagram shows ambient temperature versus mixture composition with total pressure held constant. In order to define the boundaries of an ignition diagram using a kinetic model, adequate description heat losses are necessary. An example experimental $p-T_a$ ignition diagram for stoichiometric n-butane in air is shown in Fig. 1.1. The ignition diagram is fundamental to awareness of spontaneous ignition hazards in the industrial processing of hydrocarbons and should be the first point of reference for the existence of an explosion hazard because it shows the minimum conditions at

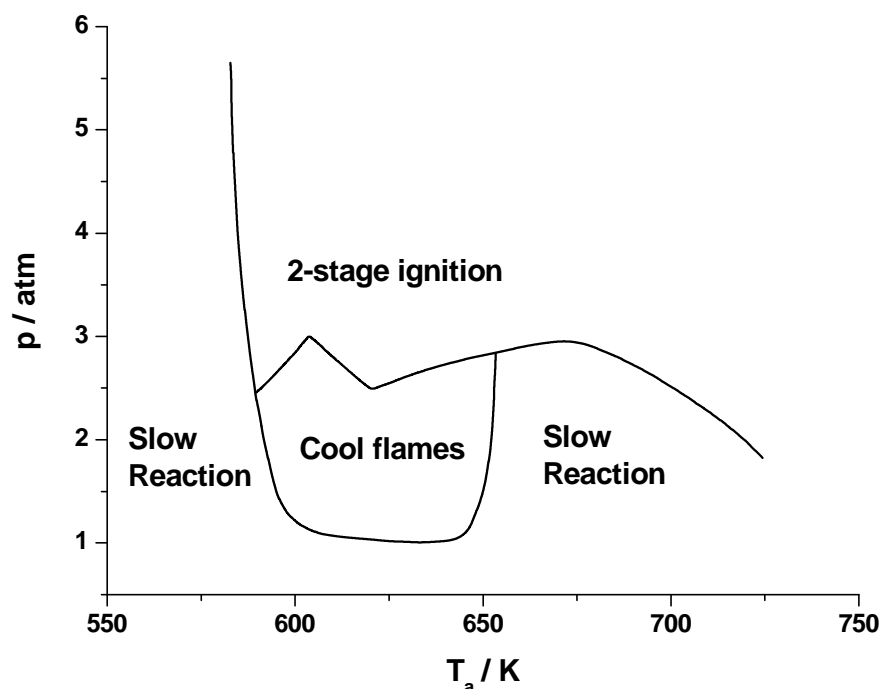


Fig 1.1. Experimental p - T_a ignition diagram for stoichiometric n -C₄H₁₀ + air, showing regions of 2-stage ignition, cool flames and slow reaction [26].

which autoignition occurs. Validation of reduced mechanisms can be made at differing levels of reduction with the output predictions of the full scheme being used as the benchmark to which the comparison is made.

Typically, the first stage of mechanism reduction is to remove unnecessary species and reactions from the mechanism whilst still retaining the essential features. Reduced mechanisms resulting from the application of these methods are collectively known as “skeleton mechanisms” and sensitivity analysis is one method which can be used to generate these. Sensitivity analysis investigates the effect of making small changes in variables or parameters on other variables e.g. the effect of small changes of concentration of each species on the rates of production of other species. The effect can be numerically quantified, ranked and then thresholds can be applied to decide which species or reactions can be retained and which can be discarded [27]. Further reduction methods may be used to analyse the time-scales of the system, identify fast reacting species which may

be decoupled from the system and hence further reduce the dimensionality and the level of stiffness of the system. Other time-scale based methods aim to find the lowest number of variables required to accurately model the system which would be useful in setting up a numerically fitted model to describe the kinetic mechanism [15].

There are a number of software available to aid the combustion kineticist or model reduction specialist. Notably, these are the KINAL [28,29] or KINALC [30,31] packages to apply sensitivity methods and the CHEMKIN family of codes [32] which are used worldwide in combustion modelling and have had a large impact on the research community by providing a common framework for communicating useable kinetic schemes via a “CHEMKIN format” [33].

Like the construction of comprehensive mechanisms their manual reduction is a laborious task. Currently, this involves running full kinetic models with multiple initial conditions in a non CFD-based environment, interpreting the results using local sensitivity methods, identifying and removing redundant species and reactions, and then testing the reduced mechanisms. To perform these tasks manually requires that the user has a detailed understanding of the principles involved and is also prone to user error. Thus the reliability of the results could be improved and many man hours saved by automating these tasks using programming techniques. The manual construction of the numerically predicted ignition diagram is also a laborious process which is amenable to automatic generation [22].

The main objectives of this thesis are to:

- (a) Assess the current state-of-art of suitable reduction methodologies.
- (b) Develop a methodology whereby comprehensive mechanisms can be evaluated via the comparison of their numerically determined ignition diagrams to the experimental versions.
- (c) Develop an automatic reduction software to produce reduced skeleton mechanisms which exhibit all the desired features of the comprehensive mechanisms from which they will be obtained.

- (d) Illustrate the application of the automatic reduction software with respect to a number of hydrocarbon oxidation mechanisms.
- (e) Make relevant kinetic investigations using the reduced mechanisms obtained from the application of the reduction software.
- (f) Develop and apply time-scale based reduction methodologies.
- (g) Evaluate the performance of the reduction methods with respect to other published techniques and CFD requirements.

In the next Chapter, we further discuss advances made in combustion kinetics and the variety of available reduction methods with attention focused on those most appropriate to the current application. More in depth descriptions of the reduction methods employed in this work are presented in later Chapters along with the results obtained from their application. Chapter 3 presents the established numerical techniques used to model chemical kinetics and employed in this work. In Chapter 4, the types of hydrocarbon oxidation phenomenon observed in experiments and mapped in ignition diagrams are discussed with respect to the kinetic foundations. A number of comprehensive mechanisms, including those sourced from the EXGAS automatic comprehensive mechanism generator, are evaluated by the automatic construction of their ignition diagrams and comparing to the available experimentally determined versions. Chapter 5 is dedicated to automated methods for reduction to a skeleton mechanism and includes the description of software which has been set up to minimise the numbers of chemical species and reactions without loss of important kinetic detail using sensitivity based reduction methods. The codes are based on the use of UNIX shell scripts to completely automate the utilisation of numerical integration and local sensitivity analysis software in a CHEMKIN format. The application of the code to a number of fuels is illustrated and reduced chemical models which can be used in higher dimensional simulations are obtained as output. The reduced schemes are kinetically analysed in Chapter 6 and their mechanistic implications are discussed. One of the reduced mechanisms obtained from the work presented in Chapter 5 is further reduced in Chapter 7 using a time-scale based method known as the quasi steady state approximation (QSSA). The main conclusions and

achievements are drawn together in Chapter 8. Areas requiring further work and possible future directions are addressed.

Chapter 2

Background to Methods

In this Chapter an overview is presented of the advances made in combustion kinetics and the experiments and computational techniques which have led to the creation, usability and refinement of large comprehensive hydrocarbon oxidation mechanisms. The development of combustion kinetics from early fundamental discoveries is introduced in Section 2.1. Further developments resulting from the implementation of the computer are reviewed, such as the use of stiff-equation solvers, kinetic databases and automatic systems for the generation of comprehensive mechanisms.

The natural follow-on from this is a review of mechanism reduction techniques which is a major focus of this thesis. To reduce a comprehensive mechanism requires that a prescribed series of formal mathematical procedures are applied in a certain order. Generally, the first of these procedures to be applied would fall into the category of skeleton reductions to purely remove all those species and reactions from the mechanism which are not required to model the kinetic features of interest. This procedure is especially applied to very large mechanisms with $N > 100$ and $n > 1000$ (where N is the number of species and n is the number of reactions). For very small comprehensive mechanisms or mechanisms provided already in a partially reduced form, it may not be possible to purely remove any species or reactions, although it may be worth applying such techniques as a check. Our objective is to reduce computational cost. Since the evaluation of the $N \times N$ Jacobian matrix constitutes the major computational

effort during the integration of large mechanisms, computational speed-ups are expected to scale with N^2 . Reductions achieved exclusively by the removal of reactions are expected to scale with n , because the effort required to compute the right hand sides of the rate equations is reduced where reactions are removed. For these reasons it is most important in skeleton reductions to first find the minimum subset of species and then apply methods to reduce the number of reactions. Amongst skeleton reductions, there are the methods of sensitivity analysis [27,30,34-36], direct relation graphs [37-40] and optimization methods [41-45] which will be later discussed. Computational singular perturbation (CSP) analysis [46] is another method which may be used to produce skeleton mechanisms, but this is often used with time-scale based techniques simultaneously and so will be discussed later.

Skeletal reductions can in many cases reduce large numbers of species and reactions thus leading to substantial computational savings. However, it is often the case that many species will remain in the mechanism and due to the large computational overheads in determining the kinetic source term in a CFD code the implementation of skeleton reduced mechanisms is still very computationally intensive. As mentioned in Chapter 1, the problem is compounded by the vast range of time-scales in the system (stiffness) which hampers the computational solution and skeleton mechanisms are often stiff. The degree of stiffness that prevails in a system will often dictate the choice of time step used by the numerical solver, with the smallest time-scale being the major controlling factor resulting in the requirement of smaller time steps. As a consequence, computational solution times are much larger than those obtained if only the slow dynamics were simulated [47]. This problem has been addressed somewhat by the development and use of dedicated stiff ODE solvers which use more sophisticated solution methods to speed up the process. One such solver is the SPRINT integration package [48] (see Section 3.4 for further details). A further class of reduction methods are known collectively as time-scale based methods and are applied after reduction to a skeleton mechanism to achieve further speed-ups. These methods also address the problem of stiffness by enabling the system to be

controlled by only the slow dynamics which are known to dictate the exhibited features in combustion kinetics. In many cases it is not possible to remove the fast species or dynamics, as one would with a skeletal reduction because they may be included in vital reaction steps in the chain of events. However, the fast species often have short lifetimes and low concentrations, making their impact negligible for most of the reaction and so may be approximated using relationships to the slower dynamics. The following techniques fall into the time-scale reduction category; computational singular perturbation (CSP) analysis [46], intrinsic low-dimensional manifold (ILDM) analysis [49], repro-modelling [50], and lumping with time scale separation [51]. The more traditional quasi-stationary state approximation (QSSA) [52] also falls into the class of time-scale based techniques and is demonstrated in Chapter 7. The QSSA was selected over the other time-scale methods in this application because it suits our intended purpose of making kinetic investigations using reduced mechanisms. Post application of the QSSA, the format of the kinetic mechanism remains intact to a large extent, whereas with the application of other methods it can be transformed into a fitted polynomial model [50,53,54] or “look-up” tabulation [55] and is hence difficult to interpret kinetically because it no longer resembles a kinetic mechanism.

Further lumping and tabulation methods are briefly reviewed. Before the further discussion of reduction techniques is a review of the developments of combustion kinetics and related computational methods.

2.1 Combustion kinetics and computational methods

The introduction of the Arrhenius rate expression in the late 19th century heralded the beginning of chemical kinetics [56]. Although originally a two parameter representation, in the present day the rate coefficient (k) for a reaction may be given in two or three parameter form as;

$$k = A \exp(-E/RT) \text{ or } k = AT^n \exp(-E/RT), \quad (2.1)$$

where A is the pre-exponential factor, E is the activation energy, R is the ideal gas constant, T is temperature and n is a number of order unity. As noted later, the values of the parameters are obtained by functional fitting of experimental data, by *ab initio* calculating or by estimation using thermochemical rules and analogy to related reaction. By combining the rate coefficient with the law of mass action, a reaction rate can be determined. At first, this equation was used in many aspects of chemistry to give a representation of a global reaction, that is, primary reactants forming final products. The next significant milestone was the realization that the behaviour of a reactive system was controlled by a number of reaction steps with reaction intermediates playing a key role, thus forming the basis of chain reaction theory. Experimental studies were undertaken to determine the parameters for a number of reactions including those of gas-phase reactions. The requirement for an understanding of gas-phase combustion kinetics was driven by the growth of automotive engines and others with initial theorizations being developed for $\text{H}_2 + \text{O}_2$ and then hydrocarbons. Small kinetic schemes were initially developed via a process of “building up” [57] which led to more realistic models for the overall reaction behaviour. However, in the pre-computer era the analytical solution of these schemes with respect to time provided a significant challenge due to the coupling of the simultaneous nonlinear ODEs representing the concentration of each species. The quasi steady state approximation proposed by Bodenstein [58,59] earlier in the 20th century provided a useful expedient for the solution of the coupled differential equations by replacing some of the ODEs with algebraic expressions. These substitutions led to efforts to construct simplified kinetic models, representing isothermal chemical reaction, by reducing the set of ODEs to a single equation [60,61]. A similar approach was used to obtain a two variable solution (reactant concentration and reactant temperature) and formed the basis of thermal ignition theory [62]. According to Turányi [63], Semenov [64-66] was the first to apply the QSSA to substantially non-stationary systems and to restrict its use to selected intermediates rather than to all of them. In 1952, the first numerical solutions of stiff systems of coupled nonlinear ODEs for chemical kinetics were developed by Curtiss and Hirshfelder [67].

The introduction of the electronic computer (*ca.* 1960) led to significant advances in the field of combustion kinetics. Early computational solutions of chemical kinetics employed the QSSA [68,69] because at that time automated computational stiff ODE solvers were not in existence. In 1969, Gear [70,71] developed the first computer based algorithms to solve stiff differential systems; these were later employed in software applications by Hindmarsh *et al* [72,73]. These methods were first applied to atmospheric chemistry problems but the same principles could be used to solve combustion kinetic problems exhibiting a higher degree of stiffness [33]. The same numerical techniques are employed today using stiff ODE solvers such as those contained in the SPRINT package [48]. Further details of the SPRINT package will be given in Section 3.4.

2.1.1 The generation of comprehensive combustion mechanisms and experimental background

The appearance of stiff ODE solvers allowed the expansion of kinetic mechanisms to include greater numbers of species and reactions with larger variations of time-scales like those of C₃₊ alkanes. Hydrocarbon oxidation mechanisms were initially assembled manually from the lists of elementary reactions that are known to occur and for which rate data had been proposed. The manual construction of mechanisms is a slow process involving many research groups which are needed to;

- a) suggest the inclusion or exclusion of certain reaction steps,
- b) establish appropriate parametric information,
- c) validate the mechanisms by comparing their output to experimental measurements.

For convenience, combustion mechanisms are categorized into those applicable to low temperature regimes ($T < 1000$ K) and those applicable to higher temperatures ($T > 1000$ K), although it must be born in mind that elementary reaction rates vary as a continuous function of temperature and do not “switch on” or “switch off”. The focus of the current work is on low temperature mechanisms.

Nowadays, many of the elementary reaction steps and corresponding reaction rate parameters included in the mechanisms can be found in online databases like the NIST program on chemical kinetics [74], although published rate data [75] which has been critically evaluated by a panel of experts using the available information regarding each elementary step is a better source. In many cases enough measurements exist to allow quality assigned error limits to be defined for all the reactions considered. The list of elementary steps of which a mechanism is composed is usually drawn from the possible molecular combinations of species that are detected during the experiments, although certain rules are adhered to in order to avoid a combinatorial explosion.

The rate parameters of a given elementary step can be determined experimentally. However, the generation of unstable intermediates presents a significant challenge. The introduction of precise diagnostic techniques to measure species concentrations, like gas chromatography in the 1950s, resulted in more accurate measurements for elementary rate constants. Work carried out by Baldwin, Walker and co workers [76-79] for example, used this technique to quantify the rates of elementary steps involving primary free radicals. The intermediate species were usually sourced by adding a small amount of a hydrocarbon to slowly reacting $\text{H}_2 + \text{O}_2$ mixtures. In experimental methods employed by Morley [80] to determine rates, mass spectrometry was used to observe the decay of intermediate species in flames. Nowadays, even more sophisticated experimental apparatus is available and the use of the laser photolysis/photo-ionization mass spectrometry technique has gained favour. Radicals are created by pulsed photolysis and the kinetics of the species are monitored in real time by photionization mass spectrometry [81]. This technique has been used by Hughes *et al* [82] to determine the rates of peroxy-hydroperoxy radical isomerizations, which is a key step in low temperature hydrocarbon mechanisms and also by Shestov and co-workers to study the kinetics of vinyl radicals and ethene [83]. Numerical methods are used to fit rate parameters to the experimental data obtained. In some cases, the experimental results show that the

reactions also exhibit a pressure dependency and further elaborations of the Arrhenius expression are therefore required.

Despite the travail of experimentalist to determine many rate parameters of elementary steps, the current position is that a large proportion of the elementary steps which make up today's comprehensive mechanisms have never been studied experimentally and are often deduced from similar reactions or by thermochemical kinetic methods such as those proposed by Benson [84]. A more rigorous numerical deduction is through the use of *ab initio* modeling techniques [85], which may be based on quantum chemical, reaction rate or transition state theory. These techniques are becoming increasingly popular because they can produce order-of-magnitude estimates in a matter of days and at a fraction of the cost of an experimental program.

Of course, a chemical kinetic mechanism must also include thermochemical data of the species; these are very important in their own right and are derived from thermochemical data tables or calculated using bond additivity rules [84]. A number of software packages are available to calculate thermodynamic data such as CHEMKIN [86] or THERGAS [87]. The thermochemical data is used to calculate enthalpies and entropies of formation as well as heat capacity and is usually in the form of 14 NASA polynomial coefficients in order to comply with the CHEMKIN mechanism format. Reverse reaction rates are calculated from the thermochemical data via the equilibrium constants. The rate and themokinetic parameters interpreted from experiments and deduced by numerical methods are often intensively debated and are usually only known to a low level of accuracy; significant uncertainties exist and these are represented by a standard deviation error percentage.

The manual assembly of large comprehensive hydrocarbon mechanisms is a laborious process which is prone to human error. Automatic procedures are advantageous and would bring a more organized structure to the generated mechanisms. Such methods draw on the lessons learned from the manual constructions, whereby the rules are converted into computer based algorithms using programming languages and techniques. Modifications can be made to the

procedure to create alternative mechanistic structures should our knowledge of the kinetic processes change [15].

A mechanism generation program usually consists of the following parts:

1. A list of species including the primary reactant “parent” species plus oxygen, intermediates and product species (the length of the list increases as reaction generation proceeds). The structures of the species are stored on file in a form which can be easily manipulated by the employed reaction generator. The symbolic representations of the species should be unique and non-ambiguous so that errors are not perpetrated by the reaction generator. They should also imply the correct chemical structure so that kinetic interpretations may be made in a user friendly way.

2. The reaction generator must consider all combinations of species but in order to avoid a massive encumbering mechanism, it should be able to identify those reactions which are most likely to occur using expert chemical knowledge.

3. Experimentally determined kinetic parameters for the generated mechanisms should be searched for in an associated database. For those reactions where no experimental or *ab initio* modeling values have been obtained, the program should include a subroutine to numerically determine them based on the size and structure of the reacting species using Benson additivity rules [84].

4. Reactions which are obviously unimportant should be filtered out at the generation stage, such as those which are highly endothermic and those which proceed at a very slow rate for the temperature and pressure ranges of interest.

Chinnick *et al* [88] appear to have been the first (in 1988) group to develop an expert system for mechanism generation based on logical programming. The POPLOG programming language was used to derive a procedure for the automatic generation of alkane pyrolysis mechanisms. Ten classes of elementary reactions were defined for alkane pyrolysis, and the mechanism generation proceeded according to the following conditions; all combinations of species and all possible reaction types for those combinations were considered, duplication of elementary reactions was prevented and ‘unlikely’ reactions were excluded, based on prescribed rules [57].

A similar approach was used by Côme *et al* [89] and after many years of work the evolution of methods led to the creation of EXGAS [19-21,90-95] – regarded as the leading software for the generation of comprehensive hydrocarbon oxidation mechanisms. The software is written in FORTRAN and is linked to the associated software of KINGAS [96] and THERGAS [87], which are used to calculate kinetic parameters and thermochemical data, respectively [21]. Mechanistic structures produced by EXGAS, for a range of normal alkanes up to n-decane, are well recognized by trained combustion chemists. Comprehensive mechanisms can also be automatically generated for the classes of compounds of branched alkanes, alkenes, cyclic alkanes and aromatic compounds. The reaction mechanisms generated are made up of three parts:

- (i) A C₀ – C₂ reaction base including all the unimolecular or bimolecular reactions involving all radicals or molecules containing up to two carbon atoms [80]. This is needed because there are no generic rules in existence for the derivation of reactions of these species [21].
- (ii) A comprehensive primary mechanism, where only the initial organic molecule or the organic molecules contained in the initial mixture and oxygen are considered as reactants.
- (iii) A lumped secondary mechanism to reproduce the consumption of the molecular products formed by the primary mechanism [90].

CHEMKIN compatible mechanisms are produced with atom balanced reactions. EXGAS is interactive in that, the freedom to choose some of the classes of reaction which appear in the primary mechanism is given to the user, i.e., those relevant to the conditions of interest. The reactant and primary radicals may be subjected to the following elementary steps;

- unimolecular initiations involving the breaking of a C–C bond,
- bimolecular initiations with oxygen to produce alkyl and HO₂ radicals,
- oxidations of alkyl radicals with O₂ to form alkenes and HO₂ radicals,
- additions of alkyl (R•) and hydroperoxyalkyl (•QOOH) radicals to an oxygen molecule,

- isomerizations of alkyl and peroxy radicals (ROO• and •OOQOOH) involving a cyclic transition state; for •OOQOOH radicals, a direct isomerization-decomposition to give ketohydroperoxides and hydroxyl radicals is considered,
- decompositions of radicals by β -scission involving the breaking of C–C or C–O bonds for all types of radicals (for low-temperature modeling, the breaking of C–H bonds is neglected),
- decompositions of hydroperoxyalkyl radicals to form cyclic ethers and OH radicals,
- metatheses involving H abstractions by radicals from the initial reactants,
- recombinations of radicals,
- disproportionations of peroxyalkyl radicals with HO₂ to produce hydroperoxides and O₂ (disproportionations between two peroxyalkyl radicals or between peroxyalkyl and alkyl radicals are not taken into account) [97].

Certain classes may have a negligible influence on the overall reaction in a given range of operating conditions. For example, below 650 K, beta-scissions are negligible, above 850 K, additions of hydroperoxyalkyl radicals to molecular oxygen are negligible compared to the formation of cyclic ethers. Above 1000 K, oxidations and any additions to oxygen are negligible compared to beta-scissions. In this way, *a priori* reductions can be made depending on the temperature range of study. Alternatively, the user could specify a low or high temperature mechanism using the EXGAS default options. A low temperature mechanism would comprise all of the above classes of reactions (except C-H β -scissions), but some classes of radicals would not be subjected to certain classes of elementary steps. A limitation to the cycle size of isomerizations would also be enforced. Selecting the default low (or high) temperature mechanism would automatically activate the generation of all possible classes of reactions in the secondary mechanisms. For further details, the reader is referred to the EXGAS user's manual [98].

Having constructed a comprehensive mechanism, by manual construction or computer based algorithm, it is essential to compare the output obtained from its integration to experimental data. Validation requires a second class of experiments and is usually conducted by several research groups. It is important to compare the mechanisms to many experiments at different process conditions to ensure they are robust. Spontaneous ignition processes are investigated in a number of apparatus such as unstirred closed vessels, the continuous-flow stirred tank reactor (CSTR), the laminar flow tube and the rapid compression machine (RCM). A review of these techniques is given by Griffiths and Mohamed [99]. The shock tube [100,101] is another method which uses high pressure inert gases to compress rapidly a reactive gaseous mixture, as opposed to the purely mechanical compression used in the RCM. The shock tube and RCM can be used to measure spontaneous ignition delay time of a given fuel/oxidizer mixture. This quantitative comparison is important with regards to mechanism validation, especially if the mechanism is to be used for engine research and development. In all these methods, it is possible to make chemical analyses during the reaction, but it should be remembered that the transient chemical composition will be heavily affected by temporal and spatial temperature variations. Supplementary thermal data is therefore required for a fully quantitative comparison to be made by the numerical modeler [57]. A further experimental/numerical comparison may be made via the ignition diagram (see Chapter 4 for more information) of a given fuel/oxidizer mixture, showing regions of cool flames, ignition, slow reaction etc. This comparison is especially important in the context of industrial explosion hazard prevention, with both qualitative and quantitative appraisals potentially being made.

The achievements in the field of hydrocarbon oxidation mechanism construction have led to detailed reaction mechanisms, whose accuracy is continuously improving. However, the requirement to incorporate large detailed kinetics into models of reactive three-dimensional flows to simulate scenarios inside industrial units and engines cannot be fulfilled at present or for the foreseeable future unless the computational burden of the kinetics can be reduced

without the loss of its descriptive value. Relevant formal mathematical techniques currently available to perform mechanism reduction are covered next.

2.2 Reduction Methodologies

As outlined in Chapter 1 and the preface to this Chapter, two major categories of reduction methodology exist, they are skeletal and time-scale based reductions. These are reviewed in the following subsections and most recent developments and achievements are reported. Several reviews on mechanism reduction have been published previously, giving further details on the subdivisions of methods. A review by Griffiths [57] focuses on reduced global mechanisms for the description of low temperature combustion. An in-depth discussion on a wide range of the techniques developed until 1997 is given by Tomlin *et al* [15]. A briefer review on lumping, sensitivity and time-scale based techniques is given by Okino and Mavrouvouniotis [102]. Reviews on the development of sensitivity analysis are given by Rabitz (1983) [34] and Turányi (1990) [103]. The review by Rabitz focuses mainly on local methods. An almost complete account of local and global methods developed before 1989 is given in the review of Turanyi. A more recent review of local methods is given in [104] and recent developments in sensitivity analysis are covered by Saltelli *et al* [105], who emphasize the highly related field of uncertainty analysis.

2.2.1 Skeletal Reduction

The first methods to be discussed are those which may be grouped as sensitivity analysis [27,30,34-36,103-105]. Many aspects of mathematical modelling use sensitivity analysis to find relationships between input and output variables and hence identify important system parameters. In the context of combustion kinetics, input variables or parameters are perturbed which are most commonly species concentrations and rate coefficients. Two distinctions of sensitivity analysis methods may be made. Local methods refer to small changes

of parameters close to their nominal values, while global methods refer to the effect of simultaneous, possibly orders-of-magnitude changes [103]. Computational tools for the application of sensitivity analysis to chemical systems have been available since the late 1980s. KINAL (a program package for KINetic AnaLysis of reactions mechanisms) [28,29] is one such software and includes subroutines for the detection of redundant species in mechanisms, principal component analysis of sensitivity matrices, rate-of-production analysis and the calculation of species lifetimes. An updated version called KINALC [30,31] was developed in the mid 1990s and is based on many of the same principles as KINAL. Sensitivity applications are set up with a user friendly interface and the program is a postprocessor of CHEMKIN-II [86]. Both KINAL and KINALC are available from the World Wide Web [29,31].

The methods employed by KINALC to identify which species may be removed from the mechanism rely on the iterative analysis of the Jacobian matrix (see Section 5.2 for further details) using algorithms that principally investigate the effect of perturbations in the concentration of each species on rates of production of important species. Thresholds are applied to the magnitudes of the sensitivity measures denoting the importance of each species in order to find a smaller subset which can give accurate output predictions relative to those produced using the full scheme. As the species are removed there will inevitably be some incurred error to output produced on integration of the reduced mechanism, so the objective is to obtain the best trade-off between reduction and accurate reproduction of the full mechanism's predictions. No information can be deduced as a guide to which thresholds will produce the most appropriate reduced mechanism prior to their application, Therefore, a trial and error approach is necessary with *a posteriori* determinations being made from the output of mechanisms of a range of sizes produced with varying thresholds. A similar approach is used to find a reduced subset of reactions by examining the effect of perturbations in the rate parameters on the rates of production of species; this is called overall rate sensitivity analysis (see Section 5.3 for further details).

Principal component analysis (PCA) [106] is a sophisticated method of identifying reactions for removal and has its foundations in sensitivity analysis. The sensitivities of each species concentration or rate of production to each reaction rate coefficient can be represented as a rate sensitivity matrix. The PCA analysis is based on an eigenvalue-eigenvector decomposition of the cross product of this matrix. The variables in the mechanism are hence changed into ‘principal components’ and we are able to study which parameters are most associated with the dominating eigenvectors. Each entry in the eigenvector represents a reaction and the magnitude of the eigenvector’s corresponding eigenvalue signifies the importance of that eigenvector. Thresholds are applied to the magnitudes of the eigenvalues and eigenvectors to find the reduced subset of reactions in the same manner for which it is performed for the other sensitivity type measures. The drawback of local sensitivity analysis methods is that in order to capture all aspects of the chemistry in the resulting reduced mechanism, the techniques must be applied to a range of time points and operating conditions. Very few attempts have been made to fully automate this process.

Sensitivity analysis reduction methods have proven successful on many occasions and are adaptable to different types of kinetic application. Turányi [27] was able to reduce a reaction mechanism for propane pyrolysis from 36 species and 98 reactions to 13 species and 38 reactions using the iterative analysis of the Jacobian and PCA which speeded up the simulation by ten times. The same techniques were applied to reduce another scheme for propane pyrolysis by Tomlin *et al* [52]. The comprehensive mechanism comprised 48 species in 422 reactions. After application of the techniques these numbers were reduced to 19 species and 122 reactions. Another study by Huang *et al* [107] used these techniques and involved the reduction of a comprehensive scheme used to simulate the generation of higher hydrocarbons during the isothermal oxidation of fuel rich methane/oxygen mixtures, comprising 155 species and 1376 reactions. The combination of Jacobian and principal component analyses resulted in the numbers of reactions being reduced to 236 reactions. The final skeletal reduction

to 75 species and 218 reactions was achieved by rate of production analysis (see Section 5.5).

Alternative approaches to the generation of skeleton mechanisms from comprehensive schemes are graph based methods. Law and co workers [37-40] have published the greatest number of articles on this reduction subcategory. The theory of Directed Relation Graph (DRG) examines the species couplings in the mechanism using rate of production analysis ratios. Analysis of the combustion mechanisms shows that groups of strongly coupled species exist due to the effect of reactions on the concentrations of species. A pair of species need not occur simultaneously in any reactions in order to be strongly coupled, as a high degree of coupling can be present through intermediates. The method proceeds by selecting a “starting set” of species which is likely to be fuel, oxidiser and any immediately produced radicals. If there is interest to accurately model the concentration of any other by-products, then these may also be included in the starting set. The degree of coupling of each species to the starting set species is quantified by a “normalised contribution” and a variety of thresholds are applied to this measure in order to find an appropriate subset of species. The existence of groups of strongly coupled species is such that if one species is removed, it becomes necessary to remove its associated group of strongly coupled species and conversely if it is desired to retain a specific species, so too must be its associated group. By consequence, sharp jumps in species numbers are witnessed when thresholds to the normalised contribution are varied. In common with local sensitivity techniques, information from simulations covering a wide parameter space is sampled in order to ensure the robustness of the resulting reduced mechanisms. Further studies conducted using DRG [40] have found that for very large kinetic mechanisms a two-stage species reduction strategy is judicious. Here, a species reduced mechanism is produced with many redundant species removed and the algorithmic procedure is repeated on the species reduced mechanism with different thresholds to remove yet more species. After the identification of the reduced subset of species, the authors of DRG often remove a proportion of unimportant reactions which still remain in the reduced mechanism but contain

the species of the reduced subset using a CSP importance index [108,109]. Applications of the DRG method have been successful on a number of occasions. A mechanism describing the autoignition of ethene in a perfectly stirred reactor was successfully reduced from 70 species and 463 reactions to 33 species and 205 reactions with little error incurred to the output of the reduced mechanism [38]. Other reductions include those for the fuels of iso-octane and n-heptane using the same application as that used for ethene [40]. The iso-octane mechanism was reduced from 857 species and 3606 reactions to 233 species and 959 reactions. The n-heptane mechanism comprising 561 species and 2539 reactions was reduced to 233 species and after reaction removal using the CSP importance index the number of reactions was reduced to 959.

Another graph based method is Detailed Reduction (DR) [110] which provides a way of removing reactions by comparing their rates to a preselected reference reaction rate. Those reactions having a very low rate in comparison to the reference rate may be discarded. This approach has been criticised for a number of reasons: Slow reactions are not necessarily always redundant especially if the products are vital intermediates. The identification of the reference reaction rate is not straightforward, especially for very large mechanisms because it is difficult to identify the overall controlling process which will often change with differing conditions [39]. Furthermore, no attempt is made to identify the most important species prior to reaction removal. As a result redundant species will remain in the mechanism and these will have a greater impact than reactions on the time to solution.

Optimization based methods can be used for mechanism reduction and are often combined with an “adaptive chemistry” approach. Green and co workers [41-43] have published a number of papers on this strategy. Adaptive chemistry aims to use a selection of highly reduced mechanisms which are applicable to a narrow parameter range. During the simulation of a temperature trajectory or flame, for example, the most appropriate and smallest sub-model is either selected from a library of previously reduced mechanisms or suitable reduced mechanisms are constructed ‘on the fly’. However, a disadvantage of this is that the

'switching' process can slow down the calculation. The model reduction and validation has been performed by inspection [41] although a more mathematically rigorous automated approach of finding the library of reduced models is advantageous. Integer programming [43] is employed to minimize the number of reactions in a model subject to some constraint, which aims to ensure satisfactory agreement between the full and reduced mechanisms. Of the optimization methods that exist, a general linear integer programming formulation was found to be most computationally viable and suitable for the generation of reduced mechanisms. Linearity is achieved by eliminating the ODE and nonlinearities in the constraint formulation and replacing with a set of algebraic point constraints. The degree of optimality of the achieved solutions is limited by the choice of linear integer problem solver technology. The methods have been applied to generate a series of reduced mechanisms to model a 2-D partially premixed laminar methane burner flame, from a 217 reactions comprehensive mechanism. A library of 657 mechanisms was produced ranging in size from 10 to 126 reactions and with an average size of 55 reactions. Implementation of the approach resulted in computational solutions being obtained 3 times faster than those using only the full mechanism [41]. Supplementary software called RIOT (Range Identification and Optimization Tool) [42] has been set up to identify the parametric ranges of applicability of each of the reduced models in the library. This is of practical importance for incorporating the reduced models into higher dimensional simulations using the adaptive approach. The techniques were applied to a comprehensive model describing the combustion of propane and comprised of 94 species and 505 reactions. The use of the adaptive chemistry/optimization based approach in conjunction with RIOT, allowed the accurate simulation of a 1-D freely propagating laminar flame under stoichiometric conditions using a library of 18 reduced models of size $\sim 30 - 475$ reactions with an average size of ~ 304 reactions.

The linear programming optimization based approach to reduction has an advantage in that the desired level of accuracy of the reduced mechanism can be assigned prior to the reduction. The optimization method should, in theory, find

the mechanism with the smallest number of reactions which satisfies an enforced agreement between the instantaneous fluxes, thus circumventing the need to make *a posteriori* validations of a number of reduced mechanisms generated using a range of thresholds [111]. However, the drawback of the methods of Bhattacharjee *et al* is that no attempt to find a reduced subset of species is made prior to reaction removal. The reduced mechanisms are not truly optimal and the opportunity to make the greatest computational savings is lost.

A different optimization reduction approach is made by Banerjee and Ierapetritou [44,45] and is also used in conjunction with an adaptive chemistry approach. Genetic algorithms (GA) were used as the solution procedure for the mechanism reduction. GA can be applied to optimization problems in which candidate solutions are represented by optimization binary variables forming a string of bits which are appended together to form a population of “chromosomes”. This population evolves towards better solutions until no further improvements can be made. In the reduction problem, the optimization variables are binary variables associated with the reactions (1 if the reaction is included in a reduced mechanism and 0 if it is not), each binary then becomes a bit in the chromosome. The GA approach is initialized by the generation of a random set of population binary strings (reaction combinations), where each member of the population represents a reduced mechanism. Evaluation of the errors associated with each of these randomly generated reduced mechanisms is assessed by their simulation which leads to a “fitness function” (a measure of the quality of the solutions). The fitness function is used by the GA operators (reproduction, crossover, mutation) to create the next generation of better populations. The procedure is repeated until a predefined termination criterion is satisfied with the end solution depending heavily on this. A mechanism comprising 14 species and 47 reactions describing the combustion of CO/H₂ in air was successfully reduced to 11 species and 26 reactions using this method and further achievements have been made in an adaptive chemistry framework [44]. The GA method has also been extended to identify species which can be eliminated from a given mechanism [33]. From a comprehensive scheme of 53 species and 325 reactions

for methane combustion a library of 12 reduced schemes ranging in size from 6 to 29 species. The reduced library was used in adaptive chemistry approach to model methane combustion in a pairwise mixed stirred reactor flow model. 78 % of the conditions encountered by the flow simulation were covered by the library of reduced mechanisms; for the remaining 22 %, none of the reduced mechanisms were found to be appropriate so the full mechanism was integrated at these conditions.

A similar use of GA for species reduction has been carried out by Elliot *et al* [112]. A comprehensive mechanism for methane combustion comprising 53 species and 325 reactions was reduced to three mechanisms of varying size and quality, consisting of 12, 16, and 20 species. The reduced mechanisms were used to model a methane burner stabilized flame. In another study by the same authors [113], the reduction of a comprehensive mechanism for surrogate aviation fuel-air combustion comprising 67 species and 338 reactions was carried out. The resulting reduced mechanism consisted of 50 species and 215 reactions. The authors claim this corresponded to a 90 % CPU time saving in each function evaluation.

Another optimization based approach is made by Petzold and Zhu [114]. Prior to the application of an integer programming method to reduce the numbers of reactions in a mechanism, a ‘greedy’ scanning method is applied to first remove species and then reactions. In the greedy method the species or reactions are deleted one by one and the errors associated with each deletion are assessed by integration. By applying an appropriate threshold to the error values, the numbers of species and/or reactions can be successfully reduced. The ensemble of techniques has been applied to reduce a mechanism with 116 species and 447 reactions describing methane combustion under the case of a mixture at the lean flammability limit. A single reduction condition was used for the techniques which yielded a reduced mechanism of 31 species and 42 reactions.

Solutions obtained by optimization approaches, such as integer programming depend strictly on the selection of constraints, which is frequently quite complicated. As a consequence, the computational cost of such approaches is

usually much greater than that of sensitivity analysis type approaches or DRG [40]. For these reasons, sensitivity analysis based approaches, which are known to be reliable, will be augmented and applied in Chapter 5 for skeletal reduction.

2.2.2 Time-scale based reductions

Post application of skeletal reduction strategies, further reduction progress can be made via the application of time-scale based methods. The first and oldest of these is the QSSA. After the advent of stiff ODE solvers in the 1970s, interest in the QSSA dwindled with many condemning it as obsolete. More recently, the QSSA has received a resurgence of interest in the field of mechanism reduction for its ability to reduce the number of ODEs and stiffness in a given mechanism. The approximation sets the net rate of production of a selected species to zero, allowing the concentration to be defined algebraically in terms of the other present species. Methods for solving the ODE/algebraic combination of equations such as inner iteration have been proposed [115]. Turanyi *et al* [63] have developed methods for selecting candidate QSS species (see Section 7.1) by calculating the instantaneous error of the QSSA. This is defined as the difference in the QSS species concentration with and without the application of the QSSA at the time of the application [52]. This measure can be applied to groups of species in unison or to single species, with the latter being the most practically viable. Species with small lifetimes are often designated as QSS species so this property may also be worth investigating. The species lifetime and instantaneous QSSA error are related but the latter has an advantage in that it can identify species with negligible rates of concentration change which may also be amenable to the application.

QSSA reductions can also be applied in an adaptive chemistry framework, as has been conducted by Løvås *et al* [116], for calculations of a natural gas fueled engine, operating under homogenous charge compression ignition (HCCI). A comprehensive mechanism comprising 53 species and 589 reactions was first reduced to a skeleton scheme based on atomic flux considerations, and comprised

43 species interacting in 481 reactions. In a pre-processing stage, a core of steady-state species which are not expected to vary during the adaptive kinetic process, were identified using a combined species lifetime and species sensitivity parameter as a selection criterion. Using a simpler lifetime analysis, online reductions were performed to identify those species which move in and out of steady state during the engine cycle. The skeleton mechanism was reduced down to 14 species in some scenarios. These methods have been extended to flame calculations (ethene) [117], whereby the online reductions were replaced by a domain splitting pre-processing stage to identify zones (or domains) with negligible chemistry changes. The domains are identified in mixture fraction space, which represent the physical zones of a flame. Species can be defined as steady state species with respect to domains instead of the entire range, resulting in a greater degree of reduction.

Another time-scale reduction technique put forward by Lam and Goussis is called computational singular perturbation analysis (CSP) [46] and is related to the QSSA. It can be used to categorise the various timescales within kinetic systems and therefore identify the fastest species which can be decoupled from the system. The method works by transforming the species in the original mechanism into variables with less direct kinetic meaning, but more directly associated with the system time-scales. The transformed variables can then be rearranged into an ordered series of vectors which represent ranked reaction groups with associated timescales of a certain magnitude. These reaction groups are known as modes. As the rates of the reactions in the modes approach zero and become exhausted, user selected thresholds are used to determine which of the modes can be categorised as ‘dead modes’, i.e. not contributing to the overall system behaviour. Information related to the dead modes can then be retransformed to a system with physical meaning in order to identify species or variables which can be eliminated or approximated using QSSA type techniques. CSP can produce reduced mechanisms consisting of a small number of global steps. However the number of species in the mechanism is often more than the number of steps and the global reaction rates involve major species and steady-state species (absent in the global

steps), which are calculated from differential and steady-state algebraic relations using an inner iteration procedure. The use of such coupled iteration techniques can in some cases add significantly to the computational burden. Using CSP, successful reductions have been undertaken on mechanisms for a methane/air flame system [108], and for that of methane combustion under mixed air-steam turbine conditions [118], both studies produced similar seven-step global reduced mechanisms. CSP has also been successfully applied to detailed mechanisms for atmospheric applications [119,120].

QSSA applications have also been developed by Lu *et al* [109] and are based on a CSP analysis of characteristic time-scales of the system to determine the quasi-steady-state species. Here, the CSP methodology also offers skeletal reduction: The CSP importance index is based on an analysis of the stoichiometric coefficient matrix and the rate vector of elementary reactions. The importance index indicates the normalised contribution of a reaction to the reaction rate of a species and user-specified thresholds applied to this value provides a way of producing the skeleton mechanisms and the global CSP reduction will follow. Alternatively, the two steps can be performed simultaneously. QSS species valid for a wide range of conditions are found by sampling data from various temperatures, pressures and equivalence ratios in a perfectly stirred reactor (PSR). Having identified the QSS species and their fast elementary reactions, algebraic procedures in matrix form are used to generate the minimum set of linearly independent global reactions and to evaluate the global reaction rates. Mechanisms for H₂/air and CH₄/air flames with 4 and 10 steps were generated, respectively. Law [38] used the same approach to reduce the skeletal mechanism describing the autoignition of ethene in a PSR consisting of 33 species and 205 reactions to 21 species and 16 lumped reactions. A discussion of the effect of QSS species on DRG applications is given in [121]. Provided that reactions are reversible and backward rates are computed from the equilibrium constant, then no impingement by the QSS species on the effectiveness of the DRG application is made. Further developments have been made by Lu and Law [122] on the type of solution methods for the mixed set of ODE and non-linear algebraic equations.

Inner iterative methods often need to run many calculations to arrive at a solution and sometimes may not converge resulting in failure [122]. This hampers the overall usefulness of the QSSA application. Graph theory based methods have been developed to significantly improve the efficiency of the solutions. If a system consists of coupled QSS species the algebraic equations are generally non-linear. However, they can be simplified on the premise that QSS species are typically in low concentration, in turn, the probability of a collision between two QSS species is low and can be disregarded. Eliminating reactions with two or more QSS species as reactants leads to a great reduction in the non-linear terms such that a linear approximation of the equations is likely to exist. The solution of the 16 lumped reactions mechanism with this approach has been achieved. Removing the QSSA species would be more computationally efficient and this will be the focus of the QSSA application presented in Chapter 7.

Intrinsic low dimensional manifold (ILDm) methods [49] rely on the same premise as CSP, in that reaction groups with a variety of time scales are separated into groups in order to decouple or eliminate the fast timescales, and thus reduce the dimensionality of the system. The fast timescales, which we wish to decouple, may occur on a scale as small as 10^{-10} s, and are therefore negligible in comparison to the duration of an ignition. In CFD applications it is the relative time-scales to the physical processes that is important. As the reaction proceeds, each of the fast “modes” collapses and reaction trajectories eventually decay to an attractor trajectory in the concentration phase space, from a number of varying initial conditions. The attractor is itself, located in what is called a slow or inertial manifold of lower dimension than the full number of system variables. The manifold describes the long-time behaviour of the system, and therefore if the system dynamics can be described on this manifold, a very much reduced model can be developed. The reduced model is usually developed in either tabulated or fitted form [54,55,107,108] and therefore has to be redeveloped when any improvements in the starting mechanism are made. However, the ILDM technique has been shown to substantially reduce computational cost when applied to methane autoignition in turbulent combustion calculations [125].

An alternative way to reduce the computational cost of CFD with incorporated chemical kinetics is by using a repro-model [50] to describe the chemical changes. A repro-model is an alternative mathematical description of a larger, more computationally intensive mathematical model and utilises functions and algebraic equations to do this. In combustion modelling, the functions of a repro-model describing a chemical mechanism can, for example, take the form of a set of high order polynomials, which represent functional relationships between selected variables of concentration or temperature over chosen time steps [50,53,54]. Before a repro-model is fitted, the influential variables that will be used to describe the low dimensional model must be selected. These can be found by using ideas related to the ILDM technique described above. Time-scale based methods can be used to identify the minimum number of variables required to describe the system on the slow manifold [126,127]. Key variables are then chosen in order to parameterise the manifold and the fitted model is developed for these variables using simulations of the full model. The term “repro-model” now becomes clear since the reduced model is nothing other than a “reproduction” of the behaviour of the full model over the chosen simulation conditions. The accuracy of the repro-model therefore depends on the range of conditions chosen for the fitting, and the accuracy of the fitting procedure. A range of fitting techniques have been utilised including high order polynomials [50], second order polynomials [124], neural networks [123] and tabulation/interpolation methods [55]. Look-up tables, in which key variables are tabulated can be constructed and then searched to obtain an interpolated estimate for the output, in contrast to evaluating a function. The *in situ* adaptive tabulation (ISAT) method of Pope [55] has been used extensively for the inclusion of chemical kinetic effects in transported probability density functions. The PRISM method (Piecewise Reusable Implementation of Solution Mapping) [124] is a hybrid of the look-up table and the polynomial fitting technique. The method uses low order (2nd order) polynomials. Both ISAT and PRISM approaches are applied in an operator splitting framework and generate the tabulation or functional fit as the calculation

proceeds. These may be stored and retrieved for future use should it be required again.

At present the application of these techniques is relatively new. It has not therefore become clear which of these methods is best suited to which types of applications. However, incorporating a repro-model into a CFD code is a viable option, because of the method of operator-splitting, whereby the physics and the chemistry are calculated separately and therefore the method of calculating the chemical changes due to reaction are unimportant to the transport phenomena calculations. A repro-model has been successfully fitted to a tropospheric chemical model and resulting in speedups of the order of a factor of 25 with errors less than 1% when compared to numerical solutions obtained from the original mechanism [54]. Simulations of the combustion of wet CO have been undertaken using a high-order polynomial, three variable repro-model [50]. The repro-model was able to achieve solution 11,700 times faster than the full.

A further method of reduction is species lumping, where two or more species are grouped together thus reducing the number of ordinary differential equations required to describe the kinetics. One of the simplest types is chemical lumping, where chemical intuition of reaction rates, mechanism and species structure is utilised. It is often possible to lump isomers using this technique. Other lumping methods, using more formal mathematical procedures, require new lumped variables which are related to the original variables by a 'lumping function' and this can be either linear or non-linear. Linear lumping is relatively straightforward and can be done in an automatic way. The new variables are often linear combinations of the original ones. The simplest case here would be that the concentration of the new lumped variable is just the summation of the concentrations of its component species. The main drawback of linear lumping is that combustion systems are highly non-linear, so a linear representation for complete reaction over all conditions can be inaccurate. A potential solution to this problem is by using the 'adaptive chemistry' approach, where a number of small linear lumped schemes are produced for different narrow ranges of operating conditions. These are stored on file and switched as input when the

conditions to which they pertain are encountered [15]. The more mathematically rigorous method of non-linear lumping can potentially solve these problems, though the complexity of the required analysis can hinder its use [51,128,129]. Non-linear lumping incorporating timescale separation techniques such as ILDM or CSP, can give insight into similar fast or slow variables which can be lumped and is a sophisticated reduction technique, applied in [130] to atmospheric chemistry [15]. Huang *et al* [107] have extended these ideas with application to a combustion system. The dimension reduction of a system describing the isothermal oxidation of fuel rich methane mixtures in a closed vessel, from 155 to 53 was achieved with little impact upon its accuracy relative to the comprehensive mechanism.

Reduction techniques specific to the present application are further discussed in Chapters 5 and 7 of this Thesis. Automated software for reduction to skeleton mechanisms is described and illustrated with respect to comprehensive mechanisms for propane, butane and cyclohexane in Chapter 5. The QSSA combined with reaction lumping is then applied to the cyclohexane skeleton mechanism in Chapter 7. The next Chapter focuses on established numerical techniques and software utilized in the present context.

Chapter 3

General Methods

The purpose of this Chapter is to outline all the basic equations, numerical methods and established techniques, which are necessary in the current work. The techniques presented do not have the direct objective of reducing a chemical mechanism, but are necessary to achieve this aim. Primarily, the essential step of numerical simulation using the information contained in a given mechanism will be covered. A CHEMKIN format mechanism will usually consist of a list of chemical elements, a list of chemical species, NASA polynomial coefficients for each species (from which temperature dependent thermodynamic properties are calculated) and a list of elementary reactions and associated Arrhenius parameters.

The use of the SPRINT integrator [48] for solving the system of ordinary differential equations and the substitution of these with algebraic equations will be covered. The derivation of reaction rate equations using Arrhenius parameters and the calculation of standard thermodynamic properties will also be described. These will allow the dynamics of individual species concentrations and non-isothermal time-dependant behaviour to be precisely modelled. The more complex rate expressions for fall-off reactions will be defined. These display a pressure dependency and are unable to be successfully represented by the standard Arrhenius expression.

Further discussion will focus on the use of the software packages CHEMKIN II [86] and MECHMOD [131]. The first of these is an openly available package

used for the efficient calculation of chemical kinetic mechanisms in standard modelling situations and is able to interface with a number of supplementary modules and post-processors, one of these being MECHMOD. This software is used for the manipulation of the data contained in a mechanisms rather than their simulation, and allows the kineticist to automatically perform a number of otherwise arduous tasks such as converting units, removing species and converting reversible reactions to irreversible form. All of these programs operate upon a LINUX platform.

3.1 Physicochemical principles

Fundamentals of chemical thermodynamics and reaction kinetics are presented in this Section, with emphasis on the specific equations calculated by the SPRINT integrator adapted to read in data from the CHEMKIN format mechanisms. The chemical mechanisms that we wish to simulate can contain reactions in either reversible, irreversible, or a combination of these forms. Comprehensive mechanisms often contain reversible reactions when they are distributed, and because reverse rate constants must be calculated from the thermodynamic properties via the equilibrium constant, it is logical to begin with a discussion of thermodynamic principles.

3.1.1 Thermochemistry

Thermodynamic data is used in the calculation of equilibrium constants and heat release rates of elementary steps, with the magnitudes of non-isothermal behaviour being affected by these values. Thermodynamic properties are calculated from 14 NASA polynomial coefficients [132-134] for each species, seven for the low temperature range (300-1000 K) and seven for the high temperature range (1000-5000 K). The polynomial coefficients can be evaluated at a given temperature (T) to obtain specific heat capacity (C_p°), enthalpy (H°) and entropy (S°), as follows;

$$\frac{C_p^o}{R} = a_1 + a_2T + a_3T^2 + a_4T^3 + a_5T^4 \quad (3.1)$$

$$\frac{H^o}{RT} = a_1 + \frac{a_2}{2}T + \frac{a_3}{3}T^2 + \frac{a_4}{4}T^3 + \frac{a_5}{5}T^4 + \frac{a_6}{T} \quad (3.2)$$

$$\frac{S^o}{R} = a_1 \ln T + a_2T + \frac{a_3}{2}T^2 + \frac{a_4}{3}T^3 + \frac{a_5}{4}T^4 + a_7, \quad (3.3)$$

Where a_n is a NASA polynomial coefficient [132-134] and R is the universal gas constant. The change of enthalpy (ΔH_j^o) and entropy (ΔS_j^o), that occurs in passing completely from reactants to products in j th reaction must also be defined;

$$\frac{\Delta S_j^o}{R} = \sum_{i=1}^I v_{ij} \frac{S_i^o}{R} \quad (3.4)$$

$$\frac{\Delta H_j^o}{RT} = \sum_{i=1}^I v_{ij} \frac{H_i^o}{RT} \quad (3.5)$$

The magnitude of heat release will depend also on the reaction rates as will be discussed, which in turn are also dependent on temperature. The temperature will depend on ambient conditions, heat release rate, heat capacity of the mixture as well as heat transfer effects. The output variables of the model are highly interrelated and the combination is thus a ‘thermokinetic model’ where chemical reaction rates and enthalpy change are computed simultaneously [57].

3.1.2 Elementary chemical reaction rate equations

The rate of change of concentration of species involved in a chemical reaction can be quantitatively described by a ‘rate law’, in terms of the product of concentration terms and a temperature dependent rate constant (or coefficient). In the present context, such descriptions refer to the multitude of elementary reactions which make up a kinetic mechanism, but also may refer to global

reaction steps. The stoichiometric description of a chemical reaction may be represented by the simple generic form;



where v_i , the stoichiometric coefficients, are normally integer values for elementary reactions. The rate law with respect to the four components takes the form;

$$\frac{-1}{v_a} \frac{d[A]}{dt} = \frac{-1}{v_b} \frac{d[B]}{dt} = \frac{1}{v_p} \frac{d[P]}{dt} = \frac{1}{v_q} \frac{d[Q]}{dt} = k_f [A]^a [B]^b \quad (3.7)$$

where k is the rate coefficient and $[\]$ represents concentration. The orders of the reaction for reactants A and B are represented by the powers a and b , respectively, and the overall order is given by $(a + b)$ [2]. The orders of reaction with respect to a reactant quantify the dependence of reaction rate on concentration. It is an experimentally determined parameter. However, for elementary reactions, the order with respect to each species is usually equal to the stoichiometric coefficient for that species, although this is usually not the case for global reactions (bimolecular reactions are the principal exception). The rate coefficient (k_f), for temperature dependent reactions, is most commonly defined by the Arrhenius equation as

$$k_f = AT^n e^{-E/RT} \quad (3.8)$$

where A (the pre-exponential factor), n (a dimensionless exponent of temperature) and E (activation energy) are the three Arrhenius rate parameters expressed in a mechanism after each stoichiometric equation on the same line. Equation 3.8 denotes the rate parameter of irreversible reactions, which are indicated in the mechanism by the signature ‘=>’ in the stoichiometric equations. Reversible reactions are defined by ‘=’ in the stoichiometric equation and the forward rate is

calculated by equation 3.8. The reverse rate (k_r) must be calculated through the equilibrium constant in concentration units (K_c), as follows;

$$k_r = \frac{k_f}{K_c} \quad (3.9)$$

The equilibrium constant is more easily calculated from the thermodynamic properties in terms of pressure for each reaction. K_c is related to the equilibrium constant in pressure units (K_p) by the following expression;

$$K_p = K_c (RT)^{\Delta v} \quad (3.10)$$

where Δv is the sum of stoichiometric coefficients products minus those of reactants i.e. $(v_p + v_q + \dots) - (v_a + v_b + \dots)$. K_p is obtained with

$$K_p = \exp\left(\frac{\Delta S^\circ}{R} - \frac{\Delta H^\circ}{RT}\right). \quad (3.11)$$

3.1.3 Third body and fall-off reactions

Extensive analysis of combustion systems has found that not all reactions have a rate parameter which may be fitted via the basic Arrhenius definition of equation 3.8, so further elaborations are necessary to enable the satisfactory fitting of data. Third body reactions show a concentration dependence on species which do not participate in the chemical interactions of a reaction, but are necessary for it to proceed. For example, the reaction



obeys third-order kinetics, and has a rate that is defined as

$$\text{rate} = k[\text{H}][\text{O}][\text{M}] . \quad (3.13)$$

The symbol M is used to denote any molecule present in the system and is known as a third body species. [M] can represent the total concentration of molecular species present in the system, or a weighted total concentration called enhanced third-body efficiencies. From (3.12) and (3.13), it can be seen that M is not consumed in the reaction but affects the rate at which the reaction proceeds. The third body is required to absorb some of the energy released by the reaction, through the molecular collisions [2]. The rate is calculated in a similar way to an ordinary elementary reaction although the inclusion of enhanced third-body efficiencies may be necessary.

Third body reaction rate constants show a strong pressure dependence, so cannot be evaluated throughout a range of pressure using the two or three parameter Arrhenius terms. At either extremes, the rate equation could be written as a third order reaction at low pressure and as a second order reaction at high pressure, thus enabling a simple fit. But between the two, the rate parameter expressions are more complicated. This is known as the “fall off region” and the reactions are known as “fall off reactions”. There are a number of representations which are used to fit the rate parameters, as discussed next. It should be noted also that the dissociation reaction, which is the reverse of the three body recombination, is similarly affected, varying between a second order at low pressure and a first order reaction at high pressure

Consider the following fall-off reaction;



where M is a third body as defined previously. Alternatively, the third body may take the concentration of a single species. Notice the distinction between the previous example; the +M within parentheses is used to denote that this is a fall-off reaction.

Equations are used to blend smoothly between high and low pressure rate expressions. The first set of Arrhenius parameters ($A_\infty, \beta_\infty, E_\infty$) are given for the high pressure limit. The second set (A_0, β_0, E_0) refer to the low pressure limit as follows:

$$k_\infty = A_\infty T^{\beta_\infty} \exp\left(\frac{-E_\infty}{RT}\right) \quad (3.15)$$

$$k_0 = A_0 T^{\beta_0} \exp\left(\frac{-E_0}{RT}\right) . \quad (3.16)$$

The rate constant at any pressure is taken to be

$$k = k_\infty \left(\frac{P_r}{1 + P_r}\right) F \quad (3.17)$$

where the reduced pressure P_r is given by

$$P_r = \frac{k_0 [M]}{k_\infty} \quad (3.18)$$

with $[M]$ defined as above.

The fall off reactions have a number of forms such as Troe [135] and Lindemann [136]. If F in equation 3.17 is unity then it is the Lindemann form. The Troe form involves more complex forms for the function F :

$$\log F = \left[1 + \left[\frac{\log P_r}{n - d(\log P_r + c)} \right]^2 \right]^{-1} \log F_{cent} \quad (3.19)$$

where c , n and d are constants given by

$$c = -0.4 - 0.67 \log F_{cent} \quad (3.20)$$

$$n = 0.75 - 1.27 \log F_{cent} \quad (3.21)$$

$$d = 0.14 \quad (3.22)$$

and

$$F_{cent} = (1 - \alpha) \exp(-T/T^{***}) + \alpha \exp(-T/T^*) + \exp(-T^{**}/T) . \quad (3.23)$$

The four parameters α , T^{***} , T^* , T^{**} must be specified and relate to the values after the word TROE in the reactions list. It is often the case, such as ours, that T^{**} is not used and only 3 parameters are listed. When a Lindemman fall off reaction is used this line is omitted.

3.1.4 Rate of production and rate of temperature change

With methods to calculate rate parameters of each elementary reaction, a system of ordinary differential equations (ODEs) can be set up. The rate of change of chemical species may be defined by a corresponding ODE. Following from equation 3.7, a rate for each elementary reaction (R_j) may be given by

$$R_j = k_j \sum_{i \in SS_j} [c_i]^{v_{ij}} \quad (3.24)$$

where $[c_i]$ is the concentration of any species, v_{ij} is the stoichiometric coefficient of the species i in the reaction j and SS_j is the set of species in the left hand side of reaction j [137]. Each reaction equation that a species appears in will then represent either a production or a loss of that species as the reaction proceeds, and

by considering all the chemical production and loss terms we can write a differential equation for each species in the chemical scheme as;

$$\frac{d[c]}{dt} = \sum_i P_i - \sum_j L_j - \sum_w L_w \quad (3.25)$$

where P_i is a production term from reaction i , L_j is a loss term from reaction j and L_w is a loss term to account for wall destruction of species. Wall loss reactions may or may not be specified in a mechanism. In zero-dimensional modeling such reactions will take the form of an elementary step with associated Arrhenius parameters. These reactions will have no products as such, instead, in their place the word ‘WALL’ will appear. The combination of production and consumption rates for each species leads to a generalised equation for the rate of production of each species in a closed vessel;

$$\frac{d [c_i]}{dt} = \sum_j v_{ij} R_j = f_i , \quad (3.26)$$

where f_i is the overall rate of production of species i . For non-isothermal reaction schemes we should include an energy balance, in order to compute the temperature profiles;

$$(C_p) \frac{dT}{dt} = \sum_j \Delta H_j^\circ R_j - \frac{UA}{V} (T - T_a). \quad (3.27)$$

The second term on the right hand side is a heat-loss term which describes Newtonian cooling through the walls, where T_a is the ambient temperature, V the volume, A the reactor surface area and U the heat transfer coefficient [15]. This term maybe manipulated so that adiabatic or non-adiabatic conditions can be explored. Equations 3.26 and 3.27 are used to model reaction in a closed vessel, under zero-dimensional, spatially uniform conditions. Extra terms maybe added at

will to describe the inflow of fresh reactants and outflow of reactor contents, as would occur during the operation of a continuously stirred tank reactor (CSTR), or these equations can be used as the chemical source term within an operator splitting environment of a CFD code. For the present purposes the above equations are sufficient.

The systems of equations outlined thus far in this Chapter are solved using the SPRINT integrator, which will be further discussed in Section 3.4. This system of equations is non-linear, due to both the non-linear nature of the simultaneous rate of production terms and the non-linearity of the Arrhenius term.

The complex system of equations maybe investigated, with the aid of a further definition called the Jacobian matrix, each element of which maybe defined as;

$$J_{ik} = \left[\frac{\partial f_i(c, k)}{\partial c_k} \right]. \quad (3.28)$$

The Jacobian matrix can be of great use in the reduction process, forming the basis of local sensitivity analysis of each species in the mechanism, as will be further discussed in Chapter 5. Investigations of the variety of timescales which exist in combustion systems may also be helped by the utilization of the Jacobian, also leading to further reductions. This will be discussed in Chapter 7.

3.2 CHEMKIN

The most widely used software for the analysis and simulation of gas phase kinetics using detailed mechanisms is the CHEMKIN family of codes, developed by Kee *et al.* [86], at the SANDIA National Laboratories in Livermore. CHEMKIN-II was significantly improved from the original version, allowing the specification of pressure dependent reactions and was available as freeware until 1985. The take-over of the project by Reaction Design, Inc. saw the commercialization of CHEMKIN, with releases 3.x and 4.x including further

expansion of functions and add-ons. Subroutines of CHEMKIN-II are used in the present work.

The CHEMKIN-II package includes a collection of Fortran application codes for a number of reactor types, including perfectly stirred reactors (AURORA), plug-flow reactors (PLUG), incident and reflected shock tube reactors (SHOCK), ignition problems (SENKIN) and laminar premixed flames (PREMIX). The package also includes a number of subroutines which allow the numerical derivation of thermodynamic and chemical kinetic quantities.

The general structure of CHEMKIN-II involves an Interpreter program which, reads in a text 'CHEMKIN format' description of the chemical kinetic reaction mechanism, including chemical species, reactions and their associated rate parameters. Thermodynamic data is available in a supplementary database, however the program is flexible in that the user may specify their own thermodynamic data, either in a separate file or written in the mechanism and hence also read in by the interpreter. The interpreter checks the validity of the mechanism written in a file called chem.inp, insofar as there is the required spacing between data and all species included in reactions are specified in the species list. The program also checks that there is no duplication of reactions unless specified and that all reactions are atomically balanced. Thus, the program offers a quick and convenient way of verifying a given text mechanisms. The results are written in a text file called chem.out and a binary file called chem.bin, the latter of which may then be used in conjunction with one of the 'Gas-Phase Subroutine Library' simulation programs for modelling the variety of reactor types.

The reasoning behind the impact and success of CHEMKIN, is not only its substantial technical contribution but also because the text format has allowed a great transferability of data and results between the people working in this field. It is now commonplace for combustion kinetic mechanisms to take this format due to the ease of analysis and ability to make understandable changes to the mechanisms. The CHEMKIN format of mechanisms, is widely regarded as an archetypal standard, however it has been criticized by Simmie [138] who states

that the notation such as inline formulas for species are cumbersome and that it is virtually impossible to specify more complicated species unambiguously in this way. Further criticism has been leveled at the subroutines of the package because many reduction techniques require modifications to be made and access to the Jacobian matrix. This is made difficult because of the ‘black box’ nature of the program [137]. Moreover, some reduction techniques, such as lumping, require pseudo species to be specified in reactions which do not obey atom balance and this is prohibited in the CHEMKIN framework.

In the present work, the bulk of the simulations are carried out by the SPRINT integrator using CHEMKIN format mechanisms as input. This format is output by the automatic mechanism generator, EXGAS and will be retained in any developed reduced mechanisms. However, some simulations are carried out by the SENKIN module of CHEMKIN, in order to interface with the kinetic analysis software KINALC. Local concentration sensitivities are processed by SENKIN and then dumped into output files. KINALC then extracts the important pieces of information from these files, and may be used for a number of functions, such as rate of production (Section 5.5 and 6.4) and atomic flux analyses (Section 6.3 and 6.5). The CHEMKIN interpreter is further used in the current work; the output text file is manipulated and used during the reduction procedures outlined in Chapter 5 and the binary chem.bin file is used as input for the MECHMOD program, the useful functions of which will be described next.

3.3 MECHMOD

Another executable program which can be of use in chemical kinetics modeling and mechanism reductions is MECHMOD [131]. This FORTRAN program is another post-processor of CHEMKIN and is freely available from the World Wide Web [131]. MECHMOD is used to manipulate the CHEMKIN format mechanisms and convert them into a form which is acceptable to simulation codes like the SPRINT integrator. The inputs to the program are the mechanism in binary format (stored in the chem.inp file) and a control file which

contains keywords denoting the user specified instructions. On execution of the program a new text file mechanism is produced based on the input mechanism but with the desired changes and improvements as specified in the control file. In fact, MECHMOD performs the reverse function of the CHEMKIN interpreter by converting a binary file mechanism into a text version.

The subroutines of MECHMOD provide the user with a number of options to make changes to mechanisms. Reversible reactions are often encountered in mechanisms when they are distributed. However, a number of reduction methods such as principle component analysis (Section 5.4) require that the techniques are applied to mechanism with only irreversible reactions. MECHMOD can convert the reversible reactions to pairs of irreversible reactions by numerically fitting three Arrhenius parameters for the rate parameter of the reverse reaction. The reverse rate parameters are calculated, as shown in Section 3.1.2, at three temperatures, chosen by the user, and then the Arrhenius parameters are fitted to this.

Unwanted or redundant species may be removed from a mechanism by using the 'KILL' function of MECHMOD. In this way, the species is removed from the species list, its thermodynamic data is removed and so too are all of the reactions in which it appears. The species will also be removed from any enhanced third body efficiency expressions. The reactions of the mechanism are then renumbered accordingly. For example, investigations of pyrolysis reactions in the absence of oxygen may use detailed hydrocarbon oxidation mechanisms as a starting point [139]. MECHMOD could then be employed to remove all the species containing oxygen atoms from the starting mechanism.

A further function is to convert units of data expressed in the mechanism such as the Arrhenius pre-exponential and activation energy parameters. This is necessary for compatibility with the SPRINT integrator. MECHMOD can also modify the room temperature thermodynamic data stored in the NASA polynomials. Thermodynamic properties can be printed in the mechanism in user selected units.

A final useful feature of MECHMOD is that it prints mechanisms in a neat and organized format with numbered reactions. This can be of help if the mechanism is required to be further manipulated using customized UNIX shell scripts, as may be required during any of the reduction procedures explained in Chapters 5 and 7. All of MECHMOD's functions would be extremely tedious, time consuming and prone to human error if they were to be performed manually. The program is easy to use and provides efficient methods for the manipulation of mechanisms.

3.4 The SPRINT Integrator

The ordinary differential equations defined in Section 3.14 for the rate of change of concentration of each species and temperature must be integrated in order to find the trajectories of these variables with time. The coupled sets of differential equations must be solved simultaneously and any later application of the quasi steady state approximation (QSSA) may require the specification of a mixed differential/algebraic system of equations. The complexity and non-linearity of the problem means that an analytical solution is highly unlikely so a suitable numerical method must be used. Furthermore, the degree of stiffness (see the preface of Chapter 2) which prevails in chemical systems, especially those of combustion, exacerbates the difficulty of solution and means the use of standard integration methods such as explicit Runge-Kutta is too inefficient because of the small time steps required [15].

Sophisticated numerical methods for the solution of stiff systems of differential equations are available in the SPRINT package (Software for Problems In Time) [48] and are particularly suited to combustion kinetic applications. SPRINT also has the ability to solve coupled differential/algebraic systems of equations, necessary for the efficient solution of QSSA problems. The development of the original SPRINT package took place during the 1980s and was primarily funded by Shell Research, Thornton [140]. The program was

originally written in FORTRAN 77, but a C version exists and has been applied in the work presented in this Thesis.

SPRINT is a modular general purpose package and so requires the user to express the rate equations explicitly within the driving program, in order for their solution to be obtained. This feature makes the package extremely versatile, unlike the SENKIN module of CHEMKIN, allowing the user to output intermediate data values which may require post-processing during the application of reduction methods such as sensitivity and principal component analyses. Jacobian entries may also be extracted during execution of program which are necessary for measuring species lifetimes and errors induced by the application of the QSSA. Comparisons of numerical predictions output from SPRINT and SENKIN under adiabatic conditions show that results from each of these programs are in good accord.

The program package includes a choice of integration routines depending on the nature of the program and these may be interchanged during execution. The numerical methods available in the package include Gear/backward differentiation formula methods [141], adaptive theta methods [142] and differential-algebraic integrators [143]. The Gear/backward differentiation formula methods were used predominantly throughout this work.

The ultimate outputs of a customized version of the code include temperature, pressure, species profiles, heat release and reaction rates. These can then be viewed using standard plotting tools such as Excel, Origin or Linux based graphical interfaces. The customized version of the program also gives the user the choice to output reaction conditions (temperature, pressure and mass fractions), at each or a selection of the time points, in a text format which is acceptable as input to SENKIN. In this way, short time-scale simulations can be performed by SENKIN and the output can be extracted by KINALC for further kinetic analysis. The choice of output time steps may be specified in an input file, with the user having the ability to make a change in step size at a selected time during the simulation. Alternatively, the output time stepping may be controlled from within the C code on the basis of reaction time passed and temperature changes. The

simulation can be terminated at a specified reaction time or temperature attained, the latter of which helps to reduce output file sizes. Heat transfer effects can be varied in the input data file. Another feature of the customized code is the ability to model conditions of a rapid compression machine, that is, pressure, temperature and heat transfer effects can be varied over a short time scale so that the effect on the evolving chemistry can be quantified. The rate expressions for each elementary reaction may be overridden by specifying alternative expressions within the C code and recompiling. These alternative expressions may take the form of algebraic combinations of other mechanism variables like rate parameters and intermediate species concentrations. This function is utilized in the application of the QSSA (see Chapter 7). The SPRINT package is further developed in Chapter 4 for the application of the automatic construction of simulated ignition diagrams, to be used as a tool for the validation of comprehensive and reduced mechanisms. The integration of sensitivity analysis type reduction methods and the simulation methodology of SPRINT via the use of UNIX shell scripts is described and discussed in Chapter 5. Individual temperature profiles output from the program package may also be used for the validation of reduced mechanisms by making a direct comparison to those of the full.

3.4.1 Measurement of computational run time

As previously discussed, the main objective of mechanism reduction is to achieve a speed up of central processing unit (CPU) time during simulation. Because reduction of the number of species directly reduces the number of ODEs to be integrated and Jacobian evaluation constitutes the major computational cost during the integration of large stiff kinetic mechanisms, then CPU time is expected to scale with the square of the total number of species (N^2). The many reactions of a mechanism involve coupling of the ODEs and will also have a burden on computational overheads, so a reduction of these will result in further computational savings. Computational savings are expected to scale linearly with

the number of reactions (n). There will be other computational costs, such as calculating various thermodynamic properties [43]. Mechanism reduction will also alleviate the impact of a CFD simulation on memory usage, but for the present purposes attention is focused on the computational run time.

In order to assess the success of any performed reduction, it is necessary to measure the computational run time of SPRINT using the reduced mechanism to simulate an autoignition process and then compare this value to those measured using the comprehensive mechanism, so a brief description of the procedure will be given. The CPU time for a given integration with a 2.4 GHz Intel Xeon processor running Linux is measured by the clock of the computer using a simple UNIX shell script to write the start and finish times in a file. A disadvantage of this approach is that the clock of the computer may not be able to accurately measure differences of very small amounts of CPU time. This is addressed by measuring and comparing the time of multiple simulations, e.g. 40 runs. Any other running applications must be closed. The speed of integration can be hampered by writing to disk, for this reason it is prudent to limit the amount of data being written by selecting large enough output time steps in the run up to ignition and also selecting the output to be only that of time, temperature and pressure. The simulation should be terminated just before the temperature has attained 1000 K, because stalling may occur during the switch of NASA polynomial coefficients and cause meaningless results. During ignition, it is necessary to switch to a smaller output time step to avoid large jumps of temperature and associated calculations of thermodynamic changes. Any error induced to the (simulated) ignition delay time output from the reduced mechanism (in comparison to that of the full) should be taken into consideration when measuring the computational run time.

3.5 Converting mechanism data files

Mechanisms must be converted to a form which is acceptable to the ensemble of programs outlined in this Chapter. The adapted SPRINT integrator accepts

CHEMKIN format mechanism, as output by MECHMOD with the units of Arrhenius parameters converted to molecules, cm^{-3} , s^{-1} and Kelvins. Species names must be 16 characters long or less, specified in uppercase alphanumeric and not include the plus sign, M, parentheses or a full stop. Third body efficiencies must appear on one line.

3.6 Summary

Established techniques and software used in the current application to model and analyse gas phase oxidation kinetic mechanisms have been outlined. The programs have been set up to be used in conjunction with one another and their interrelation is shown in Fig. 3.1. This set-up pertains to the simulation and

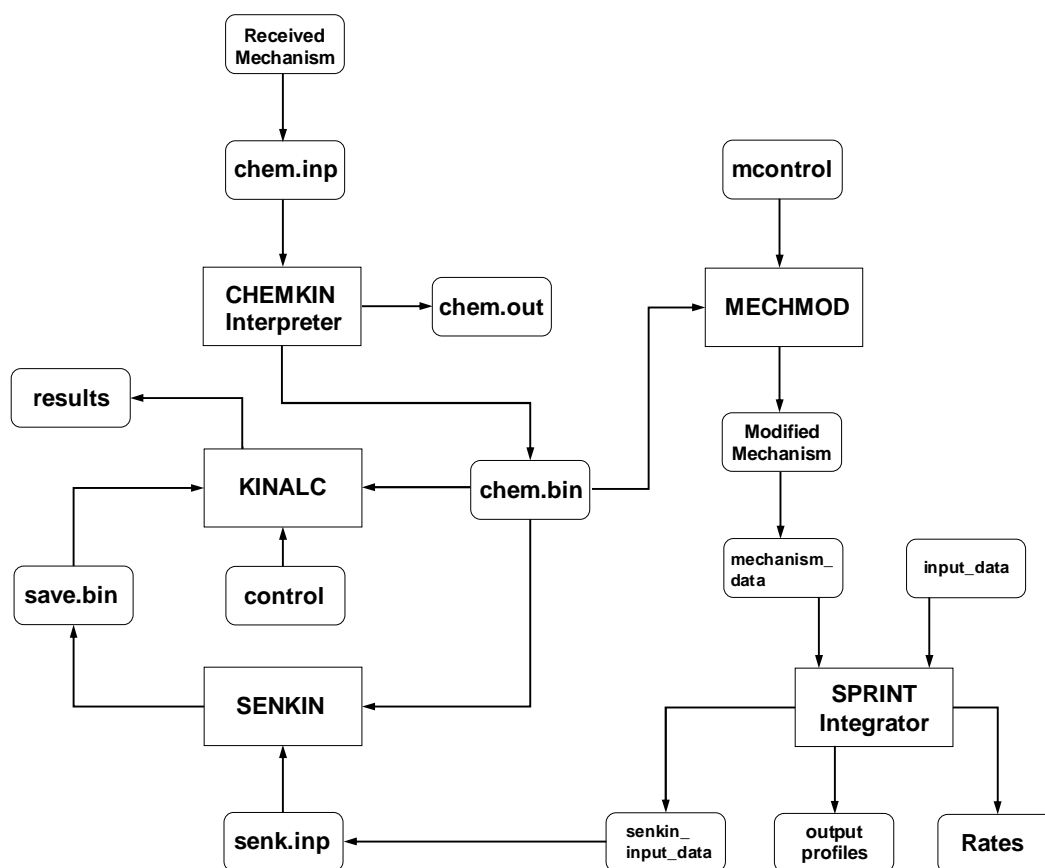


Fig. 3.1. Schematic diagram showing the structure of the suite of software packages and the relationship of executable programs and data files.

analysis of kinetic mechanisms. The identification of redundant species and reactions for mechanism reduction may be performed using the set up shown in Fig. 3.1, via the inspection and sorting of sensitivity analysis results output by KINALC. However, this procedure has been circumvented in the current application by the incorporation of sensitivity analysis algorithms into the SPRINT integrator. This will be further discussed in Chapter 5. The numerical techniques shown here can solve the coupled equations of kinetic schemes with hundreds of species and thousands of reactions, allowing a comprehensive understanding of the oxidation processes under scrutiny, for a minimal computational cost. The main drawback of all of these programs is that spatial uniformity (zero dimensions) is assumed for their implementation. Thus physical effects such as convection and diffusion cannot be accounted for. Reactor geometry is assumed to be simple and this is known to have a marked effect on real life reactive processes. To address these issues, kinetic mechanisms must be coupled to computational fluid dynamics tools for simulation of two and three dimensions. However, the kinetic mechanisms must be sufficiently reduced using mechanism reduction techniques, such as those to be discussed in Chapters 5 and 7.

Chapter 4

Comprehensive kinetic mechanisms and their validation

Selecting a suitable comprehensive mechanism to model a specific problem is an important elementary step in the development of computer tools to address problems like the elimination of explosion hazards in the chemical industries. The features of the full mechanism will be retained in the reduced mechanisms and ultimately in the application of higher dimensional simulations. Ideally, we wish to select a mechanism which accurately models all the types of behaviour seen in relevant experiments over a wide range of operating conditions. To describe a model as comprehensive implies that it has been evaluated over an enormous range of conditions of temperature, pressure and composition. The first of these is normally (but not always) satisfied but often pressure and composition variations are much more limited. This means that the starting point is that the modeller must choose the most appropriate mechanism for the specific application, analogous to “picking the right tool for the job”. Comprehensive kinetic mechanisms have been employed in combustion modelling for many years, thus there is now a wealth of mechanisms available in the public domain. To examine all of these is beyond the scope of this thesis. As time has gone by, the accuracy of combustion mechanisms has increased and is expected to further increase as poorly known parametric information is elucidated and mechanistic structures are improved. As a result, older mechanisms become superseded by the new and

improved qualitative kinetic structures; though quantitative data can always be updated. A recent review of post-1994 detailed hydrocarbon oxidation mechanisms and the experiments used to validate them is given by Simmie [138].

Our interest is to select mechanisms that incorporate appropriate low temperature chemistry ($T < 900$ K), because it is these conditions which are important to partial oxidation processing of hydrocarbons. A specific requirement of the selected mechanisms is the accurate prediction of the minimum autoignition temperature (MIT). The performance of a number of comprehensive mechanisms of different origins and fuels will be analysed via zero dimensional closed vessel simulations and the automatic construction of the pressure – ambient temperature ($p-T_a$) or composition – ambient temperature ($\phi-T_a$) ignition diagram and comparison to the experimental ignition diagram. Although not comprehensive, experimental ignition diagrams for a range of fuels are reviewed by Pollard [144]. Although now 30 years old the contents of this review remain remarkably up to date because relatively few studies of ignition diagrams have been reported since then: Griffiths and Mohamed [99] have reported more recent data. Fundamental aspects of experimental ignition diagrams and the negative temperature coefficient of reaction rate (NTC) are addressed in the following Section 4.1.

The most appropriate approach to comprehensive mechanism assembly lies with the use of expert computer systems. Today, the most advanced program system for the generation of hydrocarbon oxidation mechanisms is EXGAS and its related suite of software programs, which originate from DCPR-CNRS Nancy [19-21]. The software has been developed over several decades, at first to generate normal alkane mechanisms, now extended to isomeric structures of alkanes, alkenes, cyclic alkanes and aromatic compounds. The comprehensive mechanism, in relation to alkanes, has generalized kinetic features taking the simplified form shown in Fig. 4.1. The overall structure is described in detail elsewhere [90-95] and further information can be found in Section 2.1.1. With the aim of contributing to the further validation and development of this system, mechanisms generated using EXGAS, either at DCPR-CNRS Nancy or *in situ* by the author, are employed extensively throughout this work.

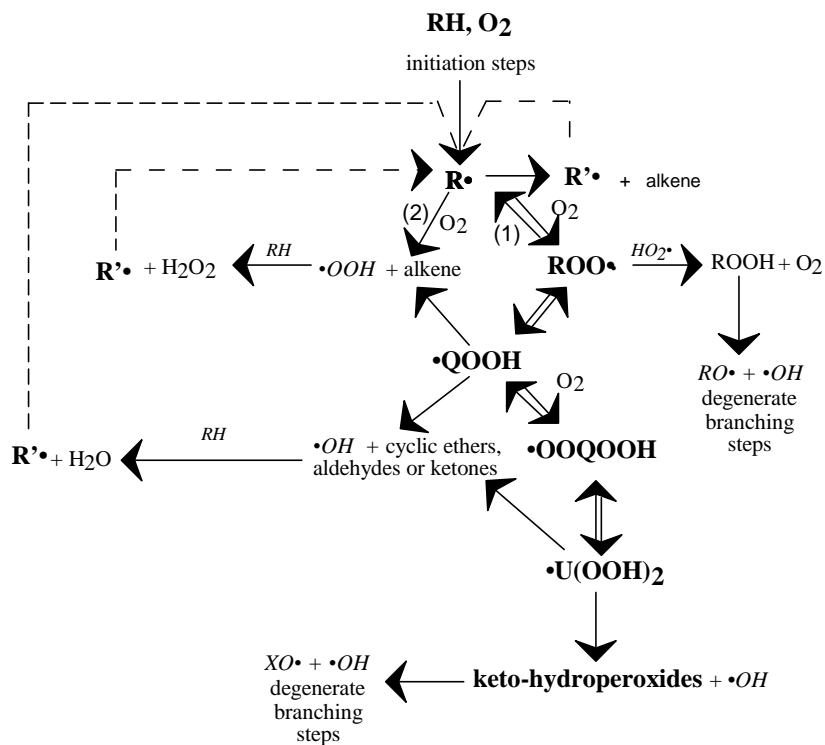


Fig. 4.1. Simplified scheme for the primary mechanism of the oxidation of alkanes (broken lines represent metathesis with the initial alkane RH.) [21].

4.1 Ignition diagrams and the negative temperature coefficient of reaction rate

Large amounts of information regarding the variety of oxidation phenomena are represented in experimental p - T_a ignition diagrams, which are constructed from the analyses of many individual runs at varying pressures and ambient temperatures in a closed vessel, typically between 500 K and 900 K. Three major classes of oxidation phenomena occur. In slow reaction, there is no sudden temperature jump, but the process is characterised by an induction time and typically limited change in temperature which evolves relatively slowly. Cool flames, either single or multiple consecutive, in which the fuel is partially oxidised to products similar to those produced during slow reaction, occur with temperature spikes in the range $20 < T/K < 200$. A very feeble bluish flame can be seen in the reactor during the occurrence of a cool flame. During Ignition, either fuel or oxidant consumption is complete, and (except in very fuel rich or lean

conditions) the reaction is accompanied by a sharp temperature spike of many hundreds of degrees. Further subdivisions of ignition may be made, depending on the number of associated cool flames, for instance a 2-stage ignition is defined as a cool flame initiated ignition, 2 cool flames and then ignition would be 3-stage ignition, etc [145].

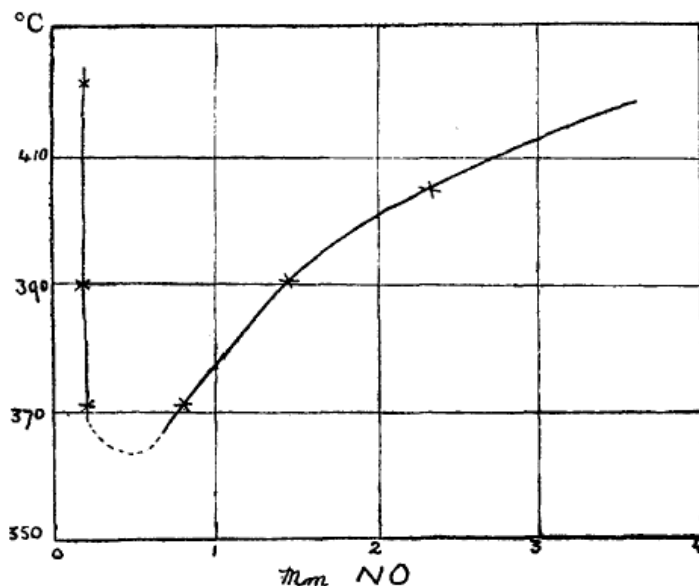


Fig. 4.2. Experimental ignition boundary showing the effect of a trace additive of NO on the AIT of $2\text{H}_2 + \text{O}_2$ at 80 kPa or 600 torr [148]. The x-axis shows partial pressure of NO in torr (mm Hg).

Rudiments of the ignition diagram appeared as early as 1883 in the form of closed vessel tests for the combustion and explosion of gaseous mixtures by Le Chatelier and Mallard [146], who were interested in mitigating methane explosions in French coal mines, although it was not until 1926 that such tests were used to measure the influence of reactant pressure or composition on autoignition temperature (AIT). Data for the explosion limits of $\text{H}_2 + \text{O}_2$ mixtures were first obtained by Dixon *et al* [147] in a rapid compression machine, though it appears that they were only tabulated by them. A little later, Gibson and Hinshelwood [148] worked with $2\text{H}_2 + \text{O}_2$ in a spherical vessel, and plotted one of the first ignition boundaries shown in Fig. 4.2, albeit for the effect of a trace additive of NO on AIT. Data obtained by Hinshelwood on the effect of total pressure on AIT was later plotted by R.N. Pease [149]. The first p- T_a hydrocarbon

limit to be plotted appears to have been undertaken by Sangulin [150], for $\text{CH}_4 + 2\text{O}_2$. Further work on methane was conducted by Prettre *et al* [151]. Then, in the early '30s there was a considerable effort to map the ignition and cool flame boundaries of hydrocarbon + air mixtures, most notably by Townend and co-workers [152,153]. Their first effort was to construct ϕ - T_a ignition boundaries for n-butane in air mixtures for a range of initial ambient temperatures from 1-15 atm [152]. They quickly turned their attention to higher hydrocarbons [153], producing p - T_a ignition diagrams showing regions of ignition, cool flames and slow reaction, such as one for pentane - air mixtures. The first sub-atmospheric p - T_a ignition diagram for “higher alkane + oxygen” was produced for propane by Newitt and Thornes [154] in 1937. Note that whichever of these two dimensional maps is produced, it constitutes a slice from the three dimensional p - ϕ - T_a phase space for a given fuel in a given closed vessel.

The generic structure of the p - T_a ignition diagram for propane and higher alkanes and alkenes is shown in Fig. 4.3. The features of the diagram are caused by the underlying kinetics of the system and are much related to the negative temperature coefficient of reaction rate or NTC, which can be defined as a temperature range, broadly between 600 - 800 K, in which overall reaction rate decreases as temperature increases. The ignition peninsular arises from changes in the kinetics as a result of the competition between temperature dependent reaction routes. The structure can be further explained by consideration of the line FG on Fig. 4.3. The slow reaction region is controlled by an overall non-branching reaction mode, with the termination rate exceeding the chain branching rate [57]. As the temperature is raised, degenerate branching is predominant at AB. The $\text{R} + \text{O}_2 / \text{RO}_2$ equilibrium is displaced towards the formation of RO_2 (see Fig. 4.1). The oxidation proceeds via alkyl hydroperoxide formation, involving RO_2 isomerization and the formation of dihydroperoxy species [2]. OH radicals are mainly formed by secondary decompositions of hydroperoxides, thus propagating the reaction [155]. Raising the initial ambient temperature further still, there is a second switch at BC to another predominantly non-branching reaction mode [2]. Although rarely acknowledged, this discontinuous transition from ignition to the

cool flame region, as temperature is raised, is the most dramatic demonstration of the negative temperature dependence of overall reaction rate in action [156]. The fraction of alkyl radicals converted to alkylperoxy radicals decreases, to the benefit of the formation of alkenes, with propagation occurring mainly via HO₂ radicals. As the temperature is increased even further, the reactivity begins to increase again during which branching reactions such as



are involved which promote autoignition [2,155]. This description encapsulates only the underlying kinetic development, but accompanying it is also heat release, which correlates to the onset of ignition. The lower temperature reactions, which are propagated by OH radicals, can be quite strongly exothermic, and this characteristic is repeated at higher temperatures. In the intermediate zone the exothermicity may be very feeble.

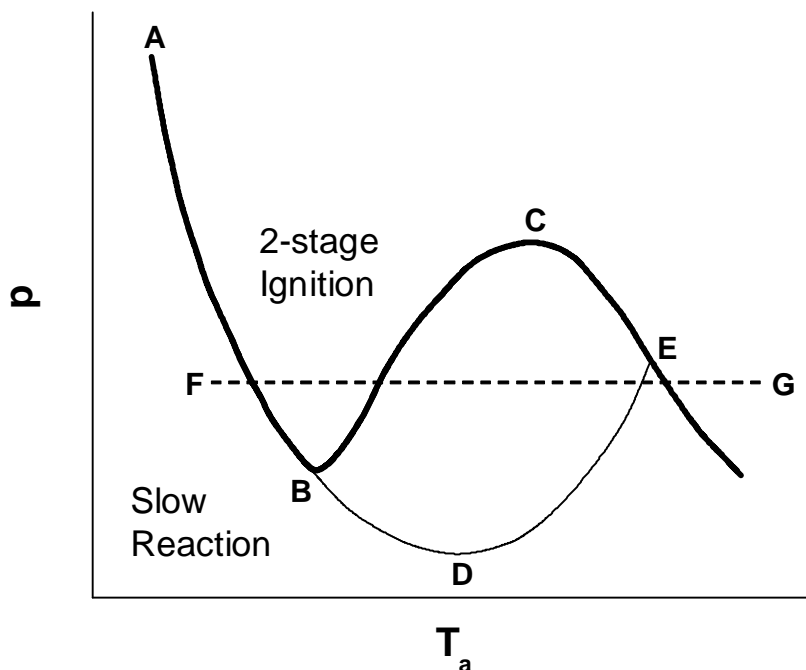


Fig. 4.3. A representative p - T_a ignition diagram for the gas phase oxidation of alkanes and other organic compounds in a closed vessel [57].

Further kinetic complexities are embedded in the various forms of the ignition diagrams of different fuels [156], especially in the region of oscillatory cool flames and multiple stage ignitions, bound by BCED on Fig 4.3. These phenomena have been studied in great detail [157-159], although only for a limited number of fuels. Amongst very few examples, a quantitative experimental assessment has been carried out for the low temperature and pressure oxidation phenomena of acetaldehyde in a continuous stirred tank reactor (CSTR) [160,161]. Chemical analysis during cool flames and ignition was carried out and the data obtained has been used in a number of efforts to model the phenomena [57,162-165].

The precise location of the boundaries distinguishing the characterized phenomena on the ignition diagram will depend on the fuel to air or oxygen ratio, as noted earlier making the p - T_a diagram one slice from a three dimensional pressure-ambient temperature-composition (p - T_a - ϕ) figure. In addition, the effect of added inert gases will be to shift boundaries to a location of higher pressure. Furthermore, the p - T_a diagram for a given mixture will behave similarly for vessels of different size and shape, however the pressure and ambient temperature required to bring about the ignition and cool flame phenomena will not be the same. As vessel size decreases, surface to volume ratio increases resulting in greater heat loss through the vessel walls and also presents a more accessible surface for termination. In consequence, higher pressures and temperatures are needed to bring about ignition [156]. Convection in unstirred vessels of different sizes can also have an effect on the position of the boundaries. As vessel size increases so too does Rayleigh number (an r^3 dependence), with increasing natural convection then enhancing heat loss. Investigations into the combustion of rich cyclohexane + air mixtures in unstirred vessels show that MIT appears to scale linearly with vessel size [166]. This would be expected in well stirred vessels, therefore this gives some justification for making comparisons of spatially uniform zero-dimensional models to experiments conducted in unstirred vessels.

A further factor which affects the form of the p - T_a diagram is the influence of heterogeneous reactions between the gas mixture and vessel wall. The effects of

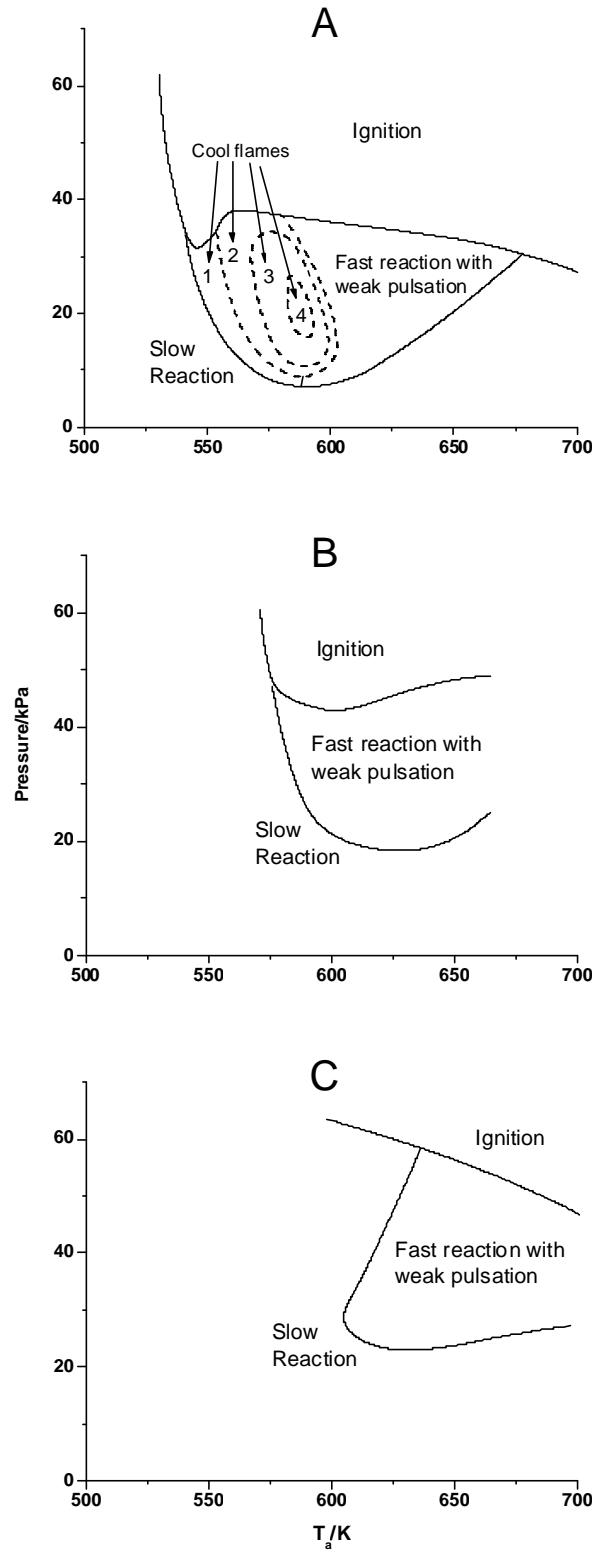


Fig. 4.4. $p-T_a$ ignition diagrams for equimolar n-butane +oxygen mixtures in a 254 cm³ cylindrical vessel with different vessel internal wall coatings. A: Untreated silica vessel. B: NiO coated. C: PbO coated [167].

surface treatment on the internal wall of a 254 cm³ cylindrical reaction vessel have been studied by Cherneskey and Bardwell [167]. The p-T_a diagrams for equimolar n-butane + oxygen in an untreated silica vessel, a vessel internally coated with NiO and a vessel internally coated with PbO, shown in Fig. 4.4, reveal that ignition and cool flame boundaries are modified by the introduction of such coatings, with the greater inhibitory effects being observed with PbO. A marked increase in the pressures and temperatures required to bring about autoignition are observed for the NiO coated vessel with further increases for the vessel coated with PbO. The coatings also have the effect of eliminating the cool flames and making the ignition peninsular far less pronounced. The phenomenon classified as 'fast reaction with weak pulsation' refers to a rapid initial acceleration of reaction with a much slower subsequent deceleration being observed, in contrast to a cool flame phenomenon. The kinetic reason for the suppression of reaction is believed to be the enhanced ability of the coatings to destroy free radical intermediates at the vessel wall. In the same study, vessels that had been thoroughly cleaned with nitric and sulphuric acid were also found to have inhibitory features relative to 'aged' vessels, in which a number of experiments had been previously carried out. Greater reproducibility of results was found in the 'aged' vessels.

4.1.1 Automatic simulation of the numerically predicted ignition diagram

The quantitative tests for the validity of hydrocarbon oxidation models include isothermal comparisons of the predicted yields of intermediates and products with experiment, and of ignition delays during non-isothermal reaction, mainly at high pressure. Only very rarely have there been tests based on the cool flame and ignition phenomena mapped in the p-T_a plane for a given composition or in the φ-T_a plane at a given total pressure. Yet in many respects these are the primary features which must be assessed if the kinetic scheme is to be used to indicate the existence of a potential industrial combustion hazard [168]. In terms of

establishing appropriate reduced models for the purpose of combustion hazard prediction, the preservation of the quantitative features of the ignition diagram is very important. Thus the comparison of ignition diagrams produced by full and reduced schemes constitutes a very important test of the validity of the reduced schemes. The construction of the numerically predicted ignition diagram is a very laborious process, and is especially slow when very large comprehensive kinetic models are being used. This process is amenable to automatic simulation [145].

In this section, we describe software, applied in the present work, which can be used to automatically identify ignition and cool flame boundaries over a range of operating conditions using comprehensive or reduced kinetic schemes¹. The p - T_a or ϕ - T_a ignition diagrams are constructed automatically using UNIX shell scripts to control the execution of a modified version of SPRINT [48] in which the various non-isothermal behaviour such as, ignition, cool flames, and slow reaction are characterised. This characterisation of the reaction modes is based on monitoring the temperature increase and temperature gradient within the simulated temperature – time profiles from given initial conditions, as would similarly be done by examining a measured experimental temperature-time profile, and making a judgement to classify the qualitative nature of the phenomenon that is displayed. The fundamental difference between this direct assessment by visual inspection and the automatic generation of a complete ignition diagram is that criteria to represent each class of behaviour have to be established on a quantitative basis within the program in order for the qualitative distinction to be made. The conditions for the location of the boundary between each kind of behaviour can then be identified. This part of the process is interactive and requires the user to have some physical perception of the nature of the phenomena that are being simulated so that appropriate criteria are defined. “Spot checks” of the categorisations should be made following the execution of the program to ensure that errors or misconceptions are not perpetrated. Typical criteria adopted are that during slow reaction ΔT does not exceed 20 K. For low initial temperatures, ignition is deemed to have occurred if T exceeds 1100 K. The

¹ The automated program was developed at the University of Leeds by Dr. K. J. Hughes.

identification of a cool flame or multiple cool flames requires not only that $\Delta T > 20$ K, but also that a maximum is identified before T exceeds 1100 K [145].

Implementation of the program requires that an initial or ambient temperature range and temperature increment must be defined, e.g. 500 – 650 K at 5 K increments. In the case of a p-T_a diagram, a mixture composition and initial pressure are defined, and simulations performed for each temperature increment within the defined range. The first pressure selected must be high enough so that throughout the entire initial temperature range, slow reaction or ignition are the only types of behaviour that are encountered. Then a bisection method is employed in which the total pressure is initially halved at each operating condition in the defined temperature range. The temperature range is repeatedly traversed. The total pressure is then progressively halved until a change in behavioral regime is detected in successive simulations at the same temperature. The region between the two is then further bisected until the conditions that distinguish the two modes of behaviour are refined to a required degree of precision to locate the boundary, typically around 0.05 kPa.

A similar procedure is used to distinguish cool flame phenomena from slow reaction in order to locate the cool flame/slow reaction boundary and likewise for boundaries between multiple cool flames or multiple stage ignitions of different order, the required level of detail being predefined by the user. At the end of the simulations, a set of files are obtained as output giving the temperature – pressure coordinates that define the various boundaries found. A similar procedure can be implemented to determine lean ϕ -T_a ignition diagrams. In this instance, the bisection method is applied on the fuel partial pressure to a desired level of accuracy while keeping total pressure constant by making compensating adjustments to the other mixture components. The calculations are looped over the defined temperature range. For the purpose of developing and testing comprehensive mechanisms, the first requirement is to set up the ignition diagram that is predicted from the full scheme in order to make a direct comparison to an experimental ignition diagram constructed at the same conditions (the same composition in the case of a p-T_a diagram or the same initial pressure in the case

of a ϕ - T_a ignition diagram). In order to validate reduced models, the ignition diagram generated by the full scheme can then be used as the benchmark against which the reduced models are tested (see Chapter 5 for further details). Fig. 4.5 shows an example p - T_a ignition diagram from the full propane oxidation scheme constructed at equimolar proportions in oxygen.

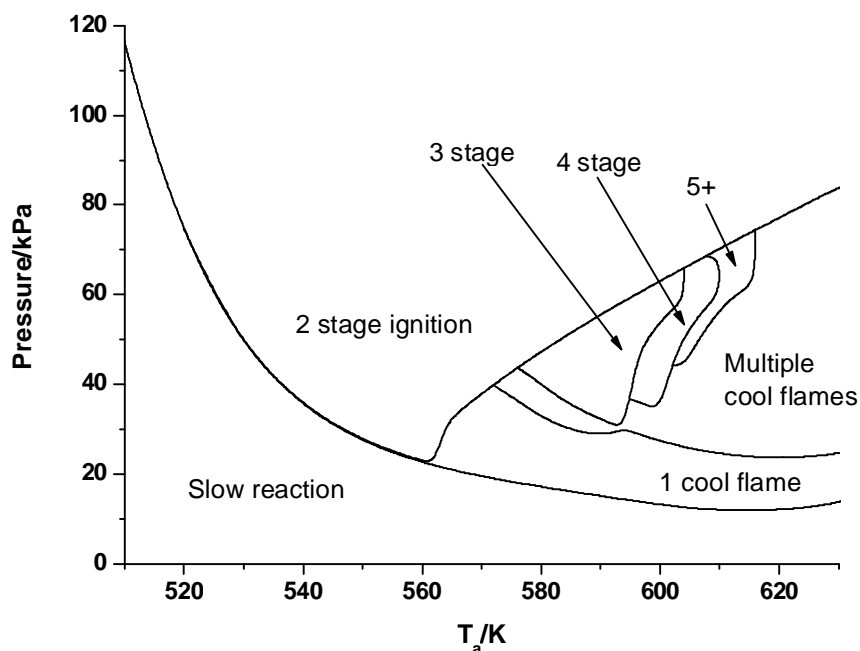


Fig. 4.5. Simulated p - T_a ignition diagram from the full, EXGAS propane mechanism, showing regions of 2 stage ignition, multiple stage ignitions, cool flames, and slow reaction. Conditions pertain to equimolar propane in oxygen, using a (Newtonian) heat transfer coefficient of $1 \times 10^{-3} \text{ W cm}^{-3} \text{ K}^{-1}$.

The number of temperature profiles generated by the numerical simulation that are required for the accurate derivation of an ignition diagram will depend on the options selected by the user, such as the temperature range, the desired level of accuracy and the extent of detail required, i.e., number of cool flames detected etc. For very detailed ignition diagrams of p - T_a format with up to 10 cool flames and 7 stage ignitions detected the number of simulations would be between 5k and 10k. For the simpler ϕ - T_a diagrams presented in this chapter for n -butane + air (e.g. Fig. 4.9), 1–1.5k simulations were made.

A further form of ignition diagram can be generated in the ϕ - T_a plane for richer mixtures. This is undertaken by conducting a series of simulations over a selected composition range and then initially halving the ambient temperature (while maintaining the same total pressure), and then progressively adjusting the temperature in order to locate the boundary between ignition and slow reaction behaviour. That is, making vertical bisections as opposed to the horizontal bisections made for the lean ϕ - T_a ignition diagram. This method is useful for providing a determination of the predicted AIT of a given fuel and is of particular relevance to the SAFEKINEX project.

4.2 Comprehensive propane model evaluation

Propane is the simplest of the alkanes that is generally acknowledged to exhibit an NTC region and associated complex oxidation phenomena such as cool flames and multiple stage ignitions. To be valid, comprehensive models must also exhibit these phenomena and it is desired that any reduced model must retain these characteristics [4]. The first set of results presented here were obtained by numerically simulating comprehensive propane + oxygen mechanisms to demonstrate the ranges of behaviour, such as oscillatory cool flames and multiple stage ignitions, found in an experimental closed vessel. The models were evaluated by the construction of their closed vessel, p - T_a ignition diagrams and comparing them with experimental results using equimolar fuel and oxygen in both cases.

The first comprehensive model presented here was generated by EXGAS [19] for propane oxidation, comprising 122 species in 1137 irreversible reactions, and is applicable to a temperature range 600 – 2000 K. The p - T_a ignition diagram produced by the automatic procedure applied to this mechanism was computed at 2 K intervals over the ambient temperature range $T_a = 500 - 650$ K, giving precision of the boundary to ± 0.07 kPa. A (Newtonian) heat transfer coefficient appropriate to a 1 dm^3 closed vessel ($1 \times 10^{-3} \text{ W cm}^{-3} \text{ K}^{-1}$) was found from the inspection of experimental thermal relaxation curves [169]. This value

incorporates the vessel surface to volume ratio and was used during the calculation. Per volume units for the heat transfer coefficient are preferred in the SPRINT calculation, as this facilitates the modelling of rapid compression machine scenarios. The p - T_a ignition diagram resulting from the procedure is shown in Fig. 4.5.

The qualitative characteristics of Fig. 4.5 compare well with the experimental ignition diagram shown in Fig. 4.6 [169], in terms of position and shape within the diagram, although there are fundamental quantitative differences. In particular, the minimum pressure at which a 2-stage ignition occurs in the simulation is 22.3 kPa, which is appreciably below that of the experiments, at 37.3 kPa (see Fig. 4.8). The most distinguishable qualitative difference between the Nancy model simulation and the experiment is regarding multiple stage ignitions. 4-stage ignitions were the maximum witnessed in the experiments whereas up to 6-stage ignitions were recorded in the simulations. In noting this distinction it should be born in mind that the region of parameter space at which these higher order phenomena are predicted is very narrow and may not be so readily identified in experimental investigations.

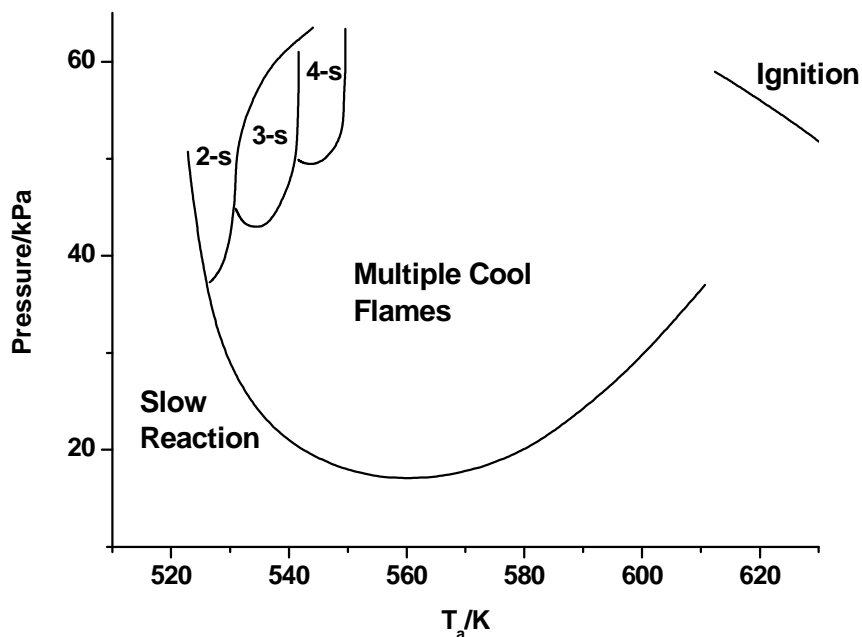


Fig. 4.6. Experimentally determined p - T_a ignition diagram for equimolar $C_3H_8 + O_2$ in a 1 dm^3 spherical vessel [169].

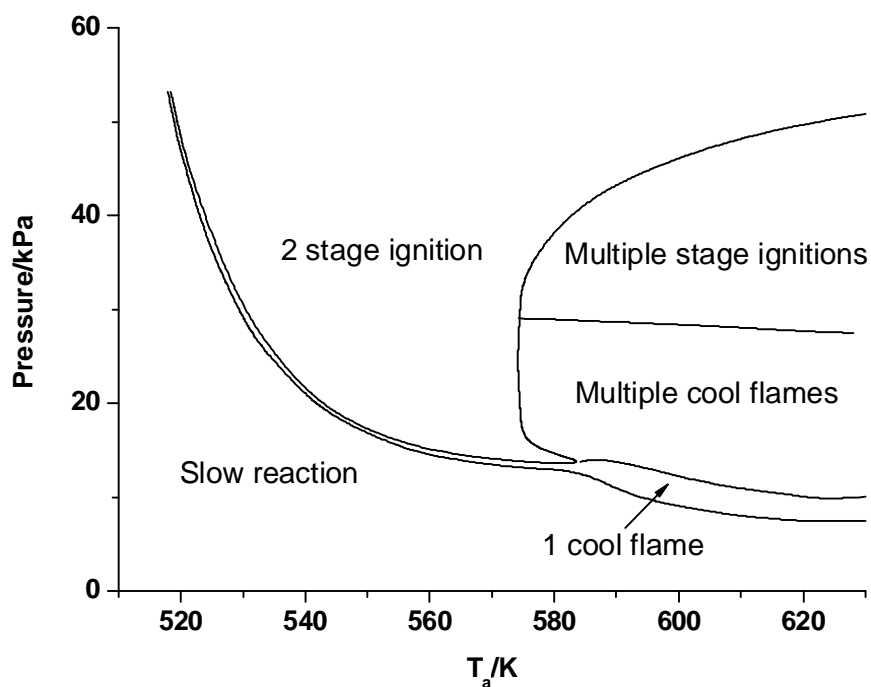


Fig. 4.7. p - T_a ignition diagram for equimolar $C_3H_8 + O_2$ in a closed vessel using a kinetic scheme derived from the comprehensive model of Westbrook *et al.* [170]. A heat transfer coefficient of $1 \times 10^{-3} \text{ W cm}^{-3} \text{ K}^{-1}$ was used.

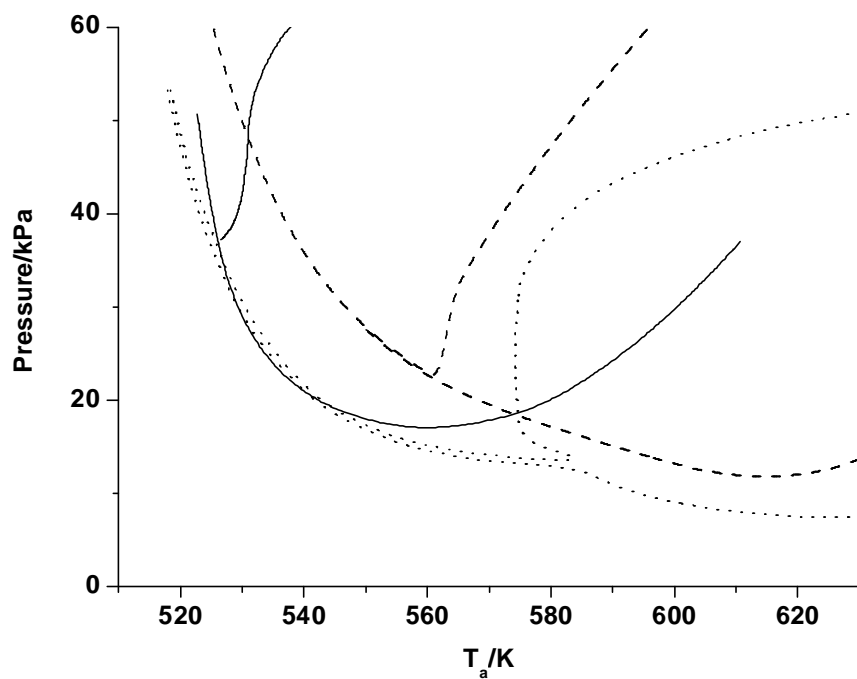


Fig. 4.8. Comparison of experimental and numerically predicted full scheme p - T_a ignition peninsulas for equimolar propane and oxygen. Solid line; Experimental. Dashed line; Nancy mechanism. Dotted line; Westbrook mechanism.

The p - T_a diagram for a second model tested for the $C_3H_8 + O_2$ system, obtained from the comprehensive C_7 model developed by Westbrook and co-workers [170], in reduced form comprising 92 species and 952 reactions (Fig. 4.7) shows a similar anomaly in terms of reactivity with respect to reactant pressure (see Fig. 4.8). The minimum pressure at which 2-stage ignition occurs with this scheme at 13.55 kPa is well below that of the experimental value (37.3 kPa). The pressures at which other complex modes of behaviour occur are also less than the experimental observations. Uncertainty analysis studies are required to explore the origin of this discrepancy in reactivity between simulation and experiment. The computational expense of these techniques requires them to be applied to suitably reduced mechanisms. A quantitative investigation of the discrepancy is presented in Section 6.2. Fig 4.7 also shows that a transitional cool flame region between the 2-stage and slow reaction regions is predicted at temperatures lower than 580 K.

Using the Nancy scheme ignition diagram as a reference (Fig. 4.5), we can further illustrate the behaviour by examining individual temperature profiles. At 600 K there is a boundary between 2 stage and 3 stage ignition (Fig. 4.9A), corresponding to pressures of 63.032 kPa and 63.030 kPa, respectively. At lower pressures there is another boundary between 3 stage and 4 stage ignition (Fig. 4.9B), corresponding to pressures of 53.803 kPa and 53.801 kPa, respectively. This level of precision could not possibly be achieved experimentally, but its accessibility by computation allows comparisons of simulations to be made at virtually identical conditions. This feature can be very useful for examining the kinetics behind the criticality of reaction modes [4]. The cool flame preceding ignition for the 3-stage ignition in Fig. 4.9A (solid line) is not distinguishable at this time-scale. However, it would become clear by zooming in on the ignition temperature spike. Correspondingly, in an experiment a photomultiplier record would have to be picked up using a high time resolution, although an observer might well see a brief blue flash preceding an orange flame. Closely examining the post ignition temperature trajectory for 2-stage ignition on Fig. 4.9A, we can see the curve does not strictly follow an exponential temperature decay and a

moderate ‘S’ shape is observed indicating a small heat release post ignition. A small heat release is also indicated by the temperature trajectories of the first cool flame in 3-stage ignition in Fig. 4.9A and of the second cool flame of the 4-stage ignition in Fig. 4.9B (solid lines). The magnitude of this post cool flame heat

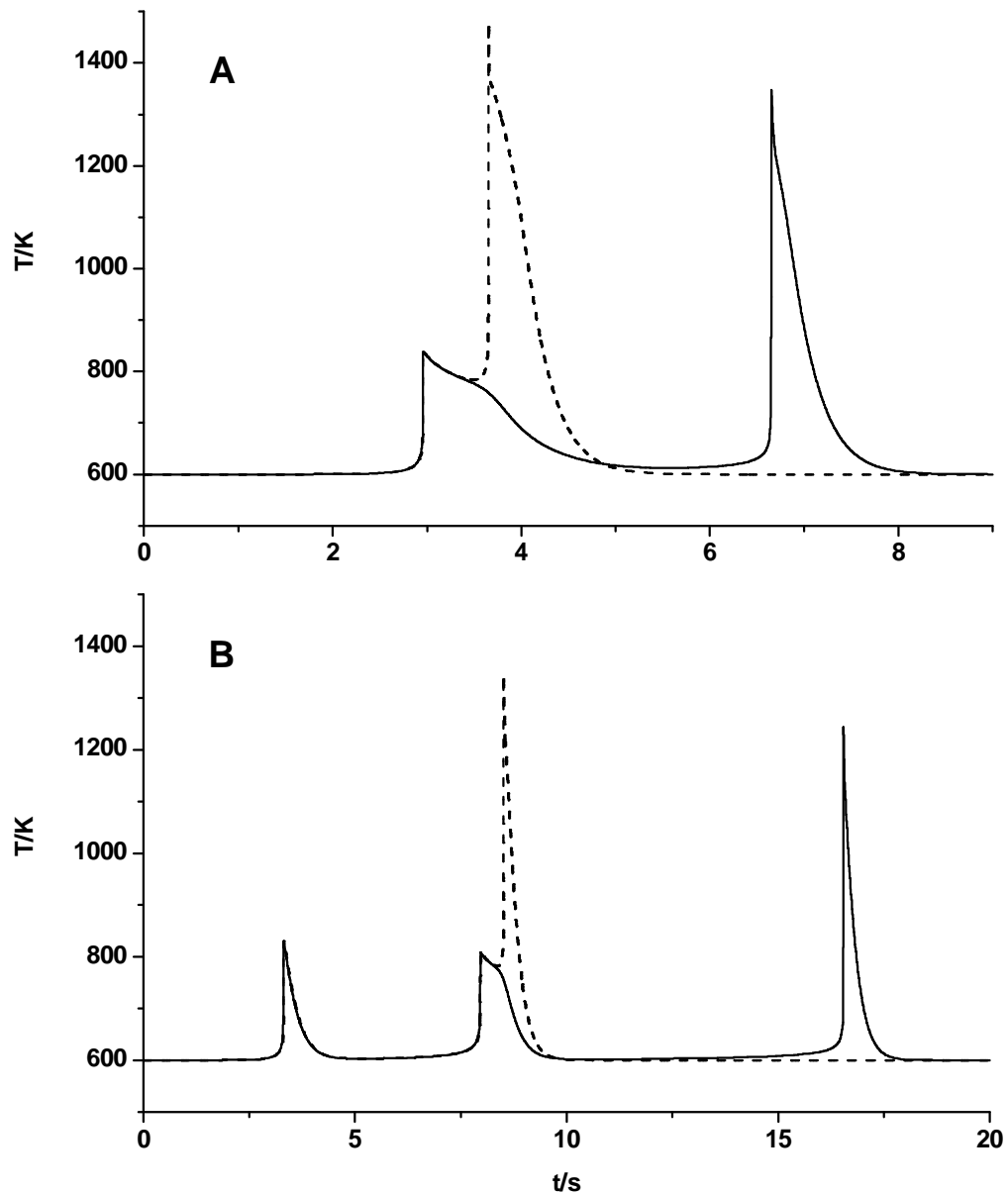


Fig. 4.9. Temperature – time profiles generated using the comprehensive EXGAS Nancy propane mechanism. (A) two-stage ignition (dashed line) and 3-stage ignition (solid line) at $p = 63.032$ and 6.030 kPa, respectively and $T_a = 600$ K. (B) 3-stage ignition (dashed line) and 4-stage ignition (solid line) at $p = 53.803$ and 53.801 kPa, respectively and $T_a = 600$ K.

release is the major controlling factor of whether or not the reaction will attain ignition. Post cool flame heat release rates and the corresponding kinetics are discussed in greater detail in Section 6.4.

Further illustrations of time dependent behaviour are made to demonstrate the range of ignition delay times during two-stage ignition as conditions vary across the ignition diagram. By defining the induction time to the first stage (cool flame) as τ_1 and the induction time of the second stage (ignition) τ_2 , we show how these features change with changing conditions in Fig. 4.10. Ignition occurring at a low initial temperature of 530 K (Figs. 4.10a and 4.10c), is characterized by a long τ_1 and short τ_2 that only becomes apparent at high resolution time-scales. As initial pressure is decreased at 530 K, τ_1 is lengthened. Increasing the initial temperature to 630 K considerably shortens τ_1 but lengthens τ_2 (Figs. 4.10b and 4.10d). The maximum temperature attained during the cool flame is decreased and the overall

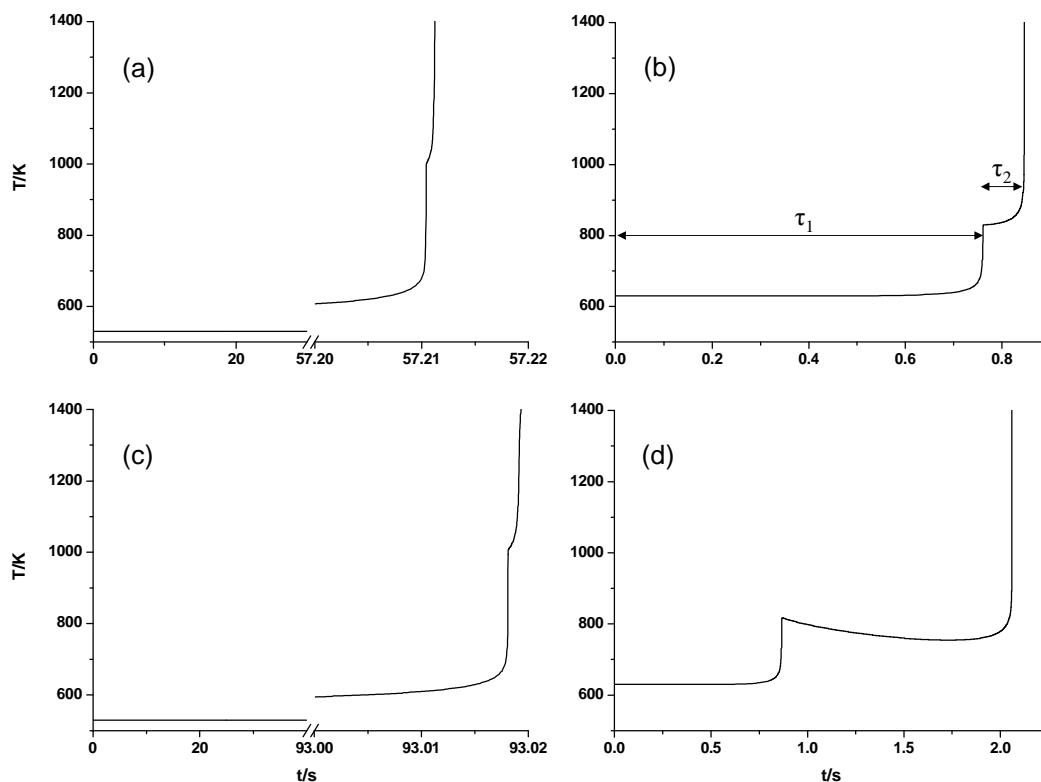


Fig. 4.10. Two stage ignition temperature – time profiles, generated using the comprehensive EXGAS Nancy propane mechanism, corresponding to conditions of equimolar propane + oxygen at; (a) 530 K and 100 kPa, (b) 630 K and 100 kPa, (c) 530 K and 50.7 kPa, (d) 630 K and 84 kPa.

time to ignition is decreased. As initial pressure at 630 K is lowered toward the ignition boundary, τ_1 increases slightly and τ_2 undergoes a marked increase, hence the ratio of τ_2 to τ_1 is increased. Similar features of the way τ_1 and τ_2 inter-relate are present even in high pressure autoignition as occurs in engines.

4.3 Comprehensive n-butane model evaluation

In this next section, comprehensive kinetic models are used to simulate the combustion of lean n-butane in air and to examine the dependence of the ignition limits on fuel/air composition above atmospheric pressure. During the processing of hydrocarbons under partial oxidation conditions in the fuel lean range, the autoignition temperature can undergo marked variations as conditions such as vessel size, or more importantly in the present context, reactant partial pressure or composition are changed. These variations can lead to autoignition occurring at temperatures well below those defined by the statutory tests, which refer to the minimum temperature at which spontaneous ignition takes place in a particular vessel (e.g. BS 4056 and IEC standard 79-4 (1975), or ASTM-E 659-78), in a mixture with air at atmospheric pressure [171]. It follows that there are potential explosion hazards on hydrocarbon processes at a wide range of conditions involving operating temperatures deemed to be safe by the statutory autoignition test procedures.

A comprehensive mechanism for n-butane oxidation was derived at CNRS-DCPR, Nancy using EXGAS [19]. The comprehensive mechanism comprises 128 species in 313 irreversible reactions and 417 reversible reactions. For comparison, a second comprehensive model for n-butane oxidation was tested which was derived from the n-heptane oxidation model developed by Westbrook et al [170]. Predictions of the full schemes were evaluated by constructing ϕ - T_a ignition diagrams over the fuel lean range, low to intermediate temperature ranges and comparing with experimental data (see Fig 4.14) [1]. Figs. 4.11 and 4.12 show the simulated ϕ - T_a ignition diagrams for n-butane + air for the Nancy and Westbrook

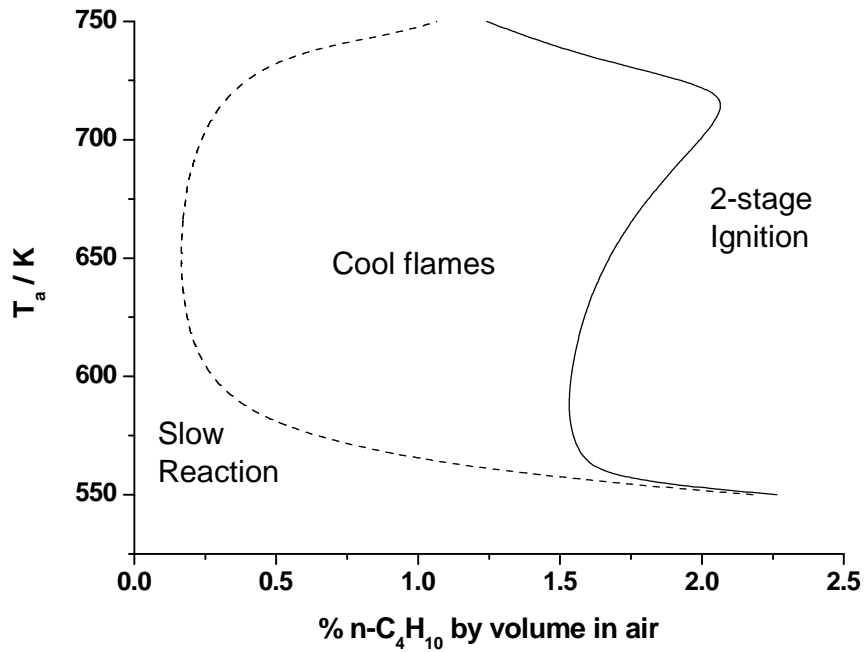


Fig. 4.11. Simulated ϕ - T_a ignition diagram at 0.2 MPa from the full, EXGAS n-butane mechanism, in a closed vessel under spatially uniform conditions. A heat transfer coefficient of $1.5 \times 10^{-3} \text{ W cm}^{-3} \text{ K}^{-1}$ was used.

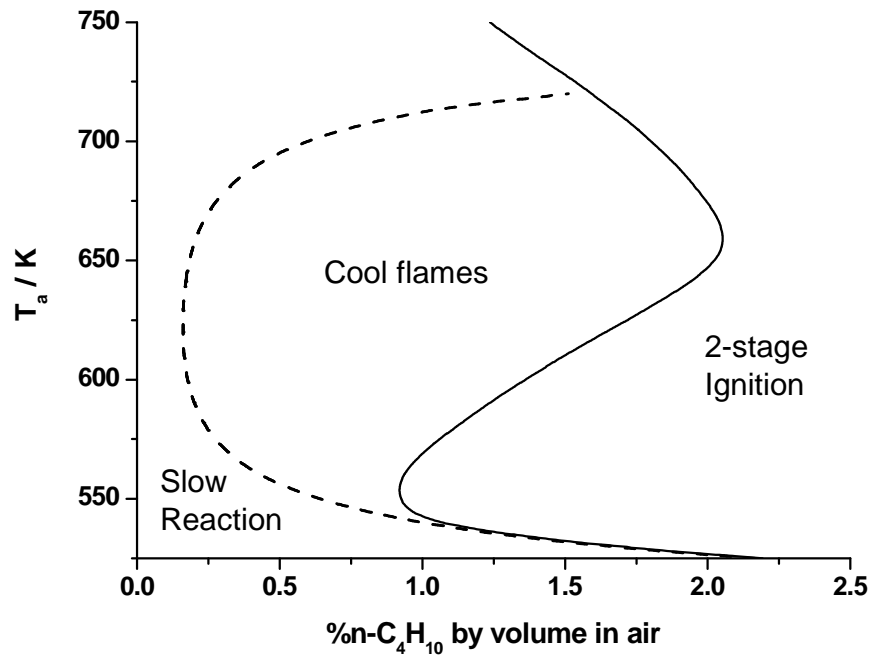


Fig. 4.12. Westbrook *et al* scheme simulated ϕ - T_a ignition diagram at 0.2 MPa for lean $n\text{-C}_4\text{H}_{10}$ + air in a closed vessel under spatially uniform conditions. A heat transfer coefficient of $1.5 \times 10^{-3} \text{ W cm}^{-3} \text{ K}^{-1}$ was used.

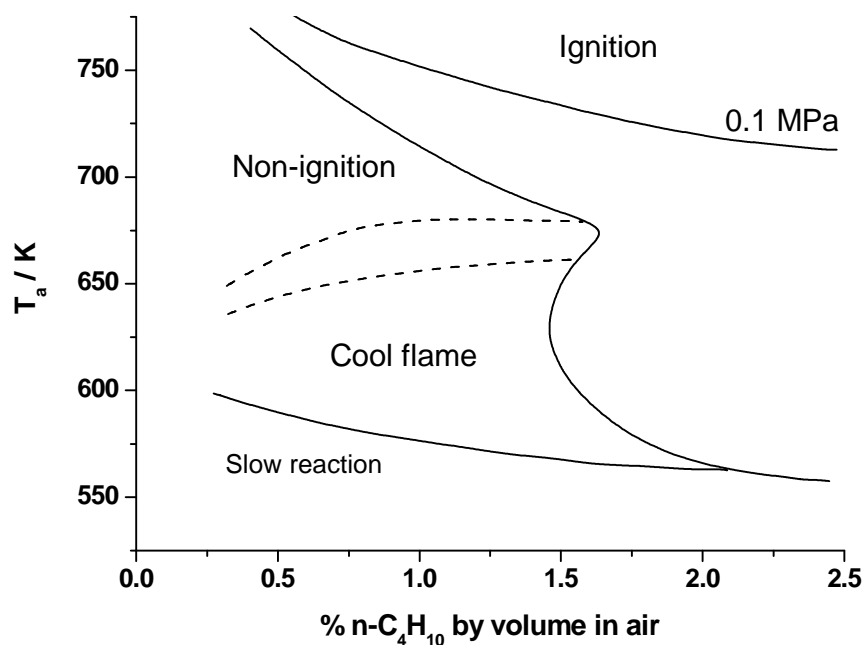


Fig. 4.13 ϕ - T_a ignition diagram for $n\text{-C}_4\text{H}_{10}$ + air at 0.2 MPa and 0.1 MPa (ignition boundary only) in an unstirred stainless steel reaction vessel (0.5 dm^3)[1].

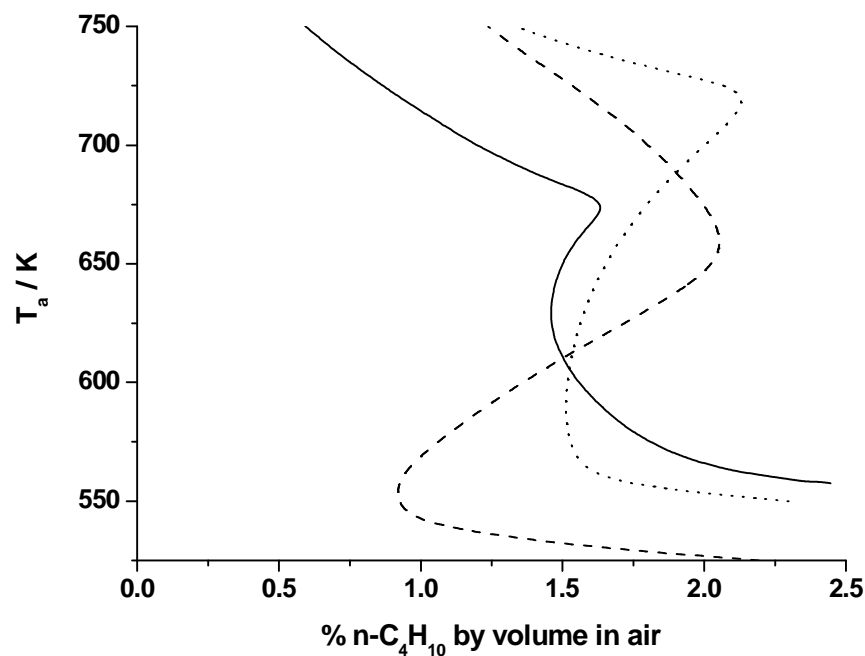


Fig. 4.14 Comparison of experimental and numerically predicted full scheme ϕ - T_a diagrams (closed vessel 0.2MPa). Solid line; Experimental. Dashed line; Westbrook mechanism. Dotted line; Nancy model.

schemes respectively. The qualitative features of the experimental ϕ - T_a ignition boundary [1], shown in Fig. 4.13, are captured by the numerical models showing both cool flame and two stage ignition behaviour. The reverse “s” shape of the boundary is displayed by both the models and this is an important feature of the validation. However Fig. 4.14 shows that at lower concentrations of fuel there are quantitative disagreements with the experiment, and both models predict the autoignition temperatures to be at too high a temperature. This may imply a shortcoming in the way that the intermediate molecular products that lead to high-temperature reactions are interpreted [172]. Poorly known mechanism parameters could be leading to an over prediction of the NTC region. There may also be some discrepancy due to inhomogeneities of temperature in the unstirred vessel [1]. Some improvement may be gained by changing the heat transfer coefficient and by including surface termination reactions. At higher concentrations of fuel the Nancy model shows very good agreement with the experiment but the autoignition temperatures in this region are under predicted by the Westbrook model. Predicted time scales are often shorter than those observed experimentally, almost certainly as a consequence of surface reactivity in the experimental vessels.

The comparison of the experimental ignition boundaries at 0.1 MPa and 0.2 MPa shown in Fig. 4.13 gives an insight into the potential hazards in industrial processing. In fact, the lowest temperature for autoignition of n-butane (the AIT) falls markedly when there is a small increase in pressure to above *ca.* 0.15 MPa. This reinforces the need for hazard prediction tools.

4.4 Comprehensive n-hexane model evaluation

The investigations of increasing carbon number for the alkane series are continued with a brief study of n-hexane. EXGAS was used by the author to generate a mechanism describing the low temperature oxidation of n-hexane ($T < 1000$ K), comprising 202 species in 600 irreversible reactions and 477 reversible reactions. A detailed p - T_a diagram showing the substructure of the cool flame region has been generated for n-hexane in oxygen at the molar proportions of 1.25

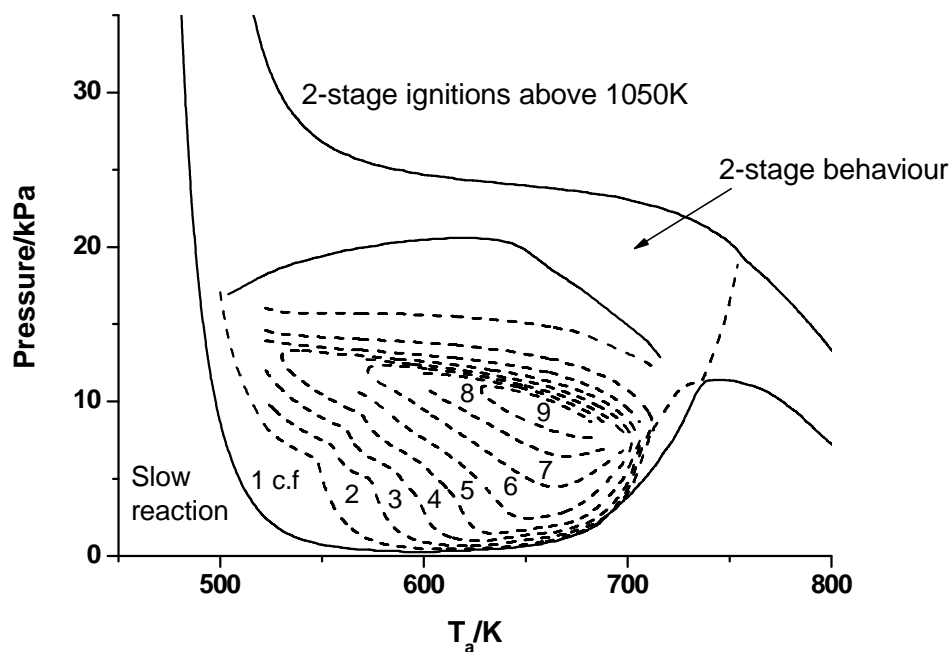


Fig. 4.15. Simulated p - T_a ignition diagram for n-hexane – oxygen in the molar proportions 1.25 to 1, from the full, EXGAS n-hexane mechanism, in a closed vessel under spatially uniform conditions. A heat transfer coefficient of $2.5 \times 10^{-3} \text{ W cm}^{-3} \text{ K}^{-1}$ was used.

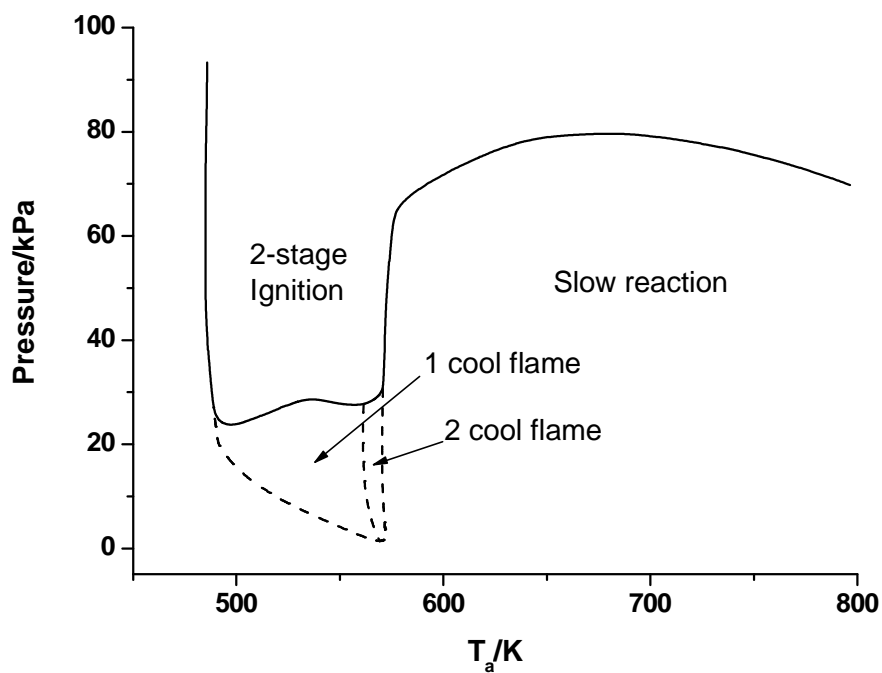


Fig. 4.16. Experimentally determined p - T_a ignition diagram for n-hexane – oxygen in the molar proportions 1.25 to 1, in a 200 cm^3 cylindrical vessel [173].

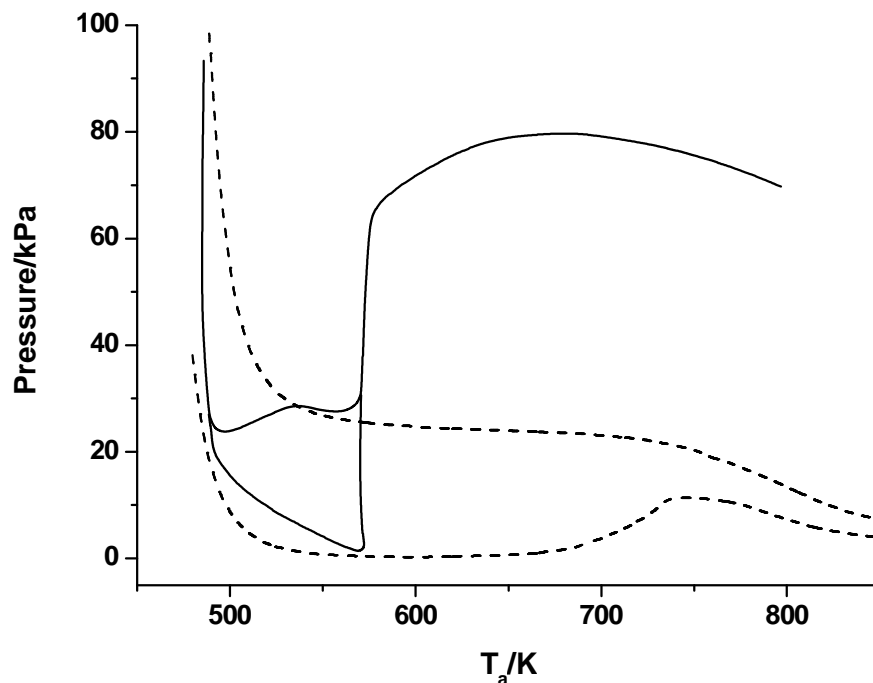


Fig. 4.17 Comparison of experimental and numerically predicted p - T_a diagrams for n-hexane – oxygen in the molar proportions 1.25 to 1. Solid line; Experimental. Dashed line; EXGAS mechanism.

to 1, and is shown in Fig. 4.15. These fuel rich conditions were selected in order to make a direct comparison to the experimental work of Cullis *et al* [173]. In the automatic program for the generation of the p - T_a diagram, the criteria for ignition was defined to be phenomena with a T_{\max} above 1050K, however, in rich mixtures 2-stage like behaviour can occur with a T_{\max} well below this threshold temperature. This phenomenon occurs because of oxygen depletion during ignition.

Some notable features can be deduced from the comparison of experimental and numerically predicted p - T_a diagrams for n-hexane (Fig. 4.17). The cool flame region exhibited by the Nancy model extends to temperatures far higher than those reported in the experiment, although it is possible that low ΔT and Δp cool flames at higher temperatures (570-740 K) may not have been detected experimentally by mercury manometers [174]. At this same temperature range, the model under predicts the minimum pressure at which 2-stage ignition occurs. However, at temperatures below 570 K the model shows good agreement with the

experiment, with both the low temperature ignition/slow reaction boundary and minimum pressure at which two-stage ignition occurs being well predicted. Although it was not our charge in the SAFEKINEX project to assess the performance of comprehensive models, the fact that discrepancies in reactivity exist cannot be disregarded. Moreover, it appears to be a generic problem. There may be a number of different reasons. First is that the qualitative structure of the models are wrong, but this is unlikely, given the widespread agreement on understanding of the main kinetic features. Second is that key quantitative data are incorrect or not known to the required precision. This is certainly a potential cause, as discussed later in Section 6.2. Thirdly, the evaluations that are being made relate to zero dimensional simulations of experiments in which there are marked spatio-temporal variations arising from mass and heat transport causes by natural convection. The qualitative investigation of such effects is only just in its infancy and has not yet been tackled yet with respect to detailed chemistry even in reduced form. However, the purpose of the present work, as discussed in Chapter 1, is to provide kinetic tools that will enable these important investigations. General trends exhibited by the mechanisms are further discussed in the final remarks of this Chapter (Section 4.8).

4.5 Comprehensive n-heptane model evaluation

The low AIT of n-heptane constitutes an explosion hazard in its storage and transportation. Moreover, the partial oxidation of alkane mixtures is likely to be an important procedure in oil reforming technology for the generation of hydrogen for use in fuel cells, with light fractions being an important feedstock for this process. Such processes must be safe and cost effective and optimum routes may be under conditions of partial oxidation using “stabilized cool flames” with low temperature products aiding the conversion [175-177]. Further ongoing research into hydrogen production is being carried out via rich combustion in silicon carbide foams [178]. In any case, the development and application of such technologies is likely to be furthered by a deep understanding of the combustion characteristics of primary reference fuels such as n-heptane, which in turn will

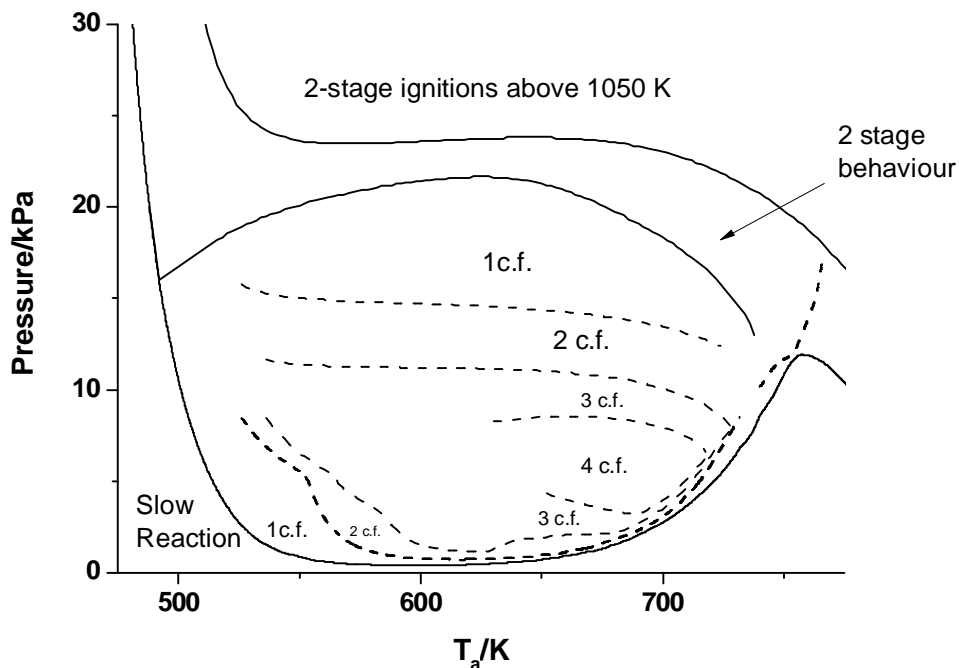


Fig. 4.18. Simulated p - T_a ignition diagram for equimolar n-heptane – oxygen, from the full, EXGAS n-heptane mechanism, comprising 268 species in 1403 reactions, in a closed vessel under spatially uniform conditions. A heat transfer coefficient of $2 \times 10^{-3} \text{ W cm}^{-2} \text{ K}^{-1}$ was used.

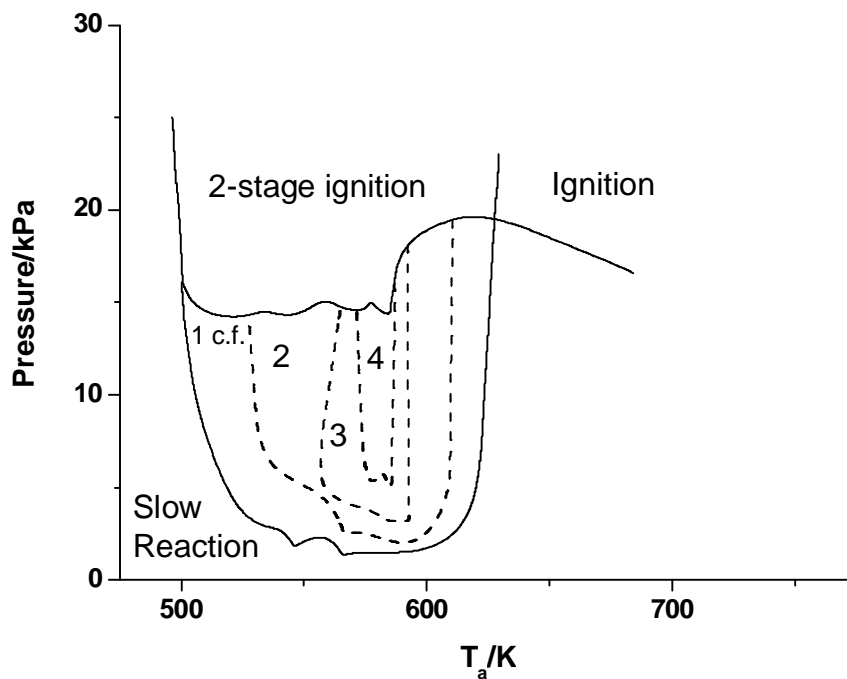


Fig. 4.19. Experimentally determined p - T_a ignition diagram for n-heptane – oxygen determined in a 330 cm^3 cylindrical vessel [179].

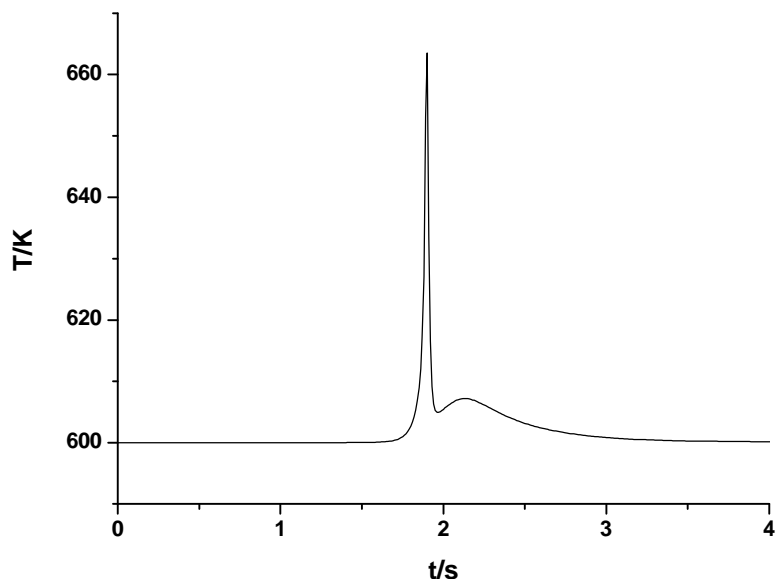


Fig. 4.20. Temperature – time profile generated using the comprehensive EXGAS n-heptane mechanism. A cool flame occurs at 600 K and 0.5 kPa.

elucidate the properties of real fuels like petroleum distillates and biofuels [174-177].

EXGAS was employed to automatically generate a mechanism describing the low temperature oxidation of n-heptane ($T < 1000$ K), comprising 268 species, 862 irreversible reactions and 541 reversible reactions. The model was evaluated via the automatic construction of the equimolar p-T_a diagram (Fig 4.18) and comparing with the experimental diagram [179] constructed at the same conditions (Fig 4.19).

From the comparison of the simulated and experimentally determined equimolar n-heptane p-T_a ignition diagram, shown in Figs. 4.18 and 4.19 respectively, we can see that the low temperature slow/reaction ignition boundary gives good agreement to that of the experiment. The minimum pressure at which two-stage ignition occurs is also reasonably well predicted by the model. The maximum initial ambient temperature at which cool flames are detected in the model is far higher than those reported in the experiment, and it is unlikely that weak cool flames went undetected in the experimental procedure because a sensitive pressure transducer was used by Burgess and Laughlin [179] in which pressure changes as little as 0.1 torr could be detected. The discrepancy could be

attributed to inhomogeneities in the unstirred vessel, parametric uncertainties in the mechanism or physical limitations of the zero-dimensional model. Another discrepancy is apparent in the minimum pressure at which cool flames occur. An individual temperature – time profile, obtained from running SPRINT at initial conditions of 600 K and 0.5 kPa, (Fig. 4.20) shows cool flame phenomena occurring at these conditions, hence, the mechanism displays a reactivity which is incompatible with anything observed in experiments.

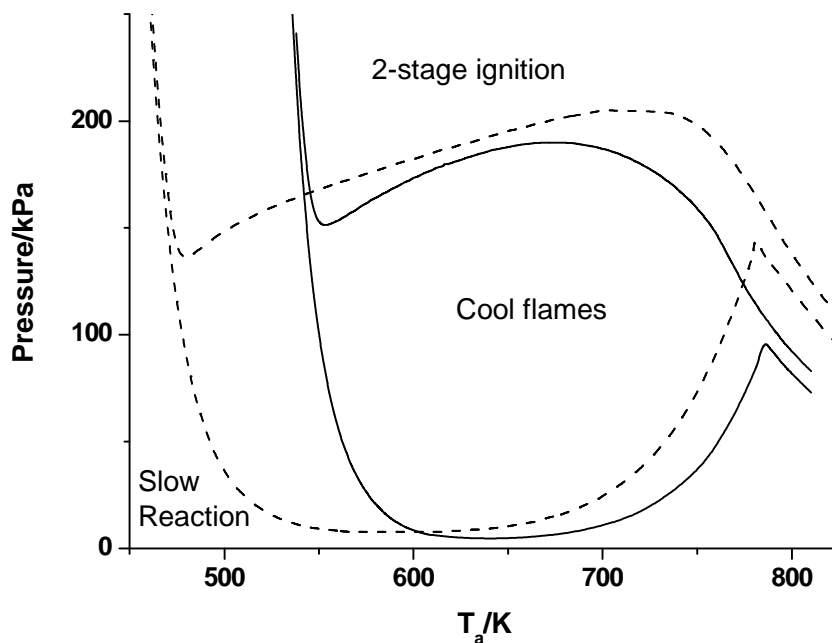


Fig. 4.21. Comparison of numerically predicted p - T_a diagrams for stoichiometric n-heptane – air. Solid line; EXGAS mechanism (boundary generated by Dr. K. J. Hughes). Dashed line; Peters mechanism.

A further comparison of model output is made with respect to the behaviour of models in stoichiometric mixtures in air. For this purpose, a larger EXGAS n-heptane mechanism consisting of 360 species in 1223 irreversible reactions and 594 reversible reactions was employed. The fundamental difference between this mechanism and the smaller 268 species mechanism is that EXGAS permits a certain amount of user interactivity, where it is possible to eliminate classes of reactions that are specifically important to temperature ranges outside the region of interest (see Section 2.1.1). In this way, *a priori* reductions can be made at the mechanism generation stage and it follows that the 360 species mechanism is

applicable to a wider range of operating conditions than the 268 species mechanism. Comparisons of temperature profiles run at the conditions encountered on the p - T_a diagram of Fig. 4.18 show a negligible difference between the two EXGAS n-heptane mechanisms at our region of interest. To be inclusive, a second model for n-heptane oxidation generated by Peters and co workers [180] was tested. The model was provided in reduced form, comprising 56 species in 136 irreversible reactions. Although not strictly a comprehensive mechanism, this chapter provides the most appropriate place for its evaluation. The automatically generated stoichiometric n-heptane – air p - T_a ignition diagrams for the 360 species EXGAS mechanism and the Peters mechanism are shown in Fig. 4.21. The two models exhibit a similar reactivity with respect to reactant pressure, although it appears that the Peters mechanism predicts the location of the low temperature slow reaction/ignition boundary at a much lower temperature than the EXGAS mechanism, which is known to be reliable at these conditions.

4.6 Comprehensive cyclohexane model evaluation

Cycloalkanes are a major constituent in automotive fuels, with up to 3% in petrol and 35% in diesel (albeit in the C_{12} - C_{20} range). However, relatively little attention has been paid to their combustion characteristics [181]. Furthermore, autoignition hazards are often encountered during the partial oxidative processing of cyclohexane due to its low minimum ignition temperature (MIT), measured at 533 K, using the standard test procedures (IEC 60079-4, DIN 51794, ASTM 659-78, BS 4056 and EN 14522) [182,183]. The best-known incident involving cyclohexane was the explosion at the Flixborough Nypro plant in 1974. Failure of a temporary pipe caused a massive release of hot cyclohexane which ignited in open air on contact with an ignition source. However, the accident was not due to the nature of the process and no explosion occurred inside the plant [7]. Studies of the autoignition properties of cyclohexane have been undertaken by Snee and Griffiths [166]. This investigation was initiated because of a need to assess potential autoignition hazards associated with batch processes in the resin manufacturing industry.

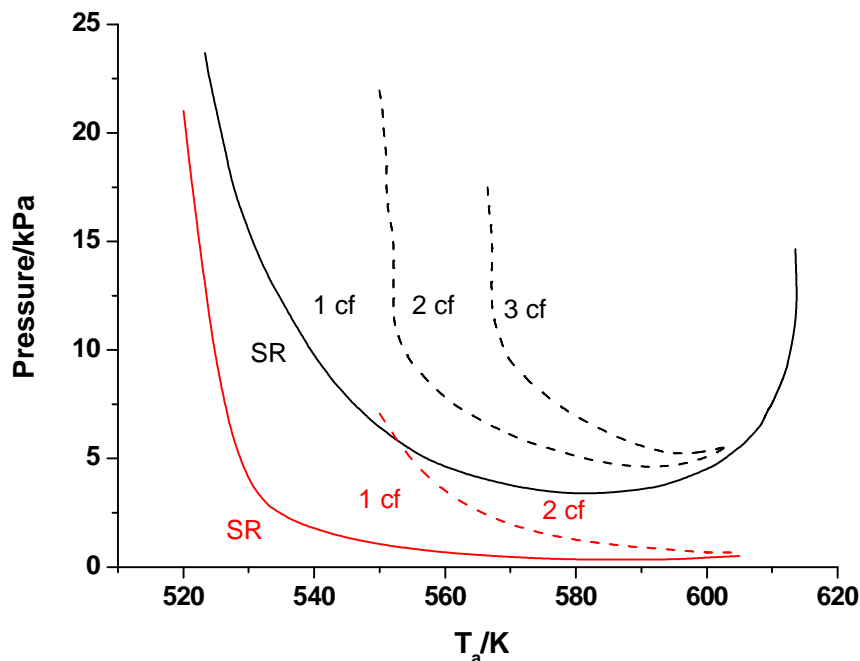


Fig. 4.22. Comparison of experimental and numerically predicted p - T_a diagrams for cyclohexane – oxygen in the molar proportions 1 to 1. Black line; Experimentally determined boundaries in a 150 cm^3 . Red line; Simulate EXGAS mechanism using a heat transfer coefficient of $3 \times 10^{-3} \text{ W cm}^{-3} \text{ K}^{-1}$.

The full cyclohexane mechanism to which the techniques were applied originates from DCPR-CNRS Nancy [19,181] and comprises 499 species in 1025 reversible reactions and 1298 irreversible reactions. The mechanism was evaluated by construction of the equimolar cyclohexane - oxygen p - T_a ignition diagram and making a comparison to the experimental cool flame boundaries at this reactant mixture composition [184], as shown in Fig. 4.22. The qualitative structure of the cool flame boundaries measured in the experiment is well captured by the p - T_a diagram generated using the Nancy model. In terms of operating temperature, the location of the slow reaction/cool flame boundary is also well represented by the model. However, like the Nancy *n*-heptane mechanism the pressure location of the slow reaction/cool flame boundary is under predicted by the model relative to the experimental boundary, leading to the conclusion that the mechanism is too reactive in this region of operating conditions.

4.7 Trends between fuels and the prediction of minimum autoignition temperature (MIT)

4.7.1 Kinetic background to the reactivity of different alkane structure

The purpose of this Section is to assess if expected patterns between fuels are well captured by the EXGAS program. As the carbon number of normal alkanes increases, so too does their reactivity. This in turn is reflected in the measured AIT, by the standard test procedures [182,183], as is shown in Fig. 4.23. The AITs of normal alkanes, e.g C_3H_8 to $n-C_9H_{20}$, show a dramatic decrease from C_3H_8 , at 790 K, through $n-C_4H_{10}$ and $n-C_5H_{12}$, at 700 and 560 K respectively, to $n-C_9H_{20}$ at 510 K [1]. As we have already seen for n-butane, the AIT of a given fuel can shift dramatically below its measured autoignition temperature when conditions are changed, however, the general hierarchy is as one would expect intuitively from chemical knowledge. The behaviour can be explained by the types of C-H bonds present on the carbon chain. With increasing carbon chain length, the ratio of primary to secondary sites decreases. The activation energy of initiations via H atom abstraction from the primary fuel, or any long chain molecule, is lower at secondary sites than it is at primary sites (and lower still at tertiary sites), although exactly how the H atom is abstracted will have a bearing on the magnitude of the demarcation of the activation energies. Further complexities arise regarding the isomeric structure of branched isomers, with AIT increasing as the main carbon chain decreases in length due to the reduced reactivity at the greater number of primary sites and other factors, as will be discussed. There is also a view that the numbers of methyl groups of branched alkane isomers is a hindrance to reactivity which relates strongly to the proportions of C-H bond types, but more specifically relates also to what happens to the methyl group endings once an H atom has been abstractions [185].

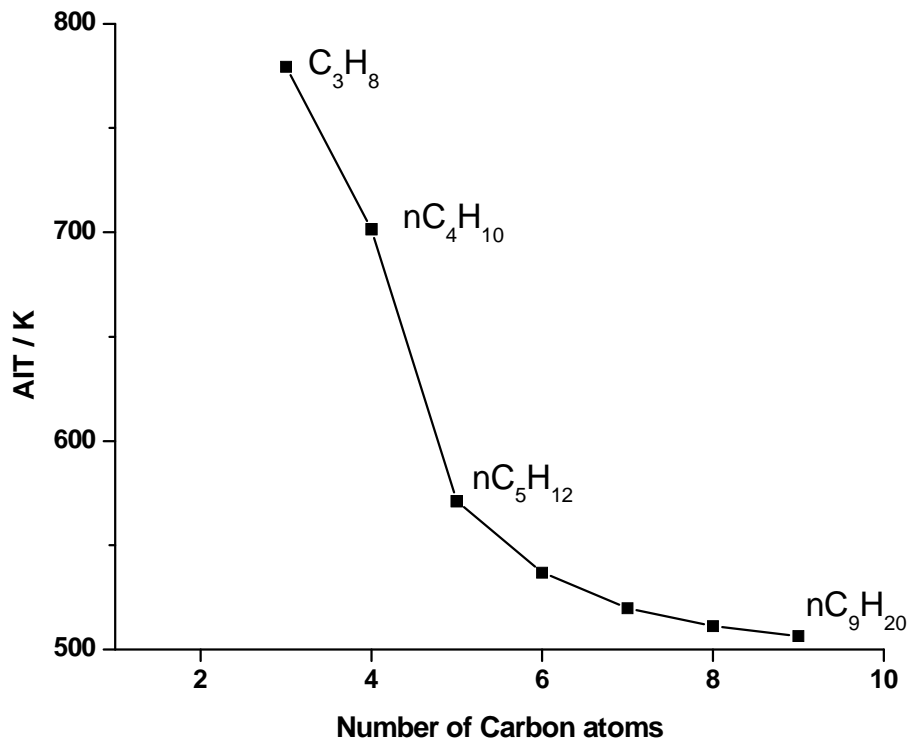


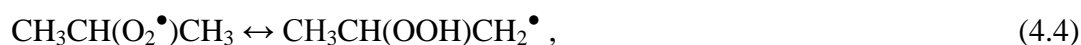
Fig. 4.23. Variation of the minimum autoignition temperature of the n-alkanes as measured in air at atmospheric pressure by ASTM, BS or EC tests [1].

Two main classes of H atom abstraction can be defined; intermolecular and intramolecular. Intermolecular H atom abstractions by HO₂ and RO₂ radicals show a marked distinction in activation energy for the three types of C-H bond (For HO₂ radicals $E > 60 \text{ kJ mol}^{-1}$ at a primary C-H bond, $> 50 \text{ kJ mol}^{-1}$ at a secondary C-H bond and $> 40 \text{ kJ mol}^{-1}$ at a tertiary C-H bond) whereas with OH radicals the difference is very small ($E < 10 \text{ kJ mol}^{-1}$). The activation energy of the intramolecular alkylperoxy radical isomerization is a major controlling factor of the AIT of a fuel. Several types of H atom abstraction may occur in the reaction;

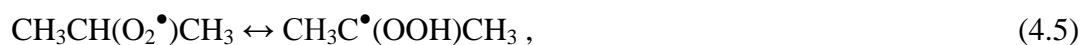


The first aspect of the magnitude of the activation energy relates to the “strain energy” of the transition state in the rearrangement. If it is a “tight” ring then there is a high strain energy. As the number of atoms in the ring increases it becomes

slightly more relaxed and so there is a lower strain energy. However, if the ring gets too large then entropy considerations may start to push the activation energy back up again. The second factor refers to the earlier point of the classification of the C-H bond, with the bond strengths being in the order of primary > secondary > tertiary. The basis on which alkylperoxy radical isomerization is classified may be illustrated with respect to the rearrangement of propylperoxy radicals, as follows: The isopropylperoxy radical may undergo two possibilities;



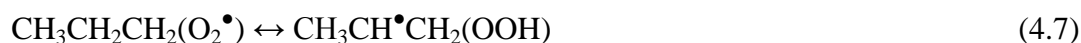
which involves the transfer of a primary C-H from four atoms away via a five membered ring. This is classified as a (1:4p) transition. There is also the possibility of a transfer of the remaining secondary H atom via



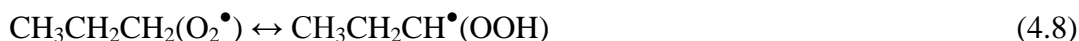
which involves a four membered ring and is classified as a (1:3s) transition. Notice that in these two cases there are six primary C-H bonds that are susceptible to transfer in the (1:4p) rearrangement, whereas there is only one secondary C-H accessible for the (1:3s) rearrangement. These probabilities also contribute to the overall rate and must be taken into account via the pre-exponential factor. A similar analysis for the normal propylperoxy radical reveals



as a (1:5p) transition with three primary H atoms being accessible,



as a (1:4s) transition with two secondary H atoms being accessible, and



as a (1:3p) transition with two primary H atoms being accessible.

If we allow that the length of the alkane chain or the position of a particular peroxy linkage does not affect the activation energy for the internal rearrangement, then a generalized table can be constructed. That is, the (1:4s) rearrangement for the n-propylperoxy radical shown above is regarded to have the same activation energy as, for example, the (1:4s) rearrangement of the secondary butylperoxy radical;



Proceeding on this basis we have activation energies, derived from EXGAS as shown in Table 4.1. Not all cases were accessible from the mechanisms that were examined. Nevertheless it can be seen that there is a trend to lower activation energy as the ring structure becomes looser and also for tertiary < secondary < primary C-H transfers. For any alkane structure, the greater numbers of isomerizations that become possible involving transfer in the bottom right hand part of the table, the greater will be the reactivity.

	1:4	1:5	1:6	1:7
Primary (p)	17900	14100	12600	12100
Secondary (s)	16400	12600	11100	10600
Tertiary (t)	14800	11100	-	-

Table 4.1. Activation energies (expressed in K as E/R) for $\text{RO}_2 \rightarrow \text{QOOH}$ reactions of normal alkanes.

These factors will affect the branched alkane isomers similarly, with only tight rings being able to be formed at a greater proportion of primary sites. The probability of a type of reaction occurring is again taken into account by the pre-exponential factor, that is, the number of H atoms that are accessible for the

particular isomerization. A combination of all these factors can “optimize” the activation energies, increasing reactivity and thus lowering the temperatures and pressures required to bring about autoignition and associated phenomenon [185].

To investigate the influence of hydrocarbon structure, a number of comprehensive mechanisms, in addition to those already presented in this chapter, were generated using EXGAS for the fuels of n-pentane, 2,3-dimethyl-pentane and 2,2,3-trimethyl-butane. The two branched alkanes were selected in order to make a direct comparison to results from n-heptane, for which they are branched isomers. The structure of n-heptane is $\text{CH}_3\text{CH}_2\text{CH}_2\text{CH}_2\text{CH}_2\text{CH}_2\text{CH}_3$, for 2,3-dimethyl-pentane it is $\text{CH}_3\text{CH}(\text{CH}_3)\text{CH}(\text{CH}_3)\text{CH}_2\text{CH}_3$ and for 2,2,3-trimethyl-butane $\text{CH}_3\text{CH}(\text{CH}_3)_2\text{CH}(\text{CH}_3)\text{CH}_3$. A qualitative analysis of the possible modes of alkylperoxy radical isomerizations for these isomers could be used to illustrate how their reactivities might be expected to differ. However, the complexity of this argument is so great that we cannot begin to attack the relative reactivity in anyway like what can be achieved in a fully quantitative computer analysis. The patterns of behaviour can be examined via p-T_a ignition diagrams as has been conducted individually in this chapter for a range of fuels. However, a problem arises in that there is a lack of experimental data conducted at similar conditions. Alternatively, we can make comparisons to the autoignition test at 1 atm, for which there is a large amount of data available, as discussed in Section 4.7.3.

4.7.2 Evaluation of numerically predicted p-T_a ignition diagrams of n-butane and n-hexane for stoichiometric mixtures in air

The experimental p-T_a ignition diagrams for stoichiometric mixtures of n-hexane and n-butane in air have been measured by Chamberlain and Townend [186] in a stainless steel closed vessel (0.19 dm³) and are shown in Fig. 4.24. Using the comprehensive EXGAS models for these fuels, a direct comparison has been made in order illustrate some of the fundamental aspects of the numerical comparisons to AIT.

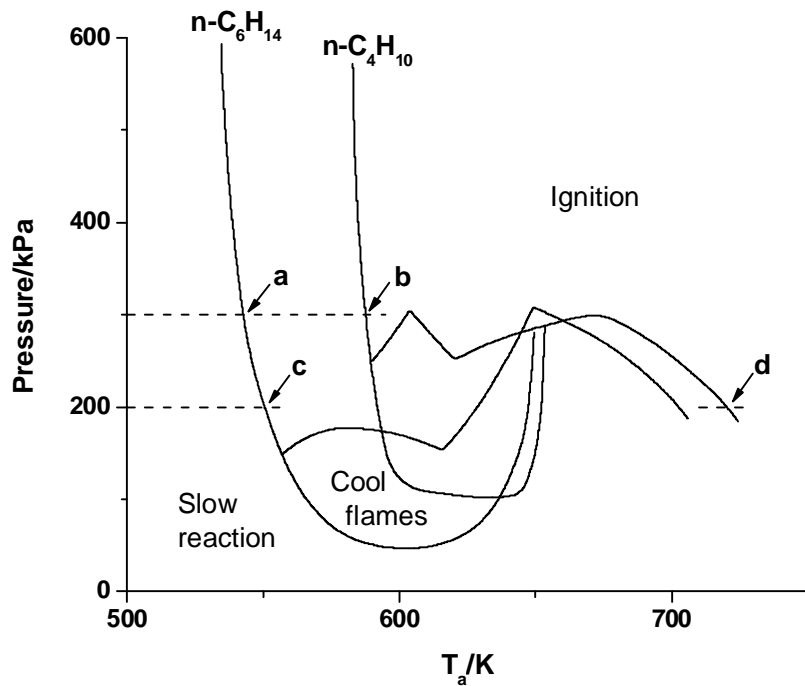


Fig. 4.24. Experimentally determined p - T_a ignition diagram for stoichiometric n-hexane in air and stoichiometric n-butane in air, in a 0.19 dm^3 cylindrical vessel [186].

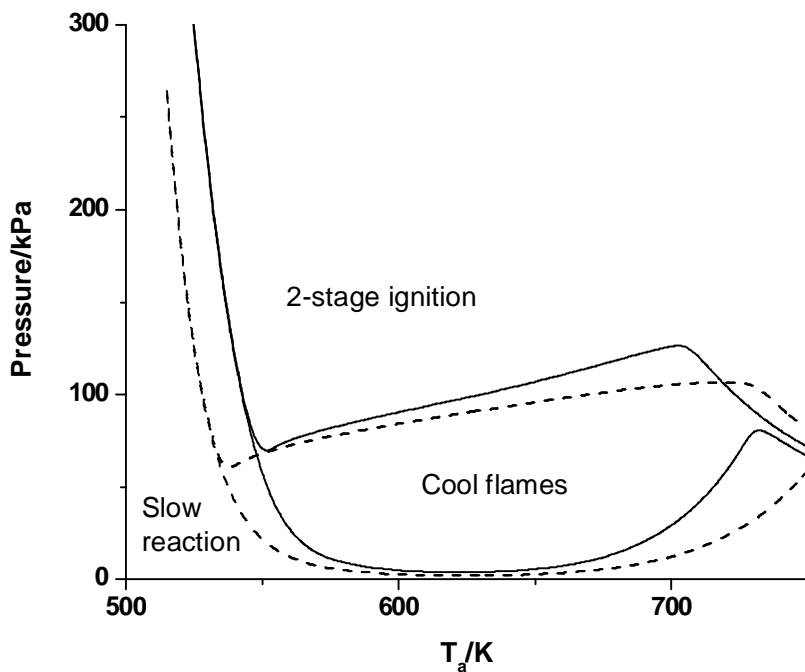


Fig. 4.25 Comparison of numerically predicted p - T_a diagrams of n-butane (solid line) and n-hexane (dashed line) for stoichiometric mixtures in air, using mechanisms generated with the EXGAS program. A heat transfer coefficient of $1.5 \times 10^{-3} \text{ W cm}^{-3} \text{ K}^{-1}$ was used.

The comparison of Figs. 4.24 and 4.25 shows that the general trend of decreasing minimum AIT with increasing carbon number for normal alkanes is reproduced by the mechanisms generated using EXGAS. However, the demarcation between magnitudes of AIT is not as pronounced in the numerical prediction as it is witnessed in the experimental results. Furthermore, at temperatures above 720 K the numerically predicted AIT reverses, in contrast to what is witnessed in the experiment. The lowest pressures at which AIT occurs are under predicted by the output from the mechanisms and the cool flame regions displayed by the generated p - T_a ignition diagrams of the mechanisms extend to temperatures higher than those observed experimentally, with both of these observations being typical of the previous experimental comparisons presented in this Chapter. The low temperature slow reaction/ignition boundaries generated by the mechanisms, on this occasion, are produced at temperatures below those observed experimentally in these reactive mixtures.

4.7.3 Predicted minimum autoignition temperature from comprehensive mechanisms for a range of alkanes and their isomers

For present purposes we focus on the general hierarchy of AIT for a range of hydrocarbon fuels and their relative positions and magnitudes, as modelled in a spatially uniform closed vessel. The experimental procedure used to quantify the AIT of a given fuel, involves the injection of a prescribed volume of liquid fuel (0.2 cm^3) or an excess of gaseous fuel into an open conical flask of volume 200 cm^3 , in which the temperature is stabilized with the use of a thermostat. Evaporation and partial mixing follows and if the temperature is sufficiently high then autoignition will occur and is detected visually. If ignition does not occur within 300 seconds, then the test result at that specific temperature is classified as non ignition. The vessel temperature is then increased in small increments in successive experiments, until ignition is observed. This temperature is defined as the minimum ignition temperature (MIT) or autoignition temperature (AIT) and is

tabulated in a variety of sources. The EC test procedure (IEC 79-4, formerly BS 4056) requires that the apparatus is calibrated to match reported data using n-heptane (220 °C), ethene (435 °C) and benzene (560 °C).

The data obtained in this way relate only to behaviour in a vessel of particular size and shape, although they do convey comparative reactivities. No information can be obtained about concentration dependence or even the concentration at which the MIT is found. Moreover, as non-isothermal reaction evolves, buoyancy and convection sets in, which may lead to loss of material from the open vessel.

Clearly the full numerical simulation of the physics and chemical development would require CFD calculations coupled to detailed chemical models. Even in closed vessels the physical effects make numerical prediction of autoignition very difficult especially since the flow fields, affecting both heat and mass transport, will be strongly pressure and vessel size dependent. Major approximations must be made to the physics and this therefore limits the possibility of obtaining a fully quantitative match [2,187].

The dependence of AIT on composition has been numerically determined for a range of fuels using mechanisms generated by EXGAS and described from Section 4.2 onwards (Fig. 4.25). The AIT boundaries were determined by conducting a series of runs over a fixed composition range at 1 atm and making bisections of ambient temperature (see Section 4.11 for further details). The procedure was repeated for each fuel. Fig 4.26 shows there to be a strong dependence of AIT on composition, with MIT occurring in very fuel rich mixtures with the majority of fuels falling in the composition range $7.49 < \phi < 9.26$, with the exception of cyclohexane whose MIT occurs at $\phi = 5.2$. It may be expected that the most reactive mixtures for n-heptane and its branched isomers would be the same. However, this is not the case with greatest reactivity for 2,3-dimethylpentane being in slightly richer mixtures than n-heptane and the greatest reactivity for 2,2,3-trimethylbutane being in slightly richer mixtures than either of its isomers. The origin of higher reactivity being observed in fuel rich mixtures can be traced to the composition dependence of the rate of heat release in the low

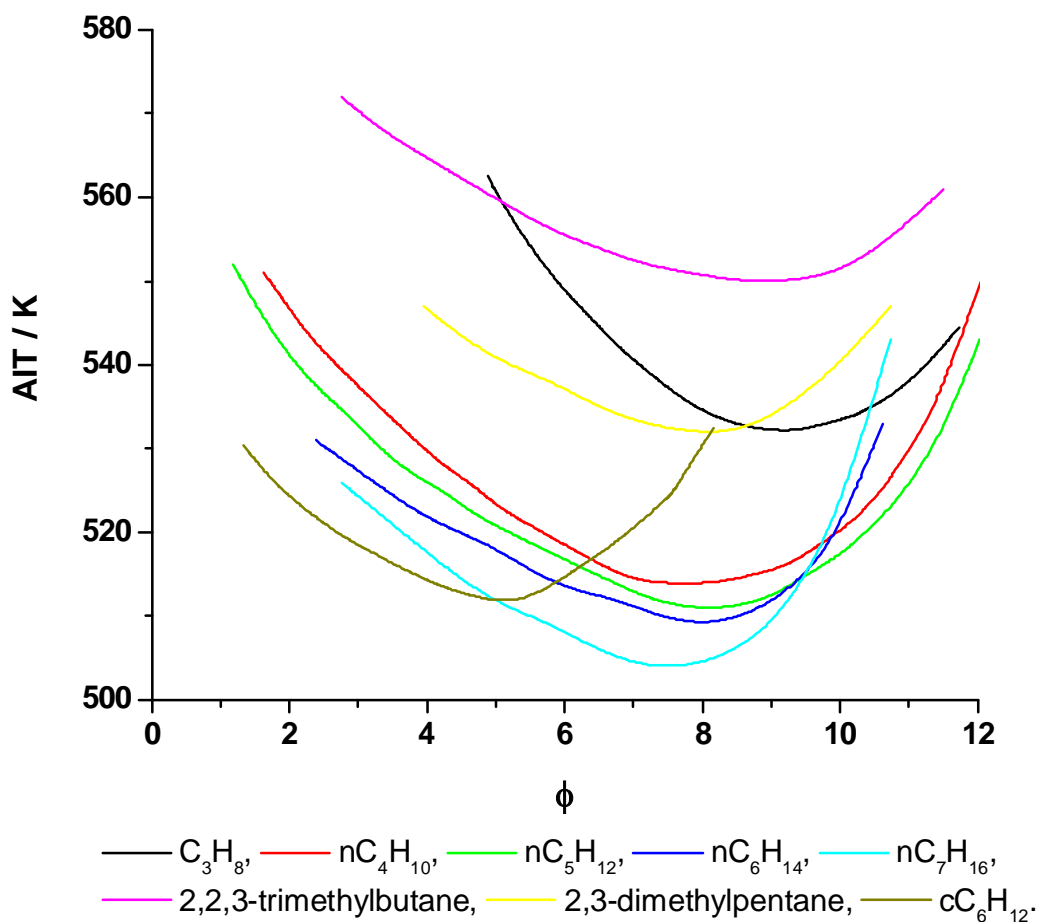


Fig. 4.26. Variation of predicted AIT for a range of alkanes, derived from comprehensive kinetic models generated by EXGAS. A heat transfer coefficient of $1.5 \times 10^{-3} \text{ W cm}^{-3} \text{ K}^{-1}$ was used and initial pressure was fixed at 1 atm.

Reactant	Measured MIT / K	Predicted MIT / K
C_3H_8	766	532
n- C_4H_{10}	705	514
n- C_5H_{12}	557	511
n- C_6H_{14}	533	509
c- C_6H_{12}	543	511.5
n- C_7H_{16}	520	504
2,3-dimethylpentane (C_7H_{16})	610	532
2,2,3-trimethylbutane (C_7H_{16})	708	550

Table 4.2. Predicted and measured minimum ignition temperatures (MIT). Experimental data are taken from Jackson [182], as determined by a modification of the ASTM method by Scott *et al* [183].

temperature range and is much related to the negative temperature coefficient (NTC), the kinetic origins of which were discussed in Section 4.1.1 [185].

Table 4.2 shows a comparison between the predicted and measured MIT values. The qualitative hierarchy of MIT for the range of compounds is well captured by the EXGAS models. However, the quantitative demarcation between fuels displayed by the models is not as pronounced as is observed experimentally. In particular, three fuels show large quantitative departures experimentally, in relation to other fuels: Propane, n-butane and 2,2,3-trimethylbutane all display experimental MIT values in excess of 700K, while the other fuels have values of *ca.* 550 K. Although no comprehensive experimental investigations have been undertaken to determine why such quantitative departures occur, the issue can be elucidated by the analysis of Fig 4.24, showing the comparison of experimental p - T_a ignition diagrams for n-butane and n-hexane at $\phi = 1$. The measurements shown in Fig. 4.23 are in much leaner mixtures than those at which MIT occurs and are therefore less reactive. For comparative reactivity, we may consider pressures above atmospheric of 200 kPa and 300 kPa. At 300 kPa, an MIT value of 530 K, as denoted by point (a) on Fig. 4.24, would be observed for n-hexane and a value of 590 K, as denoted by point (b), for n-butane. Hence, both of these values fall on the “low temperature branch” of ignition. By contrast, running the AIT test at 200 kPa would yield values of AIT of 550 K (point (c)) and 725 (point (d)) for n-hexane and n-butane, respectively. This significantly large difference arises because there is insufficient heat release for autoignition of n-butane at this pressure, whereas there is sufficient heat release for autoignition of n-hexane to occur. The cool flame phenomena exhibited by n-butane at 200 kPa would not be detected by the visual inspection employed in the AIT test. This implies that the explanation for the marked distinction between n-butane and n-hexane at 200 kPa in their stoichiometric mixtures becomes a feature in rich mixtures at 1 atm (101.325 kPa). Although there appear to be no explicit experimental results to confirm this interpretation, it is supported by the general trend of greater reactivity in richer mixtures. Another important point is in regard to why the “low to intermediate” temperature demarcations are not displayed by the numerical

predictions. Although large simplifications have been made to the physics of the numerical prediction, the root cause of this may be attributed to the general lack of distinction between fuels, which is likely to have its origins in poorly known parametric information in the mechanisms. These issues are further addressed in Section 6.2.

4.8 Discussion and conclusions

Comprehensive mechanisms for the combustion of equimolar propane + oxygen in a closed vessel at low temperature and pressure have been qualitatively evaluated. Both mechanisms exhibit excessive reactivity in terms of system pressure relative to experimental observations. Two kinetic schemes have been used to simulate ignition of lean mixtures of n-butane in air. The kinetic schemes have different strengths and weaknesses but there seems to be a common difficulty in reproducing the ignition boundary for $\phi < 0.6$. Further comprehensive mechanisms generated using the EXGAS program for the oxidation of n-pentane, n-hexane, n-heptane and cyclohexane show some general trends, they are;

- (a) Good reproduction of the experimentally observed “low temperature branch” of ignition.
- (b) The minimum pressure at which ignition occurs is lower than that observed experimentally.
- (c) Cool flames occurring at very low pressure, in contrast to experimental observations.
- (d) The cool flame region extending to temperatures higher than those measured experimentally.
- (e) Reduced distinction between the behaviour of different fuels.

There are a number of factors which may be causing the four negative trends. Firstly, there is the explanation of the over simplification of the physics in the spatially uniform numerical runs. The effects of buoyancy, convection and turbulence have been totally neglected in the numerical simulations so it may be argued that increased turbulence at intermediate temperatures may aid heat loss,

decrease reactivity and give rise to trend (d). If this were the case we might expect to see a loss of reactivity at higher pressures and effectively cancelling the trends of (b) and (c) at the same corresponding intermediate temperatures, but this is not so evident and what we get is a general horizontal “stretching” of the cool flame region. To confirm whether or not the physical effects are the cause of trend (d), a test could be carried out by coupling reduced kinetics to the appropriate heat and mass transport, and then examining its influence on the cool flame region, using two dimensional axis-symmetrical closed vessel calculations. It would not be necessary to compute the entire ignition diagram using such a higher dimensional simulation, but to ascertain whether a shift in the cool flame boundary had occurred (in terms of intermediate operating temperatures). Such calculations would, however, require significant mechanism reduction to be computationally practicable.

Further explanations for the discrepancies between experiment and numerical predictions lie in mechanistic imperfections. Heterogeneous reactions with the vessel wall are not included in any of the EXGAS mechanisms, and their inclusion may contribute to discrepancies of the ignition diagram. Moreover, poorly known rate and thermochemical parameters may be attributed to the observed discrepancies, with mechanisms exaggerating the NTC region whilst displaying an over-reactivity at other operating conditions. Mechanistic and parametric uncertainty may also explain why the numerically predicted AIT for a range of fuels, although displaying a qualitatively correct hierarchy, shows a lack of distinction between fuels when compared to the experimental results. The uncertainty of parameters in the EXGAS propane oxidation mechanism will be examined in Section 6.2.

In the next Chapter, the EXGAS generated comprehensive mechanisms for propane, n-butane and cyclohexane which have been evaluated here will have their numbers of species and reactions reduced via automated sensitivity analysis reduction procedures.

Chapter 5

Automated Sensitivity Analysis Based Reduction Methods and Rate of Production Analysis

The purpose of this Chapter is to describe the automated mathematical techniques employed, and the information required in order to be able to reduce the numbers of species and reactions in a mechanism while still retaining satisfactory agreement with the predictive behaviour of the full scheme. Applications are made to mechanisms for propane, butane and cyclohexane. The methods used in this Chapter are for reduction to a short or skeleton scheme which contains only the essential or necessary subset of species and reaction steps required to reproduce important reaction features. The skeleton scheme is produced by purely removing the unnecessary or redundant species and reactions and the resulting kinetic representation contains only the elementary reactions present in the comprehensive scheme, for which the rate constant is explicitly represented.

Having produced a skeleton scheme, there are procedures which can be applied to further reduce the numbers of system variables such as slow manifold techniques or reaction and species lumping. However, the resulting scheme produced by these further reduction methods will contain new formulations for the system variables and will no longer comprise of only the species and reactions

which were contained in the original comprehensive mechanism. The methods to enable this further reduction will be introduced and applied in Chapter 6.

To identify the necessary components, local sensitivity analysis methods available in the KINALC package [30,31] were fully incorporated into the SPRINT [48] based simulation software. Pre-processing of input variables and post-processing of sensitivity analysis results was completely automated via the use of UNIX shell scripts. KINALC subroutines were selected over those of its predecessor KINAL for the main reason that KINALC is able to interface with CHEMKIN, accepting its text file format mechanism as input. This makes the operation of the reduction software very “user friendly” and easy to interpret kinetically. KINALC is also superior in its handling of temperature dependent, pressure dependent and weighted third body reactions. There are other advantages that KINAL has over KINALC, such as unlimited reactants or products in a reaction step and the ability to calculate initial concentration sensitivities, but these were not considered essential in the present application [29].

The automated sensitivity analysis based methods presented here are applied to three Nancy kinetic schemes, describing the reactant mixtures; equimolar propane + oxygen, lean n-butane + air and stoichiometric cyclohexane + air, all previously validated in comprehensive kinetic form against experimental data in Chapter 4. The reduced mechanisms are validated at progressive stages of reduction by comparison of time dependent behaviour and ignition diagram output from the full mechanisms. The success of the techniques is evaluated by comparison with a number of reduced mechanisms produced using alternative reduction techniques and published in the available literature.

5.1 Automatic selection of time points for sensitivity analysis

By definition a local sensitivity analysis applies only to the effect of small perturbations to each variable or parameter, imposed successively on a chemical composition within a reacting system at a single point in time (or space). The resulting effect on specified output, either individually or collectively, quantifies

(and therefore ranks) the extent to which each variable or parameter controls the behaviour at that point. Because large changes in concentrations and conditions are encountered as time elapses from the start to the end of a combustion process, or as initial ambient conditions are changed, the local sensitivity information acquired from a single point would be insufficient to determine the importance of chemical reactions or species over the entire range of conditions encountered. Therefore a range of time points with varying conditions is needed, encompassing the start through to the completion of an oxidation process at a number of initial conditions, but without the unnecessary duplication of very similar conditions. Thus, the collation of information from representative local conditions allows us to gain insight into the full chemical kinetic mechanism and enables mechanism reduction to a scheme that incorporates only the relevant components for the purpose intended. The range of conditions selected will determine the domain to which the resulting reduced mechanism will be applicable and it follows that a reduced scheme that has been derived for a particular use will not necessarily serve another purpose. This effect is exploited by the techniques of adaptive chemistry [41] whereby small skeleton mechanisms are produced for narrow ranges of operating conditions.

Using the simulated ϕ - T_a ignition diagram of the system of lean n-butane in air as an example in Figure 5.1, a number of different operating conditions are selected covering a representative range of the temperature/composition space at which sensitivity analysis and mechanism reduction are to be performed. The most complex oxidation phenomena is multi-stage ignition so this is well represented by the choice of input operating conditions in the critical region close to the ignition boundary. The maximum temperature reached in the cool flame is a fundamental aspect of the transition to ignition; therefore, an operating condition in the cool flame region is selected to ensure competing reactions which contribute to the lower attainment of this temperature are adequately represented. The oxidation chemistry which evolves during slow reaction is relatively simplistic and will be covered by the other behavioural regions and so no operating conditions are required here. This selection process could be similarly

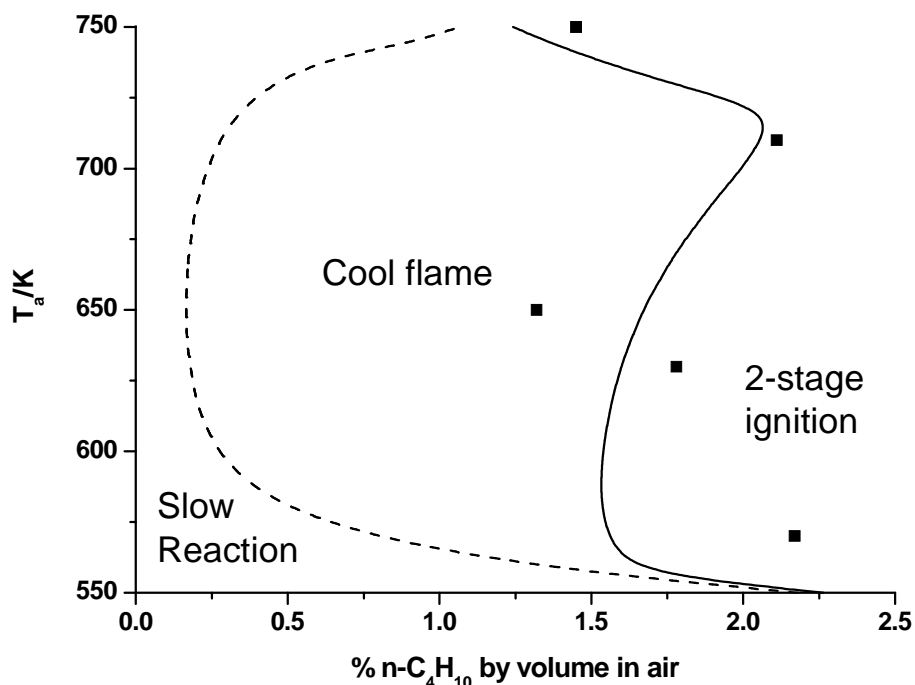


Figure 5.1. Simulated ϕ - T_a ignition diagram at 0.2 MPa from the full, EXGAS n-butane mechanism, showing regions of ignition, cool flames, and slow reaction. Black squares; user selected operating conditions of reduction.

performed using a simulated p - T_a ignition diagram for a given fuel. The procedure was then automated by the use of a UNIX shell script to run the integration code at each chosen condition, and manipulate the output data files. Time points from the calculated temperature profiles at the chosen operating conditions are automatically selected, as shown in Figure 5.2 based on the following criteria.

To capture the important species and reactions in the initial stages of reaction, the first time point is chosen to be the third integration output point. Subsequent time points are selected at ΔT values of 10, 50, 100, 200, 300 and 400 K and additionally at any temperature gradient maxima and minima. The combination of these criteria ensures that information covering the entire range of conditions applicable throughout the integration is used in the identification of important species and reactions [145].

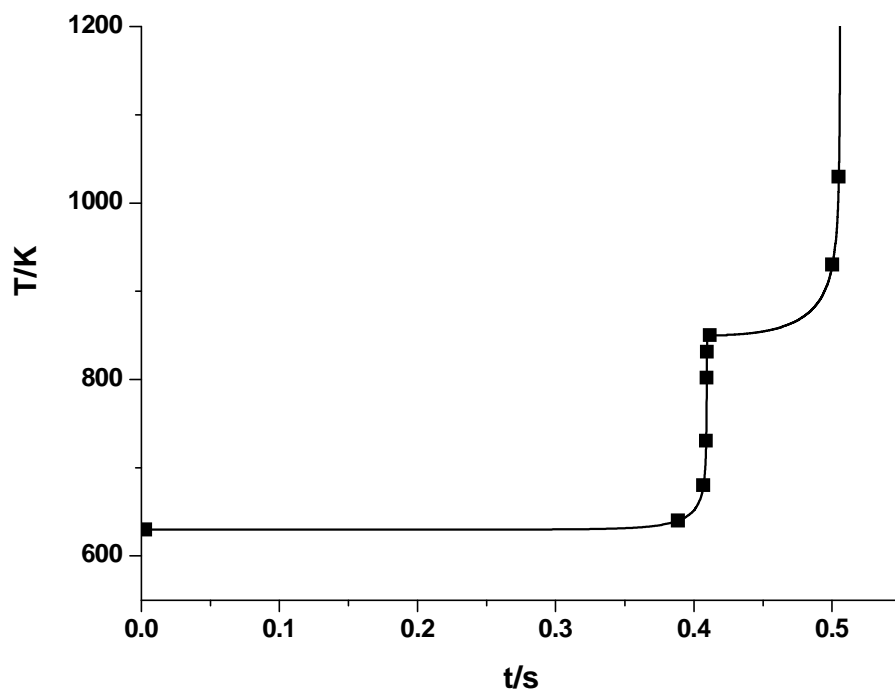


Figure 5.2. Automatically selected time points (black squares) for sensitivity analysis during simulated 2-stage ignition at 630 K, 1.78 % n-C₄H₁₀ by volume in air and 0.2 MPa total pressure.

5.2 Removal of redundant species

The initial stage in finding an appropriate sub-mechanism is the identification of redundant species which can be eliminated from the mechanism without detriment to the modelling aims. Information related to the automatically selected time point conditions and rate data from the mechanism are used to identify necessary species via the investigation of the Jacobian matrix [27]. The application of this algorithm requires that the user specifies important species. These species should be those which are essential to the modelling aims and will always include primary reactants. In a chemical engineering context, the important species may also include important bi-products. In a combustion context, these species are usually specified to be fuel and/or oxygen. Other species such as OH radicals may also be considered important, however, the desire to use chemical intuition in order to specify a larger list should be resisted in order to

allow the formal mathematical procedure to run its course. The concentration of the important species will depend heavily on those of a number of other species in the mechanism and we may classify these to be necessary species. Necessary species are required to reproduce the concentration profiles of the important species and to retain important kinetic features displayed by the mechanism. The concentration of each necessary species may effect the concentration of the important species both directly (by participating in a common elementary reaction), and indirectly (through other intermediate species). Those species not designated as important or necessary are the redundant species, although the classification of certain species may depend on the amount of error which is permissible in the reduced mechanism.

Perturbations to the concentration of a species will change the rates of those reactions in which this species is a reactant. This may have a direct effect on the concentrations of other species which are reactants or products of these reactions. The primary concentration changes then may cause perturbations to the concentration of other species through indirect couplings. The aim of the iterative analysis of the Jacobian matrix is to identify those species which are strongly coupled to the selected important species either directly or indirectly. The sensitivity of the rate of production of an N -membered group of important and necessary species to a change in concentration of species i , B_i , is given by:

$$B_i = \sum_{n=1}^N (\partial \ln f_n / \partial \ln c_i)^2, \quad (5.1)$$

where f_n is the rate of production of species n as shown in equation 3.26. The higher the B_i value the greater the direct effect of species i on the rate of production of important species. At the beginning of the iterative procedure the N -membered group will consist only of the important species (fuel and/or oxygen). After calculation of the B_i value for each species, the necessary species whose perturbation had the greatest direct effect on the rate of production of the important species and therefore having the highest B_i value (after the important species) will join the N -membered group. The iterative procedure is repeated in

order to consider necessary species with indirect effects on the important species, whereby the B_i values are calculated for all species, and then the species outside of the N -membered group with the highest B_i value is incorporated into the N -membered group. This procedure is repeated so that one by one, species join the N -membered group until there are no more species left to join. The effects of perturbations of third body species on the rates of production of the species inside the N -membered group are also taken into account by the calculation. The rates of production must be calculated to a high degree of precision because the results can be very sensitive to any rounding error. At some point during the iterations as this procedure is repeated, the vector \mathbf{B} converges and a reasonable gap appears between the ranked $\log B_i$ values of necessary and redundant species as they form definite groups. This is illustrated in Figure 5.3 in the form of a typical results file output by the program. The magnitude of this gap may then be considered during the application of thresholds, in the subsequent post-processing stage. Only the gap between $\log B_i$ values of necessary species (marked by a star on Figure 5.3) and redundant species may be considered. Each iteration may or may not be considered as a candidate for the subsequent application of thresholds. Only candidates with necessary species having the highest ranked $\log B_i$ values are considered converged and acceptable, i.e., if a redundant species has a higher $\log B_i$ value than one or more of the necessary species, then this particular iteration is disregarded.

Equation 5.1 is applied using algorithms incorporated into the SPRINT code originally implemented in the KINALC package [30,31]. Rather than treating the simulation and sensitivity analysis modules as separate entities the KINALC subroutines were embedded within the simulation code for reasons of convenience and simplicity. This speeds up the reduction process by virtue of not having to record and reread information in files, which in turn saves disk space. This strategy also pre-empts rounding errors via the avoidance of the truncation of significant figures [188]. A number of reduction thresholds are applied to the lists of iterations generated at each time point in order to identify the most appropriate

time = 4.085400e-01 T = 8.040119e+02

You are interested in how closely are the species connected kinetically to the core species below:

O2

Effect of the perturbation of the concentration of each species on the rate of the following group of species (log units) :

	O2	*	
1	O2	*	2.330
2	R11C2H5		2.057
3	R17C2H500		2.047
4	R21C4H9		0.383
5	R24C4H900		0.241
6	R4CH3		0.070
7	R8CH300		0.019
8	R20C4H9		-0.642
9	R30OH		-0.654
10	R5CHO		-0.753

Log B_i values

(Start of iterations, unconverged)

(etc. Intermediate iterations omitted for brevity)

Now let us add the highest ranked non-group member species to the group. (Calculation No 23)

Effect of the perturbation of the concentration of each species on the rate of the following group of species (log units) :

	O2	R11C2H5	R17C2H500	C3H7C000H
	C4H900H	R30OH	R20C4H9	R23C4H900
	C4H10-1	R2OH	HCHO	R1H
	R7CH30	R4CH3	N2	R15C2H50
	C2H500H	R8CH300	C2H4Z	C2H50H
	CH3CHO	H2O	C4H8Y	

1	R15C2H50	*	9.201
2	C2H500H	*	9.012
3	R11C2H5	*	8.141
4	O2	*	8.089
5	R17C2H500	*	8.082
6	R2OH	*	7.836
7	R8CH300	*	7.314
8	R1H	*	7.306
9	R7CH30	*	7.025
10	C4H10-1	*	6.983

(Converged iteration)

(Necessary species ranked 11 to 19 omitted for brevity)

20	C4H900H	*	5.619
21	CH3CHO	*	5.529
22	H2O	*	5.347
23	C4H8Y	*	5.332
24	R30C4H800H		5.065
25	R32C4H800H		5.056
26	R41C4H80000H		4.911
27	CH300H		4.724
28	R36C4H80000H		4.687
29	R31C4H800H		4.674
30	C4H700HY		4.427

Appearance of a gap between ranked log B_i values

(etc. Further iterations omitted for brevity)

Figure 5.3. Example results file for the identification of necessary species via investigation of the Jacobian matrix. Starred species represent those which are in the group of N -membered group of important and necessary species. This calculation corresponds to the 5th time point of Figure 5.2.

iterative candidates of groups of necessary species and create reduced mechanisms of varying sizes. The reduction thresholds are;

- (a) the minimum B_i value,
- (b) the minimum gap between the ranked B_i values of necessary and redundant species,
- (c) the minimum number of species and
- (d) the number of species after which criterion (a) can be ignored.

This strategy is different to the way KINALC alone would operate, where the selection is made via a time consuming visual inspection by the user. This detailed set of criteria allows the user to have good control of the size and accuracy of the resultant reduced mechanism. At each time point there may be a number of candidate ranked lists of species in the iteration which satisfy these criteria. In each case the program will identify the candidate which satisfies these criteria with the lowest number of necessary species.

Subset lists of necessary species are identified at each preselected time point, as exemplified by Fig. 5.4. The union of necessary species is taken over all the time points at each of the conditions and the irreversible consuming and reversible reactions of all redundant species are removed. After species removal there will be a certain amount of error when comparing the output from the reduced scheme to that of the full scheme. Generally, the larger the number of species removed the greater will be that error. The extent of allowable induced error of a reduced mechanism will depend on its application. So the selection of the optimum mechanism must be made on the basis of mechanism performance, assessed from comparisons of temperature profiles and ignition diagrams generated by a number mechanisms with varying numbers of species obtained by applying varying reduction criteria to the candidates produced from the iterations of equation 5.1. However, the entire recalculation of equation 5.1 for each new set of thresholds tested is avoided by saving and manipulating the output sensitivity analysis files.

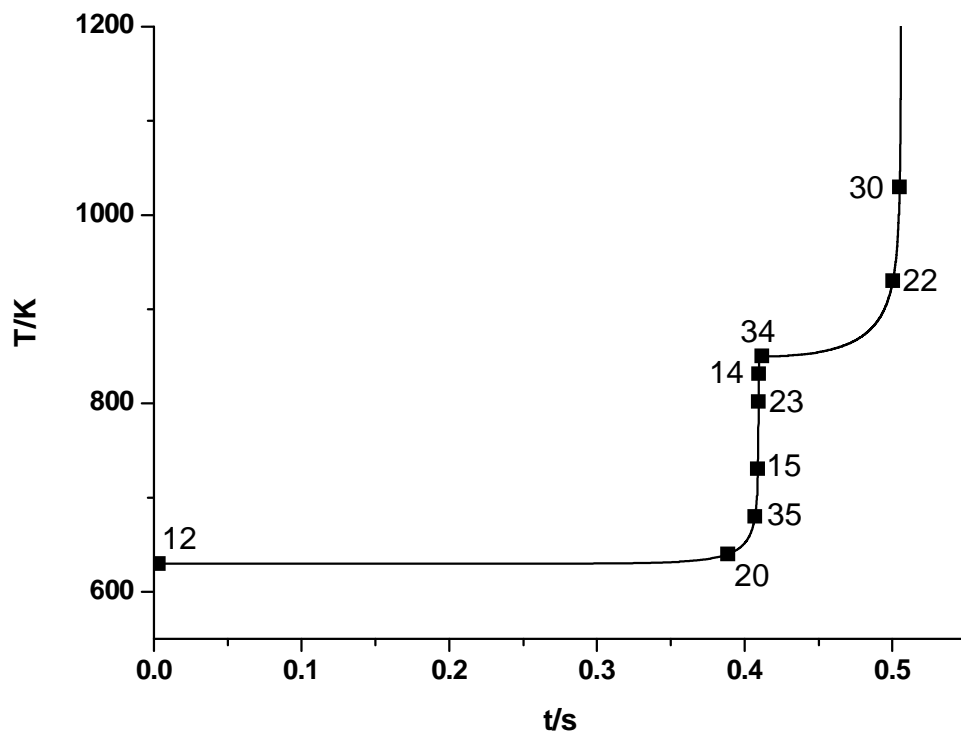


Fig. 5.4. Numbers of necessary species identified during simulated 2-stage ignition at 630 K, 1.78 % n-C₄H₁₀ by volume in air and 0.2 MPa total pressure.

Further, varying the reduction thresholds will result in mechanisms of varying size and accuracy when their output is compared to that of the full mechanism. However, two different sets of criteria may produce mechanisms of similar size but not necessarily of similar quality, due to a different combination of necessary species over all the time points considered. This is exemplified in Fig. 5.5, whereby as each criterion is varied while others are held constant, the mechanisms are progressively reduced. However, the comparison of temperature trajectories of mechanisms produced by different sets of criteria, but having the same numbers of necessary species (203), shows that the difference in their output accuracy when compared to the full scheme is considerable. Therefore, the effect of variations of the reduction criteria should be investigated in order to achieve the

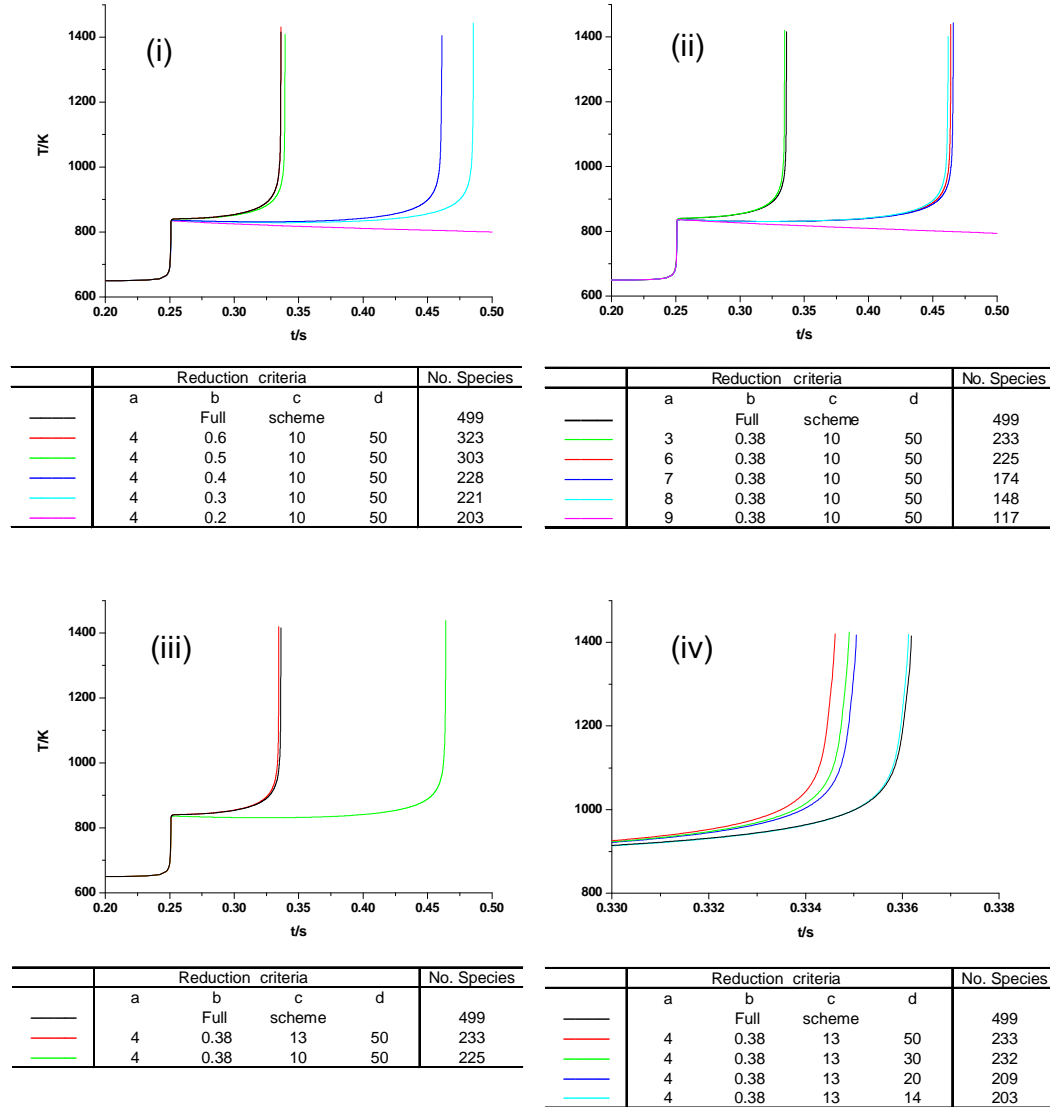


Fig. 5.5. The effect of varying each reduction criterion individually while keeping others constant at a selected operating condition of 650 K and 135.5 kPa for stoichiometric cyclohexane in air. (i) The effect of varying the minimum gap criterion. (ii) the effect of varying the minimum allowable $\log B_i$ value. (iii) the effect of varying the minimum allowable number of necessary species. (iv) The effect of varying criterion d, the number of species after which the minimum allowable $\log B_i$ value can be ignored.

optimum species reduction. A threshold of 4 for criterion (a) has proved to be successful on a number of occasions, along with values in the range of 0.25 to 0.4 for criterion (b). Criteria (c) and (d) typically achieve success in the range of 10 to 20. The drawback of this approach is that it increases the amount of required user intervention in the process.

This technique can remove large numbers of species from mechanisms, and the larger the mechanism, the larger the expected number of identifiable redundant species will be. However, it is possible that some redundant species will remain in the mechanism having not been identified as redundant by the first iterative analysis of the Jacobian matrix. It may be possible to remove these species by performing a second stage reduction on the partially reduced mechanism. For very large schemes it could be argued that more than two stages of reduction are required. In each case the majority of the redundant species are removed by the first species reduction, and the numbers of species removed by the second or subsequent species reductions are progressively less and less. The need to perform a second stage of reduction is because during the final iterations the last species to join the N -membered group of species are always redundant. However, the species that join the group in the early stages of the iterative procedure are not always necessary and redundant species may have joined the N -membered group before all necessary species have been incorporated. These incorporated redundant species can then be more easily removed by performing a second of stage reduction. The need for a two-stage reduction strategy is not unique to Jacobian analyses but has also been used by other researchers in the reduction method of direct relation graphs [40]. A two stage reduction for propane is illustrated in Section 5.6.1.

The kinetic intervention of nitrogen and the noble gases, helium and argon, are mainly as third body species in termolecular reactions, although nitrogen may react directly with species in some high temperature applications. When applying these methods to remove species, it is always the case that when these gases are not present in the initial reactant mixture they will be identified as redundant. However, the inerts will be retained in the reduced mechanisms for modelling convenience, i.e., comparison to experiments which use these gases in the reactant mixtures.

After comparison of full and reduced models via ignition diagrams and temperature trajectories the reduced mechanism with the desired degree of accuracy and reduction is selected. The resulting mechanism is then converted to

irreversible form for further analysis with respect to reaction removal and further species reduction.

5.3 Removal of redundant reactions: Sensitivity analysis

Having obtained a partially reduced scheme in which the redundant species have been removed, methods are then employed to significantly reduce the number of reactions without further detriment to model performance. Local sensitivity analysis is used to identify redundant reactions by consideration of either the sensitivity of the concentration of necessary species to perturbations in the rate parameters of each reaction given by the rate sensitivity matrix \tilde{S} , or the sensitivity of production rates of necessary species to perturbations in the rate parameters of each reaction given by rate sensitivity matrix \tilde{F} [30,31,189]. Zsély and Turányi [190] have compared the two methods as implemented in principal component analysis (PCA) (see Section 5.4 for further details on PCA), for mechanism reduction and application in a number of physical models for the case of hydrogen – air combustion. The results show that the two methods are equally effective in terms of their ability to identify an optimum subset of reactions. PCA of \tilde{F} (PCAF) proves to be simpler and faster, though PCA of \tilde{S} (PCAS) can provide additional information about the mechanistic couplings in a physical model. Due to its ease of computation, we will proceed with the local rate sensitivity matrix \tilde{F} , which is given by:

$$\tilde{F} = \frac{k_j}{f_i} \frac{\partial f_i}{\partial k_j}, \quad (5.2)$$

where k_j is the rate parameter of the j th reaction and f_i is the rate of production of species i . The effect of a change of each rate parameter on the rates of production of groups of necessary species can be quantified by a least-squares objective function B_j , where B_j is defined as:

$$B_j = \sum_i \left(\frac{k_j}{f_i} \frac{\partial f_i}{\partial k_j} \right)^2. \quad (5.3)$$

A reaction is considered important if it has a B_j value above a user-specified threshold. The calculation is applied consecutively to the automatically selected time points at a number of user-selected ambient conditions, as described in Section 5.1. The important reactions are collated from all of the considered time points and the redundant reactions (i.e. those reactions having no impact at any of the time points, as defined by the selection criteria) are then removed. The main disadvantage of the method employed in Equation 5.3 is that large amounts of data in the rate sensitivity matrix are not utilised. A more sophisticated method which examines the interactions between parameters stored in the rate sensitivity matrix is PCA [30,31,106,189] and will be discussed in the next section.

In order to be generally applicable, the reduced mechanism should contain species and reactions that have been collated over all local time-points considered. However, considerable improvement in the performance of the reduced models for a given size can be obtained by using time-point specific information about necessary species in the objective function analysed in the reaction reduction procedure. In order to achieve this, subsets of necessary species relevant for each specific time point are included within the objective function of Equation 5.3, rather than the entire group of necessary species. These subsets of necessary species have been identified via the investigation of the Jacobian matrix (Equation 5.1) at each time point considered as shown in Fig. 5.4. The effect of using this reaction reduction strategy is illustrated in Fig. 5.6 through the comparison of temperature profiles of reduced mechanism results obtained by applying Equation 5.3, with either the full set of species included in the summation i , or time point specific sets as identified by the local Jacobian matrix. Fig. 5.6 shows that by using time-point specific information, for a given size of reduced mechanism (73 species and 499 reactions), the performance is significantly improved compared to the equally sized reduced mechanism obtained using the combined species set. A similar result would follow with respect to PCA.

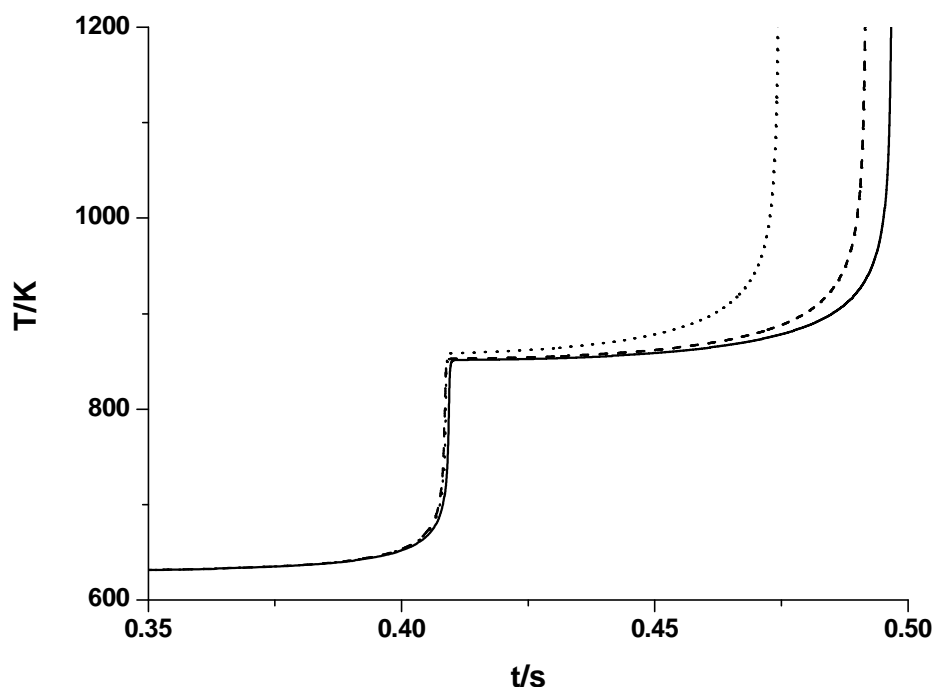


Fig. 5.6. A comparison of the effects of reaction removal using all necessary species or a subset at each time point in the objective function at $T_a = 630$ K for a mixture of 1.78 % n-C₄H₁₀ by volume in air at 0.2 MPa total pressure. Solid line: species reduced, 73 species and 715 reaction mechanism. Dashed line: subset reduced, 73 species and 449 reaction mechanism. Dotted line: all necessary species reduced, 73 species and 449 reaction mechanism.

5.4 Principal component analysis

PCA is a widely used statistical analysis tool for reducing the dimensionality of systems and finding subsets of variables which are highly correlated with each other. The analysis here is based on the eigenvalue-eigenvector decomposition of the cross-product matrix $\tilde{F}^T \tilde{F}$. The eigenvalues measure the significance of their respective eigenvector elements in the overall mechanism at the chosen time point. Each eigenvector represents a set of coupled reactions whose relative contributions are shown by the relative size of the eigenvector elements. Thresholds are defined for the significant magnitudes of the eigenvalues and eigenvectors thus providing an automatic way of deciding which reactions can be eliminated. Typically, threshold values for the eigenvalues are chosen between 1.0

$\times 10^{-2}$ and 1.0×10^{-4} and for the eigenvectors between 0.01 and 0.2 [30,191]. The choice of threshold governs the accuracy of the resulting scheme, although often for the eigenvalues a natural threshold exists where there is a large gap between successive eigenvalues. As before, the calculation is applied consecutively to several automatically selected time points at a number of user selected ambient conditions. Here also the important reactions are collated from all of the considered time points and redundant reactions are then removed. After selection of the most appropriate reduced reaction mechanism, the reduction is evaluated by comparison of ignition diagrams and temperature trajectories.

Because PCA is computationally intensive, especially for large schemes, the rational procedure is to apply it to schemes which have previously had species and reactions removed by the sensitivity methods described in Sections 5.2 and 5.3. This procedure has proved to be successful in the reduction of large schemes used to model atmospheric chemistry by Whitehouse *et al* [36]. When investigating a variety of thresholds to establish the correct sized mechanism with a balance between minimum number of reactions and accurate description of the full model, the recalculation of PCA should be avoided in order to save computational time and resources. This is achieved by saving and manipulating the output PCA results from the initial calculation using additional UNIX shell scripts.

5.5 Rate of production analysis

Redundant reactions can also be removed by the method of rate of production analysis (ROPA) as implemented in KINALC [30,31]. If a species is formed by fast reversible reactions, and if its concentration is low, it is not a significant mass reservoir. These fast producing and consuming reactions can be identified at each of the automatically selected time points along the temperature profiles at the user specified ambient conditions and eliminated from the mechanism. The KINALC output gives an ordered list of reaction contributions to the production and consumption rates of each species. The percentage contribution of each reaction to production or consumption is also calculated, which helps the user to identify the

fast pairs of producing and consuming reactions. The mechanism is then validated after removing each pair. Alternatively, these fast producing and consuming reactions can be identified via PCA as they will have large corresponding eigenvalue entries. The producing and consuming reactions will have eigenvectors of equivalent magnitude and so should appear adjacent to each other in the ranked list.

In addition to removing fast reversible pairs with high rates, ROPA techniques can be used to identify reactions that make negligible contributions to the rates of production and consumption of each necessary species. A reaction is considered important if it has a higher contribution than a certain threshold to the production rate of a species, expressed as a fraction or percentage. Other reactions are considered to be redundant. The value of the threshold can be altered, but is typically 5 – 10%. However there is a disadvantage with this method in that the application of a uniform threshold for each time point and species can result either in redundant reactions being left in the scheme, or in the oversimplification of the mechanism, to the detriment of its subsequent application. It should therefore be applied with some caution. Sensitivity based methods are generally favoured [15].

In many cases, after reactions have been removed by either sensitivity, principal component or rate of production analyses, it is possible that some species will have had all of their reactions removed, but their names still appear in the species list of the CHEMKIN format mechanism. It is therefore necessary to make a check of the mechanism to find out if this has occurred, and for which species. These species can then be removed from the species list using MECHMOD [131]. A Unix shell script has been written to automate this task.

5.6 Application of sensitivity and principal component analyses for the equimolar propane + oxygen scheme

The methods of sensitivity and principal component analyses for redundant species and reaction removal explained so far in this chapter were applied to the Nancy propane oxidation scheme to model the behaviour of an equimolar

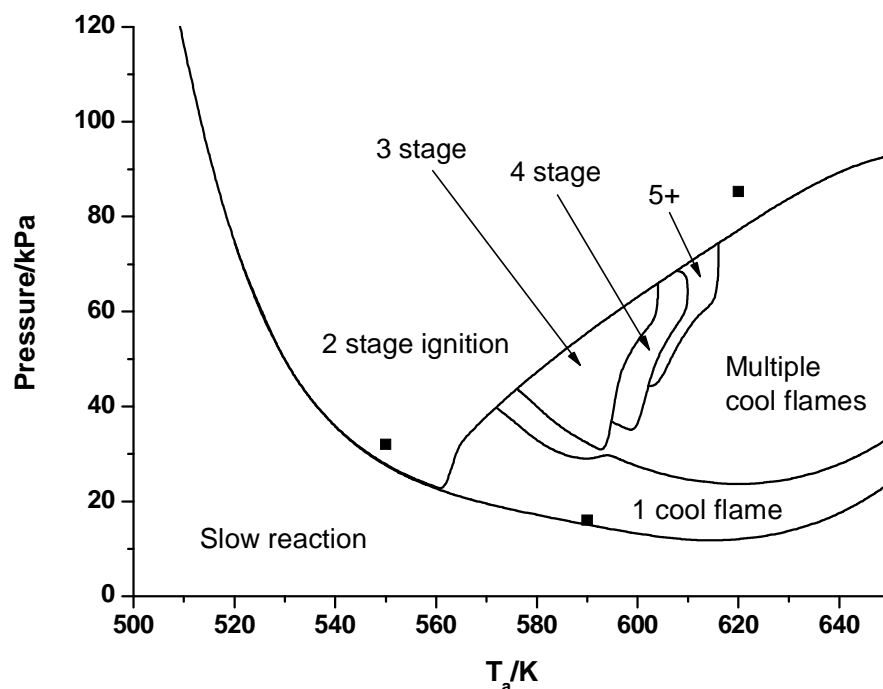


Fig. 5.7. Full Nancy scheme simulated p - T_a ignition diagram for equimolar $C_3H_8 + O_2$ in a closed vessel under spatially uniform conditions. This, and also the other C_3H_8 ignition diagrams, were computed at 2K intervals using an automatic generation procedure, giving precision of the boundary to ± 0.065 kPa. Black squares; user selected operating conditions of reduction.

composition with oxygen in a closed vessel. The model in comprehensive form consists of 122 species in 1137 irreversible reactions. A systematic reduction of the species and reactions was performed. As discussed in Chapter 4, the propane scheme exhibits a number of complex non-isothermal behavioural regimes such as single and multiple cool flames, multiple stage ignitions and slow reaction. The aim is to preserve in the reduced scheme all the ranges of behaviour displayed by the full scheme and the quantitative position of the boundaries between them. This in itself presents a significant challenge.

The first step in the reduction processes was the user selection of the operating conditions at which to perform the reduction process. For this, the full kinetic scheme p - T_a ignition diagram shown in Fig. 5.7, constructed from predictions of the time dependent behaviour over the ambient temperature range $T_a = 500 - 650$

K, was used as reference for the selection. Three operating conditions were selected, encompassing two in the 2-stage ignition region and one in the cool flame region. This number of operating conditions was found to be adequate to capture the aspects of important chemistry encountered as conditions are varied and also minimises the computational time of the reduction process. The full scheme p - T_a diagram was also used as the benchmark against which the reduced models were tested.

5.6.1 Removal of species: Iterative Jacobian analysis

A two-stage species reduction strategy was found to be appropriate for the comprehensive propane mechanism. The details of the two-stage reduction are illustrated in Fig. 5.8. A first stage reduction by investigation of the Jacobian to identify necessary species was performed using values of 4, 0.36, 10 and 20 for the reduction criteria (a), (b), (c) and (d) respectively (as outlined in Section 5.2). The partially reduced scheme, then comprising 63 species and 933 irreversible reactions, output temperature profiles which matched those of the full scheme almost perfectly, there being only tiny variations of the ignition delay time. Further species removal at this first stage yielded a mechanism of 62 species whose output ignition delay times had incurred significant error when compared to those of the full mechanism. Proceeding with the 63 species mechanism, a further level of simplification was achieved by performing a second stage species reduction via investigation of the Jacobian with altered reduction criteria of 6, 0.05, 10, 20 for (a), (b), (c) and (d) respectively. This yielded a mechanism comprising 42 species in 545 irreversible reactions. CO_2 was identified as being redundant by the analysis, but as this is a major product of combustion it was reintroduced in the species reduced scheme. Further species removal using this technique yielded a mechanism of 41 species in 507 reactions whose behaviour over the range of operating conditions gave larger quantitative departures from the behaviour predicted using the full scheme, especially the 2-stage ignition boundary of the p - T_a (see Fig. 5.9). The quantitative departures could also be

witnessed in the temperature profiles at selected operating conditions (Fig. 5.10). In consideration of the computational speed-up gained by the removal of this extra species, the quantitative departures were deemed to be unacceptable. Therefore, the 42 species mechanism was selected for further analysis and reaction reduction. The extra species which is included in the 42 species mechanism but not in the 41 species mechanism is the vinyl radical (C_2H_3). 38 consuming reactions of this species is the difference between the two mechanisms.

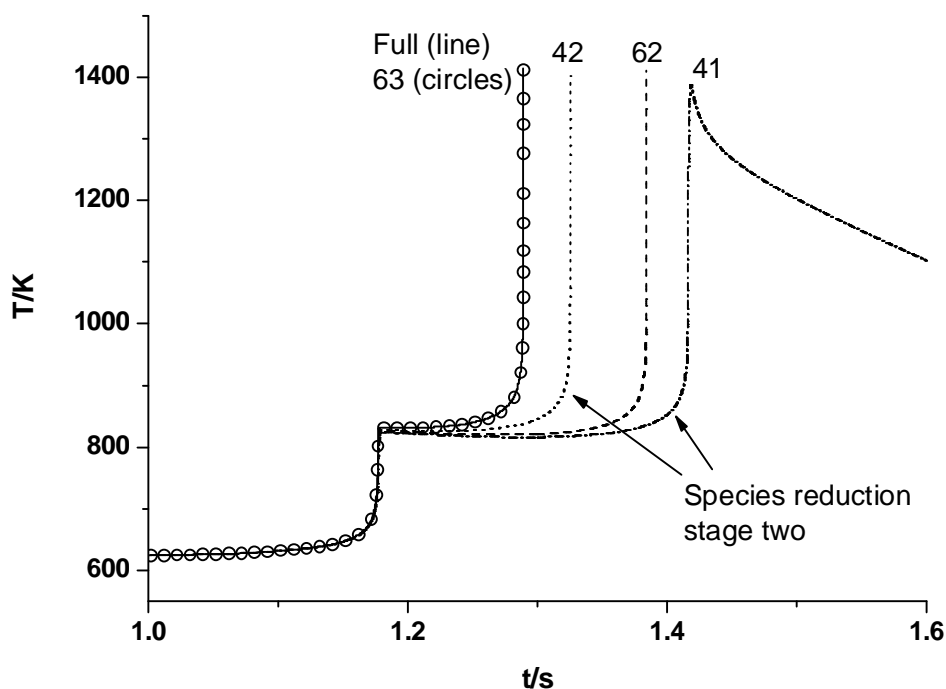


Fig. 5.8. Illustration of the two stage species reduction for equimolar propane + oxygen at 620 K and 85.3 kPa.,. The full scheme (solid line) is reduced to a 63 necessary species scheme (circles) whose agreement with the full scheme is nearly perfect. Further species removal at this stage results in a 62 species scheme (dashed line) whose output has incurred significant error when compared to the full scheme. Proceeding with the 63 necessary species scheme, a second stage reduction is performed to produce schemes of 42 species (dotted line) and 41 species (dash/dot line). The agreement of the 42 species scheme is deemed acceptable but in the case of the 41 species scheme it is deemed unacceptable.

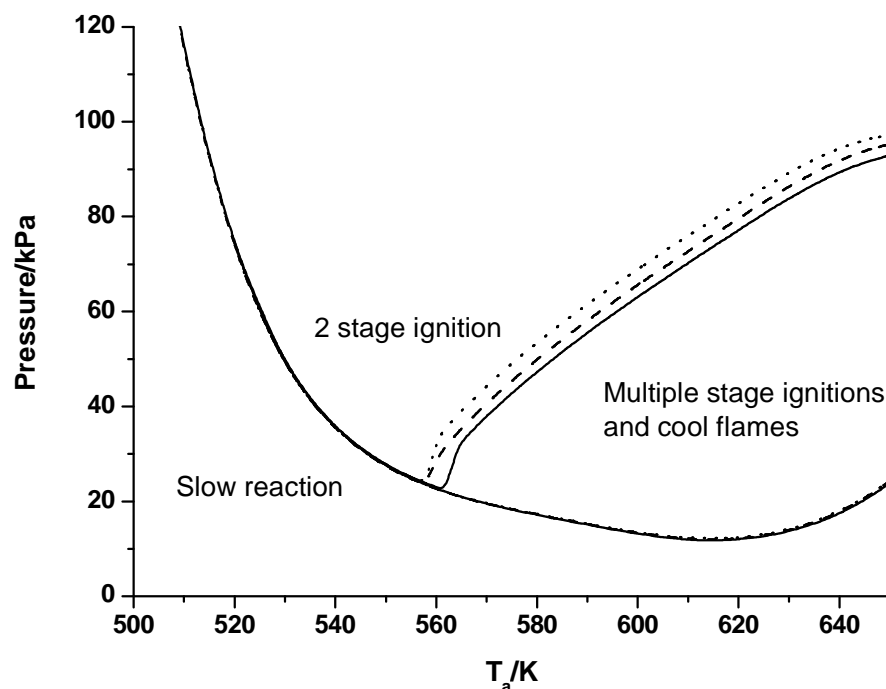


Fig. 5.9. Comparison of the p - T_a ignition diagrams produced by species reduced mechanisms for equimolar propane + oxygen. Solid line: full mechanism, 122 species and 1137 reactions. Dashed line: reduced mechanism, 42 species and 545 irreversible reactions, post Jacobian analysis. Dotted line: further species reduced mechanism, 41 species and 507 reactions.

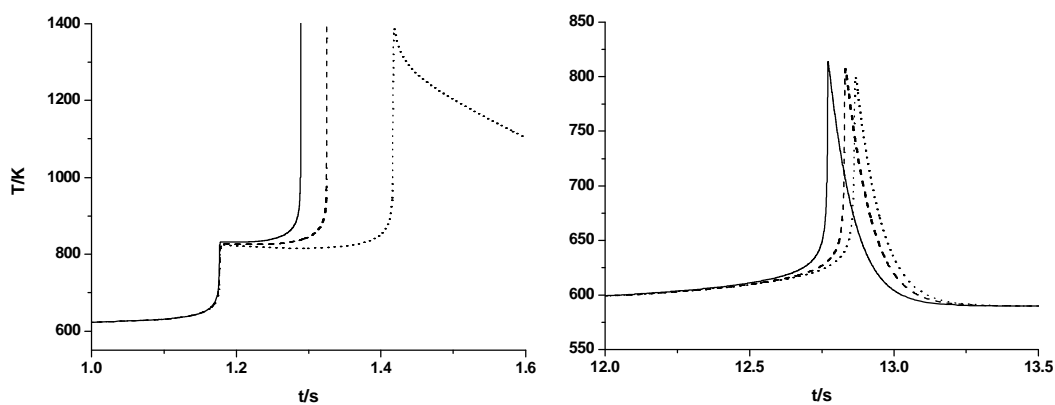


Fig. 5.10. Comparison of the temperature profiles output by species reduced mechanisms. Solid line: full mechanism, 122 species and 1137 reactions for equimolar propane + oxygen. Dashed line: reduced mechanism, 42 species and 545 reactions, post Jacobian analysis. Dotted line: further species reduced mechanism, 41 species and 507 reactions. Operating conditions: *left*: 620 K and 85.3 kPa, *right*: 590 K and 16 kPa.

5.6.2 Removal of reactions: Principal component analysis

Having identified a subset of necessary species, a principle component analysis was applied to the partially reduced mechanism in order to reduce the numbers of reactions in the scheme whilst retaining a good agreement with the output of the full scheme. The methods were applied at the same operating conditions used for the species reduction, shown in Fig. 5.7. Subsets of necessary species found from the local Jacobian analysis were included in the objective function for the PCA analysis at each time point. The investigation of a variety of thresholds showed that values of 2.5×10^{-2} for the eigenvalues and 0.15 for the eigenvectors produced a mechanism consisting of 42 species and 166 irreversible reactions which gave the best trade off between minimum number of variables and good agreement with the output from the full mechanism. Altered thresholds for the PCA tolerances resulted in further reaction removal down to 42 species and 145 irreversible reactions. However, the error introduced by the removal of these extra 21 reactions (see Figs. 5.11 and 5.12) over the range of operating conditions was deemed to be unacceptable when the low computational speed-up achieved was considered (see Section 5.6.3).

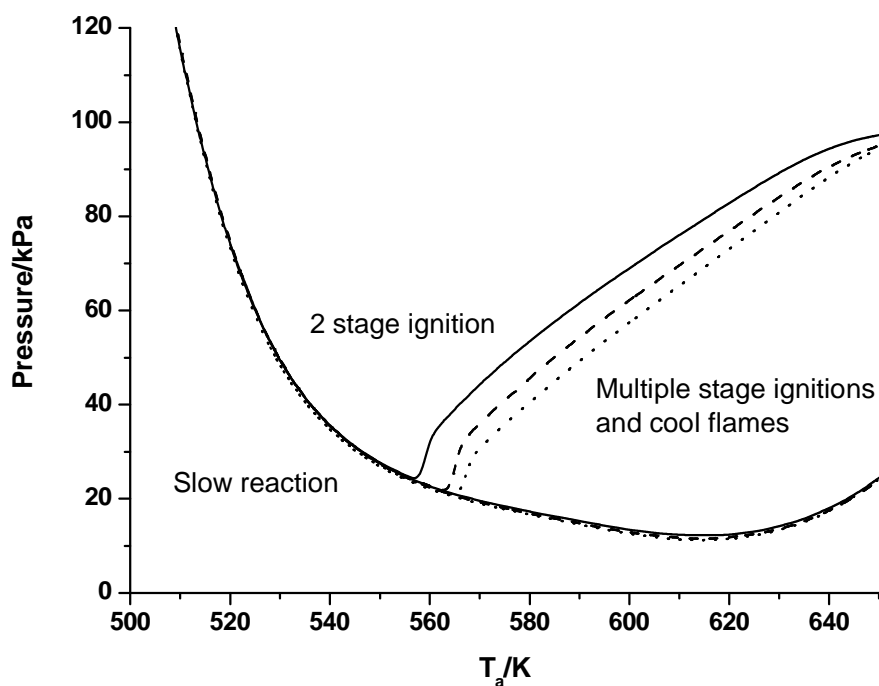


Fig. 5.11. Comparison of the p - T_a ignition diagrams produced by reaction reduced mechanisms equimolar propane + oxygen. Solid line: Species reduced mechanism, 42 species and 545 reactions. Dashed line: PCA reaction reduced mechanism, 42 species and 166 reactions. Dotted line: further PCA reaction reduced mechanism, 41 species and 145 reactions.

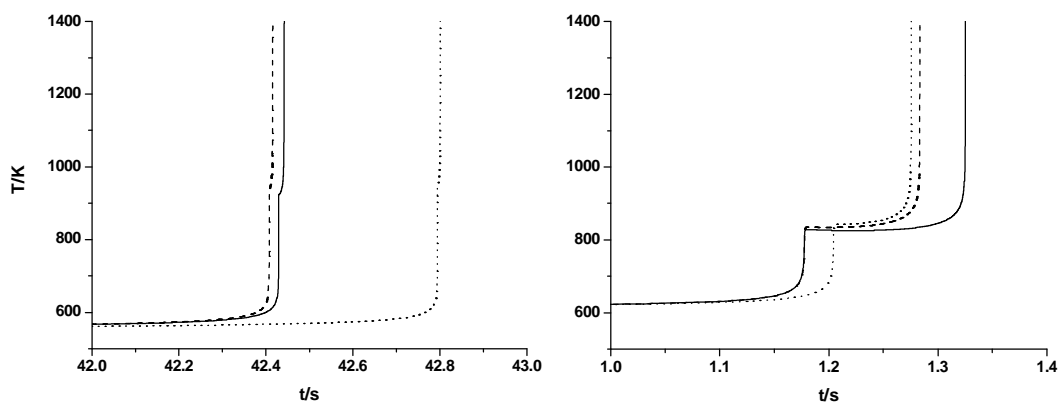


Fig. 5.12. Comparison of temperature profiles output by reaction reduced mechanisms for equimolar $C_3H_8 + O_2$. Solid line: Species reduced mechanism, 42 species and 545 reactions. Dashed line: PCA reaction reduced mechanism, 42 species and 166 reactions. Dotted line: further PCA reaction reduced mechanism, 41 species and 145 reactions. Operating conditions: *left*: 550 K and 32 kPa, *right*: 620 K and 85.3 kPa.

5.6.3 Final reduced propane scheme and computational speed-ups

The p - T_a diagram of the skeleton mechanism consisting of 42 necessary species and 166 irreversible reactions shown in Fig. 5.13 displays all the types of dynamic behaviour exhibited by the full system. Quantitatively, the agreement with the full scheme is excellent over the range of operating conditions, with only very minor differences. The agreement between the low temperature ignition boundaries produced by the full and final reduced mechanisms is nearly perfect. Good agreement can also be found between the temperature profiles of the full and final reduced schemes. After species reduction to 42 species and 545 reactions, the computational time for a single zero-dimensional calculation was 37% of that of the full scheme (to the nearest 1%). The final reduced scheme had a 15% runtime compared to the full scheme. Taking into account that the run-time of the reduced scheme should be $\propto N^2$, where N is the number of species, our calculated runtime compares well to the estimated runtime of 12% of the full mechanism. Further, in consideration that the runtime should be $\propto n$, where n is the number of reactions, our calculated run-time is the same as the estimated run-time, to the nearest 1%.

Although the size of mechanism achieved with these reduction techniques alone is still too large for application in three-dimensional, turbulent reactive flow calculations, such mechanisms could be incorporated within laminar flow, computational fluid dynamic models. Even for turbulent flows, methods such as the transported probability density function approach, which allows the incorporation of kinetic effects within turbulent flow calculations exactly, have been used to represent methane combustion for two-dimensional, axisymmetric flows with mechanisms consisting of 44 species and 256 reactions [192].

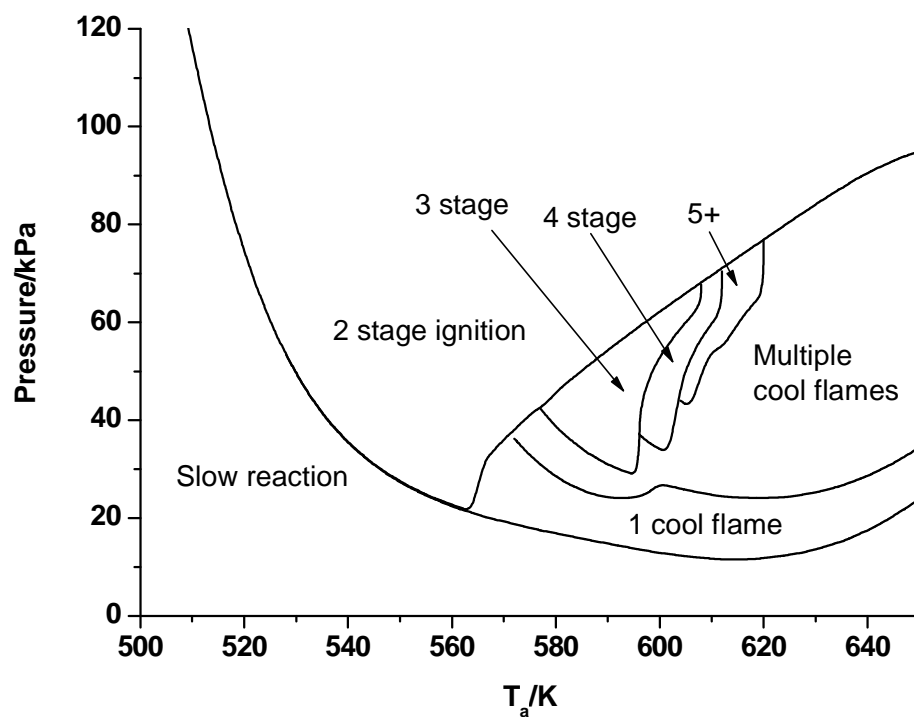


Fig. 5.13. Simulated p - T_a ignition diagram for equimolar $C_3H_8 + O_2$ in a closed vessel under spatially uniform conditions from the final reduced, Nancy scheme, comprising 42 species in 166 reactions.

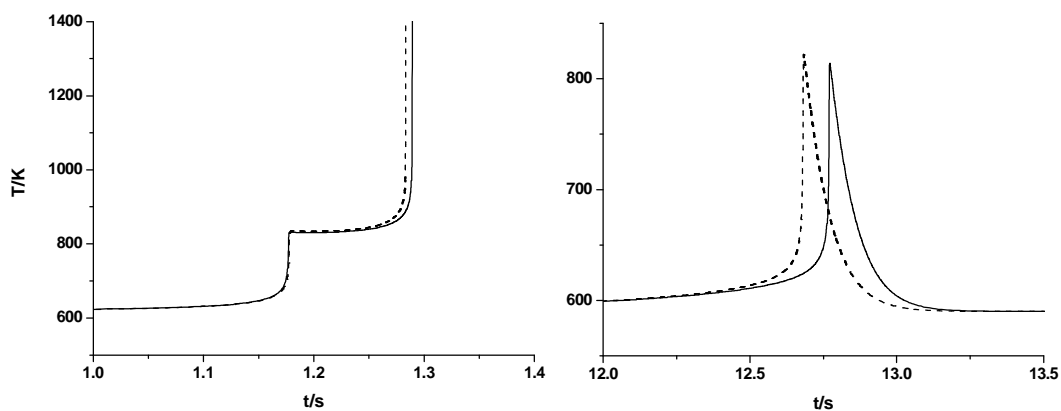


Fig. 5.14. Comparison of predictions from the full C_3H_8 mechanism (solid line) and the final reduced mechanism (dashed line), comprising 42 species and 166 reactions, following the Jacobian and principal component analyses. Operating conditions: *left*: 620 K and 85.3 kPa, *right*: 590 K and 16 kPa.

5.7 Application of sensitivity and principal component analyses for the lean n-butane + air scheme

The comprehensive model to which the methods were applied was derived at CNRS-DCPR, Nancy [19] for n-butane oxidation, comprising 128 species in 314 irreversible reactions and 417 reversible reactions. The reversible reactions can be expressed as pairs in an irreversible form, the equivalent full scheme then having a total of 1148 irreversible reactions. This mechanism is of similar size to that of propane previously discussed in this Chapter. The validation of this mechanism has been discussed in Chapter 4. The objective was to produce a reduced mechanism which agrees well with both the ϕ - T_a ignition diagram, simulated at a constant pressure of 0.2 MPa over the concentration range 0 – 2.5 % n-C₄H₁₀ by volume in air, and individual temperature profiles from selected operating conditions from the full scheme. Proceeding in a similar way to the methods discussed for propane, five operating conditions were selected using the ϕ - T_a ignition diagram shown in Fig. 5.1 as reference. Operating conditions around the critical ignition boundary with varying initial ambient temperature were selected as well as one in the cool flame region, for the reasons discussed in Section 5.1.

The first method employed in the reduction was the identification and removal of redundant species as described in Section 5.2. A single stage species reduction was performed using the values of 5, 0.2, 10 and 20 for the reduction criterion (a), (b), (c) and (d) respectively (as described in Section 5.2). This resulted in a partially reduced scheme comprising 73 necessary species and 715 irreversible reactions. The ϕ - T_a ignition diagram of this scheme matched that of the full scheme extremely well, and this comparison is shown in Fig. 5.15. This was followed by the removal of redundant reactions. Using a threshold of 0.1 for the B_j value (equation 5.3), the overall sensitivity analysis method described in Section 5.3 gave a scheme comprising 73 necessary species and 449 reactions. Further reaction removal was achieved using the PCA method described in Section 5.4 using thresholds of 1.0×10^{-4} for the eigenvalues and 0.05 for the eigenvectors. This gave a final reduced scheme consisting of 73 necessary species

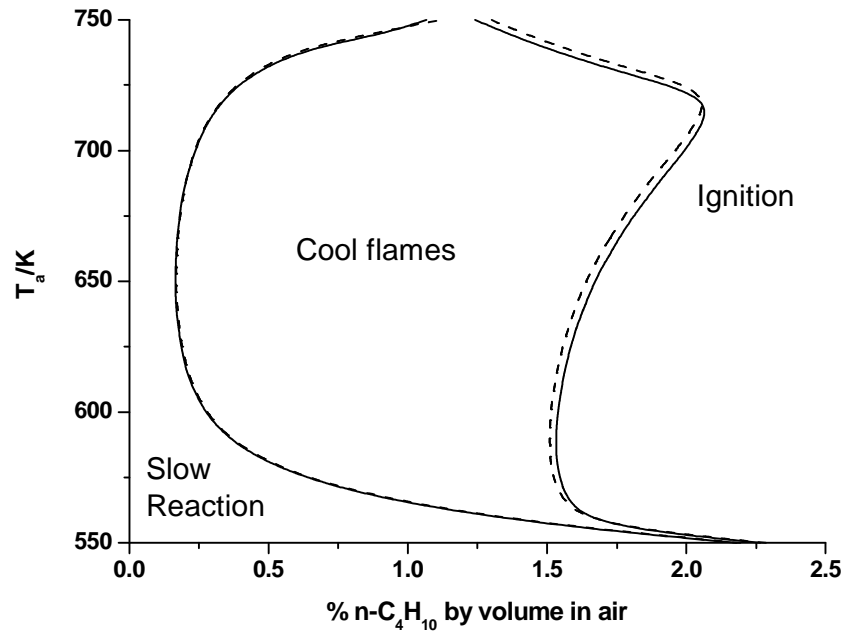


Fig. 5.15. Comparison of the predicted ϕ - T_a ignition diagram at 0.2 MPa produced by the full mechanism (solid line) and the species reduced mechanism (dashed line), comprising 73 species and 715 reactions, following the Jacobian analysis and conversion of reactions to irreversible form.

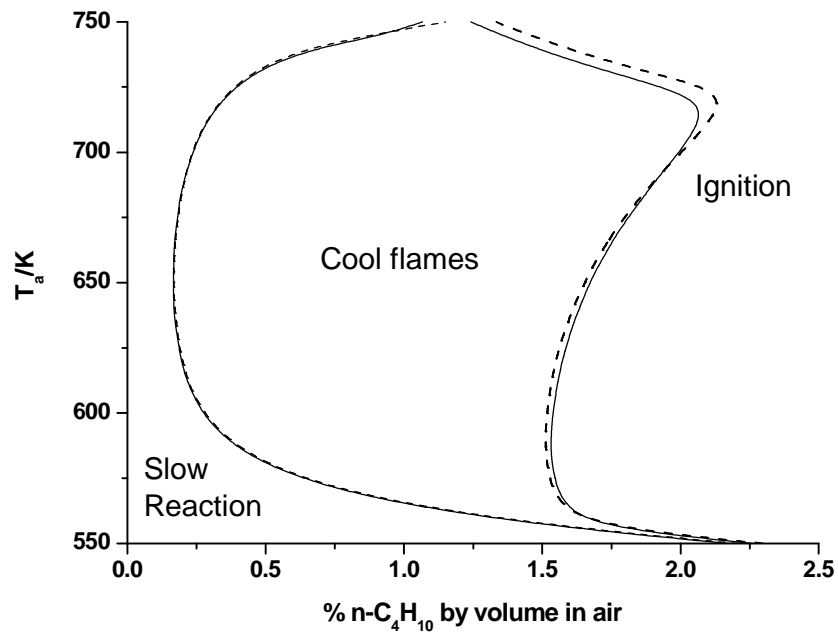


Fig. 5.16. Comparison of the predicted ϕ - T_a ignition diagram at 0.2 MPa produced by the full mechanism (solid line) and the reduced mechanism (dashed line), comprising 73 species and 300 reactions, following the Jacobian and sensitivity / principal component analysis.

and 300 irreversible reactions.

The ϕ - T_a ignition diagram showing the extent of agreement between the full and final reduced models is shown in Fig. 5.16, and a comparison of typical temperature time profiles is given in Fig. 5.17. This final reduced scheme has a computational run-time which is 22% of the run-time of the full scheme.

With this extent of species and reaction removal, there is still an excellent agreement between the simulated temperature profiles calculated with the full and reduced schemes (Fig. 5.17), which is supported by the agreement between the calculated ϕ - T_a ignition diagrams (Fig. 5.16). Greater discrepancies between the simulated temperature profiles of the full and reduced mechanisms were observed at temperatures higher than 720 K and near perfect agreement was found at temperatures lower than 570 K. These statements are reflected and supported in the comparison of full and reduced ϕ - T_a ignition diagrams (Fig. 5.16).

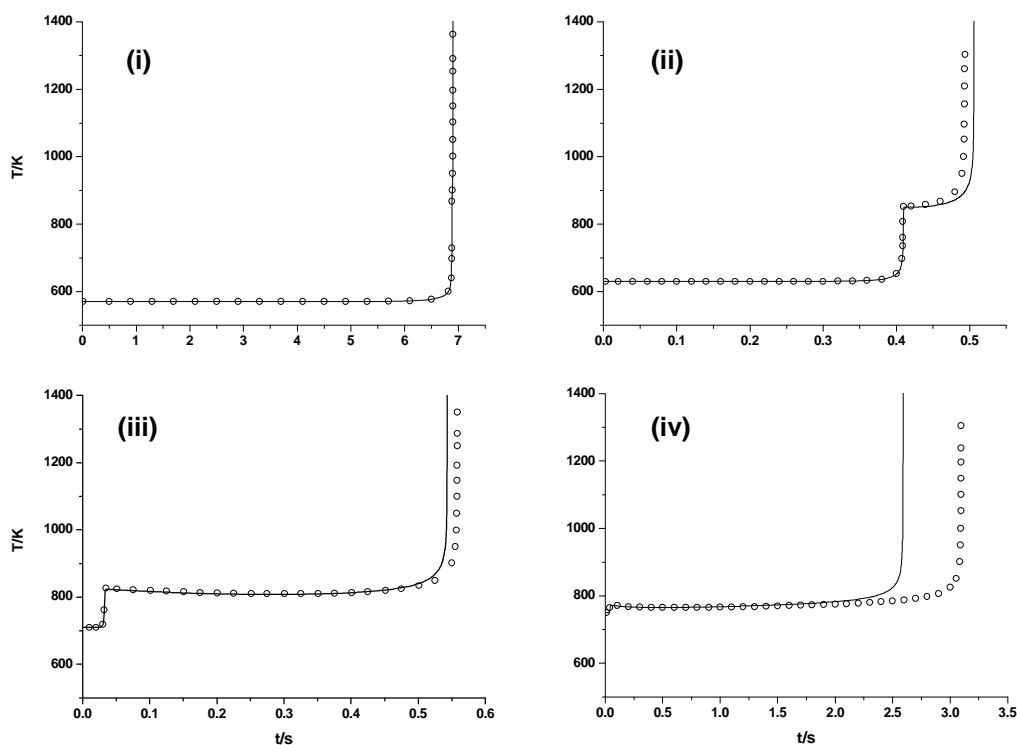


Fig. 5.17. Comparison of predictions from the full n - C_4H_{10} mechanism (solid line) and the final reduced mechanism (circles), comprising 73 species and 300 reactions, following the Jacobian and sensitivity / principal component analyses. Operating conditions: (i): 570 K, 0.2 MPa and 2.17 % fuel by volume in air (ii): 630 K, 0.2 MPa and 1.78 % fuel by volume in air, (iii): 710 K, 0.2 Mpa and 2.11 % fuel by volume in air, (iv): 750 K, 0.2 MPa and 1.45 % fuel by volume in air.

It is possible to apply different thresholds in the methods used so far in order to reduce the mechanisms still further, but at a cost of a reduced level of agreement with the full scheme. This is exemplified in Fig. 5.18 where the 73 species reduced mechanisms are compared at different levels of reduction post sensitivity and principal component analyses via ignition boundaries. When compared to the reduced mechanism without reaction removal (715 reactions), a reduced mechanism with 300 reactions gives an overall error which is deemed acceptable over the range of operating conditions. At higher specified thresholds for the eigenvalues and eigenvectors of PCA, it is possible to reduce the number of reactions to 269. However, the increasing error induced by this further reduction is considered to be inappropriate since it leads to the removal of only a further 31 reactions giving little extra computational saving.

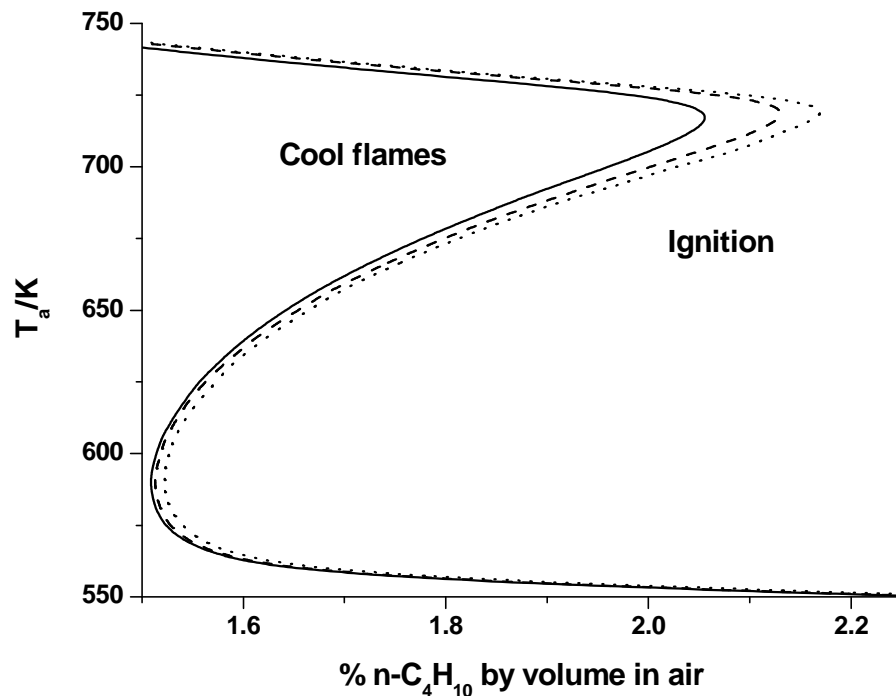


Fig. 5.18. Comparison of the ignition diagram produced by species reduced mechanism. Solid line: species reduced mechanism, 73 species and 715 reactions. Dashed line: reduced mechanism, 73 species and 300 reactions, post Jacobian and sensitivity/principal component analysis. Dotted line: further reaction reduced mechanism, 73 species and 269 reactions.

5.8 Application of sensitivity and principal component analyses for the stoichiometric cyclohexane + air scheme

The reduction methods described in this Section were applied to a Nancy generated mechanism describing the oxidation of the cyclic alkane cyclohexane. This mechanism has been validated under equimolar fuel + oxygen conditions in Chapter 4. The reduction was conducted under stoichiometric fuel in air conditions and the p - T_a ignition diagram numerically generated at this composition and temperature range of 500 – 800 K, shown in Fig. 5.19, serves as the benchmark against which the reduced models are validated. As with the reductions of propane and n-butane, our reduction aim is to remove as many redundant species and reactions as possible whilst preserving all the ranges of oxidation phenomena and the position of their boundaries within the ignition diagram. The reproduction of temperature profiles output by the full mechanism is also an important feature we wish to preserve in the reduced mechanisms where possible.

The full cyclohexane mechanism comprises 499 species in 1025 reversible reactions and 1298 irreversible reactions (2323 mixed reactions in total or equivalent to 3348 irreversible reactions) making this mechanism much larger than either of the previous comprehensive mechanisms considered in this chapter (*circa* 125 species). Pitting these techniques against a mechanism of this large size, combined with the fact that the compound whose oxidation it is describing is not a normal alkane, provides a good test of the versatility of the developed methods.

First, the reduction to a mechanism whose output gives good agreement over a wide, low temperature range (500 – 800 K) will be shown. Further, as has been shown for propane and n-butane, the application of the reduction techniques tends to incur very little or negligible error to the low temperature ignition boundary. The extent to which this feature can be exploited will be examined. To this effect, the generation of further reduced mechanisms that accurately model the low temperature ignition boundary, thus facilitating the calculation of autoignition

temperature (AIT), will be shown. In each case, the strategy of multiple stage reductions will be utilized.

5.8.1 Development of reduced cyclohexane mechanism applicable over a wide low temperature range

For the reasons discussed in Section 5.1, 3 operating conditions were selected at which to perform the sensitivity analysis for reduction, using the full mechanism stoichiometric in air p - T_a ignition diagram as reference. They encompass cool flame behaviour and 2 stage ignition at 2 different initial pressures. These input conditions are shown on Fig. 5.19. Each of these initial conditions was simulated in turn, time points were automatically selected as described in Section 5.1, and sensitivity analysis and species reduction was performed as outlined in Section 5.2.

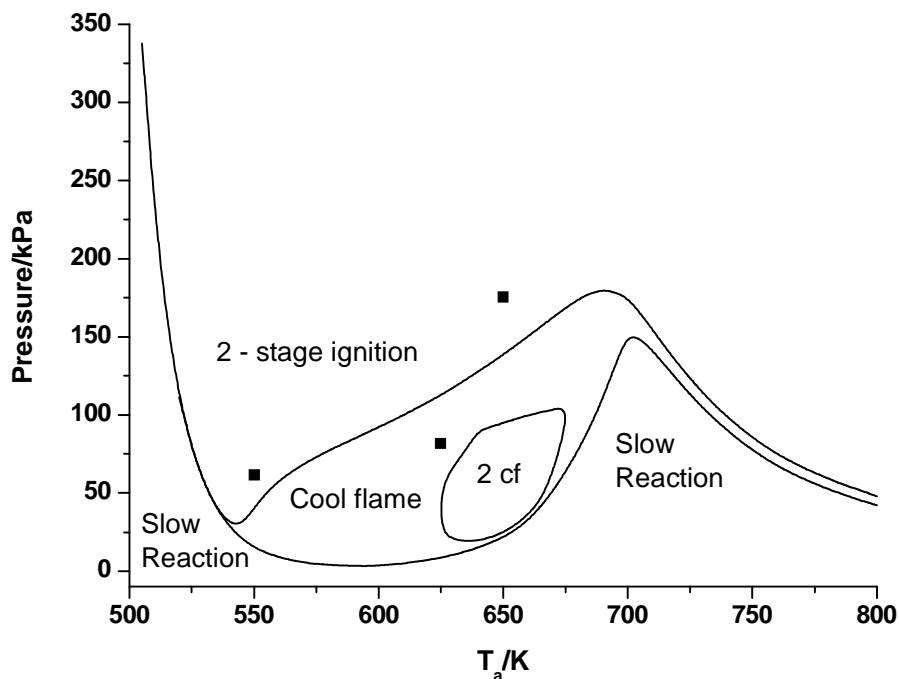


Fig. 5.19. Full Nancy scheme simulated p - T_a ignition diagram for stoichiometric c - C_6H_{12} + air in a closed vessel under spatially uniform conditions. This, and also the other c - C_6H_{12} ignition diagrams, were computed at 5K intervals using an automatic generation procedure, giving precision of the boundary to ± 0.2 kPa. Black squares; user selected operating conditions of reduction.

A number of reduction criteria were tested in order to find the optimum species reduced mechanism in a multi-stage species reduction framework. This was achieved by comparison of the reduced mechanism's output temperature profiles to those of the full mechanism (see Fig. 5.5). A three stage reduction strategy was implemented and the successful criterion at each stage are given in Table 5.1. Further species removal at each stage using altered criteria resulted in poorer quality reduced mechanisms, as reflected in the temperature profiles (an example for propane is given in Fig. 5.8) and also in their generated ignition diagrams. Consequently, the species reduction process was restarted using the successful partially reduced mechanism as the starting point for the consecutive species reduction stage. This constituted a multi-stage reduction, which resulted in a reduction of the numbers of necessary species from 499 to 104, with the numbers of reactions decreasing from 2323 (3348 irreversible) to 541 (845 irreversible). This mechanism will be referred to in the discussion as mechanism A.

Species reduction stage	Reduction criteria				No. species	No. reactions
	a	b	c	d		
Full	-	-	-	-	499	2323
1	4	0.38	13	14	203	1087
2	-8	0.4	25	35	160	888
3	2	0.24	10	20	104	541

Table 5.1. Criteria used in the three stage species reduction of stoichiometric cyclohexane in air. They are; (a) the minimum allowable $\log B_i$ value, (b) the minimum gap criterion, (c) the effect of varying the minimum allowable number of necessary species, (d) the number of species after which the minimum allowable B_i value can be ignored. The number of reactions refers to the number of mixed reversible/irreversible.

At this stage in the reduction process it is necessary to evaluate mechanism A by generation of its p- T_a ignition diagram and comparison with that of the full mechanism. This is shown in Fig. 5.20. The agreement between the two ignition diagrams is excellent at the low temperature ignition boundary and at the

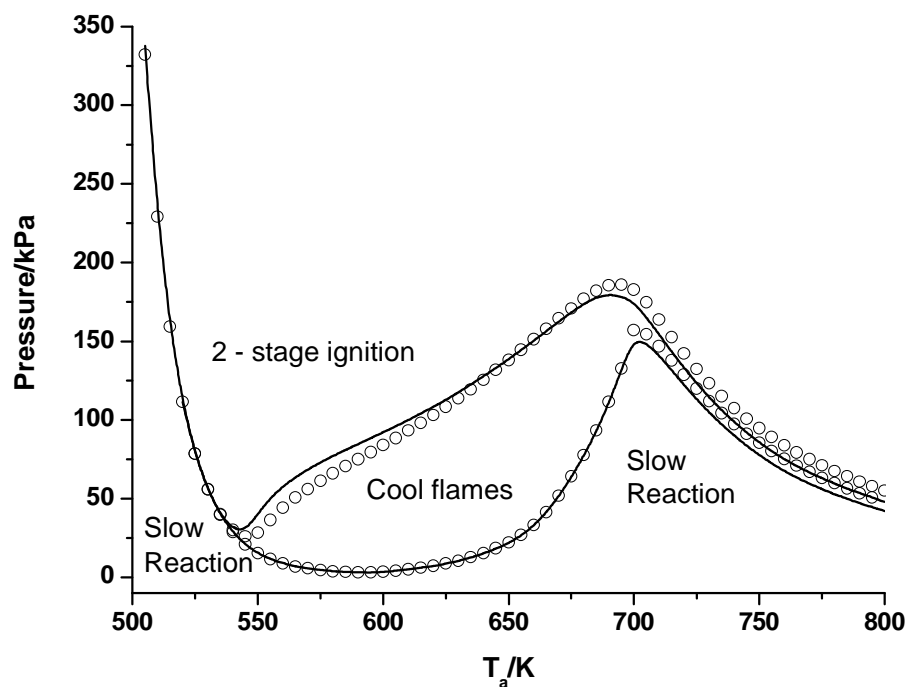


Fig. 5.20. Comparison of the p - T_a ignition diagrams produced by the full and species reduced mechanisms for stoichiometric cyclohexane in air. Solid line: full mechanism, 499 species and 2323 reactions. Circles: species reduced mechanism A, 104 species and 541 reactions, post Jacobian analysis.

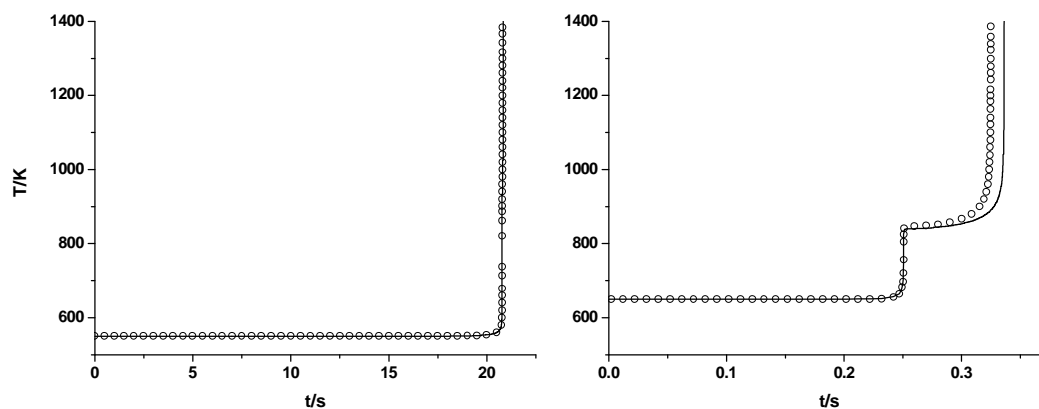


Fig. 5.21. Comparison of the temperature profiles output by the full and species reduced cyclohexane mechanisms. Solid line: full mechanism, 499 species and 2323 reactions. Circles: species reduced mechanism A, 104 species and 541 reactions, post Jacobian analysis. Operating conditions: *left*: 550 K and 61.39 kPa, *right*: 650 K and 175.41 kPa.

boundary between cool flames and slow reaction, until 700 K. Very good agreement is observed for the boundary between two-stage ignition and cool flames with only minor quantitative differences here and at temperatures above 700 K. Interestingly, the point at which the full mechanism and the mechanism A two-stage ignition/cool flames boundary intersect is roughly at the same operating temperature of the input condition for sensitivity analysis of 650 K and 175.41 kPa. In this region the agreement is excellent.

Next, the PCAF method outlined in Section 5.4 was employed to remove reactions from mechanism A. The analysis was performed at the same initial conditions used for the species reduction shown in Fig. 5.19. Before the analysis was performed the reactions of mechanism A were converted to irreversible form and this resulted in a scheme comprising 104 necessary species in 845 irreversible reactions. After testing a number of PCAF thresholds and visually inspecting the resulting output p - T_a ignition diagrams and temperature profiles, a mechanism with 100 species and 238 irreversible reactions was found to give the best trade-off between minimum number of variables and accurate description of the full model over the temperature range 500 – 800 K. This mechanism will be referred to as mechanism B henceforth in the discussion. Note that all the reactions of 4 necessary species were removed by the application of PCAF. The successful thresholds for the reaction reduction were 6.1×10^{-2} and 0.11 for the eigenvalues and eigenvectors respectively.

Comparison of output predictions of mechanism B to the full mechanism is made in Figs. 5.22 and 5.23. The agreement of the mechanism B p - T_a ignition diagram with that of the full mechanism shown in Fig. 5.22 is still very good. However, the agreement of the mechanism A p - T_a ignition diagram with that of the full mechanism, which is shown in Fig. 5.20 is slightly better, especially in the region of 660 – 720 K. Once again, the low temperature ignition boundary and slow reaction/cool flame boundary of mechanism B shows excellent agreement with those generated using the full mechanism. The removal of reactions from mechanism A to produce mechanism B incurred very little error to the resulting temperature profiles at the operating conditions tested, therefore, the comparison

of the mechanism B time dependent behaviour to that of the full scheme (Fig. 5.23) is almost identical to the performance of mechanism A (Fig. 5.21).

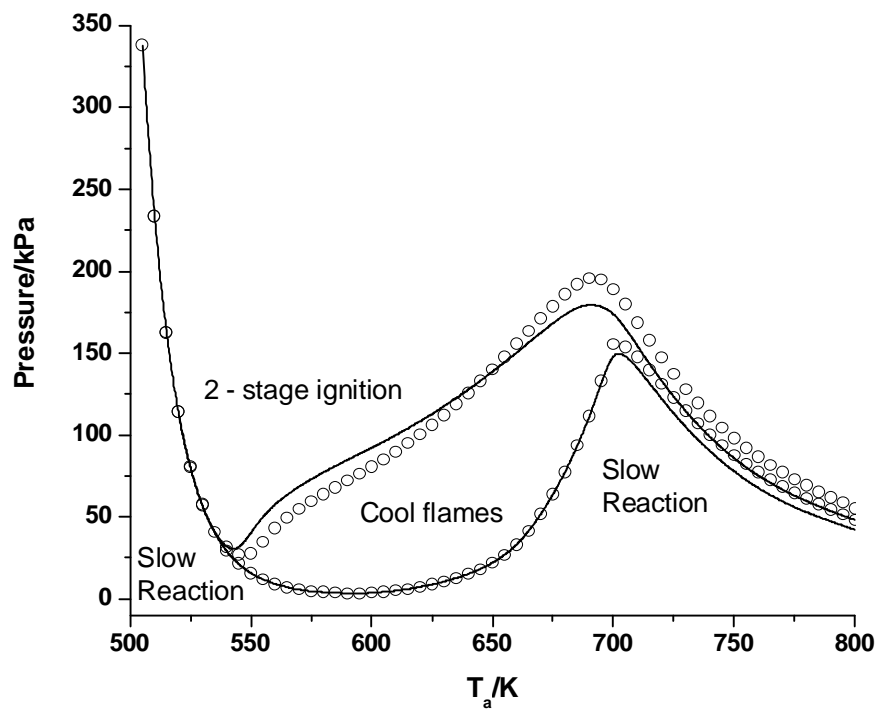


Fig. 5.22. Comparison of the p - T_a ignition diagrams produced by the full and reaction reduced mechanisms for stoichiometric cyclohexane in air. Solid line: full mechanism, 499 species and 2323 reactions. Circles: reaction reduced mechanism B, 100 species and 238 irreversible reactions, post PCAF.

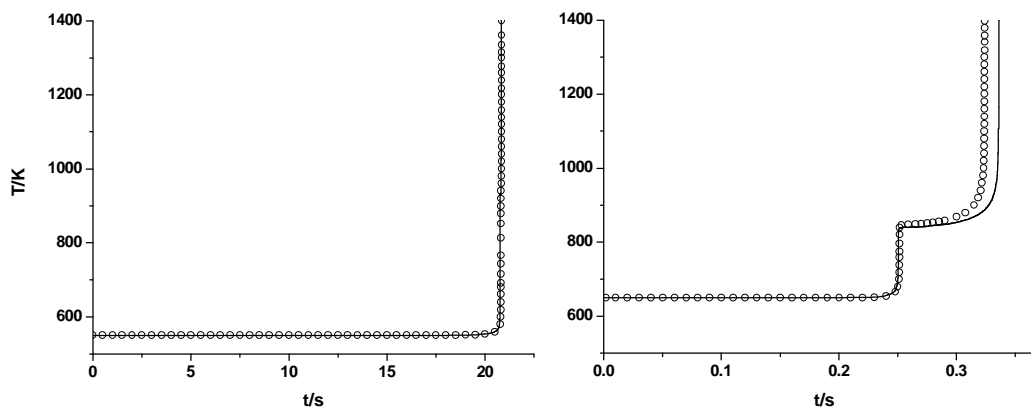


Fig. 5.23. Comparison of the temperature profiles output by the full and reaction reduced cyclohexane mechanisms. Solid line: full mechanism, 499 species and 2323 reactions. Circles: reaction reduced mechanism B, 100 species and 238 irreversible reactions, post PCAF. Operating conditions: *left*: 550 K and 61.39 kPa, *right*: 650 K and 175.41 kPa.

5.8.2 Generation of reduced cyclohexane mechanisms for the calculation of simulated autoignition temperature (AIT)

The reduction of the cyclohexane mechanism presented so far retains excellent agreement with the low temperature ignition boundary generated with the full mechanism over the temperature range of 500 – 550 K. Similar success was achieved with the reductions of propane and n-butane mechanisms. The comparisons of temperature profiles output from all of the presented full and reduced mechanisms in this region of operating conditions also show excellent agreement. Therefore, further reductions were carried out in order to assess the minimum size of mechanism which will retain these characteristics. The resulting reduced mechanisms enable a quick calculation of AIT and are useful in evaluating the underlying kinetics driving the transition from slow reaction to two-stage ignition behaviour when initial ambient conditions vary.

Mechanism A, comprising 104 species and 541 reactions, was used as the starting point for the further reductions, though the further reduced mechanisms are compared to the performance of the full mechanism. Two alternative operating conditions were selected close to the ignition boundary for the reasons mentioned in Section 5.1. These are shown in Fig. 5.24. The objective of the reduction was to produce two further reduced schemes; one which will retain the characteristics of the low temperature ignition boundary and low temperature time dependent behaviour produced using the full mechanism, whilst the second reduced mechanism had a reduction aim of only reproducing the low temperature ignition boundary produced using the full mechanism.

The reduction proceeded by performing further multi-stage species reductions to mechanism A. The criteria used for the species reduction at each stage are outlined in Table 5.2; a continuation from Table 5.1. This resulted in the creation of two reduced mechanisms of varying quality which would be further reduced via reaction removal using PCAF. The first comprised 60 necessary species in 290 reactions and the second comprised 47 species in 205 reactions. At each stage,

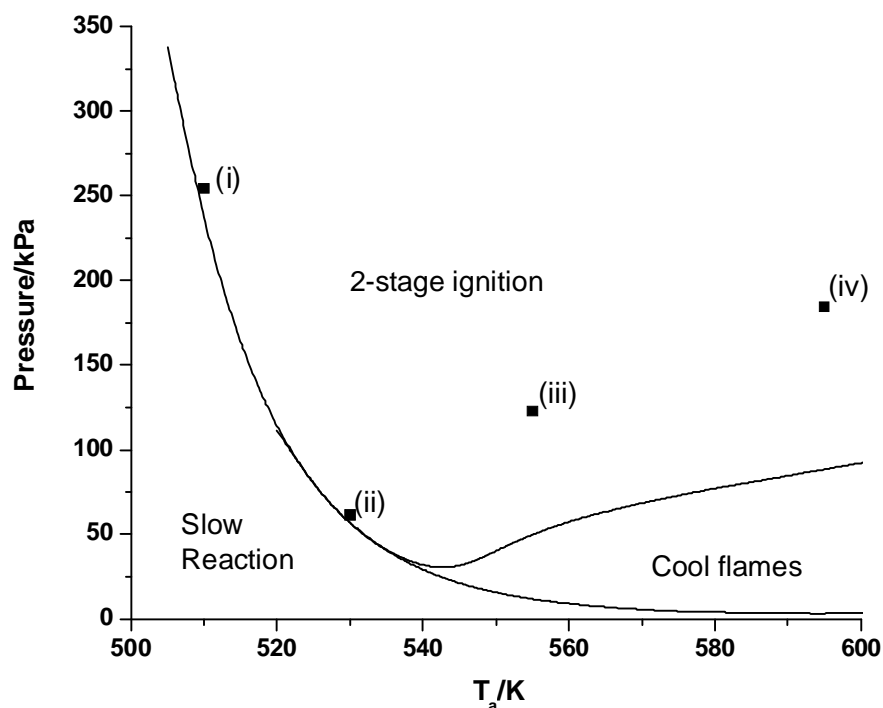


Fig. 5.24. Full Nancy scheme simulated p - T_a ignition diagram for stoichiometric c - C_6H_{12} + air over the temperature range 500 – 600 K. Black squares; (i) and (ii) are user selected operating conditions of reduction. (iii) and (iv) were used to evaluate the performance of reduced models in Fig. 5.27.

species removal further than those outlined in Table 5.2 resulted in mechanisms with undesirable performance in comparison to the performance of the full mechanism and in the case of species reduction 6, it led to the total breakdown of the mechanism with no non-isothermal time dependent behaviour being reported. Quite extreme reduction criteria were necessary in the case of species reduction 6, in order to achieve the smallest possible reduced scheme using these techniques.

Next, PCAF (see Section 5.4) was employed to remove reactions. The reactions of the 60 necessary species mechanism were converted to irreversible form and this resulted in 493 irreversible reactions. Using thresholds of 8×10^{-4} and 3.8×10^{-3} for the respective eigenvalues and eigenvectors the number of reactions were successfully reduced and this resulted in a mechanism comprising 60 necessary species and 238 irreversible reactions which shall henceforth be referred to as mechanism C. Similarly for the mechanism of 47 necessary species,

Species reduction stage	Reduction criteria				No. species	No. reactions
	a	b	c	d		
3	-	-	-	-	104	541
4	6	0.25	10	20	64	309
5	3	0.3	10	20	60	290
6	20	0	5	5	47	205

Table 5.2. Criteria used in the further multi-stage species reduction of stoichiometric cyclohexane in air. They are; (a) the minimum allowable $\log B_i$ value. (b) The minimum gap criterion, (c) the effect of varying the minimum allowable number of necessary species, (d) the number of species after which the minimum allowable B_i value can be ignored. The number of reactions refers to the number of mixed reversible/irreversible.

conversion of its reversible reactions to irreversible form resulted in 471 irreversible reactions. This number was reduced to 157 reactions using thresholds for the eigenvalues and eigenvectors of 5×10^{-4} and 1×10^{-3} . This resulted in the creation of the mechanism which will be referred to as mechanism D, comprising 47 necessary species in 157 reactions. Further reaction removal using these techniques resulted in mechanisms with unacceptable performance when a comparison of output predictions was made with the full mechanism.

The two reduced mechanisms C and D were then validated by a comparison (Fig. 5.25) of temperature profiles at the operating conditions shown by black squares in Fig. 5.24, using the full mechanism and mechanisms C and D. Further validation was by the construction of the p-T_a ignition diagrams of mechanisms C and D and making a comparison with the same diagram generated with the full mechanism: These are shown in Figs. 5.26 and 5.27 respectively.

From Fig. 5.25 we can see the major difference between mechanisms C and D. The temperature profiles of mechanism C retain excellent agreement with those of the full scheme over a number operating conditions in the region of interest. The removal of 13 more species to produce mechanism D results in the loss of reproduction of accurate ignition delay times. However, observation of the temperature profiles at a much smaller time scale than those shown in Fig. 5.25 shows that the qualitative behaviour of the two-stage ignition phenomena output from mechanism D gives good agreement with that of the full scheme at the

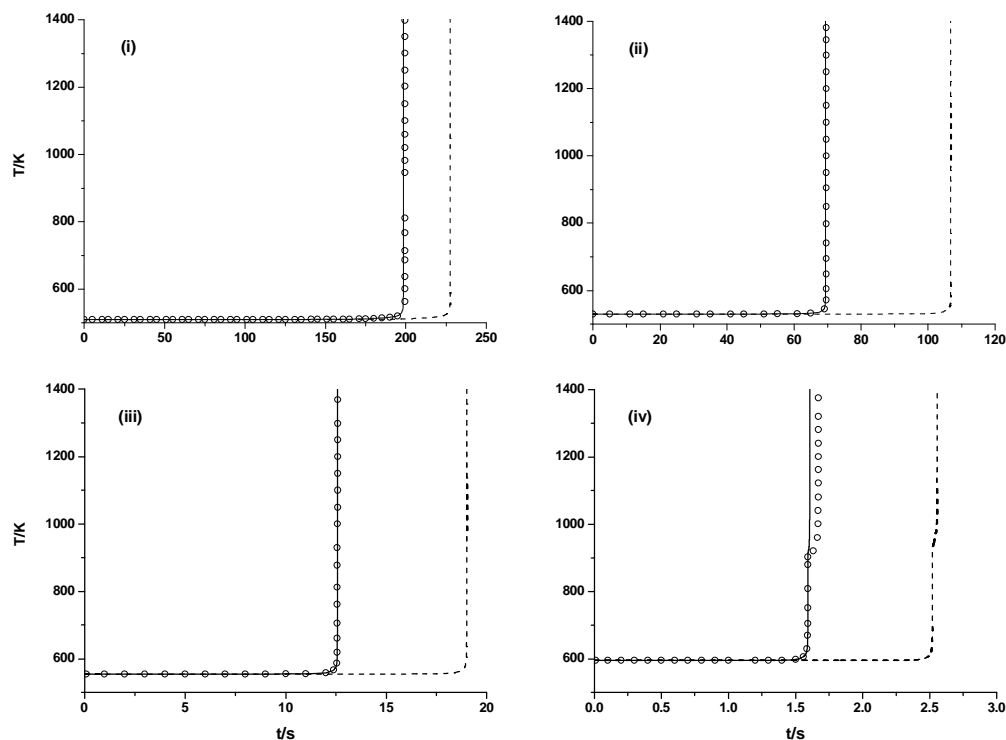


Fig. 5.25. Comparison of the temperature profiles output by the full and reduced cyclohexane mechanisms C and D. Solid line; full mechanism, 499 species and 2323 reactions. Circles; reduced mechanism C, 60 species and 238 irreversible reactions. Dashed line; reduced mechanism D, 47 species and 157 irreversible reactions. Operating conditions; (i) 510 K and 254.42 kPa, (ii) 530 K and 61.39 kPa, (iii) 555 K and 122.79 kPa, (iv) 595 K and 184.18 kPa.

operating conditions tested, with the exception of higher temperature operating condition (iv).

The comparison of the temperature profiles at the higher temperature operating condition (iv) (595 K and 184.18 kPa) of the full and reduced mechanisms C and D shows a minor corruption in the qualitative behaviour produced by both of the reduced mechanisms. The lack of good qualitative agreement is attributed to the lengthening of the τ_2 ignition delay time, which in turn is related to the behaviour exhibited by the p - T_a ignition diagrams produced by the reduced mechanisms. The comparison of the p - T_a ignition diagrams produced by the full mechanism and mechanism C (Fig. 5.26) show excellent agreement between their low temperature ignition and cool flame/slow reaction boundaries. However significant error has been incurred above the temperature of

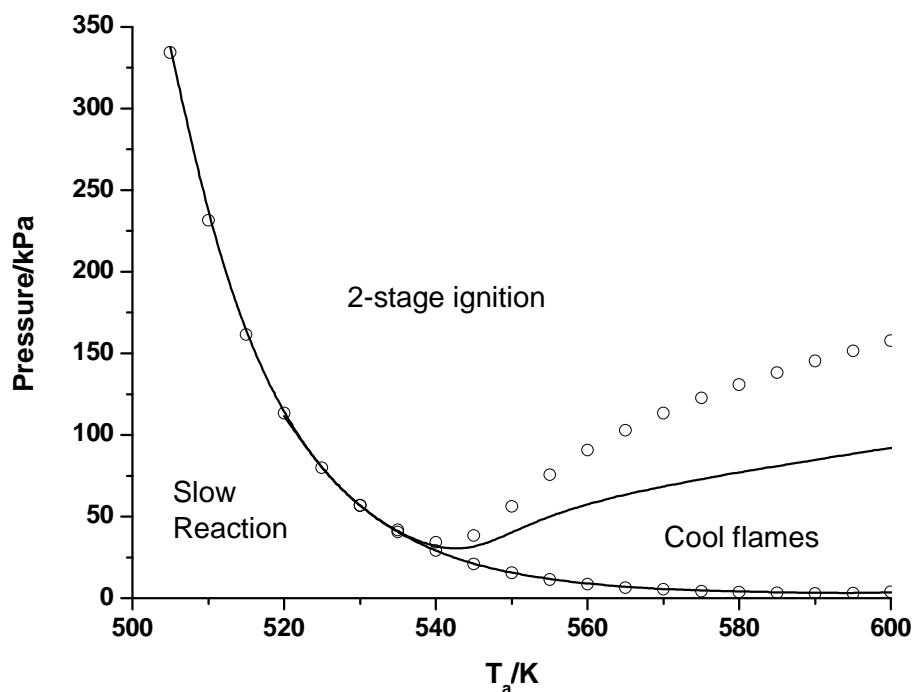


Fig. 5.26. Comparison of the p - T_a ignition diagrams produced by the full and mechanism C for stoichiometric cyclohexane in air. Solid line: full mechanism, 499 species and 2323 reactions. Circles: reduced mechanism C, 60 species and 238 irreversible reactions, post PCAF.

540 K to the ignition/cool flame boundary in the reduction. The comparison of the p - T_a ignition diagrams produced by the full mechanism and mechanism D (Fig. 5.27) shows a minor quantitative difference at the low temperature ignition boundary, incurred by the reduction. Once again, significant error has been incurred to the ignition/cool flame boundary in the reduction, but in fact the smaller reduced mechanism D gives better agreement here than mechanism C (to the performance of the full mechanism). The error incurred to the ignition/cool flame boundary in the reductions then explains the discrepancies between the full and reduced models at operating condition (iv), because as the coordinates of a two-stage ignition operating condition become closer to the ignition/cool flame boundary, or conversely in this reduction case if the ignition/cool flame boundary becomes closer to the coordinates of a two-stage ignition operating condition, the τ_2 ignition delay time lengthens, as is discussed in Chapter 4.

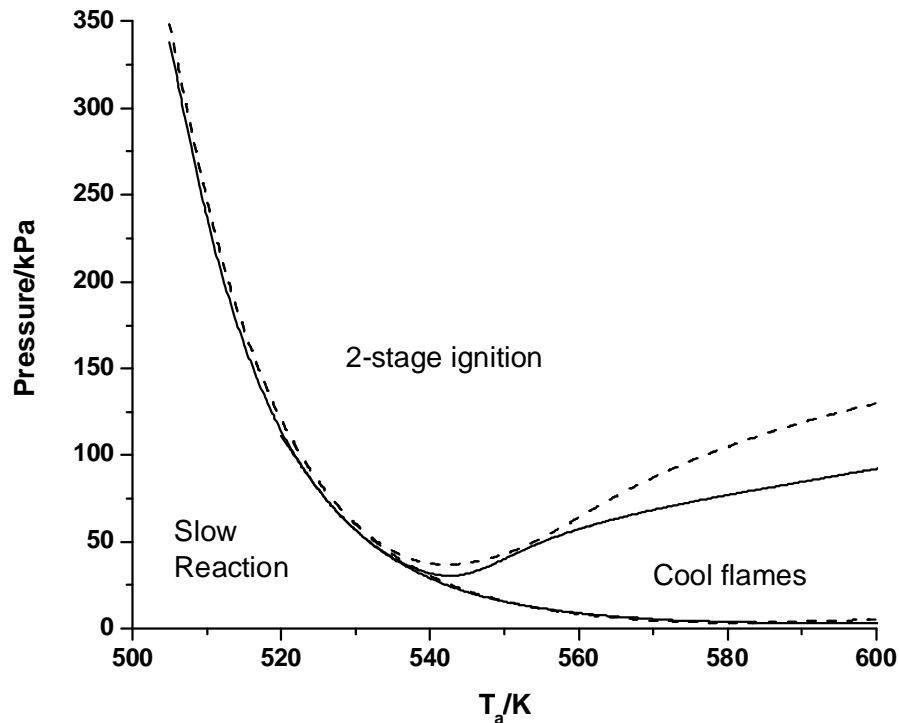


Fig. 5.27. Comparison of the p - T_a ignition diagrams produced by the full and mechanism D for stoichiometric cyclohexane in air. Solid line: full mechanism, 499 species and 2323 reactions. Dashed line: reduced mechanism D, 47 species and 157 irreversible reactions, post PCAF.

5.8.3 Summary of reduced cyclohexane mechanisms and their computational speed-ups

Using the techniques of investigation of the Jacobian matrix and PCAF, the numbers of species and reactions in the full cyclohexane mechanism have been successfully reduced from 499 species and 2323 mixed irreversible/reversible reactions to produce a number of reduced mechanisms of varying size and quality. A multi-stage species reduction strategy produced mechanism A, comprising 104 species in 541 irreversible/reversible reactions. Mechanism B was produced by employing the method of PCAF to remove reactions from mechanism A, and this yielded a reduced mechanism of 100 species in 238 irreversible reactions. The numerically predicted p - T_a ignition diagram and ignition delay times output from the reduced mechanisms of both A and B agree well with those of the full model

over a temperature range of 500 – 800 K. Using further multiple-stage species reductions and then PCAF, a further reduction was achieved to give mechanism C comprising 60 necessary species and 238 irreversible reactions, whose predictions of both p-T_a ignition diagram and ignition delay times give good agreement to those of the full scheme in the vicinity of the low temperature ignition boundary, thus facilitating the calculation of autoignition temperature or AIT. Further species and reaction removal using the sensitivity techniques alone resulted in mechanism D, comprising 47 species and 157 irreversible reactions, whose p-T_a ignition diagram gives reasonable agreement with that of the full mechanism, but whose calculated ignition delay times have incurred significant error. These species and reaction numbers are summarized in Table 5.3 along with the computational speed-ups gained from the reductions and their estimates from the size of the reduced mechanisms using a run-time $\propto N^2$ for species and $\propto n$ for reactions.

Reduced Mechanism	No. of species	No. of reactions	Runtime % of full scheme		
			Calculated runtime	Estimated from $\propto N^2$	Estimated from $\propto n$
A	104	845 irrev.	15%	4.3%	25.2%
B	100	238 irrev.	5%	4.01%	7.1%
C	60	238 irrev.	2.1%	1.5%	7.1%
D	47	157 irrev.	1.04%	0.9%	4.7%

Table 5.3. Summary of the numbers of species and reactions contained in each of the reduced mechanisms and corresponding calculated and estimated runtimes. Runtimes are estimated from runtime being proportional to the squared number of species ($\propto N^2$) and from runtime being proportional to the number of reactions ($\propto n$).

The reductions performed on the full cyclohexane mechanism are substantial and this is reflected in the computational speedups gained from the reduced mechanisms. The smallest mechanism, C, runs 95 times faster than the full scheme. The calculated runtimes are in good accordance with the estimates obtained from assuming runtime $\propto N^2$, however, this is only true for mechanisms that have had reactions removed using PCAF. The agreement of calculated

runtimes with estimates obtained from assuming runtime $\propto n$ are very approximate. Mechanism C will be kinetically analysed in Chapter 6 and in Chapter 7 it will be further reduced using the time-scale based method of the application of the quasi steady state approximation (QSSA) combined with reaction lumping to further remove species.

5.9 Comparison of reduction achievements

In order to establish the success of the reduction methods used here, comparisons to reductions by other researchers will be discussed. Where possible, the reductions have been compared to similar fuels and size of starting mechanism, however, no attempt at the reduction of a detailed n-butane combustion mechanism appears to have been previously published.

Tomlin *et al* [52] have performed species and reaction reduction on a mechanism describing pyrolysis of pure propane in a cracking tube using the techniques of identification of necessary species and PCA in a similar fashion to the techniques described in this chapter, albeit in a partially automated fashion. The full scheme to which the techniques were applied comprised 48 species in 422 reactions. After application of sensitivity and principal component analyses these numbers were reduced to 19 species and 122 reactions, which translates to a 40% reduction in species and a 30% reduction in reactions. The species reduction approximates to the propane reduction presented in this chapter of a 34% reduction in species. The reduction in reactions using PCA presented in this chapter appears to have been more effective than the methods of Tomlin *et al* [52] with 15% of the reactions remaining in the work presented here. This could be attributed to the innovation in techniques discussed in Section 5.4. However, the original mechanism used in this study could not be considered as comprehensive and was already partially lumped. Further progress was made by Tomlin *et al* by removing fast reversible pairs of reactions and application of the QSSA to a scheme with 12 coupled differential equations and 50 reactions concluding that this was an impressive reduction [137].

Green *et al* [41] use an adaptive chemistry approach to achieve computational savings, whereby a library of optimally reduced models is created. The reduction methodology, described in Section 2.2.1, uses a reaction elimination approach. Local information at a specified point in composition space is used to set up and solve an integer optimization problem and thus identify the reduced subset of reactions for the reduced models. Each reduced model is applicable over a narrow specific range of conditions and is switched to when the conditions to which they pertain are encountered. The major drawback of this technique is that no attempt is made to find a reduced subset of necessary species prior to reaction removal, and it is in this important first step that the major computational savings are made, as is demonstrated in Table 5.3, and so the resulting reduced mechanisms are not truly optimal. For a more effective reduction reduced subsets of necessary species should be identified specific to each time point as is demonstrated in Section 5.2 and Fig. 5.4.

The “optimal”-reduction/adaptive-chemistry techniques have been applied to the GRI mech 3.0 mechanism describing methane combustion in a two-dimensional flame [43]. The full mechanism comprises 53 species and 325 reactions. Nitrogen chemistry was immediately removed from the mechanism leaving a scheme with 217 reactions, because simulations were performed at temperatures lower than those for NO formation. The reduction proceeded by conversion to a library of 657 reduced models with an average size of 55 reactions. This translated to a three-fold computational speedup which compares to reduced schemes presented in this chapter of 15% and 22% runtime of the full mechanism in the cases of propane and n-butane respectively, and 5% runtime of the full mechanism in the case of the cyclohexane mechanism. The reduction methods of Green *et al* [41-43] have been applied to the case of modelling a one-dimensional propane flame using a full scheme comprising 94 species and 505 reactions [42]. The methods produced a library of 18 reduced models of size ~ 30 – 475 reactions with an average size of ~304 reactions. This is greater than the number of reactions in the propane model presented here (166 reactions). The techniques presented in this chapter appear to be more successful, doubtlessly because initial

species removal is neglected in the “optimal”-reduction/adaptive-chemistry methods, although the adaptive chemistry techniques could make more significant computational savings if they were combined with a more effective species reduction approach.

The algorithm of direct relation graph (DRG) is a reduction technique which investigates the couplings between species using ROPA. It has been applied to reduce two mechanisms describing autoignition in a PSR using n-heptane and iso-octane as the primary fuel in each case [40]. Reactions removed subsequent to species removal using a CSP importance index. The n-heptane mechanism was reduced from 561 species and over 2000 reactions down to 188 species and 842 reactions, and the iso-octane mechanism was reduced from 857 species in 3606 reactions down to 233 species in 959 reactions. With the exception of the reduction performed on the n-butane mechanism, the level of species reduction achieved using the DRG method is roughly equivalent to the reductions illustrated in this chapter, as shown in Table 5.4.

	Full mechanism		Reduced mechanism		% removed	
	species	reactions	species	reactions	species	reactions
Propane	122	1137	42	166	66%	85%
N-butane	128	731	73	300	43%	59%
Cyclohexane	499	2323	100	238	80%	90%
^a N-heptane	561	2539	188	842	66%	67%
^a Iso-octane	857	3606	233	959	73%	73%

^a Mechanism reduction performed using DRG methods.

Table 5.4. Comparison of the reduction achievements using the sensitivity techniques in this chapter to those of the DRG reduction methodology [40].

Detailed reduction (DR), proposed by Frenklach, identifies non-contributing reactions by comparing individual reaction rates with the rate of a chosen reaction such as a rate limiting step or the fastest reaction [110]. This method has proven successful in reducing a model to describe methane/air flames comprising 32 species and 163 reactions. 10 species and 124 reactions were removed from the model, translating to a 72% removal of reactions, making this reduction

comparable to the reaction reductions presented in this chapter in terms of the percentage of reactions removed. However, this method is weaker in terms of its ability to eliminate species. Like the “optimal”-reduction/adaptive-chemistry methods, this important first step was bypassed, therefore any species removed were a knock-on effect from removing reactions. The greatest computational savings are made with species removal, making this reduction stage vital.

CARM (computer aided reduction method) is an automatic reduction method proposed by Montgomery *et al* [193]. This method has been used to make dramatic reductions of detailed mechanisms, e.g. a shortened version of the detailed n-heptane mechanism of Curran *et al* [11] has been reduced to only 10 species to describe reaction in a PSR and 16-25 species to reproduce the more complex ignition delay time phenomena. At first glance, these methods appear superior to those presented in this chapter. The methods of CARM exploit the techniques of sensitivity analysis and the QSSA and some of the reactions in the scheme have hidden inner iterations. The application of the QSSA is not shown in this Chapter, however the method has been applied to successfully further remove 14 species from the n-butane mechanism. Further reductions using this technique are possible on the n-butane and propane mechanisms. The application of the QSSA in the present work will be shown in Chapter 6 and evaluated by comparison to equivalent reduction methods of other researchers, such as computational singular perturbation (CSP) analysis (Section 7.5)

5.10 Conclusions

Techniques for mechanism reduction based on local sensitivity analysis methods have been incorporated into a general numerical integration code. UNIX shell scripts have been constructed to automate the application of these techniques to accomplish the efficient reduction of full reaction models to encompass low-temperature initiation of reaction, low and intermediate temperature cool flame phenomena, and high temperature ignition at a number of initial ambient conditions. By automation of the procedures the otherwise considerable and time

consuming computational effort required is reduced to the user having only to make choices of appropriate tolerances and selection of the reduced scheme based on comparison of the ignition diagrams and temperature profiles generated from the full and reduced schemes. This also is done in an automatic way. All these techniques have been set up in a CHEMKIN framework.

The techniques have allowed the automatic and systematic reduction of an equimolar propane – oxygen, a lean n-butane - air kinetic and a stoichiometric cyclohexane – air model, simulated in a closed vessel. Comparisons of the predictions of full and reduced schemes have shown that the numbers of species and reactions have been successfully reduced in each case. Zero – dimensional runtimes of the full and reduced mechanisms have been compared and show that substantial computational savings have been made. A review of reduction achievements made by other researchers has shown that the level of reduction achieved using the techniques presented in this chapter is in line with the current state of the art for skeletal reduction.

Reducing mechanisms to this level, whilst maintaining the original kinetic form of the mechanism, facilitates the undertaking of kinetic investigations. In Chapter 6, a number of the reduced mechanisms presented here are further analysed using techniques such as global uncertainty, rate of production and element flux analyses. Further reductions can also be achieved using the QSSA combined with reaction lumping, as we will see in Chapter 7 by the application of such techniques to the 60 necessary species 238 irreversible reactions cyclohexane mechanism.

Chapter 6

Kinetic analysis of reduced hydrocarbon oxidation mechanisms

Apart from the necessity of reduced hydrocarbon oxidation mechanisms for their application in 3-dimensional models of reactive flows, they can also be used to effectively analyse the underlying kinetics of the system which drive the oxidation phenomena. There are a number of techniques available which can help scientists gain kinetic understanding of the competition between reaction steps or coupling between species such as rate of production and element flux analysis which can be used to establish and quantify the main reaction routes as time progresses. Such information can then be easily digested in tabulated form or by the use of reaction schematics for a particular range of operating conditions. Moreover, techniques which have gained increasing attention and importance recently are local and global uncertainty analyses [15], where local refers to nominal changes of parameters, while global methods refer to the effect of simultaneous, possibly orders-of-magnitude parameter changes [104].

Many of the values for rate parameters or thermochemistry in combustion mechanisms are only known to a limited degree of accuracy or range of uncertainty and these ranges are often large. The influence of each parameter on model output will vary and so making a small change to one parameter can have a huge impact on model output whilst making a large change to another could have a limited impact. These poorly known parameters can cause the large quantitative

discrepancies witnessed when model output is compared to experiment, as shown in Chapter 4. Sensitivity and uncertainty analyses can be used in order to provide information on which parameters drive the predictive uncertainty of a model and therefore require further study using experimental or *ab initio* modelling techniques. It follows that this type of analysis is an important component of model validation and development. Uncertainty analysis can be most usefully applied to combustion systems when it is employed as a global method. That is, several or all parameters are perturbed simultaneously within their entire range of uncertainty and the effect on model performance is measured. This is unlike a local sensitivity or uncertainty analysis method where only small changes in parameters are studied close to the nominal values. There are a number of global uncertainty analysis methods such as Morris-one-at-a-time and Monte Carlo simulations which work on the premise of perturbing parameters, simulating, quantifying the impact on the mechanistic feature of interest and then analysing the results using statistical methods [194].

The impact of a perturbation of one parameter can have a similar effect on model output as a perturbation of many inherently correlated parameters (within their ranges of uncertainty), where the ranges of correlated parameter values which can reproduce pertinent experimental data within their respective uncertainty bounds are known as a “feasible set” [195]. These factors are taken into account by the simultaneous nature of the global uncertainty approach. After finding our parameter or group of parameters having the greatest impact on our output of interest, then a more certain value should be found using techniques like modern quantum chemistry or detailed experimental kinetic studies and the temptation to simply tune the parameter(s) to whatever value(s) best fits the original experimental data should be resisted. Having found the more certain parameter, validation should be repeated, and if the implementation of this change negates the mechanism’s performance in a different range of operating conditions then this would suggest other uncertain parameters require the same treatment.

Although the techniques of ROPA and element flux analysis could be performed using full mechanisms, the results can be achieved much more

conveniently with the use of a reduced mechanism. In the case of global uncertainty analysis, the technique involves running many simulations, with the number of simulations often scaling with mechanism size and so mechanism reduction has been established as a prerequisite.

It is generally accepted that automatically generated comprehensive kinetic mechanisms contain information that is superfluous over all operating conditions. If there are classes of species and reactions which are always being eliminated by mechanism reduction from all types of fuel then this information could be of benefit to comprehensive mechanism generation.

In this chapter, the species and reaction elimination patterns between the fuels propane, n-butane and cyclohexane are investigated. Uncertainty analysis is used to identify parameters contributing to the over reactivity exhibited by the Nancy propane model, in reduced form, and reflected in the p - T_a ignition diagram in terms of the lowest pressure at which 2-stage ignition occurs. The uncertainty analysis presented in this chapter was not carried out by the author (work credited to Dr. K. J. Hughes) but is highly relevant to the other material in this thesis so its inclusion is deemed important. The reduced propane mechanism is examined using element flux analysis to identify major reaction pathways during two-stage ignition. The results are compared to a modelling study and the uncertainty analysis results for propane. The kinetic foundation of the n-butane scheme is analysed by formal numerical methods to trace the origins of the dramatic shifts in autoignition temperatures as conditions are changed. The most important reactions leading to hydrogen peroxide formation are identified using rate of production analysis, and the greatest heat releasing reactions are determined in the transition from cool flame to ignition [25]. The characteristics of one of the reduced cyclohexane mechanisms are analyzed during isothermal combustion and element flux analysis is used to establish the major couplings between species.

6.1 Species and reaction elimination patterns between fuels

The first step in the reduction process is the elimination of redundant species via the investigation of the Jacobian matrix. Subsequently, redundant reactions are removed via sensitivity or principal component analyses. Kinetic insights can be gained into the trends that emerge of which species or reactions are consistently eliminated for each hydrocarbon fuel type. This knowledge is potentially useful to comprehensive mechanism development and may be useful in indicating the extent of reduction achievable for higher hydrocarbons of similar classes. In the subsequent sub-sections species notations as they appear in the full and reduced CHEMKIN mechanisms are used.

6.1.1 Redundant species patterns

An analysis of the patterns of removed species has been undertaken for the mechanism reduction cases of simulated combustion of lean n-butane in air and equimolar propane in oxygen by comparison of lists of removed species. The investigation of the Jacobian matrix led to the removal 53 species from the full 128 species n-butane mechanism, leaving 75 necessary species. 80 species were removed from the full 122 species propane mechanism generating a partially reduced mechanism comprising 42 species.

Of the 53 species removed from the n-butane mechanism 42 of these (79%) were also removed from the propane mechanism. These commonly removed species are shown in Table 6.1. Notably, all the species which are classed as “secondary species” by the EXGAS program were identified as redundant with the exception of the alkene hydroperoxide species C_3H_5OOHY . Secondary species exist as a consequence of the procedures built into EXGAS for mechanism generation where, in order to provide a degree of simplification, isomeric species that are considered peripheral to the overall mechanism are represented by one generic species. There are a total of 13 secondary species for n-butane and 14 for

propane and they are virtually the same set. They include pentene, hexene, dienes, alkene alcohols and alkene hydroperoxides.

C ₀ – C ₂	C ₃ , C ₄	C ₅ , C ₆	C ₇ +
B3C	C2H3CHOZ	<u>C5H10OOY</u>	<u>C7H12Y2</u>
B4CH	C2H3O#4COOOH	<u>C5H10Y</u>	<u>C8H14Y2</u>
B6CH2	C2H6CO	<u>C5H9OHY</u>	
C2H2T	<u>C3H5CHOY</u>	<u>C6H10Y2</u>	
CH3COOOH	<u>C3H5OHY</u>	C6H10Z#6	
CH4	<u>C3H5OOHZ</u>	<u>C6H12Y</u>	
R12CHCOV	C3H6O#3		
R6CH2OH	C3H6O#4		
R9C2HT	C3H7CHO		
	C3H7OH		
	C3H8CO		
	C4H6Z2		
	<u>C4H7OHY</u>		
	<u>C4H7CHOY</u>		
	<u>C4H8OOY</u>		
	R27C4H8OOH		
	R35C4H8OOOOH		
	ZC3H4O#4OOH		
	ZC3H5O#4		
	ZCOC2H3Z		
	ZCOC3H7		
	ZCOOOC2H5		
	ZCOOOC3H7		
	ZOOC3H4O#4OOH		
	ZOOC3H5O#4		

Table 6.1. Common species removed from the comprehensive n-butane and propane mechanisms. The common “secondary species” are underlined. The species are represented by the formulation used in the EXGAS input programs, as is also the case where discussed in the text.

There are also patterns between the removed species which are not in this commonly removed list, with respect to alkanes other than the primary fuel and their sub-mechanisms as shown in table 6.2. For instance, C₃H₈ is removed from the n-butane mechanism whereas C₄H₁₀-1 is removed from the propane mechanism. Many of the species involved in the primary mechanism of C₃H₈ were also removed from the n-butane mechanism, such as, C₃H₇ (propyl radicals),

both isomers of C₃H₇O₂ (propylperoxy radicals) and of C₃H₇OOH (propyl hydroperoxide). The corresponding types of free radicals as derivatives of n-butane were removed during the propane reduction. It may seem surprising that there should be any reference to oxidation chemistry of butane in a propane oxidation scheme. It should be born in mind, however, that in the nature of a comprehensive chemical model, association reactions between radicals (for example C₃H₇ + CH₃ → C₄H₁₀) can promote subsidiary reaction chains of the higher hydrocarbons.

Methane was removed in both of the reductions. Ethane was removed in the propane reduction but was not identified as redundant in the n-butane reduction; however, the elimination of its three remaining consuming reactions does not incur a significant error leading to the conclusion that it is an unidentified redundant species. The removal of components of the sub-mechanisms of other alkanes is limited to C₃ and upwards because ethyl and methyl radicals and others are known to be integral to the reduced propane mechanism. Pentane and higher alkanes were not present in either of the full mechanisms. All cyclic species, 4 primary, 3 secondary and 8 cyclic free radicals were removed from the propane mechanism.

Species type	Removed from butane mechanism	Removed from propane mechanism
Alkane	C ₃ H ₈ , CH ₄	C ₄ H ₁₀ -1, CH ₄
Alkyl radical	R ₁₉ C ₃ H ₇	R ₂₀ C ₄ H ₉
Alkyl peroxy radical	R ₂₂ C ₃ H ₇ OO	R ₂₃ C ₄ H ₉ OO
Alkyl peroxide	C ₃ H ₇ OOH	C ₄ H ₉ OOH
Internally rearranged alkyl peroxy radical	R ₂₅ C ₃ H ₆ OOH R ₂₆ C ₃ H ₆ OOH	R ₂₇ C ₄ H ₈ OOH R ₂₈ C ₄ H ₈ OOH R ₂₉ C ₄ H ₈ OOH R ₃₆ C ₄ H ₈ OOH
Dihydro peroxy radicals	R ₃₃ C ₃ H ₆ O ₀₀₀₀ H R ₃₄ C ₃ H ₆ O ₀₀₀₀ H	R ₃₃ C ₄ H ₈ O ₀₀₀₀ H R ₃₄ C ₄ H ₈ O ₀₀₀₀ H R ₃₅ C ₄ H ₈ O ₀₀₀₀ H R ₃₈ C ₄ H ₈ O ₀₀₀₀ H
Keto hydroperoxide	C ₂ H ₅ COOOH	C ₃ H ₇ COOOH

Table 6.2. Classes of chemical species related to the submechanisms of alkanes commonly removed from the comprehensive n-butane and propane mechanisms.

An interesting question is “to what extent do these trends persist for cyclohexane?” The cyclohexane mechanism was reduced under stoichiometric conditions in air and the number of species decreased from 499 to 100 in the initial reduction. Then further reductions were made to 60 and 47 species which generated schemes of varying quality. Primarily, comparison is made to the n-butane reduction using the 100 species reduced cyclohexane mechanism.

Of the 53 species removed in the n-butane mechanism, 38 of these were present in the full cyclohexane mechanism. 31 of the 38 were removed. The exceptions were C₂H₃CHOZ, C₄H₆Z₂, C₆H₁₀Z#6, R₁₂CHOV, R₆CH₂OH, ZCOC₂H₃, CH₄. However, CH₄ had all of its consuming reactions removed at the reaction reduction stage. All of the C₃-C₅ alkanes were removed and when present in the full mechanism, so were their associated alkyl radicals, alkyl peroxy radicals, dihydroperoxides and ketohydroperoxides. Alkyl peroxides and alkanes higher than pentane were absent from the full scheme. Ethane was not removed in the reduction down to 100 species but had its consuming reactions removed in the reaction reduction of the 60 species mechanism. The trend of removal of C₃ + alkanes and their associated species has occurred in the cyclohexane reductions and is likely to occur in the reduction of other hydrocarbon mechanisms. C₂ – C₆ aldehydes were also removed from the cyclohexane mechanism. Similarly to the cases of propane and n-butane, all 17 secondary molecules were removed. The one species classed as primary cyclic and all 5 secondary cyclic species were removed, as occurred in the propane reduction. All 34 species classed as additional allene in the full mechanisms were removed, with the exception of the unidentified redundant species C₆H₆# (benzene).

It appears that alkanes and associated radicals, other than those pertaining to the primary fuel, are not required for the modeling of low temperature applications. The majority of these alkanes are produced by the recombination of radicals class of reaction, but propane and butane can be produced by metathesis involving H atom abstraction by radicals from the initial reactants and the recombination or ethyl radicals ($C_2H_5^\bullet + C_2H_5^\bullet \rightarrow C_4H_{10}$, from the C₀ – C₂ base),

respectively. However, the associated radicals are produced by unimolecular initiations involving the breaking of a C–C bond of the primary fuel or by decompositions of radicals by β -scissions involving the breaking of the breaking of C–C or C–O bonds for all types of radicals, rather than being produced via H atom abstraction from their parent alkane molecule.

6.1.2 Redundant reactions patterns

An investigation into the classes of reactions removed in the cases of n-butane and cyclohexane has been undertaken. The comprehensive cyclohexane mechanism contains 1025 reversible reactions and 1298 irreversible reactions. The numbers of reactions were reduced using principal component analysis of the rate sensitivity matrix \tilde{F} (PCAF) to 238 irreversible. This was a very substantial reduction and the many classes of reactions removed are cited in Appendix A. The comprehensive cyclohexane mechanism contains a large subsection for benzene formation reactions which has 52 irreversible reactions and 290 reversible reactions. The vast majority of these were identified as redundant and removed leaving 6 remaining. Manual removal of the remaining 6 incurs very little error to the output ignition delay times. It appears that this complete subsection of the mechanism is not necessary to study low temperature oxidation. Many of the classes of reactions involved in the C₀ – C₂ base mechanism were removed in the reduction process.

A combination of the overall sensitivity measure and PCAF was used to remove reactions from the species reduced n-butane mechanism. The comprehensive n-butane mechanism comprises 314 irreversible and 417 reversible reactions. The reduced mechanism comprises 300 reactions and the classes of reactions removed are also shown in Appendix A. Unimolecular initiations were removed in both n-butane and cyclohexane reductions. These high activation energy reactions are only important at high temperature initial conditions. Unsurprisingly, alkane reactions were commonly removed in both reductions by virtue of the removal of their species, as were the classes of alcohol

reactions, peracid radical decompositions and Dielz-Alder reactions. There are a number of reaction classes of the $C_0 - C_2$ base mechanism which were removed in both of the reductions. They are reactions of H_2 , B_4CH , B_6CH , B_5CH_2 , CH_4 , C_2H_2T , R_9C_2HT , $R_{10}C_2H_3V$, C_2H_4Z , R_6CH_2OH , $R_{12}CHCOVD$, $R_{14}CH_3CO$, CO_2 , and $R_{16}CH_3COOOH$. This suggests that a reduced $C_0 - C_2$ base mechanism may be viable for low temperature mechanisms generated by EXGAS.

The remaining species and reactions in the propane, n-butane and cyclohexane mechanisms which are important to their respective oxidation processes will be elucidated in the following Sections of the remainder of this Chapter.

6.2 Quantitative assessment of the impact of uncertainties in parameter values of the propane mechanism

As has been shown in Chapter 4 there is a quantitative discrepancy between experiment and model prediction of the pressure location for the two-stage ignition boundary. The transition from cool flame reaction to ignition can therefore be used as an appropriate basis for evaluation. Using an intermediate, 60-species reduced mechanism, global non-linear uncertainty analysis was employed in order to investigate the potential origins of the discrepancies. The quantitative impact of parameter changes on three global features were measured, namely; the temperature reached in the first stage of two-stage ignition (T_1) (on the basis that it is a fundamental aspect of the transition process [24]), the induction time to the first stage (τ_1) and the induction time of the second stage (τ_2).

A method devised by Morris [196] was used to determine an ordered ranking of the main heats of formation and reactions which contribute to output uncertainties in the selected features. In the Morris method simulations are grouped into sets in which the initial range of values for the selected input parameters are restricted (randomly) to within a given fraction at the lower end of the overall specified range. The subsequent order in which the parameters are varied is then randomly chosen. After the first simulation using the initial parameter values, variations are then applied to each parameter in turn by a fixed

Species	Absolute mean perturbation		
	τ_1 / s	τ_2 / s	T_1 / K
n-O ₂ CH ₂ CH ₂ CH ₂ OOH	13.8	19.8	166
n-C ₃ H ₇ O ₂	11.6	15.0	63.1
i-C ₃ H ₇ O ₂	3.50	6.08	32.5
CH ₂ CH ₂ CH ₂ OOH	2.13	0.225	31.8
CH ₃ CH(OOH)CH ₂	1.71	2.38	2.72
CH ₃ CHCH ₂ OOH	1.44	1.50	7.58
i-C ₃ H ₇	1.39	2.13	7.08
C ₂ H ₅ OO	1.22	4.44	5.69
n-C ₃ H ₇	0.512	1.09	10.4
CH ₃ CH(OOH)CH ₂ O ₂	0.929	1.72	1.68
C ₂ H ₅	0.890	2.50	5.36
C ₂ H ₅ OOH	0.373	0.642	18.3
CH ₃ OO	0.353	0.588	0.0928
CH ₃ CH(O ₂)CH ₂ OOH	0.103	0.199	0.335
HO ₂	0.0385	0.0980	1.56
CH ₃ OOH	0.0364	0.0768	1.27
CH ₃ O	0.0316	0.0705	1.71
CH ₃	0.0691	0.0505	0.411

Table 6.3. The 18 most important heats of formation identified by the Morris method [24].

perturbation. Within each Morris simulation, the perturbed value of each of the parameters is successively varied from its initial value by a fixed amount. The mean effect of the change in each parameter over a number of Morris runs is then evaluated and can be ranked to give the overall importance of each parameter. The results of the simulations are then analysed using standard statistical methods. Further details of the Morris method can be found elsewhere [24,194,196]. Attention was then focused on the analysis of Monte Carlo simulations based on random samples of the most important parameters as identified by the Morris method [196]. This allows a demonstration of how combinations of variations in parameter values may affect optimize the response and is necessary to assess whether the same consequent change in model output can be achieved by varying one or many uncertain parameters. An operating condition was chosen for the Morris and Monte Carlo methods constituting an equimolar propane + oxygen mixture at 400.79 torr (diluted with nitrogen to 1 atmosphere total pressure) at

Reaction	Absolute mean perturbation		
	τ_1 / s	τ_2 / s	T_1 / K
$C_3H_8+OH \leftrightarrow H_2O+n-C_3H_7$	9.62	9.20	69.1
$C_3H_8+OH \leftrightarrow H_2O+i-C_3H_7$	9.16	9.19	46.1
$O_2CH_2CH_2CH_2OOH \leftrightarrow OH+C_2H_5COOOH$	4.61	9.87	41.5
$C_3H_8+HO_2 \leftrightarrow H_2O_2+n-C_3H_7$	3.93	8.88	3.74
$2HO_2 \leftrightarrow H_2O_2+O_2$	3.26	7.78	30.3
$i-C_3H_7O_2 \leftrightarrow C_3H_6+HO_2$	4.43	3.09	23.8
$i-C_3H_7O_2+HO_2 \leftrightarrow C_3H_7OOH+O_2$	2.19	4.94	27.2
$C_3H_8+i-C_3H_7O_2 \leftrightarrow C_3H_7OOH+i-C_3H_7$	3.66	3.40	10.8
$CH_3OOH \leftrightarrow CH_3O+OH$	2.88	0.242	3.06
$n-C_3H_7O_2 \leftrightarrow C_3H_6+HO_2$	2.55	4.83	17.6
$C_2H_5+O_2 \leftrightarrow C_2H_4+HO_2$	1.26	4.83	17.0
$C_3H_8+i-C_3H_7O_2 \leftrightarrow C_3H_7OOH+n-C_3H_7$	2.55	3.39	9.02
$i-C_3H_7+O_2 \leftrightarrow C_3H_6+HO_2$	2.26	3.75	20.3
$n-C_3H_7O_2 \leftrightarrow C_3H_6+HO_2$	1.40	3.87	8.20
$n-C_3H_7+O_2 \leftrightarrow C_3H_6+HO_2$	0.795	1.69	22.9
$C_2H_5OO+HO_2 \leftrightarrow O_2+C_2H_5OOH$	1.60	3.70	17.3
$C_2H_5COOOH \leftrightarrow OH+HCHO+B_2CO+CH_3$	2.22	0.0478	3.22
$i-C_3H_7O_2 \leftrightarrow C_3H_6+HO_2$	1.90	1.52	9.83
$C_3H_8+HO_2 \leftrightarrow H_2O_2+i-C_3H_7$	1.53	3.22	1.34
$CH_3OO+HO_2 \leftrightarrow CH_3OOH+O_2$	1.54	0.670	10.6
$H_2O_2 (+M) \leftrightarrow 2OH(+M)$	0.288	2.74	0.457
$C_3H_7OOH \leftrightarrow OH+HCHO+C_2H_5$	1.44	0.240	3.59
$CH_2CH_2CH_2OOH+O_2 \leftrightarrow$	0.916	1.62	17.5
$C_2H_5OOH \leftrightarrow C_2H_5O+OH$	1.40	0.330	4.45
$C_3H_8+CH_3OO \leftrightarrow CH_3OOH+n-C_3H_7$	1.36	1.19	3.29
$O_2+CH_3O \leftrightarrow HCHO+HO_2$	0.554	1.23	5.68
$O_2+H (+M) \leftrightarrow HO_2 (+M)$	0.486	1.18	7.88
$CH_3CH(OOH)CH_2 \leftrightarrow i-C_3H_7O_2$	0.609	0.414	1.27
$C_3H_8+CH_3OO \leftrightarrow CH_3OOH+i-C_3H_7$	0.591	1.10	3.76
$CH_3CHCH_2OOH \leftrightarrow n-C_3H_7O_2$	0.561	0.390	2.20
$HCHO+OH \leftrightarrow CHO+H_2O$	0.462	1.09	16.1
$n-C_3H_7O_2+HO_2 \leftrightarrow C_3H_7OOH+O_2$	0.559	0.0466	1.40
$C_3H_8+H \leftrightarrow H_2+n-C_3H_7$	0.510	1.01	8.12
$CH_2CH_2CH_2OOH \leftrightarrow C_3H_6+HO_2$	0.372	0.688	7.33
$HO_2+CH_3 \leftrightarrow CH_3O+OH$	0.143	0.0666	20.4
$C_3H_8+CH_3O \leftrightarrow CH_3OH+n-C_3H_7$	0.280	0.624	3.69
$HO_2+HCHO \leftrightarrow CHO+H_2O_2$	0.117	0.926	1.37
$CH_3OO+HO_2 \leftrightarrow O_2+HCHO+H_2O$	0.209	0.468	3.18
$HO_2+CH_3CHO \leftrightarrow CH_3CO+H_2O_2$	0.208	0.683	1.38
$CH_3O+M \leftrightarrow HCHO+H+M$	0.144	0.433	10.71
$C_3H_6+OH \leftrightarrow CH_3+CH_3CHO$	0.0678	0.902	0.169
$2HO_2 \leftrightarrow H_2O_2+O_2$	0.140	0.624	9.98
$CH_3OO+H_2O_2 \leftrightarrow CH_3OOH+HO_2$	0.00147	0.700	0.989
$C_3H_6+OH \leftrightarrow C_3H_5+H_2O$	0.103	0.439	6.28
$C_3H_8+O_2 \leftrightarrow HO_2+n-C_3H_7$	0.0920	0.0626	7.75
$HO_2+H \leftrightarrow 2OH$	0.0216	0.0777	7.75
$C_3H_6+H \leftrightarrow C_2H_4+CH_3$	0.0239	0.307	0.634
$HO_2+C_2H_5 \leftrightarrow CH_3+HCHO+OH$	0.0228	0.102	7.08
$2CH_3 (+M) \leftrightarrow C_2H_6 (+M)$	0.00411	0.0292	5.64
$2CH_3OO \leftrightarrow 2CH_3O+O_2$	0.00330	0.0953	0.823

^a Chemkin format duplicate reactions.

Table 6.4. The 50 most important reactions identified by the Morris method [24].

$T_a = 593\text{K}$. Adiabatic conditions were maintained so that 2-stage ignition occurred rapidly on a reasonable timescale regardless of the adjustments made either to species heats of formation or to rate coefficients.

Where possible, the uncertainty of each individual ΔH_f° was taken from the work of Afeefy *et al* [197]. However, in most cases there were no data available and, therefore, an approach was taken in which simple species were assigned a ± 5 kJ mol^{-1} range, intermediate species such as n-propylperoxy ($\text{n-C}_3\text{H}_7\text{O}_2$), a ± 10 kJ mol^{-1} range, and complex species such as n-peroxyhydroperoxypropyl ($\text{n-O}_2\text{CH}_2\text{CH}_2\text{CH}_2\text{OOH}$), a ± 15 kJ mol^{-1} range. Given that the initial values in these cases all come from group additivity calculations in the generation of the mechanism [19] (as discussed in Section 2.1.1), it is reasonable to assume such levels of uncertainty. Using the Morris uncertainty analysis, the top 18 heats of formation (Table 6.3) and top 50 reaction rate parameters (Table 6.4) were then chosen from each output (τ_1 , τ_2 and T_1). By taking the union of these important parameters, a combined set was constructed that controlled τ_1 , τ_2 and T_1 . This list comprises 68 parameters in total (18 species and 50 rate coefficients). Further statistical analysis highlighted the particular importance of the heats of formation of the radicals $\text{i-C}_3\text{H}_7\text{O}_2$, $\text{n-C}_3\text{H}_7\text{O}_2$, and $\text{n-O}_2\text{CH}_2\text{CH}_2\text{CH}_2\text{OOH}$. Element flux analysis shows that these species participate in dominant reaction routes, during two-stage ignition, as will be further discussed in Section 6.3.

Morris analysis of the absolute mean values of perturbations, within their ranges of uncertainty chosen, showed that the highest ranked heats of formation exhibit a greater influence than the highest ranked rate parameters. To a certain extent the relative importance of the heats of formation with respect to the reaction rate parameters is governed by the choice of uncertainty ranges selected prior to the analysis. Assuming that the choice of uncertainty ranges are reasonable for estimated parameters, then the results support the view that sensitivity studies in general should include thermokinetic parameters since their effects can be at least as significant as those of forward rate parameters [24]. However, rate coefficient adjustments made in the Morris method, using a $\pm 25\%$ range from their initial value, showed that the three criteria, the first stage

temperature and the time dependences (τ_1 and τ_2), were highly sensitive to the magnitude of the pre-exponential term of five reactions in particular:



Reactions 6.1 to 6.4 all feature heavily in the carbon flux analysis during 2-stage ignition of propane using a reduced EXGAS mechanism (see Section 6.3 and Fig 6.3).

To exemplify the inter-relationship between some of the main controlling heats of formation, the variability of the temperature reached in the first stage of two-stage ignition and the time intervals τ_1 and τ_2 with respect to variations in ΔH_f° for n-O₂C₃H₆OOH (± 15 kJ mol⁻¹), n-C₃H₇O₂ and i-C₃H₇O₂ (± 10 kJ mol⁻¹), were evaluated from 5000 Monte Carlo simulations. The results of the calculations substantiate the Morris rankings, with variations to ΔH_f° for the n-propylperoxyhydroperoxide radical (n-O₂CH₂CH₂CH₂OOH), being the most dominant (Fig. 6.1). The scatter in Fig. 7a–c reflects the effect of the random combinations of the other 67 varied parameters, and is a consequence of the fact that more than 1 parameter contributes to the output uncertainty. The scatter plots also demonstrate regions of contrasting sensitivity to parameter variation (Fig. 6.1). τ_1 , and to a lesser extent τ_2 and T_1 , are more sensitive to an increase in ΔH_f° (n-O₂CH₂CH₂CH₂OOH) relative to its nominal value, rather than its decrease. For example, there is only ~25% reduction of τ_1 when the heat of formation is reduced by 15 kJ mol⁻¹ whereas it increases by ~165% when the heat of formation of n-O₂CH₂CH₂CH₂OOH is raised by 15 kJ mol⁻¹. There is a very marked increase in τ_2 throughout the variation range -15 to +15 kJ mol⁻¹, necessitating a logarithmic scale. This may arise because an increase of ΔH_f° (n-O₂CH₂CH₂CH₂OOH) causes

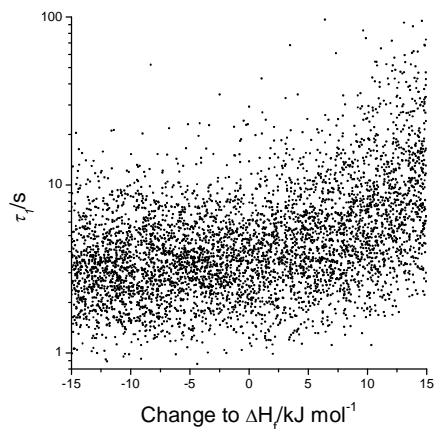


Fig. 6.1a Monte Carlo analysis of τ_1 as a function of changes in the heat of formation of n-propylperoxyhydroperoxide [24].

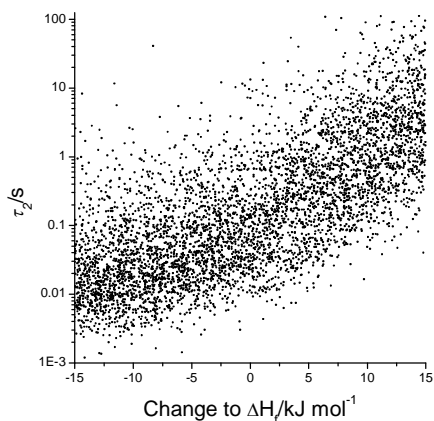


Fig. 6.1b Monte Carlo analysis of τ_2 as a function of changes in the heat of formation of n-propylperoxyhydroperoxide [24].

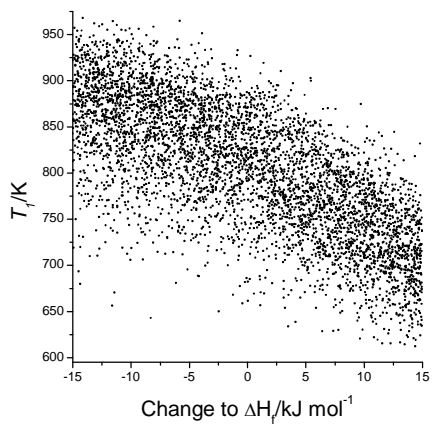


Fig. 6.1c Monte Carlo analysis of T_1 as a function of changes in the heat of formation of n-propylperoxyhydroperoxide [24].

the first stage temperature to be decreased by up to 200 K. Consequently the rate of decomposition of H_2O_2 is dramatically decreased [4,24].

6.2.1 Summary of uncertainty analysis

The reduced computational cost of the reduced C_3H_8 model has facilitated the use of global methods for assessing the impact of uncertainties in the main input parameters within the scheme for the simulation of auto-ignition. This example shows that in evaluating kinetic models it is important to address the interactions of uncertainties in parameters in a quantitative way. It should be noted also that major uncertainties reside in the parameters related to thermochemistry. The heats of formation, even of the $\text{C}_3\text{H}_7\text{O}_2$ radicals, are unlikely to be known to a precision better than $\pm (5 - 8) \text{ kJ mol}^{-1}$ [198], and that for the $\text{n-O}_2\text{CH}_2\text{CH}_2\text{CH}_2\text{OOH}$ will certainly be less precise. Amongst the three, ΔH_f° for $\text{n-O}_2\text{CH}_2\text{CH}_2\text{CH}_2\text{OOH}$ is the most important, and the question then arises as to the extent to which the p - T_a ignition diagram is affected if its heat of formation alone is increased. As an example Fig. 6.2 demonstrates that when ΔH_f° for $\text{n-O}_2\text{CH}_2\text{CH}_2\text{CH}_2\text{OOH}$ is raised by only 12.5 kJmol^{-1} there is a very pronounced effect, increasing the minimum pressure for 2-stage ignition by 180 torr, taking it higher than that found experimentally (Fig. 4.5).

It seems that parametric uncertainty alone could be enough to account for the over-reactivity of the mechanism, and that furthermore, only a few parameters may be responsible for most of the output variance. Further study of these parameters using *ab initio* techniques may help to evaluate whether such uncertainties are indeed the cause of discrepancies between the model and experiment. Without such *ab initio* studies it is difficult to say unequivocally that mechanistic uncertainty (i.e., missing or incorrect reaction steps), or problems related to the description of the physics do not play a role.

The influence of changes to the heats of formation of $\text{n-O}_2\text{CH}_2\text{CH}_2\text{CH}_2\text{OOH}$ and other highlighted species within their corresponding range of uncertainty, on the time dependence for the development of 2-stage ignition, means that

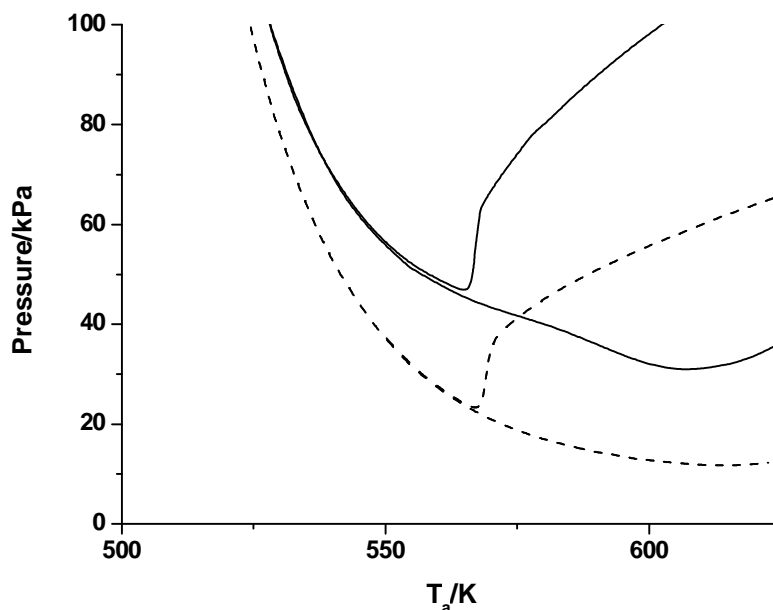


Fig. 6.2. Comparison of 2-stage ignition and cool flame/slow reaction boundaries. Dashed line – unadjusted thermodynamics, Solid line - +12.5kJ to ΔH_f^0 of $n\text{-O}_2\text{CH}_2\text{CH}_2\text{CH}_2\text{OOH}$ [168].

predictions of ignition delay times, as might be used in the interpretation of the performance of fuels, may also be in error as a consequence of the same uncertainties. This problem is not unique to the comprehensive scheme for C_3H_8 used here, but from the wider investigations appears to be a generic problem [24].

6.3 Analysis of major oxidation pathways during 2-stage ignition of equimolar propane and oxygen using element flux analysis

The creation of schematic diagrams showing the main reaction pathways of the necessary species is greatly facilitated by the application of reduced kinetic mechanisms. One approach to the generation of such schematics is in the use of element flux analysis. The idea of element flux analysis was introduced in [199] and uses reaction rates to identify the major sources and sinks of elements at a variety of reaction times. The element fluxes are most usefully calculated for C, H

or O. The instantaneous flux of an element A from species h to species i through reaction j is calculated by:

$$\dot{A}_{hij} = R_j \frac{n_{A,h} n_{A,i}}{N_{A,j}}, \quad (6.6)$$

where $n_{A,h}$ is the number of A atoms in species h , $n_{A,i}$ is the number of A atoms in species i and $N_{A,j}$ is the total number of A atoms in reaction j . Summing for all reactions that the species appear in as reactants and products gives the total transfer of element mass for any pair of species as a function of time, which leads to:

$$\dot{A}_{FROM,TO}(t) = \sum_{j=1}^{N_R} A_{j,FROM,TO}(t). \quad (6.7)$$

This is a local analysis so the fluxes should be calculated at a number of time points during the reaction simulation [200]. Showing all the species couplings would lead to an over complex figure so minor pathways should be filtered out. The element fluxes of C from species to species during 2-stage ignition in equimolar propane oxygen conditions at 630K and 640 torr were calculated by applying equation 6.7 using KINALC [31]. Time points for the analysis were automatically preselected, as shown in fig. 5.2, using a subsection of the reduction software. A program called FluxViewer [201] was then used to read the reaction flux information and view the kinetic connections between species as the reaction progresses in an animation. Using a drag and drop method software feature, the reaction schematic could be analysed in the desired species configuration and isomers could be combined. Using a slide bar in the FluxViewer window, insignificant connections could be filtered out and ignored. The magnitude of the fluxes deemed to be insignificant were subjective to reaction time or temperature because, for instance, at $t = 0.003$ and $T = 630\text{K}$ all the fluxes are very small and

will increase as time progresses. As a guide to what cut-offs were used, the threshold criteria relative to the maximum flux at each time point are outlined in Table 6.5. The insight gained from this analysis resulted in the schematic reaction pathway for propane in the low temperature regime shown in Fig. 6.3.

The reaction is initiated by H atom abstraction from the primary fuel by 9 molecules to form propyl radicals. Of these 9 molecules, OH and HO₂ radicals featured most prominently in the Morris analysis (reactions 6.1, 6.2, and 6.4), with the magnitudes of the rates of these reactions being critical to the simulated ignition. Prior to the cool flame, the major low temperature reaction pathway is

Time point	t/s	T/K	Maximum Flux of C	Threshold Flux of C
1	0.003	630	6.551×10^{-12}	1.158×10^{-14}
2	0.795	640.9	1.043×10^{-4}	1.514×10^{-8}
3	0.852	680.3	1.350×10^{-3}	4.947×10^{-7}
4	0.858	732.5	8.095×10^{-3}	9.664×10^{-7}
5	0.859	795.0	1.458×10^{-2}	3.357×10^{-5}
6	0.862	825.5	4.572×10^{-5}	2.708×10^{-8}
7	0.977	830.0	8.510×10^{-5}	6.615×10^{-8}
8	1.023	930.1	1.742×10^{-3}	1.067×10^{-5}
9	1.024	103.1	1.915×10^{-2}	4.293×10^{-4}

Table 6.5. Maximum flux of C atoms and threshold flux of C atoms at the temperature/time points used during 2-stage ignition of equimolar C₃H₈ in oxygen at initial conditions of 630 K and 640 torr total pressure. The element flux analysis was conducted using a 42 species in 166 reactions reduced mechanism.

the addition of oxygen to propyl radicals to form propyl peroxy radicals, with the simulated ignition being highly sensitive to the magnitudes of the thermochemistry of these two isomers, as was discussed in Section 6.2. The main pathway for the propyl peroxy radicals is the addition of an H atom to form propyl peroxide which subsequently breaks to form ethyl radicals and formaldehyde. Ethyl radicals form ethoxy radicals via C₂H₄, C₂H₅OO and C₂H₅OOH. Ethoxy radicals ultimately form methyl radicals, formaldehyde and carbon monoxide. A less sizeable alternative low temperature reaction pathway for the propyl peroxy radicals is

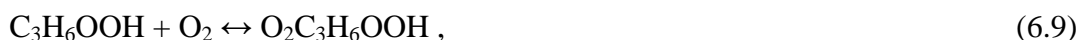
isomerization to form C_3H_6OOH . Addition of oxygen leads to $O_2C_3H_6OOH$ (propylperoxyhydroperoxide radical); three isomers of these are present and the one which has highest atomic fluxes during the induction to the first cool flame is $n-O_2CH_2CH_2CH_2OOH$ (identified in the Morris analysis as having thermochemistry to which outputs are highly sensitive). $O_2C_3H_6OOH$ then forms C_2H_5COOOH (a ketohydroperoxide), which is another highly influential reaction as identified by the Morris analysis (6.3). C_2H_5COOOH breaks to be a significant contributor to the production of methyl radicals, carbon monoxide and formaldehyde. Methyl radicals form methoxy radicals through methyl peroxide and methyl peroxy radicals. Methoxy radicals then lead to formaldehyde. Formaldehyde gets converted to carbon monoxide through the pathway of formyl radicals. When the reaction temperature exceeds 850K the secondary route for major fluxes of carbon of propyl radicals forming propene becomes more prominent and the aforementioned routes via propyl peroxy radicals become much less pronounced and in fact reverse in some reactions to take the alternative. Propene goes on to form allyl radicals which then form C_3H_5OOH and eventually formaldehyde via vinyl radicals. Above a reaction temperature of 850K there is another route for the fate of propyl radicals; they can pyrolyze to ethene and methyl radicals which will form formaldehyde via vinyl and methoxy radicals respectively. In both these higher temperature cases formaldehyde goes on to decompose in the usual way. Being located at the “confluence” of a number of major reaction pathways suggests that formaldehyde is an important intermediate.

The generic features of the flux diagram (Fig. 6.3) are in agreement with the low temperature reaction schematic diagram of Griffiths for n-butane [57]. Normal butane and isobutane begin the series of ‘higher alkanes’ but some overlap between the oxidation kinetics of propane and n-butane is known to occur.

Good agreement can also be found with the results for the Morris uncertainty analysis shown in Tables 6.3 and 6.4 with all of the 18 species with the most important heats of formation being accounted for in the schematic (N.B. three isomers of $O_2C_3H_6OOH$, three of C_3H_6OOH , two of $C_3H_7O_2$ and two of C_3H_7 are accounted for in both Table 6.3 and Fig. 6.3), except for HO_2 which would not

have been detected by the element flux analysis. 34 out of the 50 most important reactions identified by the Morris method are represented in the species couplings shown on the element flux diagram. Amongst the 16 not represented on the diagram 5 of those would not have been detected due to the absence of carbon.

There have been a number of modeling and experimental studies of the oxidation of propane, details of which can be found in [202]. Koert *et al* [203] have studied propane oxidation in a pressurized reactor under the conditions of 10-15 atm and 650 – 800 K. The experimental results clearly indicate that these operating conditions are in the negative temperature coefficient (NTC) region as described in Chapter 4. Samples from the reactor were taken at a number of operating temperatures. Concentrations of major species were measured and plotted against temperature. These experimental results were compared to a model generated by the same authors and improved since a previous study [204]. Reasonable agreement between the species concentrations predicted by the Koert model and the experimental results were shown and the model shows a distinct NTC region. Further investigation of the model was undertaken using sensitivity analysis to identify key reactions. Notably, Koert's analysis showed that some major reactions are in partial equilibrium, namely;



and to a lesser extent



Concentrations of these species are therefore controlled by the thermochemistry. These statements correlate well with the Morris analysis, with the magnitudes of the thermochemical parameters of the C_3H_7 and $\text{O}_2\text{C}_3\text{H}_6\text{OOH}$ isomers, involved in reactions 6.8 and 6.9, having been found have a strong influence on the simulated ignition. Further agreement can be found with features of the flux diagram shown

in Fig. 6.3 for the reduced Nancy scheme because reactions (6.8) and (6.10) clearly reverse during simulated ignition. Other reactions in the Koert model identified as being significant include H atom abstraction from the primary fuel by an OH radical, the production of ketohydroperoxides from propylperoxy-hydroperoxide radicals which also leads to OH production and by inference, the addition of oxygen to propyl hydroperoxide radicals to form $O_2C_3H_6OOH$. The reaction



is also significant. Again, these reactions were found to have highly influential rate parameters in the Morris analysis (Table 6.4) and are in agreement with the analysis of the Nancy scheme (Fig 6.3).

What is less significant in Koert's analysis is the decomposition of propyl peroxide to formaldehyde and ethyl radicals. This is attributed to discrepancies in the kinetic models. In Koert's model, conversion to the propoxy radical via the reaction



has the greatest significance for the fate of propyl peroxide, as identified by sensitivity analysis. This is supported by the n-butane schematic of Griffiths [57]. The Nancy models contain only one irreversible reaction for the fate of propyl peroxide. In the case of propane as the primary fuel, it is;



and similarly in the case where n-butane is the primary fuel;



According to Curran *et al* [194], alkoxy radicals (e.g. C₃H₇O) are known to be quite unstable and decompose quickly to form ketones or aldehydes in addition to an alkyl radical. The fate of the propoxy radical, for example, is generally;

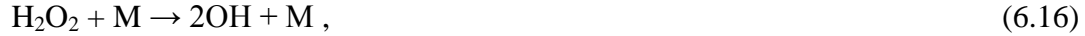


Using the Arrhenius parameters from the Konnov mechanism release 0.5 [205] the rate constant of reaction (6.15) at 630K can be calculated and is found to have a relatively high rate constant of $1.106 \times 10^{13} \text{ s}^{-1}$. The Nancy mechanisms do not appear to incorporate an RO• type of species. Therefore, reaction (6.13) appears to be an *a priori* reaction simplification, whereby the high rate of reaction 6.15 has allowed the C₃H₇O radical to be treated as a QSSA species and the 2 steps of reactions (6.12) and (6.15) have been combined into one overall global or ‘lumped’ reaction (for more details, see Chapter 7).

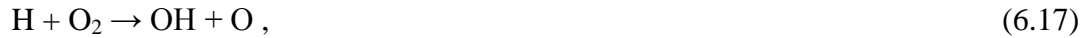
From the comparisons of the studies of Koert *et al* to the uncertainty and flux analyses, it appears that the same limited group of species and reactions are controlling the low temperature ignition behaviour. Further still, amongst this limited group, the uncertainty analysis has uncovered a smaller group of species and reactions, whose respective magnitudes of thermochemical data and rate parameters have a great influence on simulated ignition.

6.4 Numerical study of the kinetic origins of two-stage autoignition in lean n-butane-air mixtures

One of the key factors in the chemistry that promotes autoignition at low temperatures ($T < 700 \text{ K}$) is the transition from a cool flame to a second stage, within a two-stage ignition. The development of the second stage is believed to be driven by the formation and decomposition of hydrogen peroxide [162,206-208]. The kinetic significance of H₂O₂ lies in the chain branching step



which becomes important at temperatures in the approximate range 800 – 1000 K, where chain propagation by HO₂ radicals tends to predominate. Unless reaction pressures are unusually low, the reaction



does not play a major part in chain branching until the temperature is beyond 1000 K [159].

In this section, we investigate quantitatively the kinetic origins of hydrogen peroxide in the transition stage using the n-butane model reduced by formal methods in section 5.7 to 73 necessary species and 300 irreversible reactions, as this reaction scheme is of sufficient simplicity to make the kinetic analysis more manageable and less time consuming. There is also some relevance in this work to the development of fuels for use in HCCI combustion, where autoignition of fuel lean mixtures occurs with chemical kinetics playing a greater role than in other types of engine. The most important sequences of reactions leading to H₂O₂ formation are identified and the mechanistic implications are discussed.

In order to investigate the kinetic properties that lead to runaway reaction, a two-stage ignition was simulated at a specific operating condition of 600K and 1.63% n-C₄H₁₀ at 0.2 Mpa for the reduced Nancy scheme. Selected time points in the transition from cool flame to full ignition were further analyzed using rate of production analysis and calculated heat release rates. The effect of temperature on important kinetic processes involving hydrogen peroxide was then examined.

Fig. 6.4 shows the net heat release rate and temperature as functions of time from the initial conditions of 600K and 1.64% n-C₄H₁₀. The temperature stabilizes after the cool flame with a small net heat release of 1 W/cm³. The maximum heat release during the cool flame is 205 W/cm³ and in the final stage of ignition the highest predicted rate of heat release is ~16.7 kW/cm³. The rate of temperature rise is at its highest when these maxima occur. The very low heat release rate after

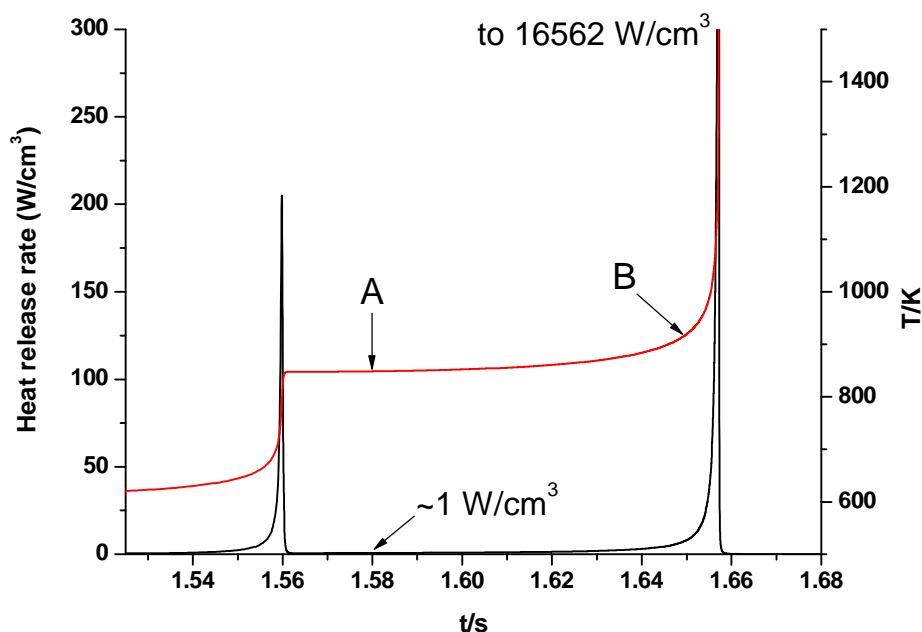


Fig. 6.4. Heat release rate during two-stage ignition (1.63 % n-C₄H₁₀ in air at 0.2 MPa and 600 K). Black line; heat release rate. Red line; temperature. Points A (t=1.58 s, T=849 K) and B (t=1.65 s, T = 919 K) were investigated kinetically.

the cool flame is symptomatic of the suppression of activity caused by the NTC of overall reaction rate [4]. Selected points for kinetic studies in the transition from cool flame to ignition are marked by arrows. Point A (t=1.58 s, T=849 K) is just after the T_{\max} of the cool flame and point B (t=1.65 s, T=919 K) is just prior to the full ignition. Here we analyse the rate of production of influential species and the highest ranked heat releasing and consuming reactions.

The rate of production analysis of influential intermediate species at points A and B is expressed in Table 6.6 as percentage contributions to the overall rate, as defined in Section 3.1.4 by equation 3.26. The greatest source of hydrogen peroxide is the quadratic interaction of HO₂ radicals. This is supplemented by H atom abstraction by HO₂ from CH₃CHO and CH₂O. At these temperatures, decomposition of the acetyl radical dominates its subsequent reactions, thereby generating CH₃ radicals as pre-cursors to formaldehyde. In fact, the most important channel to CH₂O formation is by CH₃O decomposition with C₂H₃ oxidation and C₃H₇CO₃H decomposition also making significant contributions. The major routes to HO₂ formation are by formyl and ethyl radical oxidations.

Formyl radicals are formed virtually exclusively from formaldehyde, and they yield HO₂ by oxidation. The importance of formaldehyde and its derivatives in reactions leading to hydrogen peroxide shows that it is a key intermediate in the combustion of n-butane leading to two-stage ignition. This has been shown previously for propane [4].

Formation reactions	A%	B%	Removal reactions	A%	B%
H₂O₂					
HO ₂ + HO ₂ → H ₂ O ₂ + O ₂	49.8	73.6	H ₂ O ₂ (+M) → 2OH (+M)	75.7	74.5
CH ₃ CHO + HO ₂ → CH ₃ CO + H ₂ O ₂	24.8	11.1	H ₂ O ₂ + OH → H ₂ O + HO ₂	15.6	20.9
HO ₂ + CH ₂ O → CHO + H ₂ O ₂	21.4	12.8	CH ₃ O ₂ + H ₂ O ₂ → CH ₃ O ₂ H + HO ₂	5.2	0.9
^a n-C ₄ H ₁₀ + HO ₂ → C ₄ H ₉ + H ₂ O ₂	1.9	0.8	H ₂ O ₂ + H → H ₂ O + OH	3.1	3.3
C ₂ H ₅ CHO + HO ₂ → C ₂ H ₅ CO + H ₂ O ₂	1.1	0.2	H ₂ O ₂ + H → H ₂ + HO ₂	0.5	0.5
C ₄ H ₈ + HO ₂ → C ₄ H ₇ + H ₂ O ₂	0.6	0.5			
CH₂O					
CH ₃ O + M → CH ₂ O + H + M	65.9	56.2	CH ₂ O + OH → CHO + H ₂ O	71.9	83.1
O ₂ + C ₂ H ₃ → CH ₂ O + CHO	11.2	18.1	CH ₂ O + HO ₂ → CHO + H ₂ O ₂	19.0	8.3
C ₃ H ₇ CO ₃ H → OH + CH ₂ O + CO + C ₂ H ₅	4.9	0.5	CH ₂ O + H → CHO + H ₂	7.3	7.0
C ₂ H ₄ + OH → CH ₃ + CH ₂ O	5.2	9.5	CH ₃ O ₂ + CH ₂ O → CH ₃ O ₂ H + CHO	0.8	0.1
C ₄ H ₈ + OH → CH ₂ O + C ₂ H ₄ + CH ₃	3.8	4.2	CH ₂ O + O → CHO + OH	0.6	1.0
O ₂ + CH ₃ O → CH ₂ O + HO ₂	3.4	1.4			
C ₂ H ₅ + HO ₂ → CH ₃ + CH ₂ O + OH	1.3	3.1			
C ₂ H ₅ O + HO ₂ → CH ₃ + CH ₂ O	1.3	1.1			
C ₃ H ₅ O ₂ H → C ₂ H ₃ + CH ₂ O + OH	0.9	2.8			
HO₂					
O ₂ + CHO → CO + HO ₂	58.0	60.0	HO ₂ + HO ₂ → H ₂ O ₂ + O ₂	45.8	49.6
C ₂ H ₅ + O ₂ → C ₂ H ₄ + HO ₂	12.4	14.3	CH ₃ + HO ₂ → CH ₃ O + OH	20.1	23.1
^a C ₄ H ₉ + O ₂ → C ₄ H ₈ + HO ₂	10.4	5.3	CH ₃ CHO + HO ₂ → CH ₃ CO + H ₂ O ₂	11.4	3.7
H + O ₂ (+M) → HO ₂ (+M)	10.1	8.8	CH ₂ O + HO ₂ → CHO + H ₂ O ₂	9.8	4.3
H ₂ O ₂ + OH → H ₂ O + HO ₂	3.9	8.0	C ₄ H ₇ + HO ₂ → C ₄ H ₇ O ₂ H	3.1	4.1
CH ₃ O ₂ + H ₂ O ₂ → CH ₃ O ₂ H + HO ₂	1.3	0.3	CO + HO ₂ → CO ₂ + OH	2.0	3.0
CH ₃ O + O ₂ → CH ₂ O + HO ₂	1.3	0.6	CH ₃ O ₂ + HO ₂ → CH ₃ O ₂ H + O ₂	1.6	0.4
H + O ₂ (+H ₂ O) → HO ₂ (+H ₂ O)	1.0	1.2	HO ₂ + H → OH + OH	0.8	2.2
CH ₃ CHO + O ₂ → CH ₃ CO + HO ₂	0.6	0.3	^a n-C ₄ H ₁₀ + HO ₂ → C ₄ H ₉ + H ₂ O ₂	0.8	0.3
			HO ₂ + OH → H ₂ O + O ₂	0.5	1.9
			CH ₂ CHO + HO ₂ → CH ₃ CHO + O ₂	0.5	2.1
CHO					
CH ₂ O + OH → CHO + H ₂ O	63.6	69.7	O ₂ + CHO → CO + HO ₂	99.0	97.7
CH ₂ O + HO ₂ → CHO + H ₂ O ₂	16.8	7.0	CHO + M → H + CO + M	1.0	2.1
CH ₂ O + H → CHO + H ₂	6.4	5.9			
C ₂ H ₃ + O ₂ → CH ₂ O + CHO	7.5	12.3			
C ₃ H ₅ CO ₄ H → OH + CO ₂ + CHO + C ₂ H ₄	3.8	2.6			
CH ₃ O ₂ + CH ₂ O → CH ₃ O ₂ H + CHO	0.7	0.1			

^a isomers combined

Table 6.6. Rates of production expressed as % contribution, for reaction in a closed vessel related to points A and B in Fig. 6.4.

The ten main exothermic and endothermic reactions at points A and B are shown in Tables 6.7 and 6.8 respectively. The sum of the heat release of the 20

reactions at point A is over 60% of the total heat release. As with the rate of production analysis, formaldehyde and its derivatives play a very important role in the heat released by the reaction. This vindicates the conclusion that it is equally instrumental in the development of two-stage ignition as well as the formation of hydrogen peroxide.

Heat output rates / W cm ⁻³		Heat consumption rates / W cm ⁻³	
O ₂ + CHO → CO + HO ₂	0.25	H ₂ O ₂ (+M) ↔ 2OH (+M)	0.13
CH ₂ O + OH → CHO + H ₂ O	0.15	CH ₃ O + M ↔ CH ₂ O + H + M	0.077
^a 2HO ₂ → H ₂ O ₂ + O ₂	0.12	CH ₃ CO (+M) ↔ CO + CH ₃ (+M)	0.032
O ₂ + H (+M) → HO ₂ (+M)	0.069	C ₄ H ₇ O ₂ H ↔ OH + CH ₃ CHO + C ₂ H ₃	0.026
^a C ₄ H ₁₀ + OH → H ₂ O + C ₄ H ₉	0.067	^a C ₄ H ₉ O ₂ ↔ C ₄ H ₈ O ₂ H	0.022
HO ₂ + CH ₃ → CH ₃ O + OH	0.065	CH ₃ O ₂ H ↔ CH ₃ O + OH	0.021
O ₂ + C ₂ H ₃ → CH ₂ O + CHO	0.055	C ₄ H ₉ → C ₂ H ₅ + C ₂ H ₄	0.013
C ₄ H ₉ + O ₂ ↔ C ₄ H ₉ O ₂	0.042	C ₄ H ₉ → CH ₃ + C ₃ H ₆	0.007
C ₄ H ₈ + OH → C ₄ H ₇ + H ₂ O	0.039	C ₃ H ₅ O ₂ H → OH + CH ₂ O + C ₂ H ₃	0.003
O ₂ + CH ₃ (+M) ↔ CH ₃ O ₂ (+M)	0.031	O ₂ + CH ₃ CHO → CH ₃ CO + HO ₂	0.003

^aisomers combined

Table 6.7. Individual heat output / consumption rates in the post cool flame region at point A, Fig. 6.4.

Heat output rates / W cm ⁻³		Heat consumption rates / W cm ⁻³	
O ₂ + CHO → CO + HO ₂	2.27	H ₂ O ₂ (+M) ↔ 2OH (+M)	1.75
CH ₂ O + OH → CHO + H ₂ O	1.54	CH ₃ O + M ↔ CH ₂ O + H + M	0.63
O ₂ + C ₂ H ₃ → CH ₂ O + CHO	0.84	C ₄ H ₇ O ₂ H ↔ OH + CH ₃ CHO + C ₂ H ₃	0.30
2HO ₂ → H ₂ O ₂ + O ₂	1.10	CH ₃ CO (+M) ↔ CO + CH ₃ (+M)	0.16
HO ₂ + CH ₃ → CH ₃ O + OH	0.65	C ₄ H ₉ → C ₂ H ₅ + C ₂ H ₄	0.14
O ₂ + H (+M) → HO ₂ (+M)	0.52	C ₄ H ₉ → CH ₃ + C ₃ H ₆	0.12
C ₄ H ₈ + OH → C ₄ H ₇ + H ₂ O	0.48	C ₃ H ₅ O ₂ H → OH + CH ₂ O + C ₂ H ₃	0.11
H ₂ O ₂ + OH → H ₂ O + HO ₂	0.31	C ₄ H ₇ O → CH ₂ CHO + C ₂ H ₄	0.063
^a C ₄ H ₁₀ + OH → H ₂ O + C ₄ H ₉	0.28	C ₄ H ₉ O ₂ ↔ C ₄ H ₈ O ₂ H	0.046
HO ₂ + CO → CO ₂ + OH	0.21	CH ₃ O ₂ H ↔ CH ₃ O + OH	0.044

^aisomers combined

Table 6.8. Individual heat output / consumption rates in the post cool flame region at point B, Fig. 6.4.

A supplementary point connected with development of two-stage ignition relates to the reactions in which OH radicals are consumed, and especially with regard to the reaction



In their paper on the reduced scheme modelling of n-heptane combustion, Peters *et al* [180] claimed that the onset of the second stage of two-stage ignition occurs when OH radicals cease to be removed by the primary fuel. This is not so for n-butane combustion. For example, the second stage is already well developed at 970 K in a mixture containing 1.63% n-butane at 0.2 MPa and 600 K (see Fig. 6.4). At this condition 8.9% of the fuel remains and its removal is dominated by reaction (6.18). Even by 1110 K, 1.6% of the primary fuel still remains and OH radical abstraction continues to contribute significantly to its consumption. However, still more important is the relative contribution of the primary fuel to OH radical removal during the early part of the second stage development (Table 6.9).

T / K	Reactions consuming OH	%
920	$\text{CH}_2\text{O} + \text{OH} \rightarrow \text{CHO} + \text{H}_2\text{O}$	39.5
	${}^a\text{C}_4\text{H}_{10} + \text{OH} \rightarrow \text{H}_2\text{O} + \text{C}_4\text{H}_9$	16.1
	$\text{H}_2\text{O}_2 + \text{OH} \rightarrow \text{H}_2\text{O} + \text{HO}_2$	7.4
	$\text{CH}_3\text{CHO} + \text{OH} \rightarrow \text{CH}_3\text{CO} + \text{H}_2\text{O}$	4.8
	$\text{C}_4\text{H}_8 + \text{OH} \rightarrow \text{C}_4\text{H}_7 + \text{H}_2\text{O}$	4.3
970	$\text{CH}_2\text{O} + \text{OH} \rightarrow \text{CHO} + \text{H}_2\text{O}$	40.4
	${}^a\text{C}_4\text{H}_{10} + \text{OH} \rightarrow \text{H}_2\text{O} + \text{C}_4\text{H}_9$	11.5
	$\text{H}_2\text{O}_2 + \text{OH} \rightarrow \text{H}_2\text{O} + \text{HO}_2$	6.8
	$\text{CH}_3\text{CHO} + \text{OH} \rightarrow \text{CH}_3\text{CO} + \text{H}_2\text{O}$	4.7
	$\text{CO} + \text{OH} \rightarrow \text{CO}_2 + \text{H}$	4.3
1110	$\text{CH}_2\text{O} + \text{OH} \rightarrow \text{CHO} + \text{H}_2\text{O}$	41.6
	$\text{CO} + \text{OH} \rightarrow \text{CO}_2 + \text{H}$	8.4
	$\text{C}_2\text{H}_4 + \text{OH} \rightarrow \text{C}_2\text{H}_3 + \text{H}_2\text{O}$	6.0
	$\text{C}_2\text{H}_4 + \text{OH} \rightarrow \text{CH}_3 + \text{CH}_2\text{O}$	5.8
	$\text{HO}_2 + \text{OH} \rightarrow \text{H}_2\text{O} + \text{O}_2$	5.8
	$\text{OH} + \text{H}_2 \rightarrow \text{H} + \text{H}_2\text{O}$	5.2
	${}^a\text{C}_4\text{H}_{10} + \text{OH} \rightarrow \text{H}_2\text{O} + \text{C}_4\text{H}_9$	3.4
^a isomers combined		

Table 6.9. Consumption reactions involving OH radicals

To temperatures well beyond 900 K, reaction (6.18) remains the second most important route for OH removal and even at 1110 K there is still a 3.4%

contribution of the H atom abstraction by OH from the primary fuel to this propagation route. The reaction that dominates the propagation throughout this period of development is the H atom abstraction from formaldehyde



which, of course, feeds into the formation of hydrogen peroxide and its subsequent decomposition, as discussed above [25]. Numerical analysis has shown that the onset of ignition is attributed to the heat release from reactions involving formaldehyde and related species and is not connected to the depletion of OH radical consumption by the primary fuel.

6.5 Analysis of cyclohexane oxidation under fuel rich isothermal conditions

The oxidation of cyclohexane in fuel rich + air conditions presents an autoignition hazard which is of concern in the processing industries and so it is prudent to assess the performance of oxidation mechanisms in these conditions. In this section, we present the simulation of a reduced Nancy scheme comprising 60 necessary species and 238 reactions under isothermal conditions at 1 atm, with a stoichiometry of cyclohexane + air in 1:2 molar proportions, which corresponds to an initial mixture of;



This initial mixture was chosen in order to make a direct comparison to the experimental work of Snee and Griffiths [166] who studied this composition in closed vessels, over a range of sizes, under both subcritical and supercritical conditions. Supercritical conditions refer to ambient conditions where ignition is possible and subcritical conditions refer to those where ignition does not occur. Slow reaction will occur at the low temperature ignition boundary and away from

the limiting conditions, this phenomenon can be approximated by isothermal reaction for the purposes of kinetic evaluation studies.

An ancillary study was carried out in order to assess the simulated global reaction rate. Adiabatic simulations were carried out at a range of temperatures, for which ignition is guaranteed, and times to ignition (t_{ign}) were recorded. Linear regression analysis of a plot of $\ln(t_{\text{ign}})$ versus $1/T_a$ showed the activation energy (E/R) of the global reaction to be equal to 17368K.

If it is assumed that there is a small but finite amount of autocatalyst added to the initial reactants then isothermal oxidation in fuel rich conditions appears to follow a quadratic autocatalytic rate law [166]. In a closed system the global reaction rate progresses according to;

$$v = \frac{d\xi}{dt} = \phi (\xi + \xi_0)(1 - \xi), \quad (6.21)$$

where ξ is the fractional extent of reaction of the primary reactant at time t and ξ_0 is the initial fraction of autocatalytic intermediate (x) relative to the initial concentration of the reactant (c_0). The branching factor (ϕ) can be calculated from $[\phi = k(c_0 + x_0)]$. It is therefore related to the (second order) rate constant for the autocatalytic step and the initial concentrations of material and has pseudo-first-order rate constant units (time^{-1}). The analytical solution of equation (6.21) yields a fractional extent of reaction as a function of time, giving;

$$\xi = \frac{\xi_0 [1 - e^{-(1+\xi_0)\phi t}]}{\xi_0 + e^{-(1+\xi_0)\phi t}} \quad (6.22)$$

and a fractional conversion rate as a function of time;

$$\frac{d\xi}{dt} = \frac{\phi \xi_0 (1 + \xi_0)^2 e^{-(1+\xi_0)\phi t}}{[\xi_0 + e^{-(1+\xi_0)\phi t}]^2} \cdot \quad (6.23)$$

When $\xi_0 \ll \xi$, equations 6.21-6.23 can be represented graphically as shown in Fig. 6.5. The characteristic sigmoidal curve of the ξ versus t is observed widely in experiments (see Fig. 6.6) and the maximum rate of reaction is typically at 50% consumption of the reactant [166].

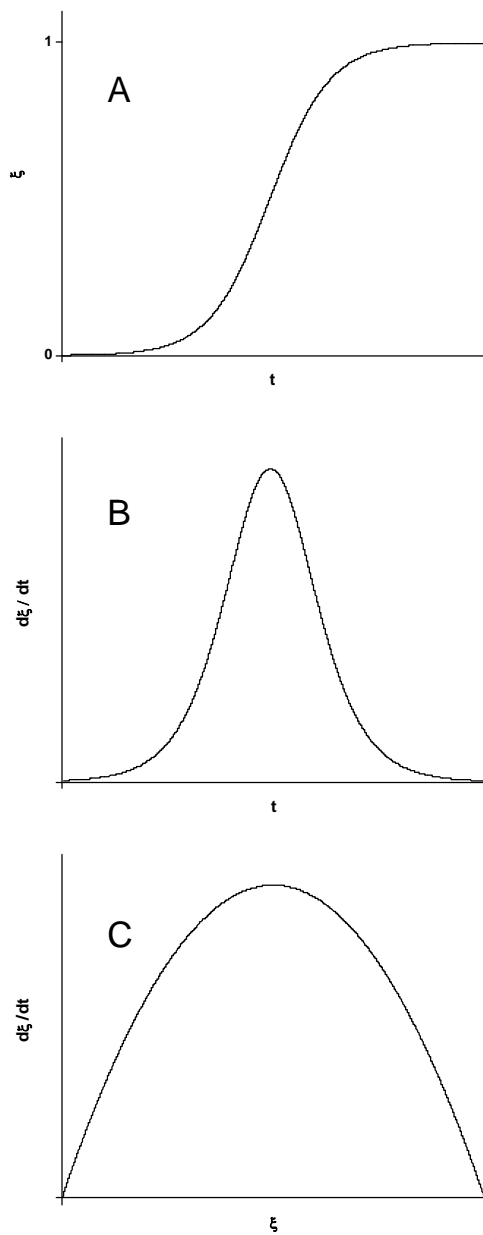


Fig. 6.5. Theoretical curves of isothermal quadratic autocatalysis in a closed vessel. A: Fractional extent of reaction versus time. B: Rate of fractional conversion versus time. C: Rate of fractional conversion versus extent of conversion [166].

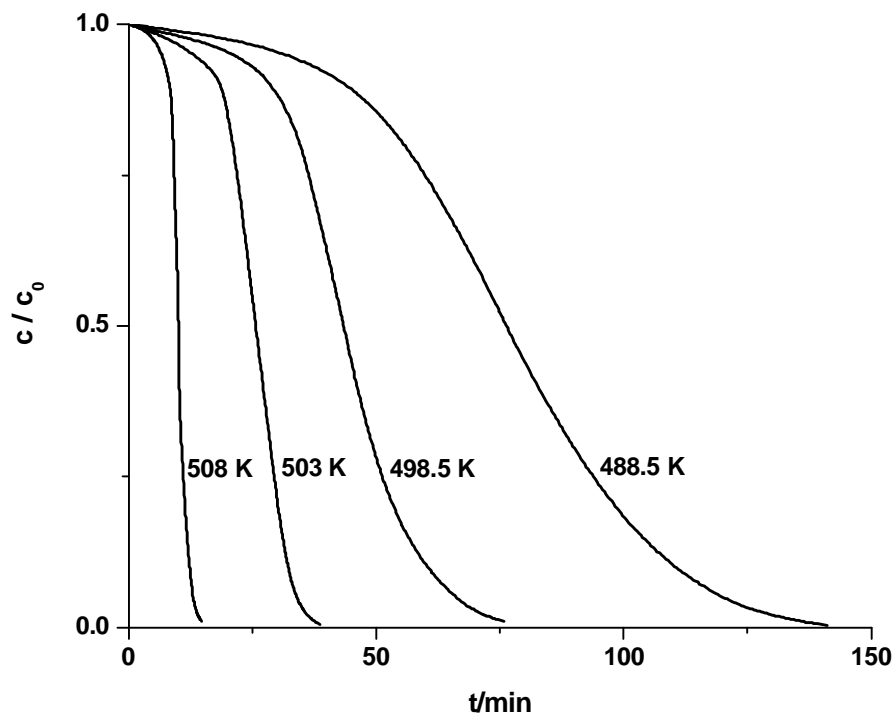


Fig. 6.6. Experimental consumption of oxygen in a 5 dm³ closed vessel during subcritical reaction of cyclohexane at different ambient reaction temperatures [166].

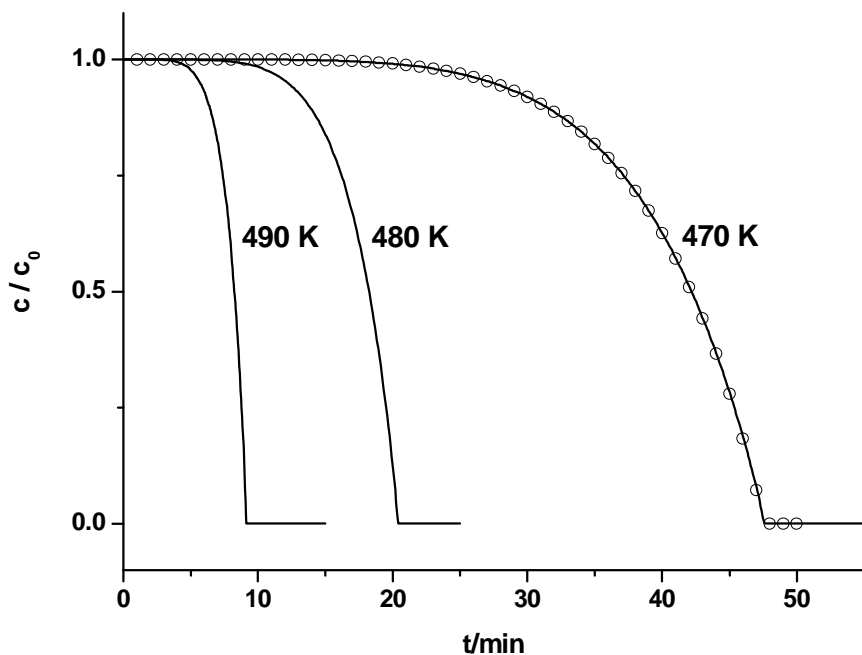


Fig. 6.7. Simulated consumption of oxygen in a closed vessel during isothermal reaction at different ambient reaction temperatures using full and reduced Nancy c-C₆H₁₂ mechanisms. Solid line – reduced mechanism. Open circles – full mechanism.

As can be seen in the experimental curves of Fig. 6.6 showing the extent of oxygen consumption versus time, the sigmoidal shape of the theoretical fractional extent of reaction versus time curve (Fig. 6.5A) is well reproduced in reality. However, the curves produce by the Nancy models (both full and reduced) under similar conditions (Fig. 6.7) fail to show the important qualitative characteristic, and oxygen consumption accelerates until its virtual total depletion. An extremely high heat transfer coefficient was selected for the simulations to ensure completely isothermal reaction and thus eliminate the possibility that the acceleration can be attributed to thermal effects. Therefore, the accelerating consumption can only be attributed to the build up or pooling of oxygen consuming intermediates, though understanding the kinetic origin of this phenomenon requires further investigation.

The qualitative discrepancy is further exemplified by gradient analysis. The simulated rate of change of oxygen concentration at 470 K was determined by numerically differentiating the concentration profiles. The dependence of reaction rate on time and extent of oxygen concentration is shown in Fig. 6.8. The maximum rate is achieved just prior to oxygen depletion and no parabolic dependence of rate on concentration is observed. The analytical expressions of Fig. 6.5 B and C are not well reproduced by Fig. 6.8.

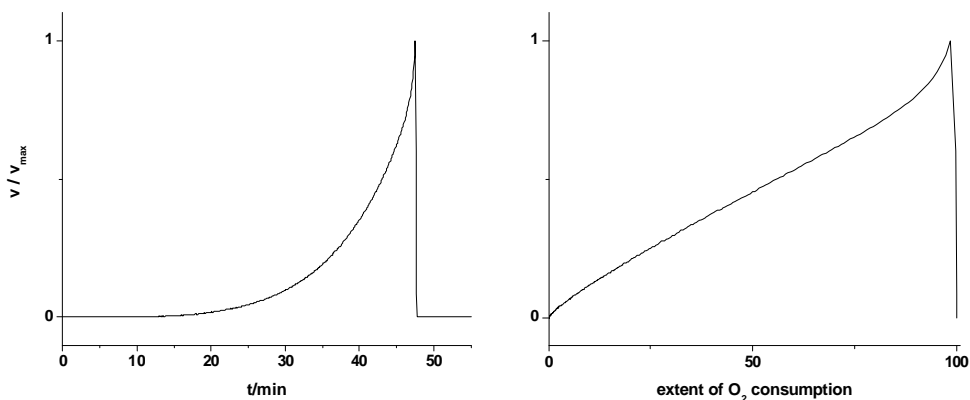


Fig. 6.8. Relationship between reaction rate, scaled to maximum rate = 1 and (*left*) time and (*right*) extent of oxygen consumption of simulations using the reduced Nancy cyclohexane model at 470K.

To investigate the underlying kinetics during reaction at these conditions, the element fluxes were calculated (see Section 6.3) using an ambient temperature of

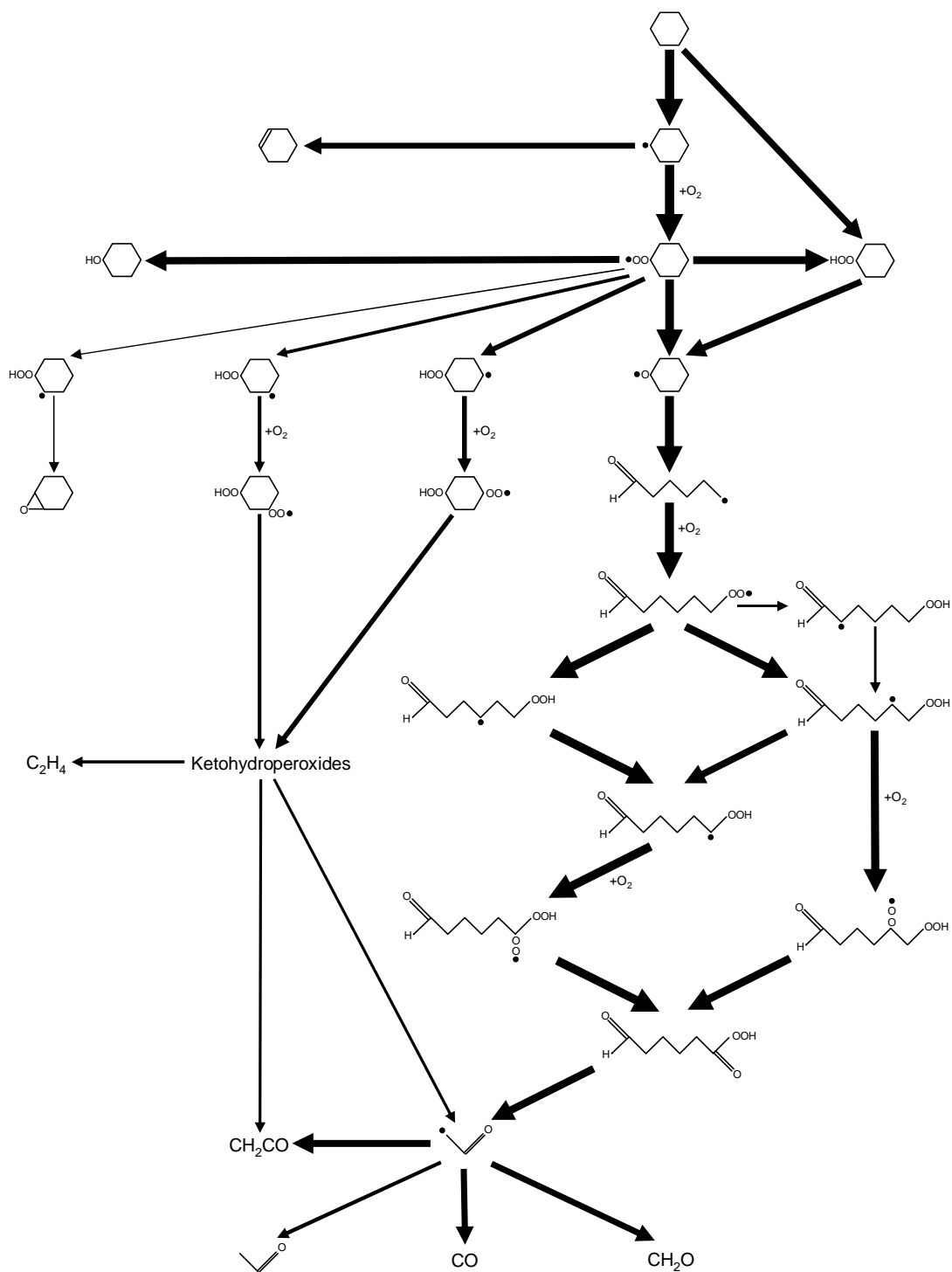


Fig. 6.9. Major fluxes of carbon atoms during isothermal oxidation of cyclohexane in air in the molar proportions 1:2, 470 K and 1 atm. Arrow thickness is scaled to magnitude of element flux.

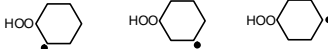
 Cyclohexane <i>C6H12#6</i>	 Cyclohexylalcoxy radical <i>RC110C6H11#6</i>
 Cyclohexyl radical <i>RC1ZC6H11#6</i>	 1,2-epoxycyclohexane <i>C6H10#6O#3</i>
 Cyclohexene <i>C6H10Z#6</i>	 6-yl-hexanal radical <i>R106C5H10CHO</i>
 Cyclohexanol <i>C6H11#6OH</i>	 Aldohydroperoxide (lumped) <i>CHOC4H8CO3H</i>
 Cyclohexylperoxy radical <i>RC2ZOOC6H11#6</i>	 Vinylloxy radical <i>R13CH2CHO</i>
 Cyclohexylperoxide <i>C6H11#6OOH</i>	 Ethanal <i>CH3CHO</i>
	Cyclohexylhydroperoxide radicals <i>RC4ZC5H9#6OOH RC5ZC5H9#6OOH RC6ZC5H9#6OOH</i>
	Cyclohexylperoxyhydroperoxide radicals <i>RC9OOZC6H10#6OOH RCD0OZC6H10#OOH</i>

Fig. 6.10. Key to species belonging to the reduced mechanism of cyclohexane and discussed in Section 6.5. Species notation, as appears in the CHEMKIN format mechanisms appears in italic.

470K. Viewing the carbon fluxes in an animation using Fluxviewer [201] and rearranging the configuration of species gives the major couplings as shown in Fig. 6.9. Unlike during 2-stage ignition of propane, no major “switching over” of or varying competition between reaction channels is observed during isothermal reaction, instead the element fluxes between species steadily increase in magnitude as time progresses. In order to show the magnitudes of the element fluxes relative to one another, the width of the arrows of the schematic were scaled to their corresponding magnitudes at a single time point during reaction.

For the reader's convenience, the molecular structures of those species discussed in the text are illustrated and labeled in Fig. 6.10.

Fig. 6.9 shows that the main oxygen consuming species are cyclohexyl radicals, 6-yl-1-hexanal radicals and two isomers of hexenalperoxide radicals. Rate of production analysis (Table 6.10) substantiates these findings and also shows the vinyloxy radical to be a significant consumer of oxygen.

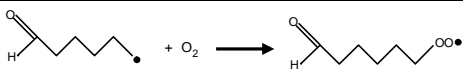
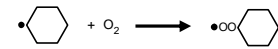
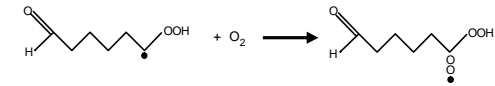
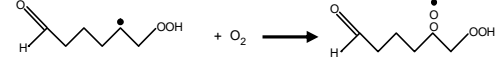
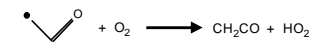
Reactions consuming O ₂	%
	30.5
	24.6
	19.8
	14.1
	4.9
	2.9

Table 6.10. Consumption reactions involving O₂ molecules. Conditions correspond to 470K after a reaction time of 46 mins and 40 seconds.

The major reaction route of the fuel is to cyclohexyl radicals, which then react with oxygen to either oxidize forming cyclohexene and HO₂, or by addition to form cyclohexylperoxy radicals. Cyclohexylperoxy radicals can form cyclohexanol, a number of isomers and cyclohexylperoxide, although the greatest pathway is to the cyclohexyl alkoxy radicals. Cyclohexylperoxide can also be formed by oxygen addition to the primary fuel. The ring of the cyclohexyl alkoxy radical breaks to form the 6-yl-1-hexanal radicals which then lead to aldohydroperoxides via a number of successive additions of oxygen and isomerizations. Aldohydroperoxides break up to become a major source of vinyloxy radicals. These form products of ketene, ethanal, carbon monoxide and formaldehyde.

Subsidiary routes of isomerizations for the fate of cyclohexylperoxy radicals lead to isomers of cycloperoxyhydroperoxide radicals; these form ketohydroperoxides except for the case of the 5 member ring which produces 1,2-epoxycyclohexane. The ketohydroperoxides decompose to ethane (C_2H_4), ketene (CH_2CO) and vinyloxy radicals.

Fig. 6.9 agrees largely with another schematic for cyclohexane produced using rate of production analysis by Buda *et al* [181] with the formation of the cyclohexylalcoxy radical being dominant route for the fate of the cyclohexylperoxy radical. The analysis was performed by modelling in a rapid compression machine at 650 K, equivalence ratio of 1 and pressure after compression of 7 – 17 bar. The fate of the cyclohexylperoxy radical depends very much on temperature. Parametric uncertainties relating to this radical could, by implication, be a cause of discrepancies between model and experiment. Preliminary uncertainty analysis runs suggest that this is the case. What is less apparent in the schematic of Buda *et al.* is the formation of cyclohexyl peroxide from cyclohexane; this must be attributed to the change of operating conditions.

The shortcoming of accelerating oxygen consumption in isothermal oxidation of rich mixtures does not appear to be limited to cyclohexane or this origin of mechanism. The full Nancy n-butane model comprising 128 species in 731 mixed reactions and the n-butane model derived from the Westbrook n-heptane model comprising 120 species in 1078 irreversible reactions were also examined under the conditions of 470 K ambient temperature, $\frac{1}{2}$ atm and 1:5 molar proportions of fuel in air. The consumption of oxygen during isothermal reaction of both of these schemes is shown in Fig. 6.11. The gradients of the oxygen consumption curves are analyzed in order to make a comparison with the expected curves for rate of fractional conversion versus time and rate of fractional conversion versus extent of conversion shown in Fig. 6.5 (B and C respectively). The mechanisms of n-butane show some improvement in performance over cyclohexane in this region of operating conditions. Both n-butane mechanisms attain their maximum rate of consumption before the total depletion of oxygen and a limited parabolic dependence on oxygen concentration can be observed for the Nancy mechanism

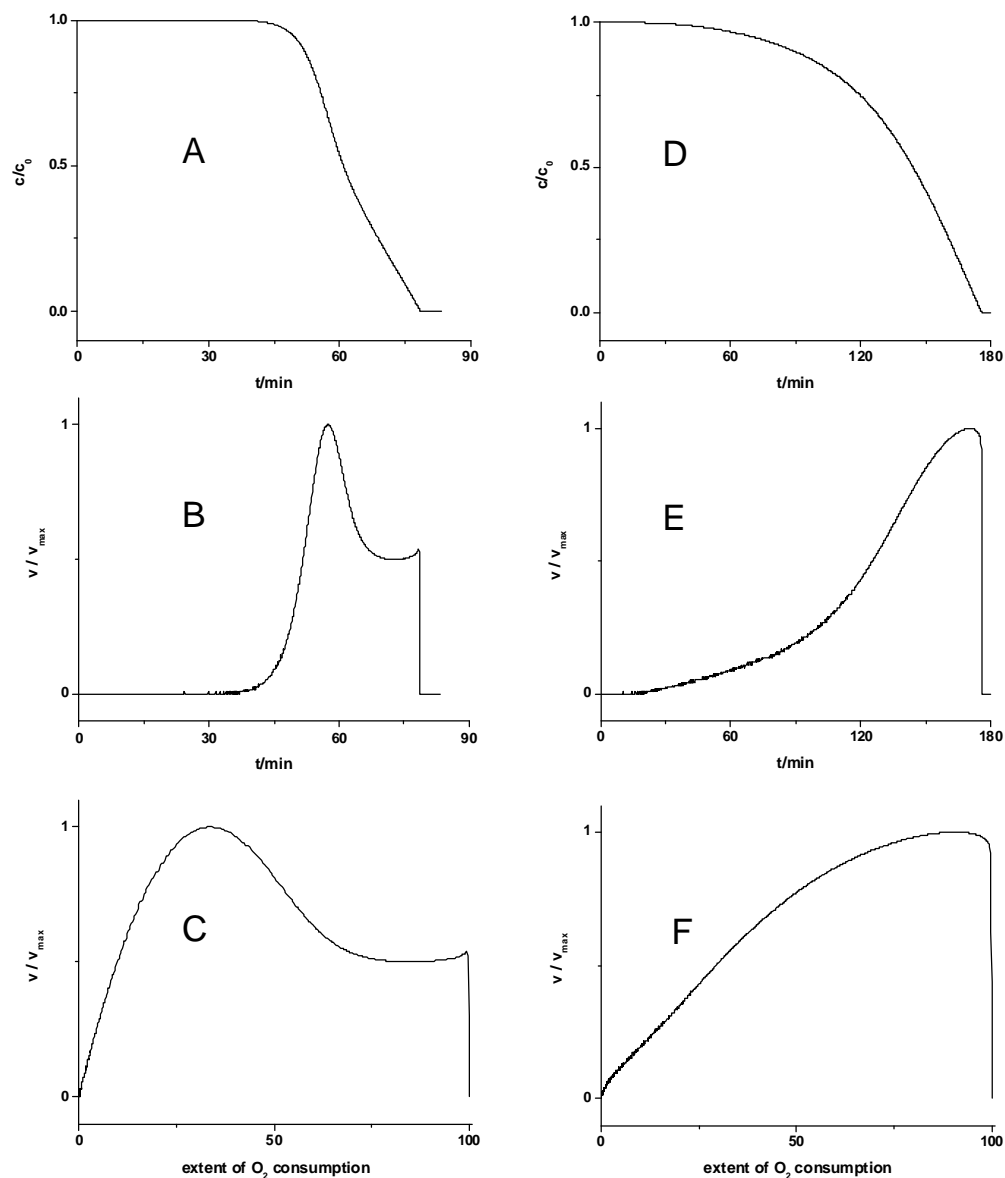


Fig. 6.11. Simulated consumption of oxygen in a closed vessel during isothermal reaction at 470K reaction temperatures using full Nancy n-C₄H₁₀ mechanism (A). Relationship between reaction rate, scaled to maximum rate = 1 and (B) time and (C) extent of oxygen consumption of simulations from the full Nancy n-C₄H₁₀ mechanism. The same analysis performed for the derived Westbrook n-C₄H₁₀ mechanism; simulated oxygen consumption (D), rate of reaction versus time (E) and rate of reaction versus extent of oxygen consumption (F).

during the start of reaction. However, towards the end of reaction, both schemes have rates for oxygen consumption which are too high and oxygen abruptly vanishes instead of the desired gradual asymptotic depletion as outlined by theory

and observed in experiments.

Uncertainty analysis could be applied in order to assess if sigmoidal oxygen consumption curves during isothermal oxidation could be output by a selected reduced mechanism with perturbed parameters within their range of uncertainties and hence identify parameters meriting further study to obtain more precise values. If this fails, it would suggest that there are missing reaction steps or the mechanistic structure is incorrect. The behaviour could also be affected by wall loss reaction steps. This is a matter for further investigation.

6.6 Conclusions

By analysing mechanisms reduced under conditions of low temperature for the fuels of propane, n-butane and cyclohexane, classes of species and reactions which are commonly removed in all reductions have been identified. In particular, sub-mechanisms pertaining to alkanes other than the primary fuel appear to be redundant in the investigated cases.

Global uncertainty analysis techniques have been applied to a reduced propane mechanism by Dr. K. J. Hughes, as part of the SAFEKINEX project. By perturbing parameters and measuring the effect on outputs such as maximum temperature in the cool flame and time to ignition, a relatively small number of thermokinetic parameters, whose values are poorly known, have been found to control the overall reactivity of the mechanism. Furthermore, most uncertainty analysis studies have generally investigated the effect of the variation of uncertain rate parameters on quantitative outputs. This study has shown that the impact on outputs of uncertain thermokinetic parameters can be as great as, if not more than, those of uncertain Arrhenius rate parameters. Amongst the thermokinetic parameters, the magnitudes of those of the intermediate radicals $n\text{-O}_2\text{CH}_2\text{CH}_2\text{CH}_2\text{OOH}$, $n\text{-C}_3\text{H}_7\text{O}_2$ and $i\text{-C}_3\text{H}_7\text{O}_2$ were found to have the greatest influence on simulated ignition.

The reduced mechanism describing the system of equimolar propane – oxygen, has also been used to identify main kinetic pathways for the major fluxes of

carbon atoms and the competition between reaction routes as reaction temperature increases has been understood. The mechanistic structure of the propane mechanism compares well to another modeling study available in the literature and many of the main reaction pathways identified using element flux analysis were found to be important when uncertainty analysis techniques were applied, such as the low temperature pathways via $C_3H_7O_2$ radicals and the pathway via C_3H_6 .

The reduced kinetic scheme for lean mixtures of n- C_4H_{10} in air has been used to kinetically analyse the ignition process. The most important reactions leading to hydrogen peroxide involve CH_2O , CHO , HO_2 , CH_3CHO and (by implication) CH_3 and CH_3O . Principal routes to heat release in the transition “plateau” region involve the molecular intermediates kinetically linked to hydrogen peroxide rather than primary fuel. The heat release and kinetic results for n- C_4H_{10} in air presented here are consistent with previously reported C_3H_8 data [4].

Simulations of isothermal cyclohexane oxidation in fuel rich mixtures have shown that there are significant qualitative discrepancies with experiments. Specifically, the concentration profiles for oxygen consumption do not follow a quadratic autocatalytic rate law as observed experimentally. Although only providing limited insight into the nature of the problem, element flux analysis has been applied to illustrate the major reaction pathways on the basis of carbon fluxes between species at the operating conditions of interest. Investigations of the behaviour of two n-butane mechanisms at similar conditions show that this issue is not isolated to cyclohexane but appears to be another generic problem. Further uncertainty analysis could be undertaken using the reduced mechanisms obtained during this work, in order to investigate this problem.

Chapter 7

Application of the Quasi Steady State Approximation

The application of the sensitivity methods demonstrated in Chapter 5 leads to a skeleton mechanism with many redundant species and reactions removed. However, in most cases, the extent of reduction achieved by such methods is insufficient for the application of the chemical model within a reactive flow simulation. Further reduction may be achieved by the exploitation of the range of time scales present in the system [127]. A number of known reliable techniques fall into this category, such as the Quasi Steady State Approximation (QSSA) [63], the Computational Singular Perturbation method (CSP) [46] and slow manifold methods like the Intrinsic Low Dimensional Manifold method (ILDM) [49] (see Chapter 2 for further discussion on these techniques). These methods take different approaches but are related by their ability to identify the ranges of system time scales and then categorise these as slow or fast. The system dynamics are usually controlled by only the slow time scales because the fast time scales quickly equilibrate with respect to the slower ones. An important and interesting feature of the system is that if the calculated concentrations of the fast species are perturbed slightly, then this perturbation will vanish or “relax” within a short time and the species with shorter lifetimes will relax more quickly. This property has been noted previously by Klonowski [209] who stated that “the fast components

‘forget’ their initial values”. Thus perturbation analysis can be used to investigate the time scales.

Since the system is controlled by the slower dynamics the fast variables can be decoupled from the system. This reduces the number of system variables and also the stiffness of the system and eases the burden on computational resources as discussed in Chapter 2. The methods of CSP and ILDM can achieve impressive reductions [46,49] and can be very effective when implemented in a reactive flow simulation. However, the time investment required to apply the ILDM technique is usually large and the resulting kinetic description is in the form of a fitted model or look up table and therefore no longer resembles a kinetic mechanism containing lists of species, reactions and associated parameters. The focus of the current work is on exploration of kinetic schemes and the kinetic insight or improvements which can be made by the analysis of reduced schemes. The implementation of a reduced kinetic scheme in computational fluid dynamics environment is a longer term goal. For these reasons, the application of the QSSA combined with reaction lumping was selected for use as a method for further reduction because the resulting further reduced schemes retain the original kinetic structure to a large extent, as will be further discussed.

The QSSA has been in use since early in the 20th century and was conceptualized during the early advances of chemical kinetics in order to simplify the analytical solution of non-linear reaction systems. More recently the technique has received increased interest for the reduction of detailed chemical mechanisms. The QSSA method can be employed in mechanism reduction to identify species which react on a very short time scale and locally equilibrate with respect to the slower species. These fast reacting species are known as quasi steady state (QSS) species. The main assumption of the QSSA is that the equilibration of the QSS species is immediate. The concentration of the QSSA species can then be approximated via an algebraic expression rather than a differential equation, obtained by setting the QSSA species rate of production (f_i^q) to zero, i.e.,

$$f_i^q = 0 \tag{7.1}$$

where the superscript q denotes a QSSA species [63,145]. This assumption is valid for a number of minor and intermediate species during combustion (not applicable to final products or reactants). The application of the QSSA for a given species is *not* equivalent to

- removing its effect from the chemical system,
- assuming its concentration does not change during reaction or
- assuming it is a redundant species [193].

The numerical solution of the combined algebraic/differential set of equations obtained by the application of the QSSA will not necessarily achieve a computational speed up as iterative methods may be needed to solve the coupled set of equations. Substantial computational savings can be made when the QSS species is removed via reaction lumping [15]. In its simplest form a reaction scheme or subset consists of a set of reactions from reactants going to intermediates, or a coupled set of intermediates, which then form products. Via reaction lumping, this set of reactions is changed to a single ‘lumped’ reaction involving only reactants going to products. Intermediates are therefore eliminated. The rates of the lumped reactions will be algebraic combinations of other rate parameters and intermediate species concentrations and are derived subsequent to the application of equation 6.1. Reaction lumping should not be confused with species lumping where two or more species are grouped together to form a composite ‘lumped’ species thus reducing the number of ordinary differential equations required to describe the kinetics, as discussed in Section 2.2.2. The reactions that involve the lumped species will also require new formulations for reaction rates. One approach for calculating the rates of reactions involving lumped species is as a weighted mean of the elementary rate constants of those reactions involving species to be lumped [210]. The fundamental differences between species and reaction lumping are illustrated in Fig. 7.1.

The application of the QSSA combined with reaction lumping was conducted in a partially automated fashion. Because the time scales can change as initial conditions vary or non-isothermal time dependant behaviour progresses, a number of initial conditions are manually selected and then simulated. Time points at

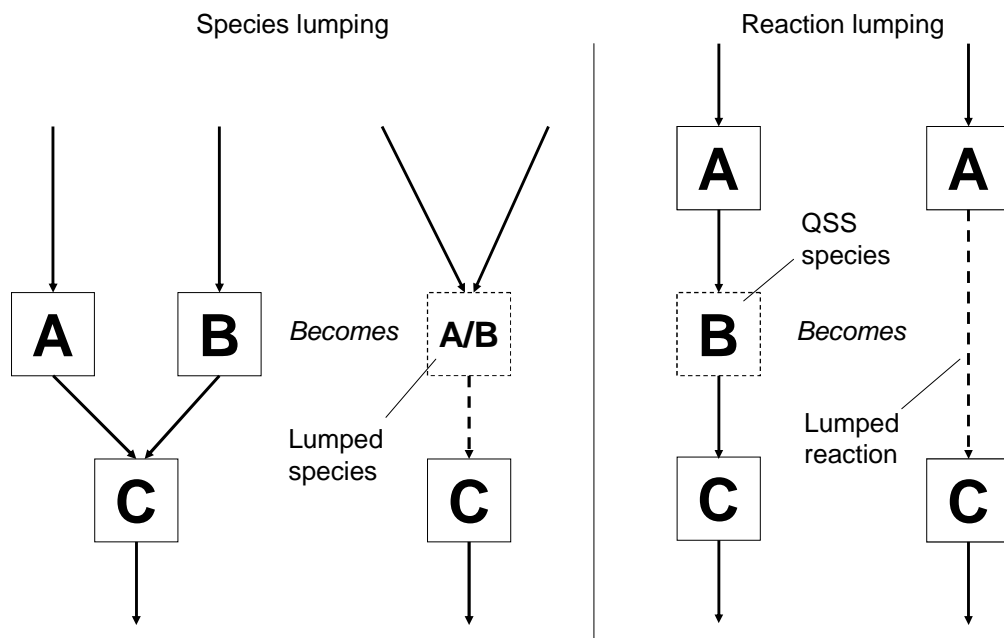


Fig. 7.1. The difference between species lumping and reaction lumping. In species lumping two or more species are combined to form a composite lumped species. Rates of reactions involving lumped species require new formulations for rate constants. Reaction lumping consists of removing intermediates via the formulation of lumped reactions with corresponding lumped reaction rates.

which the QSSA analysis will be performed are then automatically selected along the temperature profile, in the same manner as they are selected for the sensitivity analysis for reduction to a skeleton scheme, outlined in section 5.1. There are other procedures in common with those used for sensitivity analysis – further reduced schemes are validated by comparisons of temperature profiles with the bench mark set by the performance of the full scheme (or the previous stage of reduction). The QSSA reduced mechanisms are further validated via the construction of their p - T_a ignition diagrams and comparing this to the same diagram generated using the full mechanism.

In the following sections we present the methods used to identify QSS species, lump reactions and calculate lumped reaction rates. The application of the QSSA combined with reaction lumping is then illustrated with an example using one of the cyclohexane skeleton schemes from Chapter 5, Section 5.8.2, comprising 60 necessary species in 238 reactions as the starting point.

7.1 The identification of quasi steady state species

The QSSA must be applied to selected amenable species which will not incur great error to the numerical solution of the reacting system. The QSS species are usually intermediate radicals. There are algorithms available to numerically identify the QSS species. One such method is based on the use of CSP developed by Lam and Goussis [36,46]. Another method proposed by Turányi *et al* [63] works on the premise of calculating the local difference between the concentration of a species calculated using the original differential equations and the algebraic approximation of equation 7.1. This is called the instantaneous error of the quasi steady state approximation and if large can propagate to cause errors in the concentrations of important species. The instantaneous error Δc_i^s for a single species can be expressed as;

$$\Delta c_i^s = \left| \frac{1}{J_{ii}} \frac{dc_i}{dt} \right| \quad (7.2)$$

where

$$J_{ik} = \left[\frac{\partial f_i(c, k)}{\partial c_k} \right]. \quad (7.3)$$

A similar but more complex expression to calculate the instantaneous error for a group of species (Δc_i^g) has also been derived by Turányi *et al* [63];

$$\Delta c_i^g = \frac{1}{J_{ii}} \frac{dc_i}{dt} - \frac{1}{J_{ii}} \sum_{k \neq i} J_{ik} \Delta c_k^g. \quad (7.4)$$

In practice, the measure for the instantaneous QSSA error for a single species (equation 7.2) has been found to be sufficient for the identification for the candidate species [36,137,191] and in any case, the group of species to which the QSSA will be applied cannot be known prior to the application of equation 7.2 so the application of equation 7.4 would be a supplementary point of investigation. An alternative to the group QSSA error calculation is to numerically test the effect of applying the QSSA as discussed below.

The local lifetime is another measurement which can be useful for identifying QSS species, and is equal to the reciprocal of the diagonal Jacobian element for that species;

$$Lifetime = \frac{-1}{J_{ii}}. \quad (7.5)$$

Small errors stem from small lifetimes and/or slow rates of change for a species. Therefore, species lifetimes can also be a good indication of QSS species and indeed often imply small instantaneous QSSA errors. A large value of J_{ii} indicates the fast decay of perturbations, and often quite large errors can be tolerated if the lifetimes are very short [15].

In the current work, Equation 7.2 alone is used to identify candidate QSS species and has been incorporated into the automatic reduction software. Thresholds are applied to the magnitudes of the Δc_i^s over all considered time points, translated to a percentage error relative to the concentration of the specific species. Typical thresholds used to identify the candidates can be in the range of 1 – 15 % error.

Equation 7.2 may identify candidate species which in practice would not be selected for the application of the QSSA combined with reaction lumping. This is because they may be radicals which are too highly coupled with other species e.g. OH, H and HO₂ radicals. The complexity induced by such species, as we will see below, limits the application of reaction lumping to some fast reacting species and the computation of resultant long algebraic formulations for lumped rate

parameters can, in extreme cases, cancel out the speed up achieved via the elimination of these species. A negative aspect of this is that the degree of stiffness which is removed may not be as great as could be. This smaller group of species could be solved for using a domain splitting method if required, as has been conducted in reference [117]. The actual list of QSS species is then at the discretion of the user and is based on the feasibility of applying reaction lumping.

Having selected the final group of QSS species, it is necessary to numerically test the effect of applying the QSSA prior to their elimination via reaction lumping. This is done by applying equation 7.1 to the QSS species, effectively setting their rate of production to zero. Individual closed vessel simulations are then carried out at the conditions of interest and compared to those run without the application of the QSSA. Provided no major errors have been incurred to the simulations post application of the QSSA, we then proceed to eliminate the QSS species via reaction lumping.

7.2 Application of reaction lumping

Computational savings are made when the QSS species is removed via reaction lumping. Consider the simple example, where species A and C are linked by the intermediate QSS species B;



By setting $d[B]/dt = 0$, we get the expression

$$k_1[A] = [B](k_{-1} + k_2), \quad (7.7)$$

which leads to

$$[B] = [A] \left(\frac{k_1}{k_{-1} + k_2} \right). \quad (7.8)$$

By defining the lumped reaction as A going to C in a forward irreversible;



we can derive an algebraic expression for the rate parameter k' by considering the rate of change of concentration of A

$$k' = k_1 \left(1 - \frac{k_{-1}}{k_{-1} + k_2} \right). \quad (7.10)$$

An increased level of complexity is encountered, by both the involvement of second order reactions and coupled blocks of QSS species which are required to be eliminated in unison. Consider the example for lean n-butane oxidation shown in Fig. 7.2:

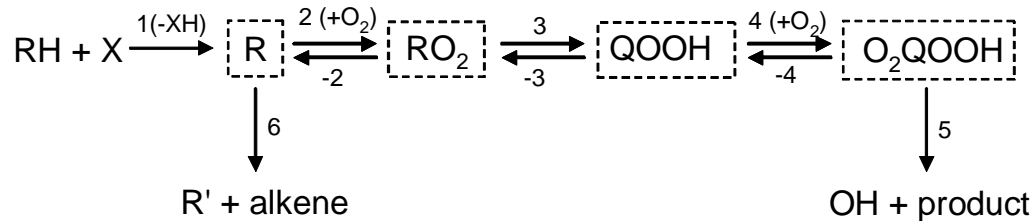
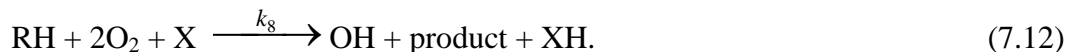


Fig. 7.2. N-butane reaction sequence to which the QSSA and reaction lumping was applied [145].

Our aim is to eliminate the QSS species R , RO_2 , $QOOH$ and O_2QOOH and replace the entire sequence with two lumped reactions with corresponding lumped reaction rates. Mass balance must be maintained so the lumped reactions will be;



Proceeding stepwise, we can first replace the central part of the reaction sequence by



which has the corresponding lumped reaction rate

$$k_2' = k_2 (1 - k_{-2} / (k_{-2} + k_3 - k_3 k_{-3} / (k_{-3} + k_4 [\text{O}_2] - k_4 [\text{O}_2] k_{-4} / (k_{-4} + k_5)))) / [\text{O}_2]. \quad (7.14)$$

The algebraic formulations for reactions 7.11 and 7.12 can then be derived as

$$k_7 = k_6 \left(\frac{k_1}{2k_2' [\text{O}_2] + k_6} \right) \quad (7.15)$$

and

$$k_8 = k_2' \left(\frac{k_1}{2k_2' [\text{O}_2] + k_6} \right). \quad (7.16)$$

The above example illustrates a ramification of applying the QSSA, in that the rate coefficients of the lumped reactions can be functions of species concentrations such as O_2 . As a consequence, the rate expressions cannot be easily replaced by a CHEMKIN style parameterization and the mechanism will no longer be CHEMKIN compatible. This means a specifically tailored integration code with embedded algebraic rate expressions must be set up to handle the complexity, exacerbating the difficulty of the practical aspects of the application. However, the kinetic structure of the mechanism is maintained to a certain extent, and the concentrations of eliminated species maybe recovered if so desired. In addition, if parametric alterations are made to the comprehensive mechanisms,

these can be easily incorporated into the reduced mechanisms since the original rate parameters are retained [145]. This is in contrast to tabulation methods where concentrations of eliminated species cannot easily be recovered and if parametric changes are made to the original mechanism the reduction process must be repeated.

As the examples of blocks of QSS species become increasingly complex, with chain branching and multiple reaction inputs and outputs to the blocks of species, manual analytical solutions become too intractable and are no longer viable. Solutions can be achieved by the use of MAPLE [211], an algebraic mathematics software package. Simultaneous equations are set up for each QSS species by considering one reaction input to the block, all reaction outputs and all reactions between QSS species. The simultaneous equations are solved with MAPLE and the process is repeated for each of the other reaction inputs to the block, one at a time. The lumped reactions are written in the mechanism and the lumped reaction rates are derived from the algebraic solution of the simultaneous equations for the specific concentrations of QSS species which reacts to form the products of the lumped reaction. Further manipulation is required by multiplying the QSS species concentration by the rate parameter for the reaction of QSS species to lumped products and other reactants in this reaction. It is then a trivial matter to find the lumped reaction rate parameter by deleting the reactants concentrations of the lumped reaction from its rate. The lumped reaction rate parameters are copied to the tailored integration code along with all the other necessary Arrhenius parameters from the original skeleton mechanism.

The description of the elimination of complex blocks of QSS species implies a slight perplexity of the reaction lumping, in that the number of reactions in the mechanism can actually increase after its application. This is because the number of lumped reactions required to eliminate a complex block of QSS species will be equal to the product of reaction inputs and outputs to the block. Potential computational speed-ups are expected to scale with N^2 or n , therefore applying these estimates can give a guide as to what may be achievable by eliminating a given group of species. Not all of the new lumped reactions will be kinetically

important and so it may be possible to remove them using skeletal reduction strategies. Extra speed-up may be achieved in a reactive flow code via the elimination of QSS species due to the reduction of the number of partial differential equations describing the transport of each species; these will be unobservable in a kinetics only scenario.

The algebraic solutions for the concentrations of QSS species can in some cases have all the terms on the denominator being multiplied by the concentration of an intermediate non QSS species. At $t=0$, the concentrations of these species are zero so the solution cannot be achieved. The problem is resolved by specifying an initial concentration of these species of 1 molecule/cm³. The QSSA is, in fact, invalid at $t=0$ [63].

7.3 Amalgamation of products

A concomitant of the sensitivity analysis reduction procedure to a skeleton mechanism is that a number of redundant species will remain in the mechanism as products, having had all their consuming reactions removed at the species removal stage. Although not contributing greatly to computational difficulty by virtue of only being involved in producing reactions, their removal is desired to achieve a further computation speed up and global reaction simplification. Many of these species can be further eliminated at the reaction removal stage. Nevertheless, some will remain in the mechanism but may be eliminated post application of the QSSA and reaction lumping. This is achieved by effectively species lumping into one ‘dummy’ product. However, no rate parameter alterations are required for the reactions of lumped products. The thermodynamic properties of carbon dioxide are selected for this purpose because amongst the product-only species this is in the highest concentration. Further incompatibility with CHEMKIN is introduced with this simplification due to the loss of mass balance from the kinetic system – a property which is maintained by the application of the QSSA/reaction lumping. If the retention of mass balance in the kinetic scheme is desired then this step can be avoided. Accurate heat release calculations are no longer preserved with the

product amalgamation simplification. In practice, however, the procedure leads to mechanisms which give excellent reproduction of temperature profiles [187].

Species	Δc_i^s %	Species	Δc_i^s %
RC4ZC5H9#6OOH	0.00049	RC1ZC6H11#6	4.6
R110C5H9CHOOOH	0.0041	-----5 % threshold -----	
R132C3H5OOZ	0.013	O2	6.0
ZCOC2H3Z	0.016	R37C3H5Y	-7.0
RC11OC6H11#6	0.026	-----10 % threshold -----	
R116C5H9CHOOOH	0.031	RC2C6H9#6Y	14
RC6ZC5H9#6OOH	0.032	-----15 % threshold -----	
RC6C6H10OH#6	0.077	CH3OH	21
R117C5H9CHOOOH	0.088	RC9OOC6H10#6OOH	23
RC5ZC5H9#6OOH	0.12	CHOC4H8COOOH	25
R108C5H9CHOOOH	0.13	R13CH2CHO	34
R14CH3CO	0.17	HCHO	-40
R5CHO	0.36	C3H5OOHY	43
R3OOH	-0.48	C6H10Z#6	47
R109C5H9CHOOOH	0.62	RCDOOC6H10#6OOH	48
R1H	0.97	R18CH3COOO	51
R2OH	1.1	RC2ZOOC6H11#6	60
R10C2H3V	1.2	C6H12#6	65
R133C5H9CHO3HOO	1.2	C2H3CHOZ	79
R106C5H10CHO	1.3	CH2COZ	-81
B1O	1.6	H2O2	95
R6CH2OH	1.8	C5H9CO#6OOH	99
R107C5H10CHOOO	1.9	C6H11#6OOH	100
R121C5H9CHO3HOO	2.0	C6H11#6OH	100
R4CH3	2.4	C2H4Z	-110
RC7OOC6H10#6OOH	2.5	CH3CHO	-200
R12CHCOV	2.6	B2CO	-4000
R8CH3OO	4.5	H2	-4300
R7CH3O	4.6		

Table. 7.1. Magnitudes of instantaneous QSSA errors for species in the cyclohexane skeleton mechanism at a single automatically selected time point relating to the ambient conditions of 510 K and 254.42 kPa, local temperature of 913.5 K and $t = 199.5$ s.

7.4 Application of the quasi steady state approximation and reaction lumping to the cyclohexane + air scheme

In this section, we show that the QSSA methods can be applied to a highly complex reaction sequence such as that for cyclohexane combustion. The comprehensive EXGAS generated scheme was simplified to a skeleton mechanism as outlined in Section 5.8 comprising 60 necessary species in 238 irreversible reactions. The analysis was performed at two operating conditions of 510K, 254.4 kPa and 530K, 61.4 kPa shown on Fig. 5.24. The aim of the QSSA application reduction was to preserve the position of the low temperature ignition

Instantaneous QSSA error		
5%	10%	15%
B1O	B1O	B1O
R107C5H10CHOOO	R106C5H10CHO	R106C5H10CHO
R108C5H9CHOOOH	R107C5H10CHOOO	R107C5H10CHOOO
R109C5H9CHOOOH	R108C5H9CHOOOH	R108C5H9CHOOOH
R10C2H3V	R109C5H9CHOOOH	R109C5H9CHOOOH
R110C5H9CHOOOH	R10C2H3V	R10C2H3V
R116C5H9CHOOOH	R110C5H9CHOOOH	R110C5H9CHOOOH
R117C5H9CHOOOH	R116C5H9CHOOOH	R116C5H9CHOOOH
R121C5H9CHO3HOO	R117C5H9CHOOOH	R117C5H9CHOOOH
R12CHCOV	R121C5H9CHO3HOO	R121C5H9CHO3HOO
R132C3H5OOZ	R12CHCOV	R12CHCOV
R133C5H9CHO3HOO	R132C3H5OOZ	R132C3H5OOZ
R14CH3CO	R133C5H9CHO3HOO	R133C5H9CHO3HOO
R1H	R14CH3CO	R14CH3CO
R2OH	R1H	R1H
	R2OH	R2OH
	R37C3H5Y	R37C3H5Y
R3OOH	R3OOH	R3OOH
	R4CH3	R4CH3
R5CHO	R5CHO	R5CHO
R6CH2OH	R6CH2OH	R6CH2OH
R7CH3O	R7CH3O	R7CH3O
	R8CH3OO	R8CH3OO
RC11OC6H11#6	RC11OC6H11#6	RC11OC6H11#6
RC1ZC6H11#6	RC1ZC6H11#6	RC1ZC6H11#6
RC3ZC5H9#6OOH	RC3ZC5H9#6OOH	RC3ZC5H9#6OOH
RC4ZC5H9#6OOH	RC4ZC5H9#6OOH	RC4ZC5H9#6OOH
RC5ZC5H9#6OOH	RC5ZC5H9#6OOH	RC5ZC5H9#6OOH
RC6C6H10OH#6	RC6C6H10OH#6	RC6C6H10OH#6
RC6ZC5H9#6OOH	RC6ZC5H9#6OOH	RC6ZC5H9#6OOH
RC7OOC6H10#6OOH	RC7OOC6H10#6OOH	RC7OOC6H10#6OOH
ZCOC2H3Z	ZCOC2H3Z	ZCOC2H3Z

Table 7.2. Overall union of QSS species, identified by applying thresholds to the magnitudes of the instantaneous QSSA error over all time points.

boundary and the magnitudes of the ignition delay times. Example results of the magnitudes of the instantaneous QSSA for a given time point are shown in Table 7.1. Thresholds were applied to the magnitudes of the instantaneous QSSA errors over all considered time point for each species calculated using equation 7.2. This led to the identification of species which satisfy the threshold criteria of 5, 10 and 15% over all of the time points and are shown in Table 7.2.

Table 7.2 shows that the same set of species were identified at 10 and 15 %, implying the existence of a natural threshold for the instantaneous QSSA error. Therefore this set of species was further examined to assess how feasible it would be to apply the QSSA and reaction lumping to them. Most of the species appeared to be good candidates for application of the QSSA, with the exceptions of B1O,

R1H, R2OH, R3OOH, R4CH3, R5CHO, R6CH2OH, R7CH3O and R8CH3OO due to the high number of reactions of these species. Individual closed vessel simulations were run, using the coupled differential-algebraic solver available in SPRINT, to numerically test the effect of applying the QSSA to the remaining 23 candidate QSS species and the results gave excellent reproduction of temperature profiles. The QSS species couplings were such that there were a number of configurations which could be solved analytically. Consider the example shown in Fig. 7.3:

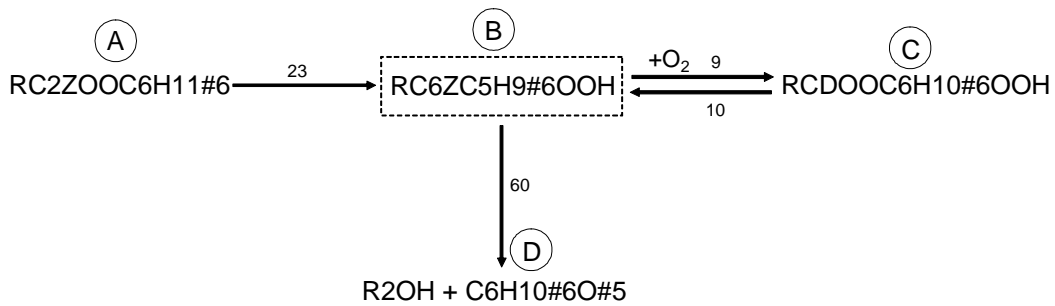


Fig. 7.3. Example of a cyclohexane QSSA problem which can be solved by hand. The QSS species is highlighted by a dashed box.

We wish to replace the above system with the set of lumped reactions;



By setting $d[B]/dt = 0$, we can derive an expression for the concentration of B;

$$[B] = \frac{k_{23}[A] + k_{10}[C]}{k_{60} + k_9[O_2]}. \quad (7.20)$$

Now, by considering the rates of change of the other species we can derive the rates of the lumped reactions.

$$\frac{d[C]}{dt} = k_9[O_2][B] - k_{10}[C] \quad (7.21)$$

$$= k_9[O_2] \left(\frac{k_{23}[A] + k_{10}[C]}{k_{60} + k_9[O_2]} \right) - k_{10}[C] \quad (7.22)$$

$$= \frac{[A][O_2]k_9k_{23}}{k_{60} + k_9[O_2]} - \frac{[C]k_{10}k_{60}}{k_{60} + k_9[O_2]} \quad (7.23)$$

Clearly the first and second terms of equation 7.23 are the rates of reactions 7.17 and 7.19 respectively. Therefore, the rate parameters of the reactions are found by simply deleting the reactant concentrations from the numerator. Now let us consider the rate of change of species D.

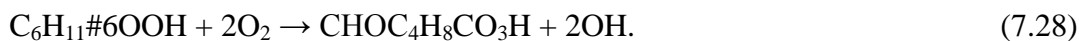
$$\frac{d[D]}{dt} = k_{60}[B] \quad (7.24)$$

$$= k_{60} \left(\frac{k_{23}[A] + k_{10}[C]}{k_{60} + k_9[O_2]} \right) \quad (7.25)$$

$$= \frac{[A]k_{23}k_{60}}{k_{60} + k_9[O_2]} + \frac{[C]k_{10}k_{60}}{k_{60} + k_9[O_2]} \quad (7.26)$$

Once again, the terms of equation 7.26 are explicit expressions of the lumped reaction rates with the first term and second terms relating to reactions 7.18 and 7.19 respectively. The actual lumped rate parameters of k_2 and k_3 are then found by eliminating $[A]$ and $[C]$ from these two terms, respectively. Rate expressions for lumped reactions could be derived for a number of other simple systems of QSS species and this led to the removal of 8 species.

More complex blocks of coupled species, such as the one shown in Fig. 7.4, required the use of MAPLE to computationally derive the rate expressions. The system of equations shown Fig. 7.4 was substituted with the two following equations:



The rate parameters of reactions shown in 7.27 and 7.28 were calculated in a stepwise manner. First the rate parameter of the lumped reaction of $\text{RC110C}_6\text{H}_{11}\#6$ to products was calculated using the MAPLE solutions from one set of simultaneous equations for the species $\text{R133C}_5\text{H}_9\text{CHO}_3\text{HO}_2$ and $\text{R121C}_5\text{H}_9\text{CHO}_3\text{HO}_2$. Using this solution, the final lumped rate parameters were calculated manually by consideration of the two input reactions. This led to the elimination of the 10 QSS species shown in Fig. 7.4.

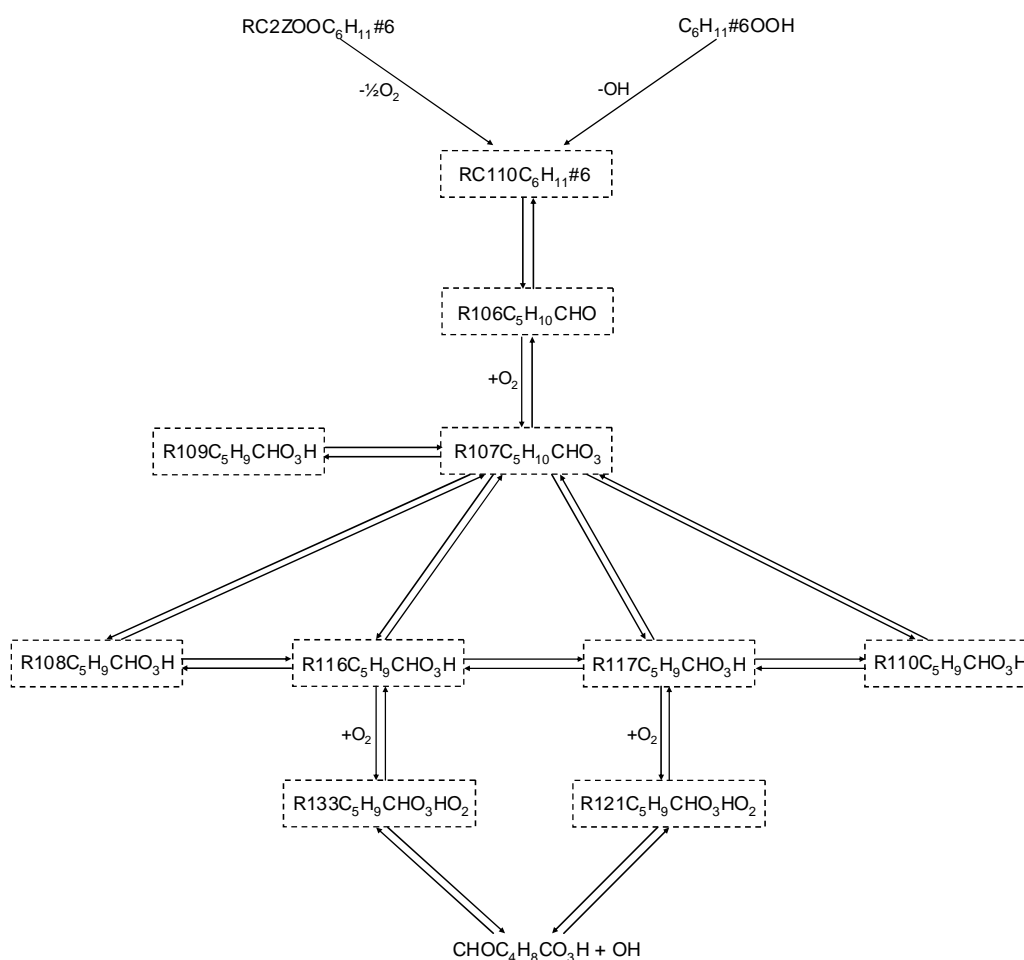


Fig. 7.4. Example of a cyclohexane QSSA problem which requires MAPLE to computationally calculate the lumped reaction rates. The QSS species are highlighted by a dashed box.

An even more complex block of 5 coupled QSS species was encountered during the reduction, which involved 13 input reactions to the block and a corresponding number of MAPLE solutions of sets of simultaneous equations. The formulation of 91 lumped reactions and the calculation of their lumped reaction rate parameters led to the successful removal of the 5 QSS species.

Hence, the 23 identified candidate QSS species were successfully removed, creating a QSSA reduced mechanism with 37 necessary species, 8 redundant products (as identified by the iterative analysis of the Jacobian matrix) plus helium and argon. These species are involved in 323 reactions, with 193 of these reactions requiring new algebraic formulations for rate parameters, embedded in the integration software.

The predicted p - T_a ignition diagram from the QSSA reduced mechanism is shown in Fig. 7.5 and compared to that of the full mechanism and the 60 species and 238 reactions mechanism to which the QSSA was applied. Up to a temperature of 530K, the QSSA reduced mechanism reproduces the ignition boundary produced by the full mechanism excellently. Excellent agreement can also be found between the cool flame/slow reaction boundaries of the full and QSSA reduced mechanisms. However, at temperatures higher than 530K there is a marked difference between the cool flame/2-stage ignition boundaries of the full and QSSA reduced mechanisms. This is partly due to inherent discrepancies from the pre-QSSA mechanism, but also attributed to the application of the QSSA raising the minimum pressure at which 2-stage ignition will occur. Very good agreement can also be observed when temperature profiles at the conditions of analysis output from the QSSA reduced mechanism are compared to those of the full mechanisms, as shown in Fig. 7.6.

A further level of simplification was achieved by amalgamating products into one 'dummy' species as outlined in section 7.3. In addition to the 8 redundant products identified by the iterative analysis of the Jacobian matrix, 2 more species became candidates for the species lumping procedure by virtue of having all their consuming reactions eliminated at the skeletal reduction stage, prior to the application of the QSSA, using principal component analysis. The 10 product

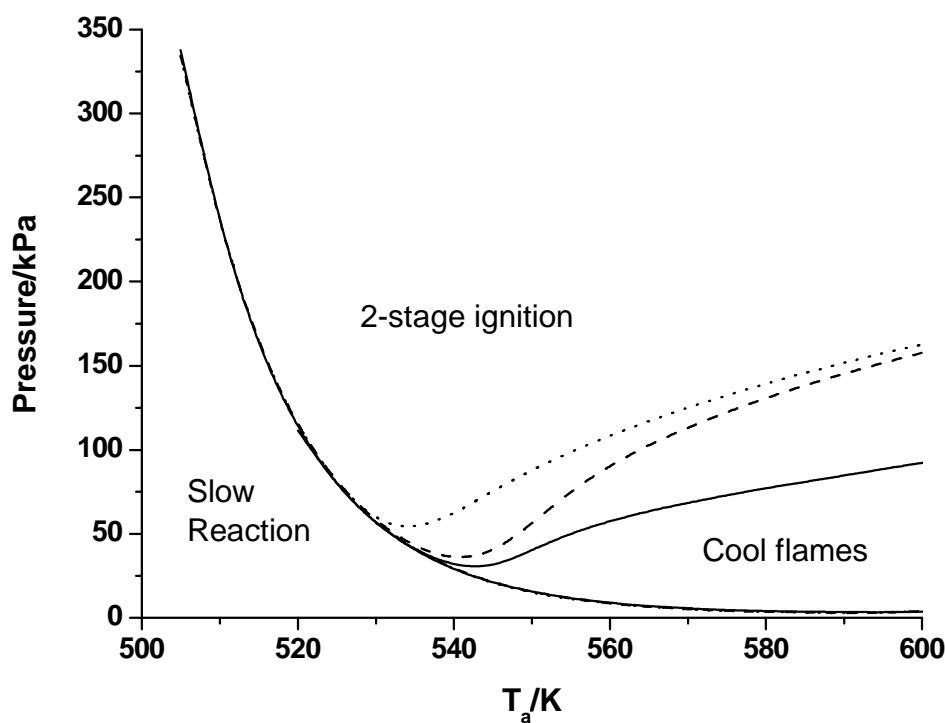


Fig. 7.5. Comparison of the stoichiometric p - T_a ignition diagrams produced by the full mechanism (solid line), the skeleton 60 necessary species and 238 reactions mechanism to which the QSSA was applied (dashed line) and the 37 species 323 reactions QSSA reduced mechanism (dotted line).

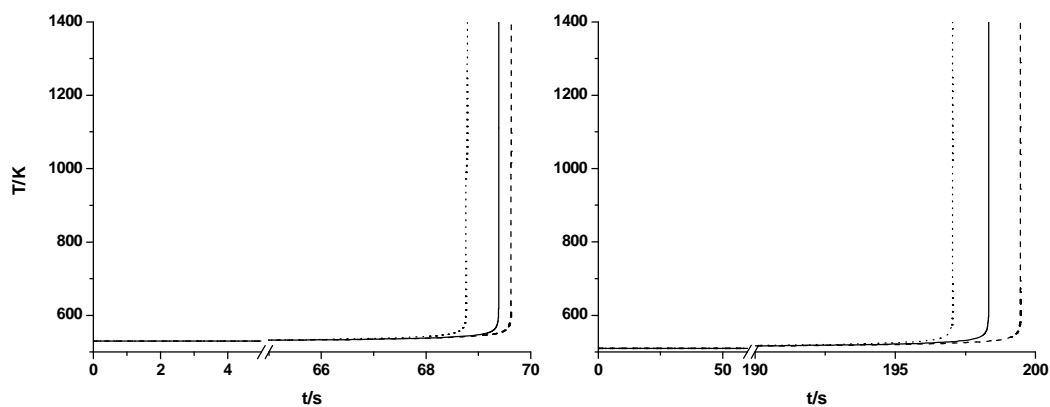


Fig. 7.6. Comparison of the temperature profiles produced by the full mechanism (solid line), the skeleton 60 necessary species and 238 reactions mechanism to which the QSSA was applied (dashed line) and the 37 species 323 reactions QSSA reduced mechanism (dotted line). *Left conditions:* 530 K and 61.39 kPa, *Right conditions:* 510 K and 254.42 kPa.

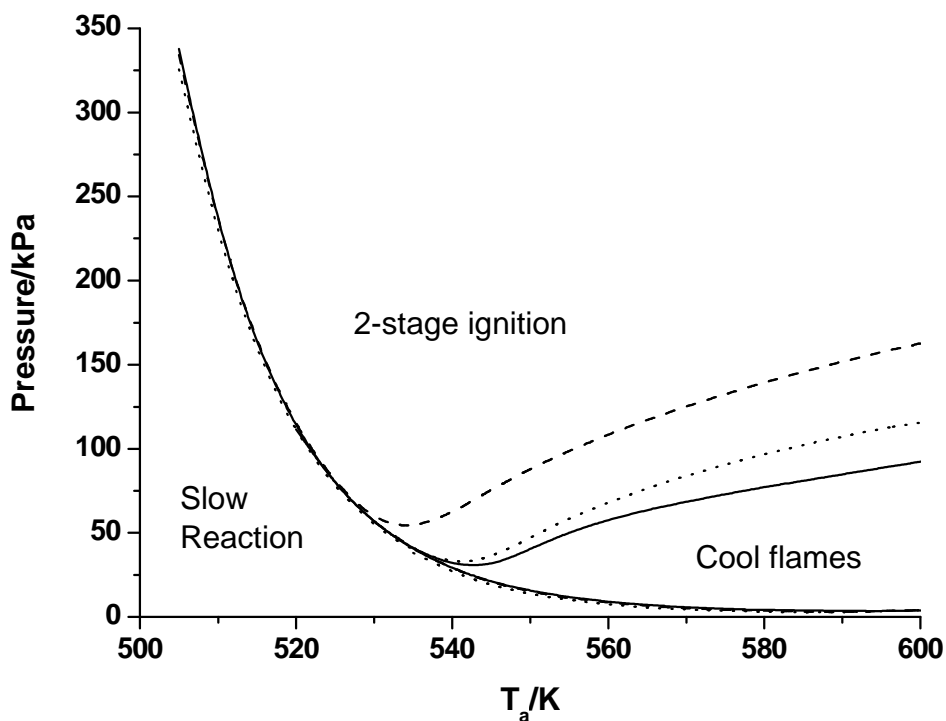


Fig. 7.7. Comparison of the stoichiometric p - T_a ignition diagrams produced by the full mechanism (solid line), the 37 necessary species 323 reactions QSSA reduced mechanism prior to product lumping (dashed line) and the 35 species 323 reactions QSSA reduced mechanism, post product lumping (dotted line).

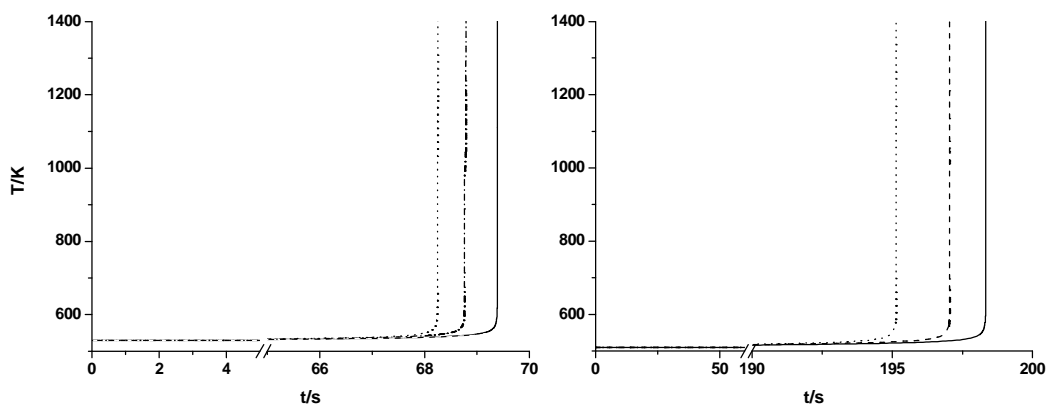


Fig. 7.8. Comparison of temperature profiles produced by the full mechanism (solid line), the 37 necessary species 323 reactions QSSA reduced mechanism prior to product lumping (dashed line) and the 35 species 323 reactions QSSA reduced mechanism, post product lumping (dotted line). *Left conditions:* 530 K and 61.39 kPa. *Right conditions:* 510 K and 254.42 kPa.

species were then amalgamated into one species which had the same thermodynamic properties of carbon dioxide. This resulted in the creation of mechanism comprising of 35 species and 323 reactions (reactions unchanged). The performance of this mechanism is evaluated by the comparison of its p-T_a ignition diagram and temperature profiles to those of the full mechanism and also to those of the QSSA reduced mechanism without this further level of simplification invoked.

Fig. 7.7 shows the comparison of p-T_a ignition diagrams. The highly reduced QSSA reduced and product lumped mechanism reproduces the low temperature ignition and cool flame/slow reaction boundaries very well. Due to the thermodynamic properties of carbon dioxide, specifically the ΔH°_f , the reactions containing the new lumped species increase in exothermicity. This results in a shift of the location of the boundary between cool flames and 2-stage ignition, with 2-stage ignition occurring at lower pressures than those exhibited by the scheme prior to the lumping of products. The location of the cool flame/2-stage ignition boundary of the QSSA reduced and product lumped mechanism is detected at magnitudes of pressure, closer to those exhibited by the full cyclohexane mechanism. Despite the shift in the cool flame/2-stage ignition boundary, the QSSA reduced and product lumped mechanism still gives an excellent reproduction of the temperature profiles, as illustrated in Fig. 7.8.

The scale of the reduction via application of the QSSA is shown diagrammatically in Fig. 7.9 via an element flux diagram under isothermal conditions. This schematic relates directly to the same diagram generated using the skeleton 60 necessary species and 238 reactions mechanism prior to the application of the QSSA shown in Fig. 6.9. Fig. 7.9 shows the mechanistic implications of eliminating the QSSA species via reaction lumping. Notable eliminations can be drawn from the comparison of Figs. 6.9 and 7.9, they are; the cyclohexyl radical, various isomers of the cyclohexylhydroperoxide radical, the cyclohexylalcoxy radical, the ring breakage of this molecule and subsequent numerous additions of oxygen and isomerizations. Interestingly, the types of radicals which were not eliminated, cyclohexylperoxy radical and the

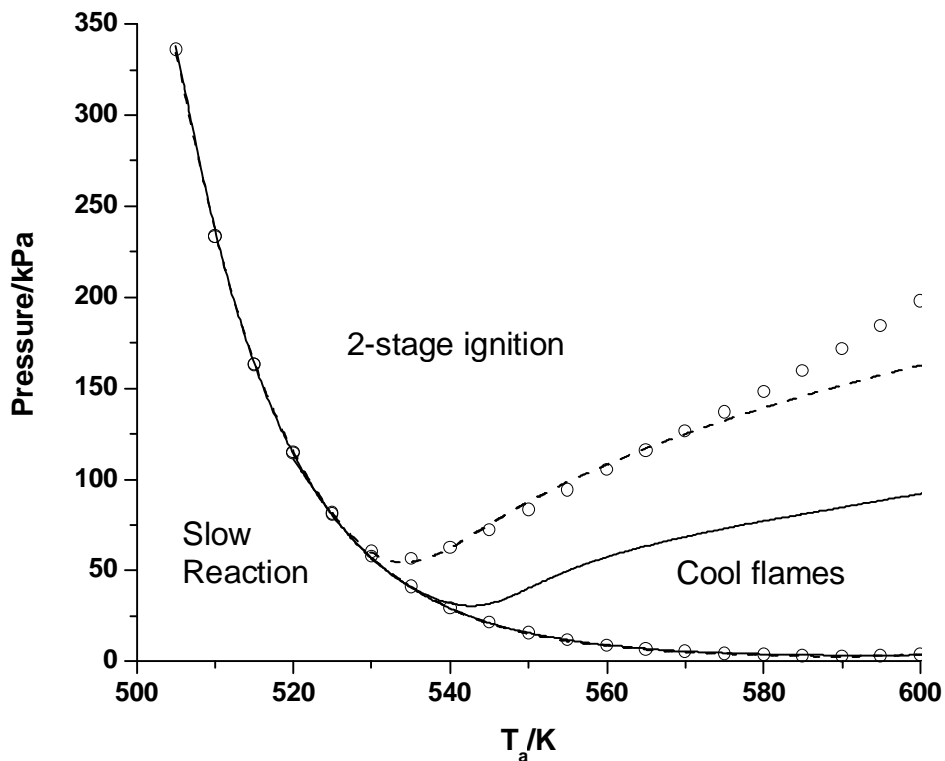


Fig. 7.10. Comparison of the stoichiometric p - T_a ignition diagrams produced by the full mechanism (solid line), the 37 necessary species 323 reactions QSSA reduced mechanism prior to product lumping (dashed line) and the 24 necessary species 135 reactions further sensitivity analysis reduced mechanism (open circles).

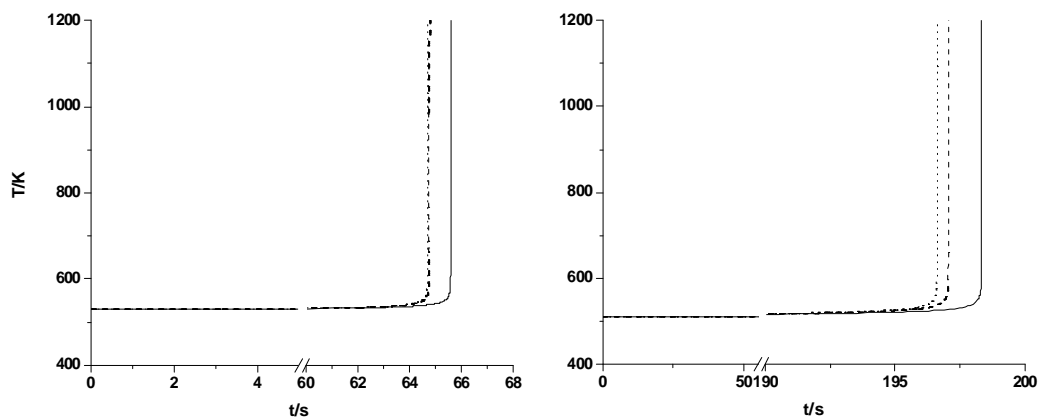


Fig. 7.11. Comparison of temperature profiles produced by the full mechanism (solid line), the 37 necessary species 323 reactions QSSA reduced mechanism prior to product lumping (dashed line) and the 24 necessary species 135 reactions further sensitivity analysis reduced mechanism (dotted line). *Left conditions:* 530 K and 74.00 kPa. *Right conditions:* 510 K and 254.42 kPa.

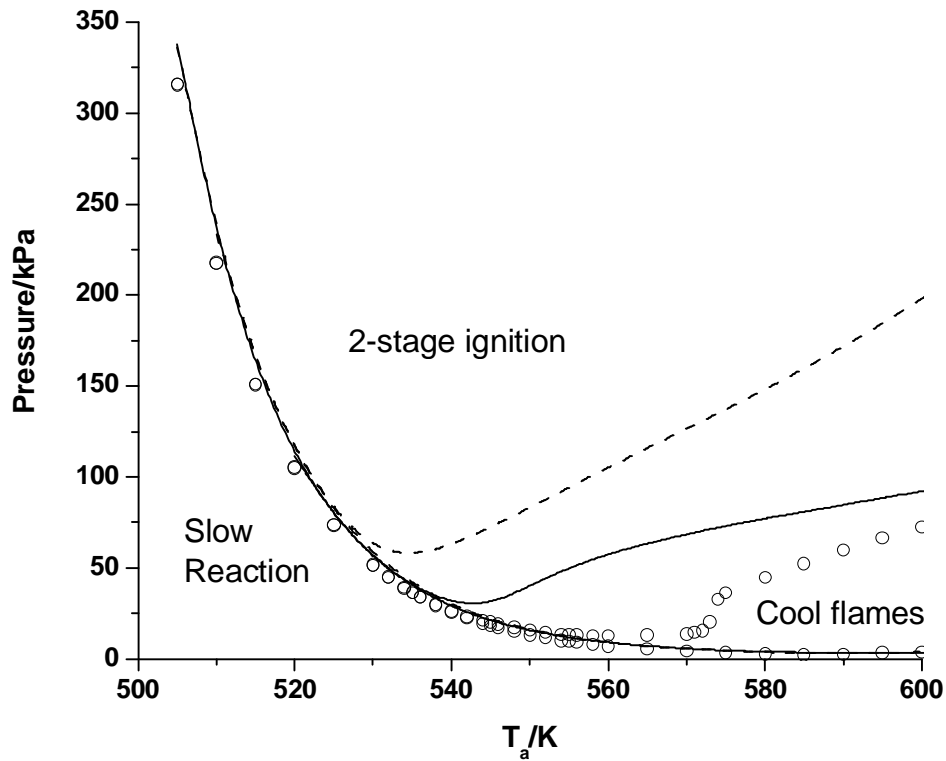


Fig 7.12. Comparison of the stoichiometric p - T_a ignition diagrams produced by the full mechanism (solid line), the 24 necessary species 135 reactions further sensitivity analysis reduced mechanism (dashed line) and the 24 species 135 reactions mechanism with amalgamated products (open circles).

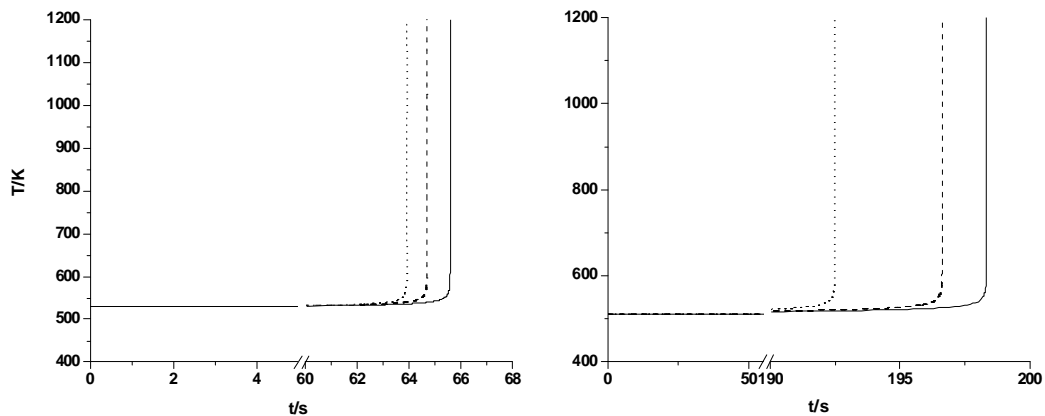


Fig. 7.13. Comparison of temperature profiles produced by the full mechanism (solid line), the 24 necessary species 135 reactions further sensitivity analysis reduced mechanism (dashed line) and the 24 species 135 reactions mechanism with amalgamated products (dotted line). *Left conditions:* 530 K and 74.00 kPa. *Right conditions:* 510 K and 254.42 kPa.

the previous Section before product lumping was applied, comprising 37 species in 323 reactions. The analysis was performed at automatically selected time points of the same two operating conditions of 510K, 254.4 kPa and 530K, 61.4 kPa shown on Fig. 5.24. The iterative analysis of the Jacobian matrix, using the threshold criteria (as outlined in Section 5.2) of (a) = 5, (b) = 0.3, (c) = 8 and (d) = 8, identified a further 7 species as being redundant. Removal of the 88 consuming reactions of these species incurred very little error to output ignition delay times. Out of the 88 reactions, 56 of these were of the new type that were created during the reaction lumping process. Further progress was made via the application of PCA using thresholds 1×10^{-4} and 1×10^{-2} for the eigenvalues and eigenvectors, respectively. This led to the removal of a further 100 reactions with 92 of these being lumped reactions with corresponding algebraic rate expressions. The reduced mechanism resulting from the reapplication of the sensitivity analysis based reduction techniques then consisted of 24 species that participate as reactants and 15 product only species, which were included in 135 reactions, with 45 of these being lumped reactions. The low temperature p-T_a ignition diagram produced by this mechanism is shown in Fig. 7.10 and compared to those of the full mechanism and the QSSA reduced mechanism. Excellent agreement can be found between the low temperature ignition boundaries produced by the full mechanism and further sensitivity analysis reduced mechanism. Little divergence is observed between the cool flame/ignition boundary produced by the further sensitivity analysis reduced mechanism and the same boundary produced using the mechanism from previous stage of reduction until 580 K temperature. The further reduction also incurs little error to the output ignition delay times as is shown in Fig. 7.11.

The further level of simplification of lumping the product only species into one dummy species can also be applied to the further sensitivity analysis reduced mechanism. The effect that this has on the simulated ignition diagram and ignition delay times is shown in Figs. 7.12 and 7.13, respectively. Some detail to the cool flame/ignition boundary is lost in this simplification. However, the reduction still

achieves its objectives of preserving the low temperature ignition boundary and ignition delay times.

7.4.2 Computational speed ups

Having virtually halved the number of species one might expect to have achieved a significant further computational saving. However, the solution of algebraic formulations for rate parameters and the increase in the overall number of reactions may not necessarily lead to a large computational time saving. Since the eliminated QSS species are fast reacting species, it is also possible that the stiffness of the system (the ratio of fast to slow time-scales) has also been reduced leading to a further speed up. The degree of stiffness removed will be limited by the retention of small fast reacting species like OH and HO₂ radicals, but the analysis of instantaneous QSSA errors shows that groups of species with the shortest lifetimes at each of the time points were successfully removed. Comparisons of the run times of the “pre” and “post” QSSA reduced cyclohexane mechanisms at the conditions of analysis, showed that despite reducing the total number of species, on this occasion, no computational speed up was perceivable in zero-dimensions. However, the reduction is still considered worthwhile because the number of dimensions of the system has been reduced and the kinetic mechanism has been simplified. The application of the QSSA reduced scheme in CFD could still achieve a further reduction in computational time in comparison to what is achieved kinetically, due to the simplification of transport calculations for these species. For instance, the solution for laminar flow which incorporates a kinetic mechanism involves the solution of a partial differential equation (PDE) for each species. A reduction of 60 to 35 PDEs could therefore give a significant speed-up [212].

The numbers of species and reactions of the post QSSA reduced scheme were successfully reduced by reapplying the sensitivity based techniques of Chapter 5. A large proportion of the created lumped reactions to remove the QSS species were found to be redundant and were removed, which also reduces the

computational overhead of their corresponding algebraic formulations. The smallest reduced mechanism presented in this Chapter (24 species, 135 reactions post further sensitivity analysis and product lumping) has a computational run time corresponding to 42 % of that of the mechanism to which the QSSA/reaction lumping was applied (60 species and 238 reactions). This translates to a 0.9 % runtime relative to that of the full mechanism. Furthermore, if it is possible to replace the algebraic formulations for the reaction rates with a standard kinetic parameterization then this may further reduce the computational run time. The procedure could involve calculating the lumped rate parameters at a number of reaction times and recording the reaction temperature and pressure. The next step would be to obtain parameterized standard CHEMKIN rate expressions by the numerical fitting of functions.

QSSA reductions using the methodology described in this section have also been applied to skeleton schemes describing the oxidation of n-butane and n-heptane². The application of the QSSA and reaction lumping to the skeleton n-butane scheme, illustrated in Section 5.7, which comprises 73 necessary species in 300 reactions, resulted in the removal of 14 QSS species and a reduction of reactions to a total of 270. This resulted in a speed-up being observed where the skeleton mechanism had a runtime equal to 19 % that of the full mechanism and after the application of the QSSA this figure stood at 16 %. This was a preliminary investigation, meaning further identified QSS species remain in the mechanism which are amenable to removal. The comprehensive n-heptane mechanism, outlined in Section 4.5, was reduced from 358 species in 2411 irreversible reactions to a skeleton form consisting of 218 necessary species in 810 reactions. Over 100 QSS species could be identified amongst the 218 species of 218 species of the skeleton scheme, and they were successfully removed. After the reapplication of the sensitivity methods outlined in Chapter 5 and the amalgamation of redundant products into one ‘dummy’ species, the size of the scheme stood at 81 species and 452 reactions. The application of the QSSA techniques to the skeleton scheme caused a significant reduction of the

² Reduction of n-heptane and n-butane QSSA reduction were performed by Dr. K. J. Hughes.

computational run time from 19 % to 5 % that of the full mechanism. The application of the QSSA combined with reaction lumping can therefore achieve significant reductions in the numbers of species. Further computational speed-ups can be obtained by performing skeletal type reductions to the post QSSA reduced mechanisms.

7.5 Comparison of quasi steady state approximation reduction achievements

In this section, the extent of the QSSA reductions, in terms of numbers of species eliminated and minimization of computational run time will be compared to other published reductions in order to assess the effectiveness of the current procedure. To be objective, these methods should be compared to other QSSA or similar reductions and not the type of reduction to a skeleton mechanism, tabulation or repro-modelling technique.

The QSSA has been applied to a mechanism describing the oxidation of carbon monoxide and hydrogen in a continuously stirred tank reactor at very low pressure by Brad *et al* [127]. Using a subset of the Leeds methane scheme [13] comprising 13 species and 69 reactions as a starting point, the mechanism was reduced via sensitivity type methods. The result was the generation of a skeleton mechanism comprising 9 species in 24 reactions. The QSSA was applied next and using similar techniques to those described here, 3 QSS species were identified. The methods illustrated in this Chapter would, at first glance, appear to be superior in terms of simplifications achieved using the QSSA; however, it is difficult to draw parallels with this reduction due to the fundamental differences in the starting mechanisms. Further ILDM techniques were applied to the carbon monoxide and hydrogen which resulted in the creation of a repro-model with only four variables needed to model the complex phenomena exhibited by the full scheme. In some cases more fast variables are identified by the ILDM since it transforms species concentrations to “time-scale” variables. Since the QSSA deals

explicitly with species, fast timescales resulting from combinations of species cannot be addressed.

A better comparison can be made to the reduction of a larger mechanism used to describe the pyrolysis of methane by Kovács *et al* [139] which used methods to reduce to a skeleton mechanism and identify QSS that are similar to those presented in this thesis. The starting point of the reduction was a mechanism comprising 165 species in irreversible 1604 reactions, after reduction to a skeleton mechanism the mechanism consisted of 61 species and 338 reactions which ran 11.5 times faster than the comprehensive mechanism. Out of the 61 necessary species, 36 of those were found to be amenable to the application of the QSSA, making this reduction to appear commensurate with those presented here, if not slightly better. However, the QSS species identified were not removed from the mechanism and no speed-up is quoted by the authors. The reduction proceeded via the employment of the ILDM to show that the dynamics of the system could be described by an 18-variate system of differential equations.

The QSSA was also used to reduce mechanisms describing atmospheric chemistry using the related CSP method to identify the fast species [119,120]. CSP can be used to make both skeletal and QSSA type reductions, with the two techniques often being performed simultaneously. The reduction was applied to the Regional Atmospheric Mechanism which comprises 77 species in 237 reactions. The most aggressive reduction in [119] led to the decoupling of 56 of the QSS species. However, significant computational speed-ups were not achieved because of the choice of inner iterative methods used to solve the resulting algebraic system. These achievements in species reduction, however, would appear to be comparable to those presented here.

A CSP application to a combustion system has been carried out by Skevis *et al* [118]. Reduced mechanisms for methane combustion, valid for high pressure and high humidity, were developed for the improvement of gas turbine operations. A 53 species and 325 reversible reactions comprehensive mechanism was used as the starting point for the construction of a reduced seven step mechanism. The steps in the reduced mechanism refer to global steps and their corresponding

global rates involve all major and steady-state species, with the latter being calculated using the inner iteration procedure. This appears to be a very impressive reduction in terms of the compactness of the resulting mechanism. The reduction of variables and stiffness will have undoubtedly led to significant computational speed-ups, although without any specific details of these it is difficult to make a comparison with the achievements presented in this Chapter. However, a very similar study has been undertaken by Massias *et al* [108] with similar results, reducing a mechanism used to describe laminar premixed methane/air flames from 49 species and 279 reactions (mostly reversible) to another seven step mechanism, including 12 major species. A four fold speed up was reported, which may appear modest in consideration of sizes of the involved mechanisms. The cause of the diminished speed up is the required calculations of the global rates which involve steady-state species. These are computed from the algebraic relations by applying the inner iteration loop several times at each spatial grid point. These extra calculations mean that any speed-up obtained is expected to scale linearly with the number of species (N); in contrast to the N^2 relation expected for skeletal type reductions. In fact, a linear relationship to N has been achieved with the QSSA/reaction lumping presented here because a 40 % reduction in species via the QSSA was obtained and a 42 % speed-up observed, making these achievements comparable to those of the Massias *et al*, in consideration of the very large skeletal reduction of the cyclohexane scheme. But for n-heptane, a nearly N^2 dependence was achieved, which implies that for some mechanisms reaction lumping can out perform inner iteration methods. The calculation of the CSP reduced mechanisms can be further accelerated via the truncation of global rates and steady-state relations or by the tabulation of the steady state relations.

Comparisons of time-scale analysis reductions have also been made by Løvås *et al* [213]. Reduced mechanisms for methane autoignition were developed using two methods; the first was a CSP analysis and the second was a lifetime analysis based on the diagonal of the Jacobian matrix (equation 7.5) combined with a sensitivity measure. From the comprehensive mechanisms consisting of 46

species and 467 reactions, a range of reduced mechanisms were produced using the two methods consisting of 10 – 20 global reaction steps. The reduced schemes comprised of similar but not identical species and had different strengths and weaknesses: The CSP appeared to give reduced mechanisms with slightly greater accuracy, however, the authors state that the lifetime analysis method produced mechanisms of sufficient accuracy and was of greater convenience in terms of the computational time required for the reduction procedure. The overall level of reduction seems to be comparable to the other CSP methods discussed in this Section and, by implication, the QSSA reduction of this Chapter.

7.6 Conclusions

The QSSA combined with reaction lumping has been applied to a 60 necessary species and 238 reactions skeleton mechanism describing the low temperature oxidation of cyclohexane, thus a number of intermediate species have been further eliminated. The resulting 37 species and 323 reactions mechanism gives an accurate reproduction of the low temperature ignition boundary and little error has been incurred to output ignition delay predictions. QSS species to be removed were identified through automated methods with user prescribed tolerances to the instantaneous error of the QSSA over a number of time points and initial ambient conditions. Ignition diagrams of QSSA reduced mechanism were generated using the automated procedures outlined in Section 4.1.1. Further reductions were made after the application of the QSSA, by reapplying the sensitivity analysis reduction methods of Chapter 5 and amalgamating redundant products into a dummy species with the thermodynamic properties of CO₂. This yielded a final reduced mechanism of 24 species and 135 reactions, including 45 lumped reactions with lumped algebraic rate expressions.

Due to the high couplings of QSS species, customized reaction mechanisms and integration codes are required to maintain a high level of accuracy, which is to the detriment of CHEMKIN compatibility. However, the kinetic structure of the original mechanism is maintained to a large extent and the concentrations of

removed species can be recovered from algebraic formulations and the concentrations of non-QSS species. Complete CHEMKIN compatibility could be restored by the fitting of lumped rate constants, which may also promote computational time savings.

The application of the QSSA and reaction lumping alone to the cyclohexane does not obtain a significant speed-up due to the overall increase in the number of reactions and complex algebraic formulations of lumped rate parameters. However, a time saving was achieved by the reapplication sensitivity type techniques (of Chapter 5) to eliminate species and reactions, corresponding to a 42 % runtime of that of the pre-QSSA skeleton mechanism to which the techniques were applied. Previous applications to oxidation mechanisms of n-butane and n-heptane showed larger time savings, due to a higher proportion of species with low couplings compared to cyclohexane. Parameterization of lumped reaction rates may also achieve extra time savings [15].

The QSSA coupled with reaction lumping application is amenable to further automation. The automatic construction of lumped mechanisms and corresponding tailored integration code could be achieved by using UNIX shell scripts to interface with MAPLE and manipulate mechanisms, integration codes and data files.

Chapter 8

Conclusions

Comprehensive hydrocarbon oxidation mechanisms often contain very large numbers of chemical species and reactions. The scale and stiffness of the resulting simultaneous equations makes their incorporation into computational fluid dynamic (CFD) tools used to model complex three dimensional reactive flows extremely difficult at present and for the foreseeable future. Therefore, there is a need for much reduced but accurate hydrocarbon oxidation kinetic mechanisms for application to process hazards mitigation and also in other areas such as engine research and development. This thesis has aimed to describe and discuss numerical techniques used for the modelling and reduction of gas phase oxidation kinetic mechanisms. The application of kinetic reduction software has been illustrated with respect to a number of fuels and numerical analysis of the resulting reduced mechanisms has elucidated a number of interesting kinetic features.

Throughout the discussion in this thesis, summaries and conclusions may be found in appropriate places such as at the end of Chapters. The following discussion aims to draw together the major findings, achievements and conclusions. Recommendations for further work will also be made.

Chapter 1 gave an outline of the requirement for mechanism reduction in the context of explosion hazard mitigation in the process industries and a brief introduction to some of the numerical techniques used to reduce mechanisms. The

discussion continued in Chapter 2, which includes a literature review on the development of comprehensive mechanisms and solution techniques followed by a review of existing skeletal and time-scale based reduction methodologies. Chapter 3 gave details on established computational techniques used in the present work for the simulation and analysis of oxidation mechanisms.

The evaluation of comprehensive mechanisms was covered in Chapter 4. Automated procedures for the generation of comprehensive mechanisms are regarded as being advantageous in comparison to manual assembly and are vital to the development of useful reduced mechanisms. EXGAS [19-21,90-95] is the most advanced comprehensive mechanism generator and provides increasingly accurate and structured hydrocarbon oxidation mechanisms. With the aim of contributing to the further development of this software package and for the congruity of the SAFEKINEX project, the majority of mechanisms studied and presented in this thesis were sourced from EXGAS.

A rarely used method for the evaluation of hydrocarbon oxidation mechanisms is the construction of the numerically predicted closed vessel $p-T_a$ or $\phi-T_a$ ignition diagram and comparison with the corresponding experimental version. This method of evaluation is important in the context of explosion hazard prediction because the ignition diagram shows the minimum conditions at which ignition will occur. A new code for the automatic construction of numerically predicted ignition diagrams was described in Chapter 4 and applied to mechanisms describing the oxidation of several fuels. Overall, the results showed that the qualitative characteristics of experimental ignition diagrams were well mimicked by the comprehensive mechanisms simulated with spatial uniformity. However, a number of quantitative discrepancies were apparent, for example; the minimum pressure at which two-stage ignition would occur in the simulation could be below the values observed in the experiments. The root cause of these discrepancies is open to debate, with both the exclusion of physical effects and heterogeneous reactions with the reactor wall being distinct possibilities. A further possibility lies in the uncertainty of rate and thermochemical parameters in the mechanism. Global uncertainty analysis can be used to elucidate the parameters whose

perturbations within their ranges of uncertainty have the greatest impact on output variables and therefore merit further study to narrow their uncertainty ranges. A quantitative assessment of the impact of uncertainties in parameter values has been undertaken and presented in Section 6.2 using a reduced propane mechanism, developed using the reduction methodology outlined in Chapter 5. The investigation revealed that output variables were highly sensitive to the magnitude of the pre-exponential term of a number of identified reactions. The thermochemistry of three species also exhibited a large influence on output variables, they were; $n\text{-O}_2\text{CH}_2\text{CH}_2\text{CH}_2\text{OOH}$, $n\text{-C}_3\text{H}_7\text{O}_2$ and $i\text{-C}_3\text{H}_7\text{O}_2$. Further work is necessary to more accurately quantify these influential parameters using experimental or *ab initio* modelling techniques. There is scope to further investigate the causes of the discrepancies between experimental and simulated ignition diagrams, with uncertainty analysis likely to feature prominently. Higher dimensional simulations of combustion processes would help to uncover what the impact of the exclusion of physics has on the comparison. Uncertainty analysis combining both kinetic and physical parameters would help to assess their relative importance. Experimental and modelling studies of the effects of heterogeneous reactions may also be helpful. In all these investigations, mechanism reduction will play a pivotal role.

A supplementary study in Chapter 4 investigated the trends between fuels and the prediction of minimum autoignition temperature (MIT), using a selection of EXGAS generated mechanisms. The dependence of MIT on composition was numerically determined for a range of fuels at 1 atm. The qualitative hierarchy of MIT for the range of compounds is well captured by the EXGAS mechanisms. However, the quantitative demarcation between fuels displayed by the mechanisms is not as pronounced as is observed experimentally. It appears that some of the large demarcations of experimentally determined MIT between fuels can be attributed to the structure of the $p\text{-}T_a$ ignition diagram. The reduced disparity between fuels as exhibited in the simulations may be attributed to uncertainty in parameters or the exclusion of physics from the zero-dimensional framework, with further studies required to clarify these issues.

In Chapter 5, details of automated techniques used for mechanism reduction based on local sensitivity analysis methods were given. The automation was achieved by incorporating sensitivity analysis algorithms into the SPRINT integration code and constructing UNIX shell scripts which manipulate data files and execute programs. Arduous tasks like the selection of time points for sensitivity analysis and the development of reduced mechanisms from the comprehensive CHEMKIN format mechanisms could all be performed without any user intervention. A number of reliable reduction techniques can then be applied to a comprehensive mechanism consecutively. An algorithm based on the iterative analysis of the Jacobian matrix is used to first remove species from the mechanism. Improved progress was noticed when incremental multi-stage reductions were performed when using this method. Subsequently, reactions could be removed using an overall sensitivity method, principal component analysis based on the local rate sensitivity matrix and/or a rate of production analysis. Of these first two reaction removal methods, modifications were made to the standard methods, in that, the effect of perturbations on rates of production of smaller groups of locally important species were analysed, instead of using the rates of production of all of the species of a (partially reduced) mechanism in the objective function of the sensitivity algorithm. Comparisons of the performance of equally sized reduced mechanisms produced using the modified and unmodified reaction removal strategies showed that the modifications led to a significant improvement in the quality of the resulting reduced mechanism for the same size of mechanism.

By the automation of the reduction procedure, the otherwise considerable and time consuming computational effort required is reduced to the user having only to make choices of the operating condition(s) of interest, appropriate threshold values and selection of the reduced mechanism based on comparisons of the temperature profiles and automatically constructed ignition diagrams from the full and reduced schemes. It may yet be possible to further automate and reduce the required user intervention by making modifications so that the user, given a comprehensive mechanism, only has to specify the conditions of interest and an error tolerance. The software program would then find the minimum skeleton

mechanism that satisfies this error tolerance, in effect, automating the stage where the user makes a judgement on the quality of the reduced mechanism based on the comparison of performance with the full mechanism. The iterative nature of this part of the procedure would need to be performed by the program.

From the comprehensive mechanisms that were evaluated in Chapter 4, the propane, butane and cyclohexane mechanisms were selected to undergo reduction using the automated procedures. Comparisons of the output from full and reduced mechanisms showed that in each case the numbers of species and reactions had been successfully reduced, in the case of cyclohexane for example, an 80 % reduction was achieved using skeletal reduction methods alone, producing a mechanism with a wide low temperature domain of applicability. The application to a range of mechanisms of different sizes demonstrated the versatility of the techniques. The extent of the reduction is shown below in Table 8.1 and will be discussed below in the context of the further reductions achieved via the application of the quasi steady state approximation (QSSA) and other reductions performed during the course of the SAFEKINEX project. The skeletal reductions of Chapter 5 were compared to similar strategies published in the available literature and were found to be in line with the current state of the art, and perhaps superior to methods where no species removal is performed at the first reduction stage. The reduction methods of Chapter 5 can achieve large reductions of species and reactions leading to substantial computational speed-ups. However, the number of residual species in the skeleton mechanisms is often still prohibitive to their application within CFD. Further reductions can be achieved via application of the QSSA to lump reactions and further reduce species, as has been demonstrated in Chapter 7 using one of the skeleton cyclohexane mechanisms. This will be discussed after a summing up of Chapter 6.

In addition to the uncertainty analysis of the propane mechanism already mentioned in this section, a number of other kinetic investigations were carried out and presented in Chapter 6, using the reduced mechanisms of propane, butane and cyclohexane obtained using the procedures of Chapter 5. Analysis of each of the reduced mechanisms revealed that there were similarities with regards to the

classes of species and reactions that were removed. Notably, all C_3+ alkanes and associated species, other than those of the primary fuel were removed in each case. A number of other species and reactions were consistently removed. With a few supplementary studies, it seems possible to use this information to make modifications at the EXGAS mechanism generation stage. For instance, a reduced C_0 - C_2 reaction base seems viable for the low temperature regime. The main kinetic pathways of the propane mechanisms were identified using element flux analysis. The qualitative features of a schematic diagram produced from these results agree well with other systems and studies proposed by other research groups. The majority of the species couplings highlighted by the element flux analysis had parameters which were correspondingly identified by the Morris uncertainty analysis as exerting a large influence on kinetic features such as time to ignition or the position of the ignition boundary.

A schematic for the low temperature isothermal oxidation of cyclohexane was also constructed via the application of element flux analysis. In this region of operating conditions, the cyclohexane mechanism displays a discrepancy with experimental observations in regards to the rate of oxygen consumption. Further analysis showed that this appears not to be limited to cyclohexane or the EXGAS source of comprehensive mechanisms. This problem is suitable for further investigation using the uncertainty analysis techniques similar to those applied to the reduced propane mechanism. Another kinetic study using the reduced n-butane mechanism tracked the heat release rate through the transition from cool flame to ignition during two-stage ignition. The principal routes to heat release in this region involve molecular intermediates rather than the primary fuel and the most important reactions leading to hydrogen peroxide have similar origins as those of the heat release rate, mainly through formaldehyde, formyl radicals and hydroperoxy radicals.

Further reduction is effectively achieved in Chapter 7 by coupling the application of the QSSA with reaction lumping. The QSSA species which may be eliminated are identified by automated procedures using a user prescribed threshold to the instantaneous error of the QSSA. Often the species are so highly

Fuel	Full mechanism	1 st Skeleton mechanism Post Jacobian analysis	2nd Skeleton mechanism Post rate sensitivity analysis	Final reduced scheme following QSSA	Runtime % of full scheme		
					Calculated run time	Estimate from $\propto N^2$	Estimate from $\propto n$
	Species (reaction)	Species (reactions)	Species (reactions)	Species (reactions)			
C ₃ H ₈	122 (1137)	42 (545)	42(166)		37% 15%	12% 12%	48% 15%
nC ₄ H ₁₀	128 (1148)	73 (715)	73 (300)	59 (270)	62.3% 22% 16.5%	33% 33% 21%	62% 26% 24%
cC ₆ H ₁₂	499 (3348)	104 (845)	100 (238) 60 (238) 47 (157)	24 (135)	15% 5% 2.1% 1.04% 0.9%	4.3% 4% 1.4% 0.9% 0.2%	25.2% 7.1% 7.1% 4.7% 4%
nC ₇ H ₁₆	358 (2411)	223 (1696)	218 (810)	81 (452)	19% 18% 5%	39% 37% 5.1%	70% 34% 19%

Table 8.1. Summary of the numbers of species and reactions contained in each of the reduced mechanisms and corresponding calculated and estimated runtimes. Runtimes are estimated from runtime being proportional to the squared number of species ($\propto N^2$) or from runtime being proportional to the number of reactions ($\propto n$). Reaction numbers correspond to equivalent number of irreversible reactions. Complete n-heptane reduction and n-butane QSSA reduction, performed by Dr. Kevin Hughes.

coupled that lumped reaction rate expressions take a complex algebraic form obtained from solutions using algebraic manipulation packages. In order to maintain the highest accuracy a customised reaction mechanism and integration code is required and complete CHEMKIN compatibility cannot be maintained as a consequence. However, there is scope for the restoring of CHEMKIN compatibility via the numerical fitting of lumped rate parameters. Having removed the QSSA species via reaction lumping further simplifications may be achieved by reapplying the sensitivity analysis reduction techniques of Chapter 5 to the altered mechanism and/or lumping redundant product species into one species.

Application of these techniques has been demonstrated with respect to the reproduction of the cyclohexane + air low temperature p-T_a ignition diagram. The preservation of accurate ignition delay times has also been achieved throughout this reduction. This reduction achievement can be found in Table 8.1 along with

other QSSA reductions for n-butane and n-heptane performed during the course of the project. The application of the QSSA/reaction lumping can often reduce the number of species by half thus making a significant computational time saving. These reductions are amenable to further automation because the manual development of customized mechanisms and integration codes are time consuming and prone to human error.

Having reduced a mechanism it is possible to make an estimate of the computational speed up by consideration of the numbers of residual species (N) and reactions (n). Computational runtime is expected to scale with N^2 or n . The removal of QSS species may also reduce the amount of stiffness that prevails during the integration of the mechanism. It is worthwhile to make comparisons of the theoretical estimates of speed-ups with those measured on integration for the reduced mechanisms produced during the course of this project. The calculated speed-ups will also clarify the potential of incorporating these reduced mechanisms within CFD since much of the computational overhead is devoted to the calculation of the chemical sub model during reactive flow calculations.

A summary of the calculated speed-ups as a percentage of the full mechanism run time for all of the reduced mechanisms obtained during this project is given in Table 8.1. In most cases, the observed speed-up compares well with the theoretical speed-up obtained from the scaling with N^2 or n . The most substantial reduction achieved was that of cyclohexane, with the smallest reduced scheme running at less than 1 % of the time required for solution of the full mechanism. This suggests that for some cases the combination of sensitivity analysis based reductions and application of the QSSA provides a sufficient degree of reduction for incorporation within a CFD simulation. For other cases, such as n-heptane, the degree of reduction is still large with the final reduced mechanism having a run time of 5 % that of the full mechanism. However, it may be that the large number of species remaining in the mechanism necessitates the use of alternative methods of incorporating the kinetics into CFD, such as the use of look-up tables. It is interesting to note that the potential for reduction does not appear to strictly correlate with the size of starting mechanism and a much higher degree of

reduction has been possible for cyclohexane in comparison to what has been achieved for the normal alkanes. This may be partly attributed to the restriction of conditions to the low T ignition boundary.

The coupling of chemical kinetics and fluid dynamics for reactive flow simulations using CFD tools is now a possibility. These methods are able to model the physical effects during fluid motion such as viscous flow, convective-diffusion effects, concentration and heat transfer. It is also possible to solve for both laminar and turbulent flow cases. However, even with the most powerful computer resources, only chemical sub models of low dimensionality can be solved within a realistic time frame using 3D CFD.

A number of methods for incorporating chemical kinetics into CFD have been proposed. A major obstacle for this aim is the kind of stiffness that arises between the physical and chemistry models. The time steps required for the chemical reactions are very short in comparison to those of the flow field. Because of this, the two terms are often computed separately using different methods in an operator splitting framework. In the repro-modelling [127,214] approach, a fitted polynomial model stored in a database is used for the chemical source term during the CFD calculation. In the ILDM approach a look-up table calculated prior to the CFD simulation is referred to. An alternative is to perform an *in situ* tabulation such as that developed by Pope [55]. Turbulent combustion is one of the most complex modelling scenarios and different approaches to those used for laminar flames are necessary. Direct numerical simulation (DNS) is an important tool for the study of turbulent combustion, and can often accommodate 10 – 20 chemical species [215,216]. Many studies have been conducted in 2D, but access to high performance computers has allowed the simulation of 3D spatially developing laboratory scale flames which incorporate detailed kinetics [217]. A more computationally viable method to simulate turbulent-reactive combustion is the transported probability density function (PDF) technique. The PDF approach may be used to simulate finite rate chemistry effects coupled to the solution of the PDF transport equation, which is most frequently obtained by a particle based Monte Carlo method [218]. A recent application of the PDF method, with some

additional simplifications, allowed the incorporation of a 44 species mechanism into 2D axisymmetric turbulent flow calculations [192]. A more recently developed and computationally reasonable method of modelling systems of complex chemistry with turbulence is known as the conditional moment closure (CMC) approach [219]. It is based on a conserved scalar approach which is used to eliminate the non-linear dependence of reaction rates on temperature in the chemical source term. A recent application to turbulent non-premixed methane flames was able to incorporate 53 species [220].

In consideration of the modelling achievements, the kinetic mechanisms derived in the present work are therefore capable of being implemented within CFD codes. Simulation of laminar flames or more computationally demanding turbulent-reactive flows are feasible, but will depend on the type of modelling approach used and whether a full 3D simulation is attempted or some simplifications are made to the geometry. The availability of computer resources is another factor which will affect the degree of complexity in the chemistry which is permissible, and exciting developments in this area will in future allow even more realistic system models with greater spatial resolution and numbers of chemical species. For example, comprehensive mechanisms for the oxidation of biofuels, will be huge due to their diversity and number of elements within them.

The versatility of the numerical methods and software presented in this work will allow the development of a range of reduced kinetic mechanisms, such as those for emerging new fuels, and which mirror well the behaviour of the comprehensive mechanisms from which they are derived. Without mechanism reduction work, the potential for incorporating large comprehensive mechanisms into reacting CFD simulations is practically impossible. The present work has resulted in much reduced hydrocarbon kinetic mechanisms, and their inclusion in CFD codes will improve the accuracy and overall usefulness of such computer tools which are relevant to the optimization and improved safety of industrial processes.

Bibliography

- [1] M.R. Chandraratna and J.F. Griffiths. Pressure and concentration dependences of the autoignition temperature for normal butane + air mixtures in a closed vessel. *Combustion and Flame*, 99 (1994) 626-634.

- [2] J.F. Griffiths and J.A. Barnard. *Flame and Combustion, Third Edition*. Blackie Academic and Professional, London, 1995.

- [3] H.J. Pasmann, SAFEKINEX proposal, Proposal No. EVG1-2001-00098-SAFEKINEX, 2003. <http://www.morechemistry.com/SAFEKINEX/>

- [4] J.F. Griffiths, K.J. Hughes and R. Porter. The role and rate of hydrogen peroxide decomposition during hydrocarbon two-stage autoignition. *Proceedings of the Combustion Institute*, 30 (2004) 1083-1091.

- [5] A.A. Pekalski, J.F. Zevenbergen, H.J. Pasman, S.M. Lemkowitz, A.E. Dahoe and B. Scarlett. The relation of cool flames and auto-ignition phenomena to process safety at elevated pressure and temperature. *Journal of Hazardous Materials*, 93 (2002) 93-105.

- [6] M.F. Pantony, N.F. Scilly and J.A. Barton. *International Symposium on Runaway Reactions 1989*, March 7-8, 1989, Cambridge, Massachusetts, 504-510.

- [7] T.A. Kletz. Causes of hydrocarbon oxidation unit fires. *Loss Prevention*, 12 (1979) 96-102.
- [8] T.A. Kletz. Fires and explosions of hydrocarbon oxidation plants. *Plant/Operations Progress*, 7 (1988) 226-230.
- [9] E.J. D'onofrio. Autoignition risks in hydrocarbon oxidation. *Loss Prevention*, 13 (1979) 89-95.
- [10] L.G. Britton. Lagging fires of ethylene oxide processes. *Plant/Operations Progress*, 10 (1991) 27-33.
- [11] H.J. Curran, P. Gaffuri, W.J. Pitz and C.K. Westbrook. A comprehensive modeling study of n-heptane oxidation. *Combustion and Flame*, 114 (1998) 149-177.
- [12] G.P. Smith, D.M. Golden, M. Frenklach, N.W. Moriarty, B. Eiteneer, M. Goldenberg, C.T. Bowman, R. Hanson, S. Song, W.C. Gardiner Jr., V. Lissianski and Z. Qin, 1995. http://www.me.berkeley.edu/gri_mech/
- [13] M.J. Pilling, T. Turányi, K.J. Hughes and A.R. Claque. *The Leeds methane oxidation mechanism*. 1997.
<http://www.chem.leeds.ac.uk/combustion/methane.htm>
- [14] L.B. Harding, S.J. Klippenstein and Y. Georgievskii. Reactions of oxygen atoms with hydrocarbon radicals: a priori kinetic predictions for the $\text{CH}_3 + \text{O}$, $\text{C}_2\text{H}_5 + \text{O}$, and $\text{C}_2\text{H}_3 + \text{O}$ reactions. *Proceedings of the Combustion Institute*, 30 (2005) 985-993.

- [15] A.S. Tomlin, T. Turányi and M.J. Pilling. Mathematical tools for the construction, investigation and reduction of combustion mechanisms. In M.J. Pilling, (ed.) *Autoignition and low temperature combustion of hydrocarbons*. Elsevier, Amsterdam, 1997 p. 293-437.
- [16] D.M. Matheu, W.H. Green, Jr., J.M. Grenda. Capturing pressure-dependence in automated mechanism generation: Reactions through cycloalkyl intermediates. *International Journal of Chemical Kinetics*, 35 (2003) 95-119.
- [17] D.M. Matheu, A.M. Dean, J.M. Grenda and W.H. Green, Jr.. Mechanism generation with integrated pressure dependence: A new model for methane pyrolysis. *Journal of Physical Chemistry Series A*, 107 (2003) 8552-8565.
- [18] W.H. Green, P.I. Barton, B. Bhattacharjee, D.M. Matheu, D.A. Schwer, J. Song, R. Sumathi, H.H. Carstensen A.M. Dean and J.M. Grenda. Computer Construction of Detailed Chemical Kinetic Models for Gas-Phase Reactors. *Industrial and Engineering Chemistry Research*, 40 (2001) 5362-5370.
- [19] F. Battin-Leclerc. <http://www.ensic.u-nancy.fr/DCPR/Anglais/GCR/software.htm>
- [20] F. Buda, R. Bounaceur, V. Warth, P.A. Glaude, R. Fournet and F. Battin-Leclerc. Progress toward a unified detailed kinetic model for the autoignition of alkanes from C₄ to C₁₀ between 600 and 1200 K. *Combustion and Flame*, 142 (2005) 170-186.

- [21] V. Warth, F. Battin-Leclerc, R. Fournet, P.A. Glaude, G.M. Côme and G. Scacchi. Computer based generation of reaction mechanisms for gas-phase oxidation. *Computers and Chemistry*, 24, (2000) 541-560.
- [22] R. Porter, M. Fairweather, J.F. Griffiths, K.J. Hughes and A.S. Tomlin. Automatic generation of reduced reaction mechanisms for hydrocarbon oxidation with application to autoignition boundary prediction for explosion hazards mitigation. *Proceedings of ESCAPE*, 16 (2006) 383-388.
- [23] J.F. Griffiths, D. Coppersthaite, C.H. Phillips, C.K. Westbrook and W.J. Pitz. Auto-ignition temperatures of binary mixtures of alkanes in a closed vessel: Comparisons between experimental measurements and numerical predictions. *Proceedings of the Combustion Institute*, 23 (1990) 1745-1752.
- [24] K.J. Hughes, J.F. Griffiths, M. Fairweather and A.S. Tomlin. Evaluation of models for the low temperature combustion of alkanes through interpretation of pressure-temperature ignition diagrams. *Physical Chemistry Chemical Physics*, 8 (2006) 3197-3210.
- [25] F. Battin-Leclerc, F. Buda, M. Fairweather, P.A. Glaude, J.F. Griffiths, K.J. Hughes, R. Porter and A.S. Tomlin. A numerical study of the kinetic origins of two-stage autoignition and the dependence of autoignition temperature on reactant pressure in lean alkane-air mixtures. *Proceedings of the European Combustion Meeting 2005*, April 3-6, 2005, Louvain-la-Neuve, Belgium, Paper # 25.

- [26] D.T.A. Townend, M.R. Mandlekar. The Influence of Pressure on the Spontaneous Ignition of Inflammable Gas-Air Mixtures. I. Butane-Air Mixtures. *Proceedings of the Royal Society of London*, A141 (1933) 484-493.
- [27] T. Turányi. Reduction of large reaction mechanisms. *New Journal of Chemistry*, 14 (1990) 795-803.
- [28] T. Turányi. KINAL - a program package for kinetic analysis of reaction mechanisms. *Computers and Chemistry*, 14 (1990) 253-254.
- [29] T. Turányi. <http://www.chem.leeds.ac.uk/Combustion/kinal.htm>
- [30] T. Turányi, Applications of sensitivity analysis to combustion chemistry. *Reliability Engineering and System Safety*, 57 (1997) 41-48.
- [31] T. Turányi. <http://www.chem.leeds.ac.uk/Combustion/kinalc.htm>
- [32] R.J. Kee, F.M. Rupley, E. Meeks and J.A. Miller. *CHEMKIN: A Software Package for the Analysis of Gas-Phase Chemical and Plasma Kinetics*. Reaction Design Inc., 2000.
- [33] C.K. Westbrook, Y. Mizobuchi, T.J. Poinso, P.J. Smith and J. Warnatz. Computational combustion. *Proceedings of the Combustion Institute*, 30 (2005) 125-175.
- [34] H. Rabitz, M. Kramer, and D. Dacol. Sensitivity analysis in chemical kinetics. *Annual Review of Physical Chemistry*, 34 (1983) 419-461.

- [35] A.S. Tomlin, M.J. Pilling, T. Turányi, J.H. Merkin, and J. Brindley. Mechanism reduction for the oscillatory oxidation of hydrogen: Sensitivity and quasi-steady-state analysis. *Combustion and Flame*, 91 (1992) 107–130.
- [36] L.E. Whitehouse, A.S. Tomlin, and M.J. Pilling. Systematic reduction of complex tropospheric chemical mechanisms, part 1: sensitivity time-scale analyses. *Atmospheric Chemistry and Physics*, 4 (2004) 2025–2056.
- [37] C.K. Law, C.J. Sung, H. Wang, T.F. Lu. Development of comprehensive detailed and reduced reaction mechanisms for combustion modeling. *AIAA Journal*, 41 (2003) 1629-1646.
- [38] C.K. Law. Comprehensive description of chemistry in combustion modeling. *Combustion Science and Technology*, 177 (2005) 845-870.
- [39] T.F. Lu and C.K. Law. A directed relation graph method for mechanism reduction. *Proceedings of the Combustion Institute*, 30 (2005) 1333-1341.
- [40] T.F. Lu and C.K. Law. Linear time reduction of large kinetic mechanisms with directed relation graph: n-Heptane and iso-octane. *Combustion and Flame*, 144 (2006) 24-36.
- [41] D.A. Schwer, P. Lu and W.H. Green. An adaptive chemistry approach to modeling complex kinetics in reacting flows. *Combustion and Flame*, 133 (2003) 451-465.
- [42] O.O. Oluwole, B. Bhattachargee, J.E. Tolsma, P I. Barton and W.H. Green. Rigorous valid ranges for optimally reduced kinetic models. *Combustion and Flame*, 146 (2006) 348–365.

- [43] B. Bhattacharjee, D.A. Schwer, P.I. Barton and W.H. Green. Optimally-reduced kinetic models: reaction elimination in large-scale kinetic mechanisms. *Combustion and Flame*, 135 (2003) 191–208.
- [44] I. Banerjee and M.G. Ierapetritou. Development of an adaptive chemistry model considering micromixing effects. *Chemical Engineering Science*, 58 (2003) 4537–4555.
- [45] I. Banerjee and M.G. Ierapetritou. An adaptive reduction scheme to model reactive flow. *Combustion and Flame*, 144 (2006) 619–633.
- [46] S.H. Lam and D.A. Goussis. Understanding complex chemical kinetics with computational singular perturbation. *Proceedings of the Combustion Institute*, 22 (1988) 931-941.
- [47] G.D. Byrne and A.C. Hindmarsh. Stiff ODE Solvers: A Review of Current and Coming Attractions. *Journal of Computational Physics*, 70 (1987) 1-62.
- [48] M. Berzins and R.M. Furzeland. *A User's Manual for SPRINT - A Versatile Software Package for Solving Systems of Algebraic, Ordinary and Partial Differential Equations: Part 1 - Algebraic and Ordinary Differential Equations*. Report TNER.85.058, Shell Research Ltd, Thornton Research Centre, Chester (1985).
- [49] U. Maas and S.B. Pope. Simplifying chemical kinetics: Intrinsic low-dimensional manifolds in composition space. *Combustion and Flame*, 88 (1992) 239-264.

- [50] T. Turányi. Application of repro-modelling for the reduction of combustion mechanisms. *Proceedings of the Combustion Institute*, 25 (1994) 949-955.
- [51] G. Li, A.S. Tomlin, H. Rabitz and J. Toth. A general analysis of approximate nonlinear lumping in chemical kinetics. I. Unconstrained lumping. *Journal of Chemical Physics*, 101 (1994) 1172-1187.
- [52] A.S. Tomlin, M.J. Pilling, J.H. Merkin, J. Brindley, N. Burgess and A. Gough. Reduced mechanisms for propane pyrolysis. *Industrial and Engineering Chemistry Research*, 34 (1995) 3749-3760.
- [53] T. Turányi. Parameterization of reaction mechanisms using orthonormal polynomials. *Computers and Chemistry*, 18 (1994) 45-54.
- [54] R. Lowe and A.S. Tomlin. The application of repro-modelling to a tropospheric chemical model. *Environmental Modelling and Software*, 15 (2000) 611-618.
- [55] S.B. Pope. Computationally efficient implementation of combustion chemistry using in situ adaptive tabulation. *Combustion Theory Modelling*, 1 (1997) 41-63.
- [56] S Arrhenius. On the reaction velocity of the inversion of cane sugar by acids. *Zeitschrift für Physikalische Chemie* 4, 1889. *Translated and published in* Margaret H. Back and Keith J. Laidler, (eds.), *Selected Readings in Chemical Kinetics*. Pergamon, Oxford, 1967.
- [57] J.F. Griffiths. Reduced kinetic models and their application to practical combustion systems. *Progress Energy and Combustion Science*, 21 (1995) 25-107.

- [58] M. Bodenstein. *Zeitschrift fur Physikalische Chemie*, 85 (1913) 329.
- [59] H. Lutkemeyer and M. Bodenstein. *Zeitschrift fur Physikalische Chemie*, 114 (1924) 208.
- [60] N.N. Semenov. *Chemical Kinetics and Chain Reactions*. Clarendon Press, Oxford 1935.
- [61] C.N. Hinshelwood. *The Kinetics of Chemical Change*. Clarendon Press, Oxford, 1940.
- [62] N.N. Semenov. Zur Theorie des Verbrennungsprozesses. *Zeitschrift fur Physikalische Chemie*, 48 (1928) 571-582.
- [63] T. Turányi, A.S. Tomlin, and M.J. Pilling. On the Error of the Quasi-Steady-State Approximation. *Journal of Physical Chemistry*, 97 (1993) 163-172.
- [64] N.N. Semenov. On the kinetics of complex reactions. *Journal of Physical Chemistry*, 7 (1939) 683-699.
- [65] N.N. Semenov. Advances of chemical kinetics in the Soviet Union. *Zhurnal Fizicheskoi Khimii*, 17 (1943) 187-198.
- [66] N.N. Semenov. Kinetics of complex homogenous reactions. 1. General theory of complex reactions. *Acta Physicochim, USSR*, 18 (1943) 433-472.
- [67] C.F. Curtiss and J.O. Hirschfelder. Integration of stiff equations. *Proceedings of the National Academy of Sciences, USA*, 38 (1952) 235-243.

- [68] R.H. Snow. A chemical kinetics computer program for homogeneous and free-radical systems of reactions. *Journal of Physical Chemistry*, 70 (1966) 2780-2786.
- [69] T.J. Keneshea, Report No. 67-0221, *Env. Res. Paper: US Air Force* Cambridge, Res. Lab. 1967.
- [70] C.W. Gear. *Numerical Initial Value Problems in Ordinary Differential Equations*. Prentice-Hall, Englewood Cliffs, New Jersey, 1971.
- [71] C.W. Gear. The automatic integration of stiff ordinary differential equations. In A.J.H. Morrell (ed.), *Information Processing*, North-Holland, Amsterdam. 1969, p. 187–193.
- [72] A.C. Hindmarsh. *GEAR: Ordinary Differential Equation System Solver*. Lawrence Livermore Laboratory report UCID-30001, Rev. 3, 1974.
- [73] A.C. Hindmarsh, G.D. Byrne. *EPISODE: An Effective Package for the Integration of Systems of Ordinary Differential Equations*. Lawrence Livermore Laboratory report UCID-30112, Rev. 1, 1977.
- [74] <http://www.nist.gov/srd/chemkin.htm>
- [75] D.L. Baulch, C.J. Cobos, R.A. Cox, P. Frank, G. Hayman, Th. Just, J.A. Kerr, T. Murrels, M.J. Pilling, J. Troe, R.W Walker and J. Warnatz. Summary table of evaluated kinetic data for combustion modeling: Supplement 1. *Combustion and Flame*, 98 (1994) 59-79.

- [76] R.R. Baker, R.R. Baldwin, and R.W. Walker. The addition of neopentane to slowly reacting mixtures of hydrogen and oxygen at 480°C I: Formation of primary products from neopentane. *Combustion and Flame*, 25, (1975) 285-300.
- [77] R.R. Baker, R.R. Baldwin, and R.W. Walker. Addition of neopentane to slowly reacting mixtures of H₂ + O₂ at 480°C. Part II. The addition of the primary products from neopentane, and the rate constants for H and OH attack on neopentane. *Combustion and Flame*, 27 (1976) 147-161.
- [78] R. R. Baldwin and R. W. Walker. The role of radical-radical reactions in hydrocarbon oxidation. *Combustion and Flame*, 21 (1973) 55-67.
- [79] R.R. Baldwin, D.E. Hopkins, A.C. Norris, and R.W. Walker. The addition of methane to slowly reacting hydrogen-oxygen mixtures: Reactions of methyl radicals. *Combustion and Flame*, 15 (1970) 33-46.
- [80] C. Morley. The formation and destruction of hydrogen cyanide from atmospheric and fuel nitrogen in rich atmospheric-pressure flames. *Combustion and Flame*, 27 (1976) 189-204.
- [81] V.D. Knyazev and I.R. Slagle. Kinetics of the reaction between propargyl radical and acetylene. *Journal of Physical Chemistry A*, 106 (2002) 5613-5617.
- [82] K.J. Hughes, P.D. Lightfoot and M.J. Pilling. Direct measurements of the peroxy-hydroperoxy radical isomerisation, a key step in hydrocarbon combustion. *Chemical Physics Letters*, 191 (1992) 581-586.

- [83] A.A. Shestov, K.V. Popov, I.R. Slagle and V.D. Knyazev. Kinetics of the reaction between vinyl radical and ethylene. *Chemical Physics Letters*, 408 (2005) 339–343.
- [84] S.W. Benson. *Thermochemical Kinetics, Second Edition*. Wiley, New York, 1976.
- [85] J.A. Miller, M.J. Pilling and J. Troe. Unravelling combustion mechanisms through a quantitative understanding of elementary reactions. *Proceedings of the Combustion Institute*, 30 (2005) 43–88.
- [86] R.J. Kee, F.M. Rupley and J.A. Miller. *Chemkin II: A Fortran Chemical Kinetics Package for the Analysis of a Gas-Phase Chemical Kinetics*, SAND89-8009B, Sandia Laboratories, 1993.
- [87] C. Muller, V. Michel, G. Scacchi and G.M. Côme. THERGAS: a computer program for the evaluation of thermochemical data of molecules and free radicals in the gas phase. *Journal De Chimie Physique Et De Physico-chimie Biologique*, 92 (1995) 1154-1178.
- [88] S.J. Chinnick, D.L. Baulch, and P.B. Ayscough. An expert system for hydrocarbon pyrolysis reactions. *Chemometrics and Intelligent Laboratory Systems*, 5 (1988) 39-52.
- [89] G.M. Côme, P. Azay, D. Alran and M. Niclause. *AIChE 72nd Annual Meeting*, 21a (1979).
- [90] V. Warth, N. Stef, P.A. Glaude, F. Battin-Leclerc, G. Scacchi and G.M. Côme. Computer-aided derivation of gas-phase oxidation mechanisms: Application to the modelling of the oxidation of n-butane. *Combustion and Flame*, 114 (1998) 81–102.

- [91] G.M. Côme, V. Warth, P.A. Glaude, F. Battin-Leclerc and G. Scacchi. Computer aided design of gas-phase oxidation mechanism: Application to the modelling of normal-heptane and iso-octane oxidation. *Proceedings of the Combustion Institute*, 26 (1997) 755–762.
- [92] P.A. Glaude, V. Warth, R. Fournet, F. Battin-Leclerc, G.M. Côme, G. Scacchi. Modeling of n-heptane and isooctane gas-phase oxidation at low temperature by using computer-aided designed mechanism. *Bulletin des Societes Chimiques Belges*, 6 (1997) 343–348.
- [93] P.A. Glaude, V. Warth, R. Fournet, F. Battin-Leclerc, G. Scacchi, G.M. Côme. Modeling of the oxidation of n-octane and n-decane using an automatic generation of mechanisms. *International Journal of Chemical kinetics*, 30 (1998) 949–959.
- [94] F. Battin-Leclerc, R. Fournet, P.A. Glaude, B. Judenherc, V. Warth, G.M. Côme and G. Scacchi. Modeling of the gas-phase oxidation of n-decane from 550 to 1600 K. *Proceedings of the Combustion Institute*, 28 (2001) 1597–1605.
- [95] P.A. Glaude, V. Warth, R. Fournet, F. Battin-Leclerc, G.M. Côme, G. Scacchi, P. Dagaut and M. Cathonnet. Modeling the oxidation of mixtures of primary reference automobile fuels. *Energy and Fuels*, 16 (2002) 1186–1195.
- [96] V. Bloch-Michel. *Logiciel d'estimation de paramètres cinétiques de processus élémentaires en phase gazeuse*. Thèse de l'INPL, Nancy 1995.

- [97] P. Barbé, F. Battin-Leclerc and G.M. Côme. Experimental and modelling study of methane and ethane oxidation between 773 and 1573 K. *Journal De Chimie Physique Et De Physico-chimie Biologique*, 92 (1995) 1666-1692.
- [98] F. Battin-Leclerc, R. Bounaceur, G.M. Côme, R. Fournet, P.A. Glaude, G. Scacchi and V. Warth. *A software for the automatic generation of mechanisms for the oxidation of alkanes*. November 2004, <http://www.ensic.u-nancy.fr/DCPR/Anglais/GCR/software.htm>
- [99] J.F. Griffiths and C. Mohamed. Experimental and numerical studies of oxidation chemistry and spontaneous ignition phenomena. In M.J. Pilling, (ed.) *Autoignition and low temperature combustion of hydrocarbons*. Elsevier, Amsterdam, 1997 p. 545-653.
- [100] R. Fournet, J.C. Bauge and F. Battin-Leclerc. Experimental and modeling of oxidation of acetylene, propyne, allene and 1,3-butadiene. *International Journal of Chemical kinetics*, 31 (1999) 361–379.
- [101] N. Belmekki, P.A. Glaude, I.Da Costa, R. Fournet and F. Battin-Leclerc. Experimental and Modeling Study of the Oxidation of 1-Butyne and 2-Butyne. *International Journal of Chemical kinetics*, 34 (2002) 172–183.
- [102] M.S. Okino and M.L. Mavrouniotis. Simplification of mathematical models of chemical reaction systems. *Chemical Reviews*, 98 (1998) 391-402.
- [103] T. Turányi. Sensitivity analysis complex kinetic systems. Tools and applications. *Journal of Mathematical Chemistry*, 5 (1990) 203-248.

- [104] T. Turányi and H. Rabitz. Local Methods. In A. Saltelli, K. Chan, E.M. Scott (eds.) *Sensitivity Analysis*. Wiley, Chichester, UK, 2001 p. 78-99.
- [105] A. Saltelli, M. Ratto, S. Tarantola and F. Campolongo. Sensitivity analysis practices: Strategies for model-based inference. *Reliability Engineering and System Safety*, 91 (2006) 1109–1125.
- [106] S. Vajda, P. Valko, and T. Turányi. Principal component analysis of kinetic models. *International Journal of Chemical Kinetics*, 17 (1985) 55-81.
- [107] H. Huang, M. Fairweather, J.F. Griffiths, A.S. Tomlin and R.B. Brad. A systematic lumping approach for the reduction of comprehensive kinetic models. *Proceedings of the Combustion Institute*, 30 (2005) 1309–1316.
- [108] A. Massias, D. Diamantis, E. Mastorakos and D.A. Goussis. An algorithm for the construction of global reduced mechanisms with CSP data. *Combustion and Flame*, 117 (1999) 685–708.
- [109] T.F. Lu, Y. Ju and C.K. Law. Complex CSP for chemistry reduction and analysis. *Combustion and Flame*, 126 (2001) 1445–1455.
- [110] H. Wang and M. Frenklach. Detailed Reduction of Reaction Mechanisms for Flame Modeling. *Combustion and Flame*, 87 (1991) 365-370.
- [111] B. Bhattacharjee. *Kinetic model reduction using integer and semi-infinite programming*. PhD Thesis, Massachusetts Institute of Technology, Department of Chemical Engineering, 2003.

- [112] L. Elliott, D.B. Ingham, A.G. Kyne, N.S. Mera, M. Pourkashanian and C. W. Wilson. Reaction mechanism reduction and optimization using genetic algorithms. *Industrial and Engineering Chemistry Research*, 44 (2005) 658-667.
- [113] L. Elliott, D.B. Ingham, A.G. Kyne, N.S. Mera, M. Pourkashanian and S. Whittaker. Reaction mechanism reduction and optimisation for modelling aviation fuel oxidation using standard and hybrid genetic algorithms. *Computers and Chemical Engineering*, 30 (2006) 889–900.
- [114] L. Petzold and W. Zhu. Model reduction for chemical kinetics: An optimization approach. *AIChE Journal*, 45 (1999) 869-886.
- [115] W. Wang and B. Rogg. Premixed ethylene/air and ethane/air flames: reduced mechanisms based on inner iteration. In N. Peters and B. Rogg, (eds.) *Reduced Kinetic Mechanisms for Applications in Combustion Systems*. Springer, Berlin, 1992 p. 76-82.
- [116] T. Løvås, F. Mauss, C. Hasse and N. Peters. Development of adaptive kinetics for application in combustion systems. *Proceedings of the Combustion Institute*, 29 (2002) 1403-1410.
- [117] T. Løvås, E. Blurock and F. Mauss. Automatic reduced mechanisms based on domain splitting methods. *Proceedings of the European Combustion Meeting 2005*, April 3-6, 2005, Louvain-la-Neuve, Belgium, Paper # 10.
- [118] G. Skevis, A. Chrissanthopoulos, D.A. Goussis, E. Mastorakos, M.A.F. Derksen and J.B.W. Kok. Numerical investigation of methane combustion under mixed air-steam turbine conditions – FLAMESEEK. *Applied Thermal Engineering*, 24 (2004) 1607–1618.

- [119] T. Løvås, E. Mastorakos and D.A. Goussis. Reduction of the RACM scheme Using Computational Singular Perturbation Analysis. *Journal of Geophysical Research-Atmospheres*, vol. 111, D13302, doi: 10.1029/2005JD006743.
- [120] M.K. Neophytou, D.A. Goussis, M.van Loon and E. Mastorakos. Reduced chemical mechanisms for atmospheric pollution using Computational Singular Perturbation analysis. *Atmospheric Environment*, 38 (2004) 3661–3673.
- [121] T. Lu and C.K. Law. On the applicability of directed relation graphs to the reduction of reaction mechanisms. *Combustion and Flame*, 146 (2006) 472–483.
- [122] T. Lu and C.K. Law. Systematic approach to obtain analytic solutions of quasi steady state species in reduced mechanisms. *Journal of Physical Chemistry A*, 110 (2006)13202-13208.
- [123] J.A. Blasco, N. Fueyo, C. Dopazo and C. Ballester. Modelling the temporal evolution of a reduced combustion chemical system with an artificial neural network. *Combustion and Flame*, 113 (1998) 38-52.
- [124] S.R. Tonse, N.W. Moriarty, N.J. Brown and M. Frenklach. PRISM: Piecewise Reusable Implementation of Solution Mapping. An economical strategy for chemical kinetics. *Israel Journal of Chemistry*, 39 (1999) 97-106.
- [125] Z.Ren and S.B. Pope. *Proceedings of the Combustion Institute*, 30 (2005) 1293-1300.

- [126] A.S. Tomlin, L. Whitehouse, R. Lowe and M.J. Pilling. Low-dimensional manifolds in tropospheric chemical systems. *Faraday Discussions*, 120 (2001) 125-146.
- [127] R.B. Brad, A.S. Tomlin, M. Fairweather and J.F. Griffiths. The application of chemical reduction methods to a combustion system exhibiting complex dynamics. *Proceedings of the Combustion Institute*, 31 (2007) 455-463.
- [128] G. Li, H. Rabitz and J. Tóth. A general analysis of exact nonlinear lumping in chemical kinetics. *Chemical Engineering Science*, 49 (1994) 343-361.
- [129] G. Li and H. Rabitz. Combined symbolic and numerical approach to constrained nonlinear lumping - with application to an H₂/O₂ oxidation model. *Chemical Engineering Science*, 51 (1996) 4801-4816.
- [130] B. Sportisse and R. Djouad. Reduction of chemical kinetics in air pollution modeling. *Journal of Computational Physics*, 164 (2000) 354-376.
- [131] T. Turányi, <http://www.chem.leeds.ac.uk/Combustion/mechmod.htm>
- [132] A Burcat. Thermochemical data for combustion calculations. In W.C. Gardiner (ed.) *Combustion Chemistry*. Springer-Verlag, New York, 1984 p. 455-504.
- [133] B.J. McBride, S. Gordon and M.A. Reno. *Coefficients for calculating thermodynamic and transport properties of individual species*. Technical Report TM-4513, NASA, 1993.

- [134] S. Gordon and B.J. McBride. *Computer program for calculation of complex chemical equilibrium composition, rocket performance, incident and reflected shocks and chapman-jouguet detonations*. Technical Report SP-273, NASA, 1971.
- [135] R.G. Gilbert, K. Luther and J. Troe. Theory of thermal unimolecular reactions in the fall-off range. II. Weak collision rate constants. *Berichte Der Bunsen-Gesellschaft-Physical Chemistry Chemical Physics*, 87 (1983) 169-177.
- [136] F.A. Lindemann. The radiation theory of chemical action. *Transactions of the Faraday Society*, 17 (1922) 598-599.
- [137] R.B. Brad. *Reduced Kinetic Mechanisms for Chemical and Process Engineering Applications*. Phd Thesis, University of Leeds, The School of Process Environment and Materials Engineering, 2005.
- [138] J.M. Simmie. Detailed chemical kinetic models for the combustion of hydrocarbon fuels. *Progress in Energy and Combustion Science*, 29 (2003) 599-634.
- [139] T. Kovács, I. G. Zély, A. Kramarics and T. Turányi. Kinetic analysis of mechanisms of complex pyrolytic reactions. *Journal of Analytical and Applied Pyrolysis*, 79 (2007) 252–258.
- [140] <http://www.scs.leeds.ac.uk/cpde/SPRINT1.html>
- [141] M. Berzins. A C1 interpolant for codes based on backward differentiation formulae. *Applied Numerical Mathematics*, 2 (1986) 109-118.

- [142] M. Berzins and R.M. Furzeland. An adaptive theta method for the solution of stiff and non-stiff differential equations. *Applied Numerical Mathematics*, 9 (1992) 1-19.
- [143] A.J. Preston and M. Berzins. On algorithms for the location of discontinuities for dynamic simulation problems. *Computers in chemical engineering*, 15 (1991) 701-713.
- [144] R.T. Pollard. Gas-Phase Combustion. In C.H. Bamford and C.F.H. Tipper (eds.) *Comprehensive Chemical Kinetics, Volume 17*. Elsevier, Amsterdam, 1977 p. 249-278.
- [145] M. Fairweather, J.F. Griffiths, K.J. Hughes, R.Porter and A.S. Tomlin. *SAFEKINEX Public Deliverable 37*. <http://www.safekinex.org>
- [146] <http://www.woodrow.org/teachers/ci/1992/LeChatelier.html>
- [147] H.B. Dixon, J. Harwood and W.F. Higgins. On the ignition-point of gases. *Transactions of the Faraday Society*, 22 (1926) 267-272.
- [148] C.H. Gibson and C.N. Hinshelwood. The influence of nitrogen peroxide on the union of hydrogen and oxygen. - A problem of trace catalysis. *Transactions of the Faraday Society*, 24 (1928) 559-562.
- [149] R.N. Pease. *Equilibrium and kinetics of gas Reactions*. Princeton University Press, Princeton, 1942.
- [150] A. Sangulin. *Zeitschrift fur Physikalische Chemie B*, 1 (1928) 273-280.
- [151] M. Pettre, P. Dumanois, and P. Laffite. *Compte Rendu*, 191 (1930) 329-338.

- [152] D.T.A. Townend and M.R. Mandlekar. The influence of pressure on the spontaneous ignition of inflammable gas-air mixtures. I. – Butane-air mixtures. *Proceedings of the Royal Society of London, Series A*, 141 (1933) 484-493.
- [153] D.T.A. Townend, L.L. Cohen and W.F. Mandlekar. The influence of pressure on the spontaneous ignition of inflammable gas-air mixtures. III. – Hexane- and isobutene-air mixtures. *Proceedings of the Royal Society of London, Series A*, 146 (1934) 113-129.
- [154] D.M. Newitt and L.S. Thorne. The Oxidation of Propane. Part III. The Kinetics of the Oxidation. *Journal of the Chemical Society*, 350 (1937) 1669-1676.
- [155] F. Battin-Leclerc, R. Bounaceur, F. Buda, V. Conraud, R. Fournet, P.A. Glaude, S. Touchard, M. Fairweather, J.F. Griffiths, K.J. Hughes, R. Porter and A.S. Tomlin. *SAFEKINEX Public Deliverable 35*. <http://www.safekinex.org>
- [156] J.F. Griffiths and S.K. Scott. Thermokinetic interactions: Fundamentals of spontaneous ignitions and cool flames. *Progress in Energy and Combustion Science*, 13 (1997) 161-197.
- [157] P.G. Lignola and E. Reverchon. Cool flames. *Progress in Energy and Combustion Science*, 13 (1987) 75-96.
- [158] J.F. Griffiths. Thermokinetic oscillations in homogeneous gas-phase oxidations. In R.J. Field and M. Burger, (eds.) *Oscillations and Travelling Waves in Chemical Systems*, pages 529--564. John Wiley & Sons, New York, 1985 p. 529-564.

- [159] J.F. Griffiths. The fundamentals of spontaneous ignition of gaseous hydrocarbons and related organic compounds. *Advances in Chemical Physics*, 64 (1986) 203-304.
- [160] P. Gray, J.F. Griffiths, S.M. Hasko and P.G. Lignola. Oscillatory ignitions and cool flames accompanying the non-isothermal oxidation of acetaldehyde in a well stirred, flow reactor. *Proceedings of the Royal Society of London, series A*, 374 (1981) 313-339.
- [161] P. Gray, J.F. Griffiths, S.M. Hasko and P.G. Lignola. Novel, multiple-stage ignitions in the spontaneous combustion of acetaldehyde *Combustion and Flame*, 43 (1981) 175-186.
- [162] C. Gibson, P. Gray, J.F. Griffiths and S.M. Hasko. *Twentieth Symposium (International) on Combustion*. The Combustion Institute, Pittsburgh (1984), p. 101-109.
- [163] A.J. Harrison and L.R. Cairnie. The development and experimental validation of a mathematical model for predicting hot-surface auto-ignition hazards using complex chemistry. *Combustion and Flame*, 71 (1988) 1-21.
- [164] J.F. Griffiths and A.F. Sykes. Numerical studies of a thermokinetic model for oscillatory cool flame and complex ignition phenomena in ethanal oxidation under well-stirred flowing conditions. *Proceedings of the Royal Society of London, series A*, 422 (1989) 289-310.
- [165] J. Cavanagh, R.A. Cox and G. Olson. Computer modeling of cool flames and ignition of acetaldehyde. *Combustion and Flame*, 82 (1990) 15-39.

- [166] T.J. Snee and J.F. Griffiths. Criteria for spontaneous ignition in exothermic, autocatalytic reactions: Chain branching and self-heating in the oxidation of cyclohexane in closed vessels. *Combustion and Flame*, 75 (1989) 381-395.
- [167] M. Cherneskey and J. Bardwell. Surface effects in butane oxidation. *Canadian Journal of Chemistry*, 38 (1960) 482-492.
- [168] F. Battin-Leclerc, F. Buda, M. Fairweather, P.A. Glaude, J.F. Griffiths, K.J. Hughes, R. Porter and A.S. Tomlin. The effect of formal mechanism reduction on simulated propane autoignition and a quantitative assessment of the impact of uncertainties in parameter values. *Proceedings of the European Combustion Meeting 2005*, April 3-6, 2005, Louvain-la-Neuve, Belgium, Paper # 16.
- [169] J. F. Griffiths, B.F. Gray and P.Gray. Multistage ignition in hydrocarbon combustion: Temperature effects and theories of nonisothermal combustion. *Proceedings of the Combustion Institute*, 13 (1971) 239-248.
- [170] C.K. Westbrook, http://www-cms.llns.gov/combustion/combustion_home.html
- [171] F.P. Lees. *Loss Prevention in the Process Industries (Vols 1 and 2)*. Butterworths, London, UK (1980).
- [172] J.F. Griffiths, K.J. Hughes, M. Schreiber and C. Poppe. A unified approach to the reduced kinetic modeling of alkane combustion. *Combustion and Flame*, 99 (1994) 533-540.

- [173] C.F. Cullis, A. Fish, M. Saed and D.L. Trimm. Alkylperoxy radical isomerization and cool flames. *Proceedings of the Royal Society of London, series A*, 289 (1996) 402-412.
- [174] J.F. Griffiths. Cool flames, a hot prospect? *Proceedings of the European Combustion Meeting 2005*, April 3-6, 2005, Louvain-la-Neuve, Belgium, Paper # 259.
- [175] D. Kolaitis and M. Founti. Comparative assessment of thermokinetic mechanisms for the cool flame region of n-heptane at low Pressures. *Proceedings of the European Combustion Meeting 2005*, April 3-6, 2005, Louvain-la-Neuve, Belgium, Paper # 249.
- [176] L. Hartmann, K. Lucka and H. Koehne. Mixture preparation by cool flames for diesel-reforming technologies. *Journal of Power Sources*, 118 (2003) 286-297.
- [177] A. Naidja, C.R. Krishna, T. Butcher and D. Mahajan. Cool flame partial oxidation and its role in combustion and reforming of fuels for fuel cell systems. *Progress in Energy and Combustion Science*, 29 (2003) 155-191.
- [178] H. Pedersen-Mjaanes, L. Chan, and E. Mastorakos. Hydrogen production from rich combustion in porous media. *International Journal of Hydrogen Energy*, 30 (2005) 579-592.
- [179] A.R. Burgess and R.G.W. Laughlin. The cool flame oxidation of n-heptane. Part I. The kinetic features of the reaction. *Combustion and Flame*, 19 (1972) 315-329.

- [180] N. Peters, G. Paczko, R. Seiser and K. Seshadri. Temperature cross-over and non-thermal runaway at two-stage ignition of n-heptane. *Combustion and Flame*, 128 (2002) 38-59.
- [181] F. Buda, B. Heyberger, R. Fournet, P.A. Glaude, V. Warth and F. Battin-Leclerc. Modeling of the gas-phase oxidation of cyclohexane. *Energy and Fuels*, 20 (2006) 1450-1459.
- [182] J.L. Jackson. Spontaneous ignition temperatures; commercial fluids and pure hydrocarbons. *Industrial and Engineering Chemistry*, 43 (1954) 2869-2870.
- [183] G.S. Scott, G.W. Jones and F.E. Scott. Determination of ignition temperatures of combustible liquids and gases. *Analytical Chemistry*, 20 (1948) 238-241.
- [184] B.H. Bonner and C.F.H. Tipper. The cool flame combustion of hydrocarbons I-Cyclohexane. *Combustion and Flame*, 19 (1965) 317-327.
- [185] J.F. Griffiths. Personal communication.
- [186] G.H.N. Chamberlain and D.T.A Townend. Processes in the vapour phase oxidation of ethers. III. *Proceedings of the Combustion Institute*, 3 (1949) 375-390.
- [187] M. Fairweather, J.F. Griffiths, K.J. Hughes, R.Porter and A.S. Tomlin. *SAFEKINEX Public Deliverable 38*. <http://www.safekinex.org>
- [188] K.J. Hughes. Personal communication.

- [189] T. Turányi, T. Bérces and S. Vajda. Reaction rate analysis of complex kinetics systems. *International Journal of Chemical Kinetics*, 21 (1989) 83-99.
- [190] I.G. Zsély and T. Turányi. The influence of thermal coupling and diffusion on the importance of reactions: The case study of hydrogen-air combustion. *Physical Chemistry and Chemical Physics*, 5 (2003) 3622-3631.
- [191] A.C. Heard, M. J. Pilling and A.S. Tomlin. Mechanism reduction techniques applied to tropospheric chemistry. *Atmospheric Environment*, 32 (1998) 1059-1073.
- [192] K. Gkagkas and R.P. Lindstedt. Transported PDF modelling with detailed chemistry of pre- and auto-ignition in CH₄/air mixtures. *Proceedings of the Combustion Institute*, 31 (2007) 1559–1566.
- [193] C.J. Montgomery, M.A. Cremer, J.-Y.Chen, C.K. Westbrook and L.Q. Maurice. Reduced chemical kinetic mechanisms for hydrocarbon fuels. *Journal of Propulsion and Power*, 18 (2002) 192-198. www.reaction-eng.com/downloads/redchemhydrocarb.pdf
- [194] A. Saltelli, K. Chan and E.M. Scott. *Sensitivity analysis*. Wiley, Chichester, UK, 2001.
- [195] M. Frenklach. Transforming data into knowledge - Process informatics for combustion chemistry. *Proceedings of the Combustion Institute*, 31 (2007) 125–140.
- [196] M.D. Morris. Factorial sampling plans for preliminary computational experiments. *Technometrics*, 33 (1991) 161-174.

- [197] H.Y. Afeefy, J.F. Liebman, and S.E. Stein. "Neutral Thermochemical Data" in *NIST Chemistry WebBook, NIST Standard Reference Database Number 69*. P.J. Linstrom and W.G. Mallard (eds), March 2003, National Institute of Standards and Technology, Gaithersburg MD, 20899 (<http://webbook.nist.gov>).
- [198] S. Klippenstein. Personal communication.
- [199] J. Revel, J.C. Boettner, M. Cathonnet and J.S. Bachman. Derivation of a global chemical kinetic mechanism for methane ignition and combustion. *Journal de Chimie Physique et de Physico-Chimie Biologique*, 91 (1994) 365-382.
- [200] I.P. Androulakis. New approaches for representing, analyzing and visualizing complex kinetic transformations. *Computers and Chemical Engineering*, 31 (2006) 41–50.
- [201] T. Turányi. <http://garfield.chem.elte.hu/Combustion/fluxviewer.htm>
- [202] H.J. Curran, T.M. Jayaweera, W.J. Pitz and C.K. Westbrook. A detailed modeling study of propane oxidation. *Western States Section of the Combustion Institute 2004 Spring Meeting*, 29 – 30 March 2004, Davis, CA, United States, UCRL–CONF- 203063.
www.llnl.gov/tid/lof/documents/pdf/306130.pdf
- [203] D.N. Koert, W.J. Pitz, J.W. Bozzelli, N.P. Cernansky. Chemical kinetic modeling of high pressure propane oxidation and comparison to experimental results. *Proceedings of the Combustion Institute*, 26 (1996) 633-640.

- [204] W.J. Pitz, C.K. Westbrook and W.R. Leppard. The autoignition chemistry of paraffinic fuels and pro-knock and anti-knock additives: A detailed chemical kinetic study. *SAE Transactions*, SAE Paper No. 91-2315, 1991.
- [205] A. Konnov. <http://homepages.vub.ac.be/~akonnov/>
- [206] C.K. Westbrook. Chemical kinetics of hydrocarbon ignition in practical combustion systems. *Proceedings of the Combustion Institute*, 28 (2000) 1563-1577.
- [207] M.P. Halstead, A. Prothero and C.P. Quinn. *Combustion and Flame*, 20 (1973) 211-221.
- [208] S.W. Benson. The kinetics and thermochemistry of chemical oxidation with application to combustion and flames. *Progress in Energy and Combustion Science*, 7 (1981) 125-134.
- [209] W. Klonowski. Simplifying principles for chemical and enzyme reaction kinetics. *Biophysical Chemistry*, 18 (1983) 73-87.
- [210] F. Battin-Leclerc, P.A. Glaude, V. Warth, R. Fournet, G. Scacchi, and G.M. Côme. Computer tools for modelling the chemical phenomena related to combustion. *Chemical Engineering Science*, 55 (2000) 2883-2893.
- [211] <http://www.maplesoft.com>
- [212] M. Fairweather, personal communication.

- [213] T. Løvås, P. Amnéus, F. Mauss and E. Mastorakos. Comparison of automatic reduction procedures for ignition chemistry. *Proceedings of the Combustion Institute*, 29 (2002) 1387-1397.
- [214] A. Büki, T. Perger, T. Turányi and U. Maas. Repro-modelling based generation of intrinsic low-dimensional manifolds. *Journal of Mathematical Chemistry*, 31 (2002) 345-362.
- [215] E.R. Hawkes and J.H. Chen. Direct numerical simulation of hydrogen-enriched lean premixed methane–air flames. *Combustion and Flame*, 138 (2004) 242–258.
- [216] E.R. Hawkes and J.H. Chen. Comparison of direct numerical simulation of lean premixed methane–air flames with strained laminar flame calculations. *Combustion and Flame*, 144 (2006) 112–125.
- [217] R. Sankaran, E.R. Hawkes, J.H. Chen, T. Lu and C.K. Law. Structure of a spatially developing turbulent lean methane–air Bunsen flame. *Proceedings of the Combustion Institute*, 31 (2007) 1291–1298.
- [218] A.T. Norris and S.B. Pope. Modeling of extinction in turbulent Diffusion flames by the velocity-dissipation-composition PDF method. *Combustion and Flame*, 100 (1995) 211-220.
- [219] A.Y. Klimenko and R.W. Bilger. Conditional moment closure for turbulent combustion. *Progress in Energy and Combustion Science*, 25 (1999) 595-687.
- [220] M. Fairweather and R.M. Woolley. First-order conditional moment closure modeling of turbulent, nonpremixed methane flames. *Combustion and Flame*, 138 (2004) 3–19.

Appendix A

A.1 Classes of reactions removed from the cyclohexane mechanism

Molecular elimination reactions

Retro-ene reaction

Unimolecular initiations

Alkane reactions

Addition of oxygen on cyclo-ether radicals

Isomerization of peroxy radicals

Addition of oxygen on cyclo-peroxy radicals

Formation of cyclo-ether ketohydroperoxides

Decomposition of cyclo-ether ketohydroperoxides

Alkene reactions

Addition of OH on alkenes

Addition of O on alkenes

Addition of OOH on alkene

Alkene to dienes

Metathesis with (YH) (alkenes)

Addition of .Y on (YH) (alkenes)

Alcohol reactions

Ketoradicals addition to O₂

Peracide radical decomposition

Diels alder

.Y termination (Alkene)

unimolecular initiations of C₆H₁₀Z#6

Beta scissions (cyclohexene submechanism only)

Cyclization of molecule C₆H₈Z3-135

The C₀ – C₂ lumped reactions of:

H₂, B₄CH, B₆CH, B₅CH₂, CH₄, C₂H₂T, R₉C₂HT, R₁₀C₂H₃V, C₂H₄Z, C₂H₆, R₆CH₂OH, R₁₂CHCOVD, R₁₄CH₃CO, C₂H₄O#, R₁₅C₂H₅O, C₂H₅OH. CO₂, R₁₇C₂H₅OO, R₁₆C₂H₄OOH, R₁₈CH₃COOO, CH₃COOOH

Reactions producing C2+ radicals and C2+ molecules

Reactions of C2H2T, C2H3, C2H4, C2H5, HCO, CH3O, CH2OH, CH3CO

Benzene formation reactions of;

C3H2, C3H3, C3H4T, C3H4T, C3H4Z2, cC3H4 (cyclopropene), sC3H5 (2-methyl vinyl), tC3H7 (1-methyl vinyl), C3H6Y (propene), cC3H6, C3H7.

Non oxygen C4 reactions

C2H4, nC4H3, iC4H3, C4H4, tC4H4, iC4H5, C4H5-1s, C4H5-1p, C4H5-2

Reactions deducted from those of C3H3

Reactions of C4H6(12) (1,2 butadiene), c-C4H6 (methyl cyclopropane), C4H6-1 (1 Butyne), C4H6-2 (2-butyne), iC4H8Y

A.2 Classes of reactions removed from the n-butane mechanism

Unimolecular initiations removed.

Alkane reactions.

Addition of of .Y on YH (Alkenes)

Alcohol reactions

Peracide radical decompositions

Ketone reactions

Dielz Alder

The lumped base C0-C2 reactions of:

Reactions of the matrix O(0)C(y)H(z)

H2, B4CH, B6CH, B5CH2, CH4, C2H2T, R9C2HT, R10C2H3V, C2H4Z

Reactions of the matrix O(x)C(y)H(z)

H2O, R6CH2OH, R12CHCOVD, R14CH3CO, CO2, R16CH3COOOH

Reactions of:

C2H2T, C2H3, C2H4, CH3O, CH2OH, CH3CO

Reactions added to hold count of propenal

Appendix B

Publications and Conference Presentations

Papers published in peer reviewed journals

J.F. Griffiths, K.J. Hughes and R. Porter. The role and rate of hydrogen peroxide decomposition during hydrocarbon two-stage ignition. *Proceedings of the Combustion Institute*, 30 (2005) 1083 – 1091.

F. Buda, P.A. Glaude, F. Battin-Leclerc, R. Porter, K.J. Hughes and J.F. Griffiths. Use of detailed kinetic mechanisms for the prediction of autoignitions. *Journal of Loss Prevention in the Process Industries*, 19 (2006) 227-232.

Poster presentations (published proceedings marked*)

M. Fairweather, J.F. Griffiths, K.J. Hughes, R. Porter and A.S. Tomlin. Kinetic modelling of two-stage autoignition of alkanes and the effect of formal mechanism reduction on autoignition temperatures. *Institute of Physics Current Research in Combustion: A Forum for Research Students and Young Researchers*, Loughborough University, UK, 2005.

* F. Battin-Leclerc, F. Buda, M. Fairweather, P.A. Glaude, J.F. Griffiths, K.J. Hughes, R. Porter, and A.S. Tomlin. The Effect of Formal Mechanism Reduction on Simulated Propane Autoignition and a Quantitative Assessment of the Impact of Uncertainties in Parameter Values. *Second European Combustion Meeting, ECM 2005*, Louvain-la-Neuve, Belgium, Paper 16, 2005.

* Battin-Leclerc, F. Buda, M. Fairweather, P.A. Glaude, J.F. Griffiths, K.J. Hughes, R. Porter, and A.S. Tomlin. A Numerical Study of the Kinetic Origins of Two-Stage Autoignition and the Dependence of Autoignition Temperature on Reactant Pressure in Lean Alkane-Air Mixtures. *Second European Combustion Meeting, ECM 2005*, Louvain-la-Neuve, Belgium, Paper 25, 2005.

* R. Porter, M. Fairweather, J.F. Griffiths, K.J. Hughes and A.S. Tomlin. Automatic generation of reduced reaction mechanisms for hydrocarbon oxidation with application to autoignition boundary prediction for explosion hazards mitigation. *16th European Symposium on Computer Aided Process Engineering*, Garmish-Partenkirchen, Germany, 2006 p.383-388.

M. Fairweather, J.F. Griffiths, K.J. Hughes, R. Porter and A.S. Tomlin. Automatic generation of reduced reaction mechanisms for hydrocarbon oxidation with application to auto ignition boundary prediction for explosions hazards mitigation. *CAPE research poster day*, University College London, UK, 2006.

R. Porter, M. Fairweather, J.F. Griffiths, K.J. Hughes and A.S. Tomlin. The automatic generation of reduced reaction mechanisms for hydrocarbon oxidation with application to auto ignition boundary prediction for explosions hazards mitigation. *Thirty-first International Symposium on Combustion*, Heidelberg, Germany, 2006.

K.J. Hughes, M. Fairweather, J.F. Griffiths, R. Porter and A.S. Tomlin. Systematic application of the QSSA to combustion mechanism reduction via reaction lumping. *Thirty-first International Symposium on Combustion*, Heidelberg, Germany, 2006.

* R. Porter, M. Fairweather, J.F. Griffiths, K.J. Hughes and A.S. Tomlin. Simulated autoignition (AIT) and oxidation of cyclohexane using a QSSA reduced mechanism. *Third European Combustion Meeting, ECM2007*, Chania, Greece, 2007.

Conference presentations (published proceedings marked*)

* F. Buda, P.A. Glaude, F. Battin-Leclerc, R. Porter, K.J. Hughes and J.F. Griffiths. Use of detailed kinetic mechanisms for the prediction of autoignitions. *5th International Symposium on Hazards, Prevention and Mitigation of Industrial Explosions*, ISHPMIE, Krakow, Poland, 2004.

R. Porter. Kinetic Mechanism Reduction for Chemical Process Hazard Application. *SPEME research meeting*, University of Leeds, UK, 2006.